Genetic changes in melanoma progression

Weiling Li

Thesis presented for the degree of PhD

The University of Edinburgh

2011

Declaration

I hereby declare that this thesis has been composed by me and it has not been accepted in any previous application for a degree at this time or at any other university. The work described has been performed by me, except where expressly indicated otherwise. All sources of information have been specifically acknowledged. The experiments were designed in collaboration with my supervisor Prof. David W. Melton.

Acknowledgement

I am very grateful to Prof. David Melton for his very kind support and guidance over past years. I also would like to thank my second supervisor Dr. Jim Selfridge for his kind help. Many thanks to the members in Melton group: Ann-Marie Ritchie, Liang Song, Yan Xu and Ewan McNeil. I also have to give my thanks to those working in Dr. Liz Patton's and Dr. Val Brunton's group for their advice and technical support. I would like to thank Huizhong Hu for his advice and enthusiasm on cell signaling pathways. I am also grateful for my friends in Edinburgh: Liting Sun and Xiaoxia Liu. Finally, I am indebted to my parents for their unwavering support.

Table of contents

Abstract

Melanoma is a highly aggressive tumour with a poor prognosis for patients with advanced disease because it is resistant to current therapies. Therefore, the development of novel strategies for melanoma treatment is important. The characterization of the molecular mechanisms underlying melanoma proliferation, progression, and survival could help the development of novel targeted melanoma treatments. The MAPK and PI3K pathways both play important roles in melanoma progression. In the MAPK pathway, DUSP6, which acts as a phosphatase to negatively control the activation of ERK1/2, is involved in the development of human cancers. The MAPK pathway also regulates expression of the DNA repair gene *ERCC1* following EGF treatment. ERCC1 is essential for nucleotide excision repair, which is one of the major systems for removal of cisplatin induced DNA lesions. The aims of this project were: 1, to investigate the molecular changes in our immortal mouse melanocyte cell lines that were needed for them to form tumours in a xenograft model; 2, to investigate whether the MAPK pathway regulates ERCC1 following cisplatin treatment and protects melanoma cells from death.

Through comparison of the RAS/RAF/MEK/ERK (MAPK) and the PI3K/AKT (AKT) signalling pathways between our immortal mouse melanocyte cell lines and their tumour derivatives in our xenograft model, we identified a molecularly distinct subtype of mouse melanoma characterized by reduced ERK and AKT activity and increased expression of DUSP6. Functional analyses employing ectopic overexpression indicated that increased expression of DUSP6 enhanced anchorage independent growth ability and invasive ability in our mouse melanocytes, suggesting that increased DUSP6 expression may contribute to melanoma formation in the xenograft assay. We also demonstrated that higher expression of p-ERK suppressed invasion, but not anchorage independent growth, in our subtype of mouse melanoma by enforced expression of constitutively active MEK1 and MEK2. In addition, the role of DUSP6 in classical human melanoma was investigated in this

study. Inhibition of anchorage independent growth and invasion were observed after exogenous expression of DUSP6 in human melanoma cells. This suggested that DUSP6 played different roles in classic human melanoma than in our distinct subtype of mouse melanoma. Our study also investigated the phosphorylation level of ERK1/2 and the mRNA and protein level of ERCC1 and its partner XPF in the human melanoma cell line following cisplatin treatment. Significant increases in expression of p-ERK, ERCC1 and XPF were found in cisplatin treated cells. Moreover, a MEK inhibitor inhibited ERCC1 induction by cisplatin, but did not significantly affect XPF induction. This suggested that the MAPK pathway was involved in regulation of ERCC1 but not XPF. Furthermore, the DUSP6 level decreased after cisplatin treatment and overexpression of DUSP6 inhibited ERCC1 and XPF induction and reduced resistance to cisplatin. DUSP6 seems to play a crucial role in resistance of melanoma to cisplatin. In addition, a novel larger *ERCC1* transcript was identified in human cell lines and was found to be upregulated by cisplatin. The ratio of larger *ERCC1* transcript relative to the normal *ERCC1* transcript increased following cisplatin treatment. The functions of this larger *ERCC1* transcript in cisplatin resistance deserve further study.

Abbreviations

A: adenosine

AP-1: activated protein 1

APS: ammonium persulphate

APS: agouti signaling protein

BCA: bicinchoninic acid

BSA: bovin serum albumin

Bp: base pair

BRCA-1: breast cancer 1

C: cytosine

CDK: cyclin-dependent kinase

CDDP: cisplatin

cDNA: complementary DNA

CO_2 : carbon dioxide

CPDs: cyclobutane pyrimidine dimers

CS: cockayne syndrome

CSA: cockayne syndrome protein A

CSB: cockayne syndrome protein B

DDB: damage-specific DNA binding protein

DMSO: dimethyl suphoxide

DMEM: Dulbecco's Modified Eagle' Medium

DSB: double strand break

DTIC: dacarbazine

DUSPs: dual-specificity protein family of phosphatases

ECL: enhanced chemiluminescence solution

ECM: extracellular matrix

EDTA: ethyleneiaminetetraacetic acid

EGF: epidermal growth factor

ERCC1: excision repair cross-complementing group 1

ERK: extracellular signal regulated kinase

EST: expressed sequence tag

FCS: foetal calf serum

FDA: U.S. Food and Drug Adiministration

FGF: fibroblast growth factor

FNE-1: flap endonuclease

G: Guanosine

GAPDH: glyceraldehyde-3-phosphate dehydrogenase

GGR-NER: global genomic repair

HBS: HEPES buffered saline

HGF: Hepatocyte growth factor

hHR23B: human homolog of yeast RAD23

HR: homologous recombination

HRP: horseradish peroxidase

ICL: interstand crosslinks

IGFBP7: insulin-like growth factor-binding protein 7

JNK: c-jun-NH_2-kinase

Kb: kilobase

KIM: kinase interaction motif

LB: Luria-Bertani

LPS: bacterial lipopolysaccharide

MC1R: melanocortin 1 receptor

MEK: mitogen-activated protein kinase

MITF: microphthalmia-associated transcription factor

MKP: dual-specificity MAPK phosphatase

MMP: matrix metalloproteinases

MSH: melanocyte stimulating hormone

NaPy: sodium pyruvate

NEAA: non-essential amino acids

NER: nucleotide excision repair

NSCLC: non-small-cell lung carcinoma

PAGE: polyacrylamide gel electrophoresis

PBS: phosphate buffered saline

PCA: phenol-chloroform-isoamyl alcohol

PCNA: proliferating cell nuclear antigen

PCR: polymerase chain reaction

PI3K: phosphatidylinositol 3′-kinase

PKA: protein kinase A

PTC: papillary thyroid cancer

PTEN: phosphatase with tensin homolog

qPCR: real-time polymerase chain reaction

RACE: rapid amplification of cDNA Ends

RFC: replication factor C

RGP: radial-growth phase

RPA: replication protein A

RRM1: ribonucleotide reductase 1

RTK: receptor tyrosine kinase

RT-PCR: reverse transcription polymerase chain reaction

SAPK: stress-activated protein kinase

SCCHN: advanced squamous cell carcinoma of the head and neck

SDS: sodium dodecyl sulphate

siRNA: small interfering RNA

SNP: single nucleotide polymorphism

SRB: sulforhodamine B

SSA: single-strand annealing

T: thymidine

TAE: Tris Acetate EDTA

TBE: Tris Borate EDTA

TBS: Tris Buffered Saline

TBST: Tris Buffered Saline with Tween

TCA: trichoroacetic acid

TCR-NER: transcription-coupled repair

TE: Tris EDTA

TEMED: tetramethylethylenediamine

TFIIH: transcription factor with helicase activity

TGCT testicular germ cell tumour

TMZ: temozolomide

TTD: trichothiodystrophy

uPA: urokinase plasminogen activator

UV: ultraviolet

VGP: vertical-growth phase

w/v: weight against volume

X-gal: 5-Bromo-4-chloro-3-indolyl β-D-galactopyranoside

XP: xeroderma pigmentosum

Chapter 1

General introduction

1.1 Melanoma

1.1.1 General introduction to melanoma

Melanoma is an aggressive, therapy-resistant malignancy of melanocytes. The incidence of melanoma has risen at an astonishing rate worldwide. Cutaneous melanoma is the sixth most common cancer in the UK and the second commonest in young people (Gandini et al. 2005). Approximately 85 percent of patients with primary cutaneous melanoma who are diagnosed at an early stage enjoy long- term survival and a high cure rate (Tsao and Sober 2005). However, average survival durations in patients with metastatic melanoma range from 6 to 9 months, because of the high resistance of the disease to therapy and its very fast progression (Casula et al. 2007).

Melanocytic transformation is generally believed to occur by sequential accumulation of genetic and molecular changes (Miller and Mihm 2006). Although the molecular basis of human malignant melanoma progression has remained largely unknown, several genes and metabolic pathways have been shown to carry molecular alterations during this process. Mutations of BRAF, CDKN2A and PTEN have been proposed to contribute to melanoma progression. Both the RAS/RAF/MEK/ERK (MAPK) and the PI3K/AKT (AKT) signaling pathways are reported to be involved in melanomagenesis (Takata and Saida 2006).The characterization of the molecular mechanisms involved in melanoma proliferation, progression, and survival could help to identify the molecular profiles underlying aggressiveness, clinical behaviour, and create many opportunities for targets, drugs and new therapeutic approaches for this disease.

1.1.2 Introduction to melanocytes

Melanocytes are specialist pigment cells that are located in the lower layers of the skin, the middle layer of the eye, the inner ear, heart, bones and meninges. Cutaneous melanocytes originate in the neural crest and migrate to the basal layer of the epidermis and the hair follicles during embryonic development. Melanocytes produce melanin which is responsible for skin and hair colour (Lin and Fisher 2007).

There are two main types of melanin-eumelanin and pheomelanin. Eumelanin is brown to black and is the main type in dark skin and hair, while pheomelanin is red to yellow and is the main type in red hair and freckled individuals. Both types of melanin are regulated by a common tyrosinase-dependent pathway with the same precursor, tyrosine. Production of eumelanin or pheomelanin depends on the interaction of the melanocortin 1 receptor (MC1R) on the surface of the melanocyte with melanocyte stimulating hormone (MSH) or with the agouti signaling protein (ASP). The binding of MSH to MC1R leads to the production of eumelanin while the binding of ASP to MC1R results in the formation of pheomelanin (Jimbow et al. 1979, Prota et al. 1976). MSH is a ligand of the receptor MC1R, and activation results in an increase in cellular cAMP. ASP antagonizes the effects of MSH at MC1R. Overexpression of ASP in mice results in yellow coat colour. The role of ASP in humans is still unclear. It seems that the MC1R receptor has some degree of constitutive (ligand-independent) activity. The increased cAMP leads to activation of protein kinase A (PKA), which results in an increase in microphthalmia transcription factor (MITF). MITF seems to play an important role in control of melanogenesis that leads to increased transcription of many genes (including genes encoding tyrosinase and tyrosinase-related protein 1 and 2). These genes are involved in the control of the relative and absolute amounts of eumelanin and pheomelanin (Rees 2004).

Melanin production takes place in unique organelles known as melanosomes. Melanosomes usually cluster together near the centre of the cell but can rapidly redistribute themselves to the ends of dendritic processes projecting from cells. Two types of transport are responsible for melanosome redistribution: long-range transport from the center along microtubules and along the periphery; short range capture and transport. External stimuli such as UV radiation or mutations in the transport system can affect melanosome distribution (Hirobe 1995, Sulaimon and Kitchell 2003).

The function of melanocytes is best studied and defined in skin. In the basal layer of the epidermis, each melanocyte can distribute melanin to about 30 surrounding keratinocytes through melanocytic dendritic processes. The melanin granules orient in an umbrella-like fashion over the keratinocyte nucleus parallel to the skin surface. It is generally believed that melanin absorbs ultraviolet radiation (UVR) and possesses antioxidant properties which can neutralize UVR-induced free radicals. When the skin is exposed to UVR, melanocytes synthesize more melanin and transfer it to keratinocytes to dissipate ultraviolet energy and protect cells (Agar and Young 2005). Eumelanin is more protective against UVR exposure than pheomelanin. Tanning of the skin due to UV exposure represents an increase in the content of eumelanin within the epidermis and its major purpose is increased photoprotection.

1.1.3 Melanoma epidemiology, risk factors and prevention

The latest statistics show that 11,767 new malignant melanoma cases were diagnosed in the UK during 2008 and there were 2,067 deaths at the same year. Among these cases, 6,183 cases were diagnosed in women and 5,584 cases diagnosed in men. It was the sixth most common cancer in females and the ninth in males in the UK. The commonest site of melanoma is on the legs in female; while over a third of male cases arise on the trunk of the body. Melanoma is notorious for affecting young

people, unlike other solid tumours, which mainly affect older adults. The age specific rates of malignant melanoma in UK show that about 30% of all cases occur in people aged less than 50 years and malignant melanoma is the second most common cancer in young people (aged 15-34) (Cancer Research UK, 2009, http://info.cancerresearchuk.org/cancerstats/types/skin/incidence/).

The incidence rates vary 100 fold among different populations. The highest rates occur in Queensland, Australia where fair skinned individuals have high UV radiation exposure, the cumulative incidence in the population older than 50 years is 1 in 19 for men and 1 in 25 for women (Goldstein and Tucker 1993). Scotland has the highest rate of melanoma compared to other countries in the UK. The incidence of malignant melanoma is dramatically increasing in most white populations. The increase is occurring at a faster rate than any other common cancer in Scotland: the rate has increased from only 633 cases in 1998 to 1,164 cases in 2008 (NHS National Services Scotland, 2009, http://www.isdscotland.org/isd/1048.html).

Several factors have been reported to be responsible for the world wide increase in the incidence of melanomas. A large number of studies have shown an increased melanoma risk in individuals who have sunburn history in childhood, and a lower melanoma risk for sunburn with older age. Higher incidences of melanoma occur in the population who live in low latitudes or close to the coast during childhood. In contrast, people living in high latitudes or who never lived near the coast have lower incidences of melanoma (Oliveria et al. 2006). Some studies also showed that intermittent sun exposure from recreational and vacation activities during childhood increased melanoma risk (Elwood 1992, Nelemans et al. 1995)

The risk of melanoma has been directly related to the presence of multiple naevi on the body. The risk is approximately 1.5 times higher in people with 11 to 25 naevi and seems to be doubled with every 25 naevi increase (Bevona et al. 2003, Garbe et

al. 1994). Dysplastic nevi are strongly associated with the risk of melanoma. Patients with dysplastic nevus syndrome have almost a 100-times increased risk of developing melanoma, and approximately 50% of these patients would have melanoma by the age of 50 years (Tucker et al. 1993).

A family history of melanoma is another risk factor for developing melanoma. Patients with a family history of melanoma have double the risk of developing melanoma than patients without a family history. About 10% of all melanoma is familial melanoma (Meyer and Zone 1994). Mutations in CDKN2A and CDK4 have been reported to occur in the patients with a family history of melanoma (Tsao and Niendorf 2004). The roles of the CDKN2A mutations will be discussed in Introduction 1.2.3. Variation in melanocortin-1 receptor has been found to predispose to the development of melanoma. Red hair, fair skin, presence of freckles, and sun sensitivity are associated with variation in the melanocortin-1 receptor and may be related to the increasing risk for melanoma in these phenotypes (Titus-Ernstoff et al. 2005, Veierod et al. 2003).

Primary prevention of melanoma is by reduction of risk factors. Reducing intense, intermittent sun exposure and avoiding sunburn in childhood are the most important behaviours to prevent development of melanoma (Kaskel et al. 2001). However, there has been some concern that reduction of sun exposure will disturb the synthesis of vitamin D which may have a negative impact on health (Weinstock et al. 1992). Research on how much UVR exposure is required to synthesize the optimal vitamin D levels is ongoing. Early diagnosis and treatment of melanoma are the secondary steps to prevent metastatic melanoma. People with high risk for development of melanoma such as xeroderma pigmentosum and familial multiple mole syndrome patients and people with a family history of melanoma and men older than 50 years should be identified and receive skin screening by a dermatologist (Geller et al. 2003a, Geller et al. 2002, Geller et al. 2003b).

1.1.4 Melanoma stages and diagnosis

The “ABCDE” mnemonic is used to examine and interpret pigmented lesions of melanoma. These include: asymmetric moles, border irregularity of moles, colour variability in a lesion, diameter greater than 6mm and evolving (or changing). Evolving is defined as any significant change in shape, surface, colour, or symptoms (Goldstein and Goldstein 2001).

Melanomas are histologically classified into five distinct stages according to their location and progression: benign nevus; dysplastic nevus; radial-growth phase (RGP) melanoma; vertical-growth phase (VGP) melanoma; and metastatic melanoma (Fig. 1.1). Both benign nevus and dysplastic nevus are characterized by increased numbers of melanocytes and disruption of the epidermal melanin unit. During the radial-growth phase, cells grow laterally and remain largely confined to the epidermis. In addition, the cells can penetrate the papillary dermis singly or in small nests but fail to form colonies in soft agar. When lesions progress to the vertical-growth phase, cells aquire ability to invade the upper layer of the epidermis, and penetrate into the underlying dermis and subcutaneous tissue through the basement membrane, forming expansile nodules. The cells are capable of growth in soft agar. The final step is metastatic melanoma: cells are spread to other areas of the skin and other ogans, where they can proliferate and form metastatic foci (Miller and Mihm 2006)

Figure 1.1 Progression of melanoma

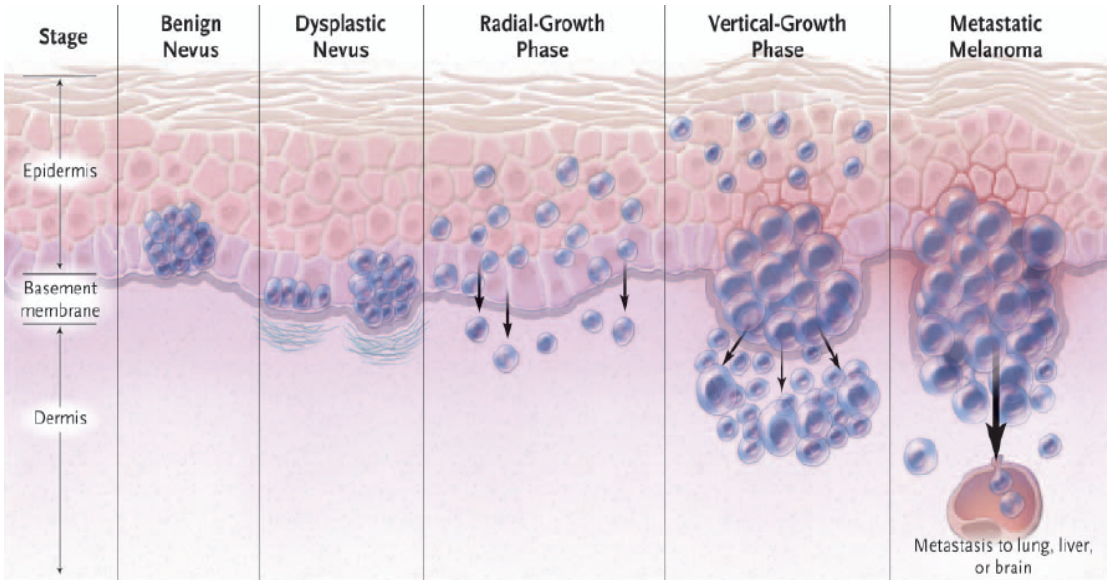

The stages of melanoma progression. For explanation, see text. Taken from Miller and Mihm, 2006.

Cutaneous melanomas are classified as superficial spreading, acral lentiginous, nodular, and lentigo maligna. Superficial spreading is the most common type of melanoma, accounting for 70% of cases. It tends to be found on the back of the legs of women and on the backs of men (Newell et al. 1988). These tumours are usually composed of epithelioid melanoma cells and are linked with intermittent sun exposure (Markovic et al. 2007). Acral lentiginous melanomas account for 5% of melanomas in white people. However, it is the most common type of melanoma in the non-caucasian population, accounting for 50% of cases (MacKie 1985). Acral lentiginous melanomas are usually found on glabrous skin, the palms of hands and the soles of feet (Cascinelli et al. 1994). Nodular melanoma often occurs on the trunk and limbs of patients, accounting for 5% of melanoma cases. It only has a vertical growth phase without a radial growth phase (Markovic et al. 2007). Lentigo maligna generally occurs on sun-exposed regions in the elderly, accounting for 4% to 15% of cutaneous melanoma. It correlates with long-term sun exposure and increasing age (Clark and Mihm 1969, Flotte and Mihm 1999).

Several clinical and histological parameters that influence the prognosis of cutaneous melanoma have been identified (Balch et al. 2000). Three clinical parameters are considered: anatomical site, gender, and age. Patients with melanoma on the trunk, head or neck have poorer prognosis than patients with melanoma on the extremities. As the histological parameters, depth of invasion and ulceration are considered for melanoma prognosis. There is a linear correlation between patient survival and tumour thickness. Female and young people have higher survival rate compared to male and older people. Tumour thickness (Breslow) and Depth of invasion (Clark) are the most important melanoma prognostic factors. 20-25% of all melanomas harbour ulceration. Based on these clinical and histological parameters, melanoma can be staged (Table 1.1).

Stage I and II melanomas are characterized by tumour thickness and ulceration status. There is no evidence of regional lymph node or distant metastasis. Stage III melanoma is characterized by the level of lymph node metastasis without distant metastasis. Stage IV melanoma patients have distant metastatic spread of melanoma (Goldstein and Goldstein 2001). Although staging patients is helpful for clinical treatment, sometimes the parameters are not reliable. Some thin lesions may become metastatic, while some deep melanomas lack metastatic potential.

Stage	TNM classification	Histological/Clinical Features	5 Year Survival
0	Tis0 N0 M0	intraepithelial/in-situ melanoma	100%
IA	T1a N0 M0	<1mm without ulceration and level II/III	>95%
IB	T1b N0 M0	<1mm with ulceration and level III/IV	
	T2a N0 M0	1.01-2cm without ulceration	89-91%
IIA	T2b N0 M0	1.01-2cm with ulceration	
	T3a N0 M0	2.01-4cm without ulceration	77-79%
IIB	T3b N0 M0	2.01-4cm with ulceration	
	T4a N0 M0	>4cm without ulceration	63-67%
IIC	T4b N0 M0	>4cm with ulceration	45%
IIIA	T1-4a N1a M0	1 nodal micrometastases, nonulcerated 1	
	T1-4a N2a M0	2-3 microscopic nodes, nonulcerated 1	63-69%
IIIB	T1-4b N1a M0	1 nodal micrometastases, ulcerated 1	46-53%
	T1-4b N2a M0	2-3 microscopic nodes, ulcerated 1	
	T1-4a N1b M0	1 nodal micrometastases, nonulcerated 1	
	T1-4a N2b M0	2-3 macroscopic nodes, nonulcerated 1	
	T1-4a/b N2c M0	In-transit mets and/or satellite lesions	30-50%
IIIC	T1-4b N2b M0	1 macroscopic region node, ulcerated 1	
	T1-4a/b N2a M0	2-3 metastatic nodes, ulcerated 1	
	Any T N3 M0	4 or more metastatic nodes	24-29%
IV	Any T any N M1a	Skin, or nodal mets with normal LDH	
	Any T any N M1a	Lung mets with normal LDH	
	Any T any N M1a	Mets with elevated LDH or visceral mets	7-19%

Table 1.1 AJCC 2002 Revised Melanoma Staging. The table shows 5 year survival for patients with different stages of melanoma determined by Breslow thickness, presence of ulceration, nodal involvement or presence of metastatic disease. TNM means tumour, nodes and metastases. LDH means lactate dehydrogenase.

1.1.5 Melanoma therapy

Surgery is the standard treatment for melanoma in situ, Stage I, Stage II, and Stage III melanoma and may be considered for Stage IV melanoma. The aim of surgery is

to remove the tumour and its surrounding normal skin. Surgery in early-stage melanoma can be curative. The goal of surgery in late-stage melanoma is to remove the tumours or lymph nodes from spread to other areas of the body. Adjuvant therapy including chemotherapy, radiation, and immunotherapy can be applied to late-stage patients after surgery (McMasters and Swetter 2003)

Melanoma is not so sensitive to chemotherapy as other types of cancers. However, application of chemotherapy can relieve the symptoms of some late-stage patients. The most common single agents used for melanoma therapy are dacarbazine (DTIC), temozolomide (TMZ), and cisplatin (CDDP). Dacarbazine is approved by the U.S. Food and Drug Administration (FDA) for treatment of melanoma. Studies indicate that dacarbazine results in melanoma shrinkage in 15% to 20% patients for an average of six months before the melanomas resume growth. Dacarbazine does not significantly prolong the overall survival (Kirkwood and Agarwala 1993). Temozolomide is another agent used in treatment of advanced metastatic malignant melanoma. It can be given as outpatient treatment which is easier to administer with fewer side effects. Temozolomide is as effective as DTIC according to a phase III trial. Median overall survival times were 7.7 months with TMZ vs 6.4 months with DTIC (Middleton et al. 2000). Besides DTIC and TMZ, cisplatin has achieved higher response rate in advanced melanoma patients. The functions of cisplatin will be discussed in detail in the following section. Cisplatin has been tested as a single agent at doses of up 200mg/m^3, with response rate in the range of 0-53% (Al-Sarraf et al. 1982, Glover et al. 1987, Schilcher et al. 1984). However, high dose cisplatin can result in therapy resistance and side effects. Combination of cisplatin, dacarbazine and tamoxifen (a hormonal therapy drug used in breast cancer treatment) known as the Dartmouth regimen is also applied for treatment of advanced melanoma (Chapman et al. 1999). However, the clinical trials have not shown that this combination is more effective than dacarbazine alone.

Radiation therapy can be applied to advanced melanoma where surgery is not possible. It is used to relieve symptoms where the melanoma has metastasized to areas such as the brain or bone. Radiation therapy can prevent melanoma recurrence after surgery as well (Berk 2008, Guadagnolo and Zagars 2009). Various immunotherapeutic strategies are also used for treatment of advanced melanoma. These strategies include interferon-alpha and interleukin-2 (IL-2). Interferon-a2b is approved for stage III melanoma in the USA, however its efficacy is limited. Interferon-a2b has demonstrated a 10-20% improvement in overall survival, but without a clear effect on mortality (Fecher and Flaherty 2009). Interleukin-2 is used for stage IV melanoma. High-dose Interleukin-2 produces durable responses in 10-20% patients with metastatic melanoma (Atkins et al. 2000).

The improved understanding of molecular changes underlying melanoma initiation and progression resulted in the development of novel targeted melanoma therapy. Given BRAF V600E mutations occur in up to 70% of human melanoma (Dong et al. 2003), there has been intense interest in selective BRAF inhibitors. Sorafenib is one of the earlier BRAF inhibitors which targets BRAF, CRAF and receptor tyrosine kinases (Wilhelm et al. 2004). Although sorafenib showed limited activity against melanoma alone, it showed greater activity when combined with other chemotherapeutic agents (Amaravadi et al. 2009, Flaherty 2006). PLX4032 is a more selective BRAF inhibitor which suppresses BRAF V600E with 30-fold selectivity relative to the wild type BRAF kinase. It produced about 70% objective response rates in patients with metastatic melanoma harbouring BRAF mutations in the phase I trial and has already proceeded to phase II/III trials (Ko and Fisher 2010). However, recent study also indicated that patients with melanomas frequently acquire resistance to PLX4032 after initial responses. Melanomas escape BRAF(V600E) targeting through RTK-mediated activation of alternative survival pathways or activated RAS-mediated reactivation of the MAPK pathway, suggesting additional therapeutic strategies (Nazarian et al. 2010). The c-KIT RTK has been reported to be amplified or mutated in some subtypes of melanoma (Curtin et al. 2006), suggesting that c-KIT is another novel drug target. Several phase II trials are ongoing to evaluate

KIT-targeted agents, including imatinib, sunitinib, inlotinib and dasatanib, in melanoma patients who have KIT amplifications or mutations. Targeted therapies, specifically those against BRAF V600E and mutant KIT open a new era in melanoma treatment.

1.2 Molecular changes in melanoma progression

1.2.1 The RAS/RAF/MEK/ERK pathway

1.2.1.1 Overview of the RAS/RAF/MEK/ERK pathway

The RAS/RAF/MEK/ERK pathway, also known as the MAPK (mitogen-activated protein kinase) pathway, is a signaling cascade relaying extracellular signals from plasma membrane to nucleus via a series of consecutive phosphorylation events (Fig. 1.2). A variety of cellular stimuli, such as growth factors, bind to their respective receptor tyrosine kinase (RTK), and receptor dimerization results in activation of intrinsic tyrosine kinase activity followed by autophosphorylation of specific tyrosine residues on the intracellular portion of the receptor. Then the sequence homology 2 (SH2) domains of adaptor proteins such as GRB2 recognize tyrosine phosphate docking sites located on the receptor or on receptor substrate proteins and recruit SOS (son of sevenless), a cytosolic protein, to the plasma membrane (Chin 2003). The binding of SOS to RAS switches the RAS-family GTPases from the inactive GDP-bound state to the active GTP-bound state (Cobb 1999, Kolch 2000). The activation of RAS leads to recruitment of RAF, which includes 3 isoforms: ARAF, BRAF and CRAF, from the cytosol the cell membrane where it becomes activated (Stokoe et al. 1994). Once active, RAF results in phosphorylation and activation of MAP kinase extracellular signal regulated kinases 1 and 2 (MEK1 and MEK2), which in turn phosphorylate extracellular signal regulated kinases 1 and 2 (ERK1 and ERK2) (Crews et al. 1992). The activated ERK either phosphorylates a variety of

cytoplasmic targets or migrates to the nucleus to phosphorylate several transcriptional factors such as Elk-1, Fos, CREB and Myc (Lenormand et al. 1993, Treisman 1994). These transcriptional factors bind to the promoters of many genes that regulate cell proliferation, differentiation and survival.

For many years, RAS signalling has been implicated in initiation and progression of melanoma. Approximately 15–20% of human melanomas have mutations in RAS genes (Fecher et al. 2007). Knockdown of NRAS by RNA interference results in apoptosis in melanoma cells carrying a NRAS mutation, suggesting the important role of NRAS in maintaining the growth of melanoma cells (Eskandarpour et al. 2005). Most of the RAS mutations in melanoma involve a substitution of leucine for glutamine at residue 61 of N-RAS, which remains constitutively GTP bound and active. K-RAS and H-RAS mutations are relatively rare in melanoma, suggesting that RAS activities are dependent on specific isoforms (Whitwam et al. 2007).

Although RAS clearly plays a role in human melanoma, BRAF mutations in human melanoma have recently received much attention. BRAF mutation occurs in approximately 70 percent of melanomas (Dong et al. 2003). The most frequent mutation in BRAF is a glutamic acid for valine substitution (V600E), which produces a protein that induces constitutive activation of ERK (Wan et al. 2004). One possible explanation for the high rates of BRAF mutation in melanoma is that the mutation is UV-induced. However, the T>A transversion of this mutation is not a typical UV-induced lesion(C>T or CC>TT), which makes this hypothesis unlikely. Others have proposed that UVB-induced DNA photoproducts account indirectly for BRAF mutation in melanoma (Thomas et al. 2006). According to this hypothesis, the BRAF mutations may arise from UV-induced oxidation of melanin, resulting in the formation of reactive oxygen species and leading to increased DNA damage. None of these hypotheses have been proved; therefore the mechanism of BRAF mutation remains unclear. Mutations of ARAF and CRAF are not found in melanoma, which may be because BRAF just needs one genetic mutation for oncogenic activation,

while ARAF and CRAF both need two mutations to activate, and this is rare (Emuss et al. 2005, Lee et al. 2005).

Figure 1.2 The RAS/RAF/MEK/ERK pathway

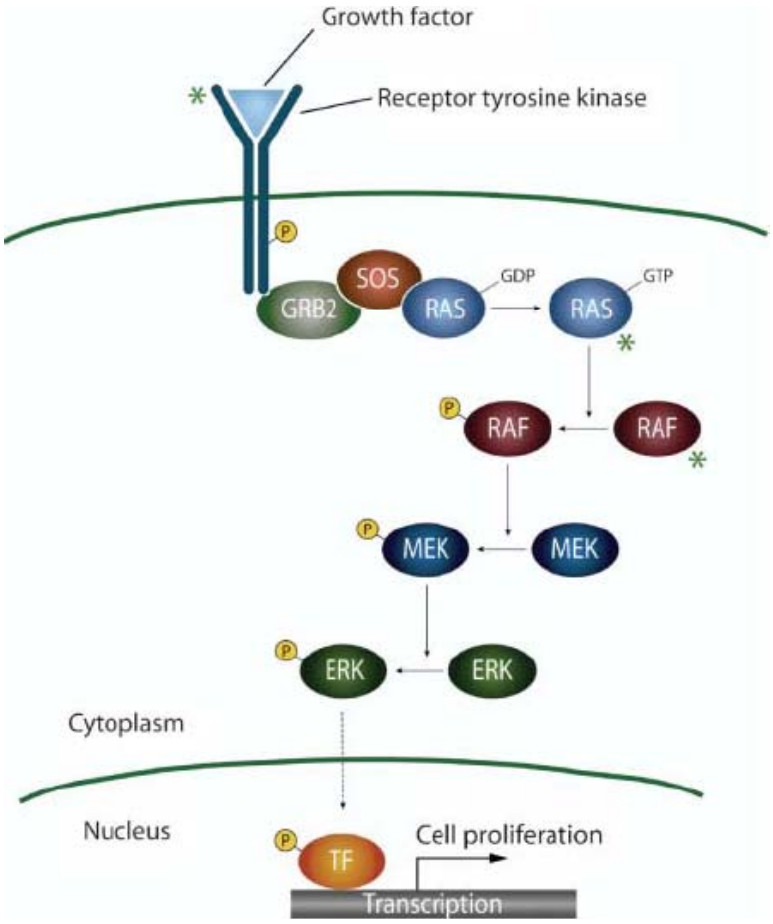

Growth factors bind to cell surface receptor RTK to activate RAS though various adaptor proteins. Once activated, RAS triggers phosphorylation of a series of kinases: RAF, MEK and ERK. Activated ERK transmits signals to the nucleus by activating transcription factors to stimulate cell proliferation. RTK genes, NRAS, and BRAF are oncogenes in malignant melanoma (indicated by green asterisks). Taken from Dahl and Guldberg, 2007.

1.2.1.2 Roles of the RAS/RAF/MEK/ERK pathway in cell proliferation and invasion

Cell proliferation is regulated at the G1 restriction checkpoint. Progression through G1 into S phase of the cell cycle is controlled by CDK4 and CDK6, which interact with the cyclin D family of proteins, and by CDK2, which interacts with cyclins A/E (Polyak et al. 1994, Sherr 1994, Sherr and Roberts 1995). Sustained ERK activation is reported to stimulate cells to pass the G1 restriction (Pages et al. 1993). Microinjection of active-RAS resulted in proliferation in fibroblasts (Feramisco et al. 1984). Mutant BRAF V600E can initiate the formation of papillary thyroid cancer (PTC) and maintain the proliferation and tumorigenicity of papillary thyoid cancer cells (Liu et al. 2007). However, the MAPK pathway is downregulated in some types of tumours. There is a pronounced decrease in p-ERK levels with increasing tumour stage in colorectal cancer (Gulmann et al. 2009). The expression of the MAPK pathway may shut off in some prostate cancers isolated from advanced prostate cancer patients by the deletion of PTEN gene, which regulates AKT activity (Shelton et al. 2005). Moreover, under some circumstances, a constitutively active MAPK pathway can lead to cell cycle arrest instead of proliferation. This pre-G1 arrest and subsequent senescence are driven by ERK-mediated upregulation of p53 and p16 (Lin et al. 1998). Recently, it has been demonstrated that BRAF mutation can induce isulin-like growth factor-binding protain 7 (IGFBP7) which may take part in arrest of the cell cycle (Wajapeyee et al. 2008).

In melanoma, the roles of ERK activity in proliferation are still controversial. Classical studies have indicated that uncontrolled growth of the majority of melanoma cells results from constitutive activation of the MAPK pathway. ERK activity controls the proliferation of human and mouse melanoma cell lines, which can be blocked by administration of a MEK inhibitor (Kortylewski et al. 2001, Smalley and Eisen 2000). Inhibition of the MAPK pathway is associated with G1-phase cell cycle arrest via the downregulation of pRB phosphorylation and CDK2

activity, and the upregulation of p27 activity (Kortylewski et al. 2001). In contrast, other studies indicated that there was little correlation between the inhibition of phospho-ERK levels and growth of melanoma cells following MEK inhibitor treatment (Smalley et al. 2006). It suggests that there are likely other molecular changes in the pathways involved in regulation of cell proliferation. Some subtypes of melanomas without MAPK activation seem to stimulate cell proliferation by reduction of RB activity or overexpression of c-kit (Shields et al. 2007, Smalley et al. 2008). Furthermore, BRAF mutations also occur in naevi. Mutant BRAF protein induces cell senescence by increasing expression levels of p16 protein, which in turn, could limit the hyperplastic growth of melanocytes by BRAF mutation. (Michaloglou et al. 2005)

In normal skin, melanocytes interact with keratinocytes through the adhesion molecule E-cadherin. Downregulation of E-cadherin and upregulation of N-cadherin were reported during melanoma development (Kuphal and Bosserhoff 2006). The switch of cadherin subtypes frees melanoma cells from keratinocyte-mediated control and allows tumour cell invasion and migration. The decrease of E-cadherin is regulated by autocrine hepatocyte growth factor (HGF) which is expressed in melanoma cells. Inhibition of the MAPK pathway by the MEK inhibitor can partially block the downregulation of E-cadherin. It suggests that the MAPK pathway is involved in this process (Meier et al. 2005). The MAPK pathway is also involved in the upregulation of integrins which promote survival and invasive growth of melanoma cells in the extracellular matrix (ECM) (Schwartz et al. 1995). The expression of $\alpha_V\beta_3$ integrin is involved in transition from radial to vertical growth of melanoma (Albelda et al. 1990). Introducing $\alpha_V\beta_3$ integrin into a benign melanoma can induce invasion and metastasis in mouse xenograft models (Li et al. 1998b). The expression of α6 is also involved in melanoma invasion: human melanoma cells injected into nude mice were diminished in their metastatic potential by anti-α6 antibodies (Ruiz et al. 1993). The sustained activation of MAPK is associated with the expression of β3 and α6 in melanoma cell lines. The expression of β3 and α6 integrin in WM793, WM9, WM164 and WM1205 melanoma cell lines was

completely inhibited by the MEK1 inhibitor U1026 (Woods et al. 2001). Another important factor contributing to the metastatic spread of melanoma is the proteolytic enzymes which break down the surrounding matrix and facilitate cell migration though the basement membrane. Matrix metalloproteinases (MMPs) and the urokinase plasminogen activator (uPA), two families of proteases, are involved in matrix remodelling. With regard to melanoma, the expression of MMP-9 is linked with highly invasive melanoma and the expression of MMP-2 is a prognostic factor for survival of melanoma patients (MacDougall et al. 1999, Vaisanen et al. 1999). The expression of the MMP family is regulated by the MAPK pathway. Treatment of melanoma cells with MEK inhibitor reduced invasion of human melanoma A375 cells. This reduced invasion is due to downregulation of uPA and MMP-9 (Ge et al. 2002). However, in MeWo melanoma cells, MEK inhibitor had no affect on invasion (Denkert et al. 2002b). The functions of the MAPK pathway in the regulation of melanoma invasion still need further investigation.

1.2.1.3 Roles of the RAS/RAF/MEK/ERK pathway in cisplatin resistance

For the past 14 years, a large number of studies have revealed that the DNA cross-linking agent diamminedichloroplatinum (II) (cisplatin; CDDP) could activate the MAPK pathway. It is generally believed that MAPK activation is a major component in deciding the cell fate in response to cisplatin. However, the role of the MAPK pathway in response to cisplatin is complex because this pathway, in some cases, is able to induce apoptosis, but in other cases, has no roles in this process, or even suppresses apoptosis. The final outcome depends on the cell type, proliferation and differentiation status of tumour cells (Brozovic and Osmak 2007).

In Hela cells, activation of ERK is important for the induction of cisplatin-induced apoptosis. Downregulation of ERK results in an inhibition of CDDP-induced apoptosis, while enhanced activation of ERK contributes to cell death. Activation of ERK by cisplatin could release cytochrome c which is involved in mediating CDDP induced apoptosis. The influence of the ERK pathway on CDDP-induced apoptosis is not limited to Hela cells, but also occurs in lung cancer cell line A549 cells (Wang et al. 2000). In contrast to the foregoing results, there are also reports which indicate that the activation of ERK signaling enhances the resistance to cisplatin. Inhibition of ERK activity has been shown to increase sensitivities to cisplatin by accumulation of p53 in ovarian cancer (Brown et al. 1993). In melanoma, overexpression of activated N-RAS has been reported to protect melanoma cells and induce cisplatin resistance (Jansen et al. 1997). Treatment of melanoma cells with cisplatin caused a time dependent increase in activation of ERK and enhanced cisplatin resistance through activation of survival protein RSK1 (Mirmohammadsadegh et al. 2007). The molecular mechanisms underlying activation of the ERK pathway by CDDP and protecting melanoma cells from death need further investigation.

1.2.1.4 Feed-back loop of the RAS/RAF/MEK/ERK pathway

The duration and magnitude of kinase activation determine the biological outcome of the MAPK pathway. It depends on a balance between the activation of the upstream components and various negative regulatory mechanisms, which inhibit pathway activation. Studies indicated that activities of specific MAPK phosphatases are responsible for negative regulation of the MAPK pathway activation. Activation of the MAPK pathway require phosphorylation of both threonine and tyrosine residues. Therefore, dephosphorylation of either of these residues is sufficient for kinase inactivation. Serine/threonine phosphatases, tyrosine specific phosphatases and dual-specificity phosphatases are involved in this task (Keyse 2000, Saxena and Mustelin 2000). Among these three classes of protein phosphatases, dual-specificity MAPK

phosphatases (MKPs) are the largest group of phosphatases to specifically regulate the phosphorylation and activities of the MAPK pathway.

The MKPs are a subgroup of ten catalytically active enzymes within the cysteine-dependent dual-specificity protein family of phosphatases (DUSPs) (Theodosiou and Ashworth 2002). They share a similar structure with a noncatalytic NH_2-terminal domain and a catalytic COOH-terminal domain. The NH_2-terminal domain contains highly conserved sequences involved in MAPK recognition, known as the kinase interaction motif (KIM). The catalytic COOH-terminal domain shares an active site sequence similarity with the prototypic VH-1 DUSP encoded by vaccinia virus (Owens and Keyse 2007). Based on the sequence similarity, substrate specificity and subcellular localization, these ten MKPs can be divided into three subclasses. The first subclass contains DUSP1/MKP-1, DUSP2/PAC-1, DUSP4/MKP-2, and DUSP5. These phosphatases are encoded by inducible genes which contain four exons with introns in highly conserved positions. They are all nuclear proteins and can be rapidly upregulated in response to stimuli at the transcriptional level. All of these phosphatases are shown to dephosphorylate ERKs, JNK, and p38 MAPKs. The second subclass consists of DUSP6/MKP-3, DUSP7/MKP-X and DUSP9/MKP-4. The genes of these phosphatases also have four exons. They all are cytoplasmic enzymes and highly selective for ERK1/2. The third subclass of MPKs comprises DUSP8/hVH-5, DUSP10/MPK-5 and DUSP16/MKP-7. The genes of these phosphatases have six exons. They are located in both cytosol and nucleus and can inactivate p38 and JNK MAPKs (Keyse 2008).

Although the structures and catalytic mechanism of MPKs are described in detail in many studies, the knowledge of their biological functions is less complete. One study indicated that DUSP1 knock out mice are resistant to diet-induced obesity (Wu et al. 2006). However, the main roles of MKPs are regulation of the immune system and in cancer development. Some data indicated that DUSP1, DUSP10, and DUSP2 seem to be involved in regulation of immune response. DUSP1 is required to regulate

cytokine synthesis in response to bacterial lipopolysaccharide (LPS) (Chi et al. 2006). DUSP1 knock down animals are more sensitive to lethal endotoxic shock and have a high rate of induced autoimmune arthritis (Hammer et al. 2006). DUSP10 also plays an important role in regulation of immunity through the JNK pathway in immune effector cells (Zhang et al. 2004). DUSP10 knock out macrophages could produce more pro-inflammatory cytokines in response to LPS. In contrast, DUSP2 is a positive regulator of inflammatory response because DUSP2 knock out mice have reduced inflammation and macrophages from these mice produce less pro-inflammatory cytokines exposed to LPS (Jeffrey et al. 2006). Given the roles of the MAPK pathway in cancer progression, it is not surprising to see MPKs involved in the initiation and development of cancer though regulation of the MAPK pathway. High levels of DUSP1 are found in many human epithelial tumours, including prostate, colon, and bladder cancers (Loda et al. 1996). Interestingly, overexpression of DUSP1 is found in the early stage of these epithelial tumours and then drops during tumour progression. For example, DUSP1 expression is high in the early stage of prostate cancer, while its expression is lost in later stages of this cancer (Magi-Galluzzi et al. 1998). However, DUSP1 is also increased in invasive stages of certain cancers. Strong expression of DUSP1 is detected in 60% of invasive ovarian carcinomas and the DUSP1 level appears to be a prognostic marker for shorter progression-free survival (Denkert et al. 2002a). DUSP1 is also expressed at higher levels in poorly differentiated and late stages of breast cancer, which may be related to regulation of the JNK pathway (Small et al. 2007). Another member of the MPKs involved in tumour progression is DUSP6, the functions of DUSP6 will be discussed in detail in the next section.

1.2.1.5 DUSP6 functions

DUSP6 plays an important role in embryonic development according to knock down and overexpression studies in Drosophila, zebrafish and chick embryos. Fibroblast

growth factors (FGFs) are secreted molecules that activate the MAPK pathway and have crucial functions during embryonic development. DUSP6 is responsible for regulation of the MAPK pathway in response to FGF signaling in the early embryo of zebrafish (Tsang et al. 2004). Small interfering RNA (siRNA) studies showed that DUSP6 could protect cells from apoptosis though controlling the MAPK pathway in chicken limb (Kawakami et al. 2003). Overexpression of DUSP6 in Drosophila disturbs photoreceptor differentiation and wing vein formation (Kim et al. 2004).

Many studies show that DUSP6 is involved in cancer progression. The first evidence came from the studies of its role in pancreatic cancers associated with frequent loss of heterozygosity at 12q21 where the DUSP6 gene was located. The expression of DUSP6 is selectively abrogated in invasive carcinoma, especially in the poorly differentiated type. In contrast, most dysplastic carcinoma cells have high level of DUSP6. Moreover, the reintroduction of active DUSP6 into pancreatic cancer cell lines could lead to suppression of cell growth and induced apoptosis. Furthermore, some invasive carcinomas that had lost expression of DUSP6 also harboured a K-RAS mutation (Furukawa et al. 2003). This suggests that loss of DUSP6 is associated with progression of pancreatic cancer from dysplastic carcinoma to invasive carcinoma and absence of DUSP6 combined with K-RAS mutations contribute to hyperactivation of ERK. DUSP6 expression levels are also reported to be lower in lung cancer and ovarian cancer cells and DUSP6 restoration suppresses cell growth (Chan et al. 2008, Okudela et al. 2009). In contrast, DUSP6 and Sprouty 2, an inhibitor of the MAPK pathway at the level of RAF, are upregulated in melanoma cell lines with BRAF mutation (Bloethner et al. 2005). In addition, DUSP6 is overexpressed in human breast cancer cells and keratinocytes stably habouring an H-RAS mutation (Warmka et al. 2004). The activation of the MAPK pathway in these cell lines possibly induces DUSP6 expression at the transcriptional level. While this increase in turn increases the negative feedback control of the MAPK pathway to keep the pathway in balance.

1.2.2 Phosphatidylinositol 3′-kinase (P13K) pathway

The P13K pathway is also important in melanoma progression. Activation of RTKs by growth factors leads to activation of PI3K, which then converts membrane lipid PIP_2 into the second messenger, PIP_3. This activation step leads to activation of AKT kinase, in turn p-AKT phosphorylates several proteins affecting cell growth and survival (Fig. 1.3) (Cristina et al., 2007). Phosphatase with tensin homolog (PTEN) is a protein and lipid phosphatase that inhibits AKT activation by PI3K (Takata and Saida 2006).

Figure 1.3 The PI3K pathway

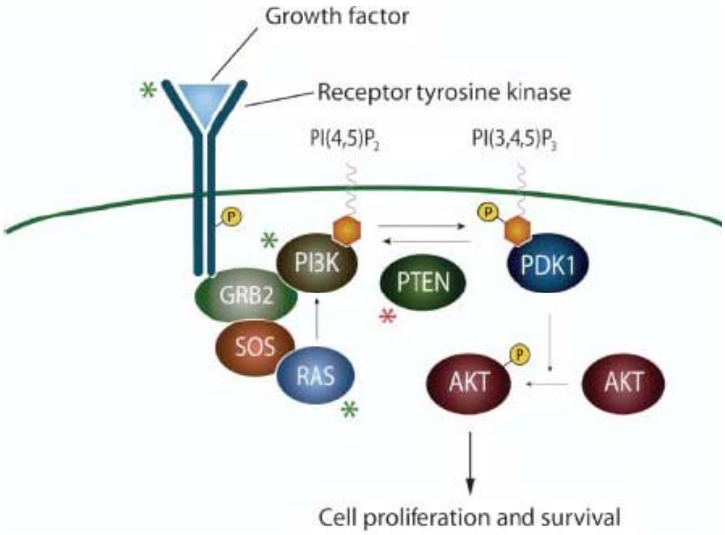

Activation of RTKs by growth factors leads to activation of PI3K, which then converts membrane lipid PIP2 into the second messenger, PIP3. This activation step leads to activation of AKT kinase and phosphorylation of AKT, which in turn phosphorylates several proteins affecting cell growth and survival. PTEN is an inhibitor of the PI3K pathway, which can dephosphorylate PIP3. Activation of RAS also increases signalling of the PI3K pathway. NRAS and PI3K are oncogenes (indicated by green asterisks) and PTEN is a tumour suppressor (indicated by red asterisks) in malignant melanoma. Taken from Dahl and Guldberg, 2007.

The expression of phosphorylated AKT protein increases dramatically with melanoma invasion and metastasis. Loss of heterozygosity in the region of chromosome 10q, which harbours the PTEN locus, was demonstrated in melanomas. It has been shown that 30-40% of melanoma cell lines and 5-15% of uncultured melanoma specimens carried homozygous deletion and inactivating PTEN mutations (Tsao et al. 1998). Interestingly, PTEN mutations are often found coincident with BRAF mutations, whereas they are not found together with RAS mutations (Fecher et al. 2007). It suggests that there may be cooperation between BRAF activation and PTEN loss in melanoma progression.

The MAPK pathway is intimately linked with the P13K pathway. RAS can not only regulate the MAPK pathway, but also control the PI3K pathway. Moreover, RAF activity is negatively regulated by AKT suggesting that cross-talk occurs between these two pathways. Interestingly, mutations of RAS and RAF can result in different outcomes. Mutations of RAS could lead to activation of both MAPK and PI3K pathways. Activation of the PI3K pathway could result in the inhibition of the MAPK pathway though cross-talk. Mutations of either BRAF or CRAF could result in only activation of the MAPK pathway (McCubrey et al. 2007).

1.2.3 $p16^{INK4A}$ and $p14^{ARF}$

CDKN2A mutations are identified in 25% of familial melanoma kindreds (Arlo et al. 2006). The $p14^{ARF}$ and $p16^{INK4A}$ proteins are both encoded by the CDKN2A gene. $p16^{INK4a}$ inhibits cyclin-dependent kinases 4 and 6, thereby causing pRB to accumulate in its hypo-phosphorylated form (Fig. 1.4). In this way, pRB acquires increased affinity for and inhibits E2F, the transcription factor which is involved in cell cycle progression, DNA replication and repair (Michaloglou et al. 2008). ARF, known as p19 in the mouse and p14 in the human, antagonizes the function of

MDM2 to induce a protective response that depends on the p53 transcription factor and its many target genes (Fig. 1.5) (Sviderskaya et al. 2002). Recent studies have shown that mutations of the INK4A-ARF locus may favour tumourigenesis from melanocytes by impairing senescence and cell death (Sviderskaya et al. 2002). Cellular senescence, the acquired inability of normal somatic cells to divide after a finite number of divisions, is controlled by key tumour suppressors including p53 and $p16^{INK4a}$. The best known form of senescence is affected by the p53 pathway. However, expression patterns of senescence mediators and markers in melanocytic lesions provide strong evidence that cell senescence in benign naevi does not involve p53 upregulation, while $p16^{INK4a}$ is widely expressed. It suggests that $p16^{INK4a}$ rather than p53 plays a key role in cellular senescence of benign naevi (Gray-Schopfer et al. 2006) The inactivation of $p16^{INK4a}$ expression in early melanomas may make it possible to bypass cellular senescence and subsequently to acquire epigenetic and genetic changes, which may be associated with tumour progression.

Figure 1.4 The p16-CDK4/6-RB pathway

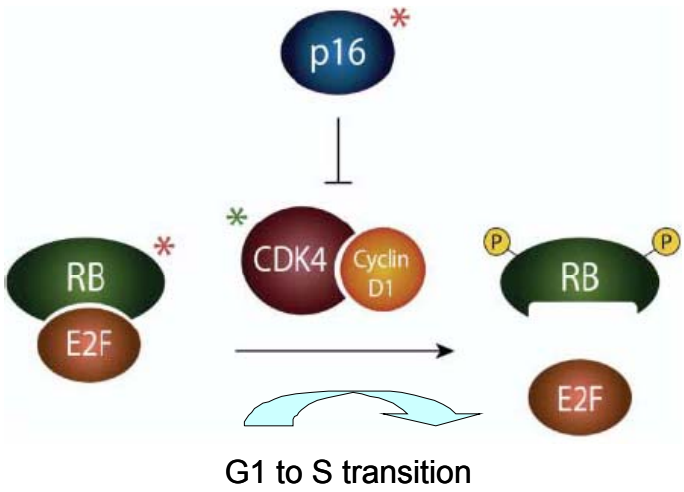

p16 inhibits the G1 cyclin-dependent kinases CDK4 and CDK6 to keep RB in an activated state. Inhibition of p16 increases CDK4/6 activity leading to hyperphosphorylation of RB and release of E2F transcriptional factors needed to activate genes essential for S phase. In this way, cells can pass G1 phase to S phase. CDK4 is an oncogene (indicated by green asterisks) and p16 and RB

are tumour suppressors (indicated by red asterisks) in malignant melanoma. Adapted from Dahl and Guldberg, 2007.

Figure 1.5 ARF and p53

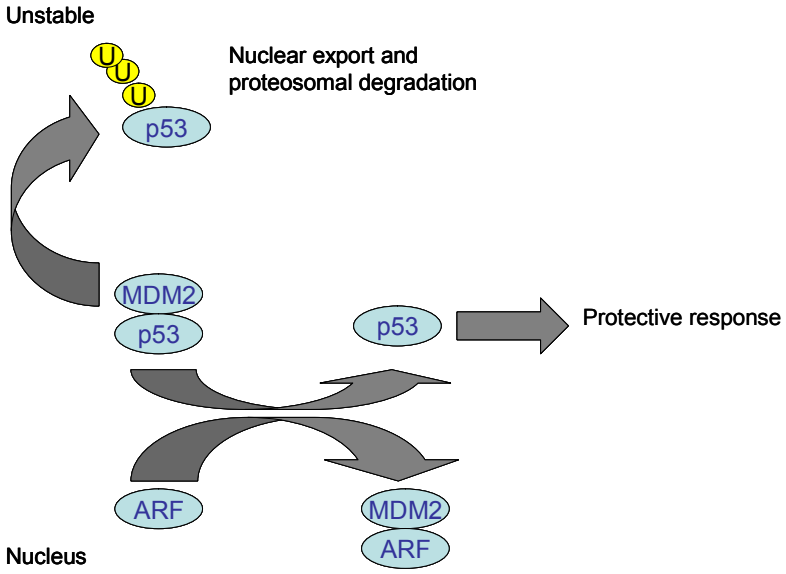

ARF can release p53 from MDM2-p53 complex and induce protective reponse. For explanation, see text. Adapted from Miller and Mihm, 2006.

1.2.4 Other genes and pathways involved in melanoma progression

It is generally believed that MITF plays an important role in regulation of melanocyte specific transcription. Several pathways could affect MITF expression by binding to the MITF promoter. MSH binds to the G protein-coupled MC1R, which acts through adenylate cyclase to stimulate binding of CREB1 to the MITF promoter. WNT and Endothelin signaling could also regulate MITF expression. Several growth factors such as C-KIT and hepatocyte growth factor (HGF) are involved in regulation of phosphorylation of MITF through the MAPK pathway. Both increased expression of MITF and phosphorylation of MITF stimulate its target genes including numerous

markers important in melanoma (MLANA, TRPM1, and SILV), genes important for survival (BCL2) and genes involved in melanin production (TYR, TRP1 and DCT) (Fig 1.6) (Sekulic et al. 2008). MITF plays an important role in pigment cell behaviour.

Figure 1.6 MITF and β-catenin signalling

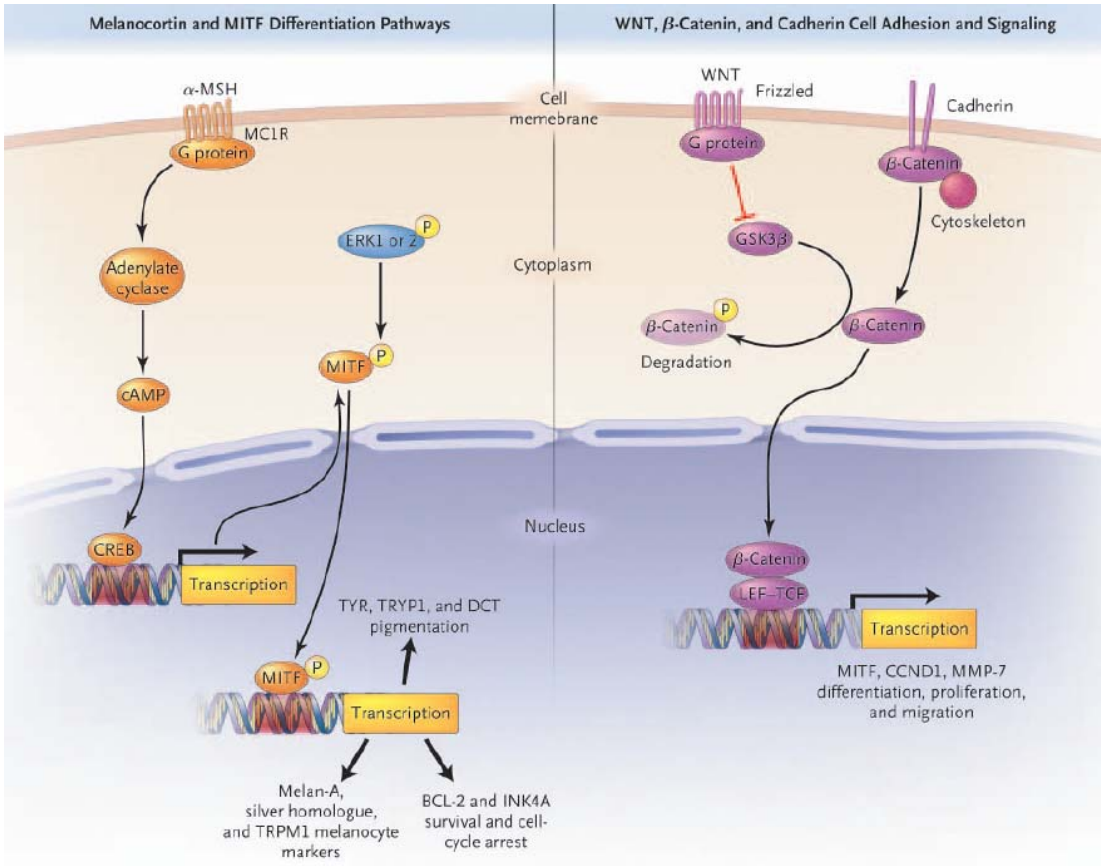

MITF and β-catenin signalling are also involved in progression of melanoma. For explanation, see text. Taken from Miller and Mihm, 2006.

High levels of MITF activity result in cell cycle arrest and differentiation, whereas low levels of MITF activity lead to cell cycle arrest and death. Therefore, MITF can contribute to melanoma development or suppress melanoma progression and its ability to control cell fate decisions depends on its expression levels or activity levels.

MITF expression or activity may be carefully regulated in melanoma cells to ensure that the levels are not so low or so high as to prevent cell growth (Wellbrock et al. 2008).

Beta-catenin is a key component of the canonical WNT transduction pathway. Signalling through this pathway controls a wide range of cellular functions, and aberrant WNT signalling can induce progression of cancer (Giles et al. 2003). When WNT proteins bind their receptors, they inactivate the kinase GSK3β, an enzyme which phosphorylates β-catenin and targets it for destruction in the proteosome. As a result, β-catenin accumulates in the cytoplasm and goes to the nucleus where it binds to lymphoid enhancer factor-T-cell factor (Fig. 1.6) (Dahl and Guldberg 2007). High levels of nuclear β-catenin can increase the expression of MITF (Widlund et al. 2002) and cyclin D1 (Patil et al. 2009) and MMP-7 (Miller and Mihm 2006), and these in turn increase the survival, proliferation and migration of melanoma cells. Nuclear or cytoplasmic localization of β-catenin is a potential indicator of WNT pathway activation and has been found in one third of melanoma specimens (Omholt et al. 2001).

1.3 Cisplatin resistance and the NER pathway in melanoma

1.3.1 Cisplatin induced DNA damage and repair

Cisplatin, cis-diamminedichloroplatinum (II), or CDDP, was synthesized first in 1845 but its anticancer activity was not discovered until 1965 (Lippard 1982). Cisplatin is most effective in the treatment of testicular tumours (Bosl and Motzer 1997). The cure rate for testicular cancer is greater than 90% (Bosl and Motzer 1997). Cisplatin is also used to treat other kinds of malignancies, including ovarian, lung, cervical, head and neck, and bladder cancer (Keys et al. 1999, Loehrer and Einhorn 1984, Morris et al. 1999, Rose et al. 1999).

Although the mechanism is not yet fully understood, cisplatin is generally believed to kill cancer cells by activating apoptosis leading to cell death (Rosenberg 1985). Both prokaryotic and eukaryotic cells deficient in DNA repair are particularly sensitive to cisplatin (Beck and Brubaker 1973). Cisplatin and its analogues are heavy metal complexes which contain a central atom of platinum, two chloride atoms and two ammonia molecules in the cis position. In the cells, one of the cisplatin chloride ligands is displaced by water to form a highly reactive charged platinum complex $[Pt(NH_3)_2ClH_2O]^+$. This complex binds to the N7 atom of either guanine or adenine bases. The remaining choloride ligand is then displaced to allow platinum to bind to a second nucleotide base (Jamieson and Lippard 1999). Cisplatin forms various DNA adducts, the most notable one is the 1,2-intrastrand crosslink with purine bases. The inactive isomer of cisplatin, trans-DDP, can not form this crosslink. It suggests that this kind of lesion is involved in the biological activities of cisplatin. In the 1,2-intrastrand crosslink, the DNA is unwound and bent towards the major grove. Interstrand crosslinks caused by cisplatin induce even more steric changes in DNA which prevent chromosome segregation and block DNA and RNA polymerases and are therefore a particularly toxic class of DNA damage. Other DNA adducts include the monofunctional and the 1,3- and longer range intrastrand, and protein-DNA crosslinks. Each of these adducts forms a distinct structural element and interacts with DNA differently.

As mentioned before, cells deficient in DNA repair are more sensitive to cisplatin. It suggests that the DNA repair system plays an important role in cisplatin activities. Repair of cisplatin induced DNA damage is mainly performed through the nucleotide excision repair (NER) pathway (Chu 1994). The inherited disease xeroderma pigmentosum (XP) is characterized by hypersensitivity to UV radiation and a predisposition toward skin cancer because of deficiency in the NER pathway (Sancar 1995, Wood 1997). Cell lines cultured from XP patients are hypersensitive to

cisplatin (Fraval et al. 1978). It provides the evidence that the NER pathway is important in the cellular processing of cisplatin. In addition, the repair of cisplatin adducts has been investigated directly in reconstituted repair systems. The activity of nucleotide excision repair in E.coli results from the ABC excinuclease which includes three subunits, UvrA, UvrB, and UvrC (Sancar 1996). The UvrB gene is reported to be important for repair of ciplatin induced DNA damage, indicating NER to be the primary pathway to repair these adducts (Popoff et al. 1987). Increased expression of several NER genes has been correlated with cisplatin resistance. In ovarian cancer, higher levels of expression of *XPA, ERCC1, XPF and ERCC3* (*XPB*) have been observed in tumours of patients resistant to cisplatin treatment (Rabik and Dolan 2007). In addition, gastric cancers display a correlation between *ERCC1* and *XPF* mRNA levels and cisplatin resistance (Matsubara et al. 2008). In contrast, testicular cancers with low levels of XPA and ERCC1-XPF are highly responsive to cisplatin (Welsh et al. 2004). Furthermore, among these proteins in the NER pathway, ERCC1-XPF has been shown to have an important role in determining the overall NER capacity of ovarian cell lines resistant to cisplatin (Ferry et al. 2000).

The NER endonuclease-complex ERCC1-XPF is also reported to be crucial for the repair of cisplatin induced interstand crosslinks (ICL) by making the incision at the DNA lesions (Chipchase and Melton 2002, Niedernhofer et al. 2006). The mechanism of ICL repair in mammalian cells is still poorly understood. It is reported that the ICL repair is initiated by the formation of a Y structure near the DNA damage due to replication folk stalling or with the help of DNA helicase. ERCC1-XPF complex then cleaves at the 3′ side of one arm of the crosslink and then makes an additional cleavage at the 5′ side. The fork collapses and recombination and NER events take place to complete the repair (Fisher et al. 2008, Kuraoka et al. 2000). Thus, the ERCC1-XPF complex seems to play an important role in initiating the ICL repair process for this most toxic lesion in mammals.

ERCC1-XPF complex is also thought to be involved in homologous recombination (HR) which has been proposed to repair double strand break (DSB) caused by cisplatin (Frankenberg-Schwager et al. 2005). The HR mechanism consists of two categories: gene conversion and single-strand annealing (SSA). The ERCC1-XPF complex is reported to be involved in both SSA and gene conversion to repair DSB in mammalian cells (Al-Minawi et al. 2008). However it seems not to be an essential factor in the recombination repair pathway. When murine cells deficient in ERCC1 were examined for induction of interstrand crosslinks by mitomycin, only a moderate sensitivity was observed (Melton et al. 1998). It suggests that ERCC1 is not essential for homologous recombination and there are other DNA repair pathways to deal with this DNA damage. However, impairment of the HR pathway in ICL repair is observed in *ERCC1* deficient cells, suggesting that the ERCC1-XPF complex plays a role in completion of HR in ICL repair (Al-Minawi et al. 2009).

Taken together, the ERCC1-XPF complex is involved in multiple DNA repair pathways to deal with cisplatin-induced DNA damage. High *ERCC1/XPF* mRNA and protein levels in cancer patients cause enhanced DNA repair and lead to chemotherapy resistance. Cancer patients who have lower expression of *ERCC1/XPF* are hypersensitive to cisplatin treatment. This makes the *ERCC1/XPF* heterodimer a potentially interesting drug target.

1.3.2 Cisplatin resistance

Resistance of tumours to cisplatin is one of the main reasons for failure of cisplatin treatment. There are two kinds of resistance to cisplatin: acquired resistance and intrinsic resistance. Acquired resistance develops in patients undergoing the cisplatin treatment and in cell lines exposed to cisplatin. Some type of malignancies, such as ovarian cancer, may be sensitive to cisplatin initially but can acquire resistance to the

drug during treatment. Intrinsic resistance occurs when the patient tumours are inherently resistant to cisplatin and naturally unaffected by the treatment. Some cell lines isolated from these patients are more proficient at removing cisplatin induced DNA adducts compared with cell lines with normal cisplatin sensitivity (Zamble and Lippard 1995).

Because of its clinical importance, the mechanisms of cisplatin resistance have been studied over time. Resistance of tumours to cisplatin seems to be a multifactor cellular response, rendering it more difficult to understand the process fully. Generally, three main activities have been identified as potential mechanisms involved in cisplatin resistance (Kartalou and Essigmann 2001):

1) Inhibition of drug uptake and increase in the production of cellular thione. Reduced intracellular accumulation of cisplatin because of decreased uptake or increased efflux plays an important role in cisplatin resistance. Another cellular response that can modulate cisplatin resistance is to increase the level of intracellular thiol (such as metabolic synthesis of glutathione and metallothionein) that can react with and inactivate cisplatin.

2) Changes in the concentrations of regulatory proteins. Alteration in the expression of oncogenes (such as c-fos, c-myc, H-ras, c-jun, and c-abl) and tumour suppressor genes (such as p53) have been implicated in the cellular resistance to cisplatin.

3) Increase in the repair of cisplatin DNA adducts. Based on current literature review, an increase in DNA repair is the key to determine clinical outcome and clinical resistance to cisplatin based chemotherapy in human cancer. The increase in DNA repair with cisplatin resistance could be due to enhanced expression of

proteins involved in repair. High levels of ERCC1 and PCNA were observed in cisplatin resistant tumour cells.

Many mechanisms involved in cisplatin resistance are still not fully understood. An improved understanding of cisplatin resistance may lead to improved chemotherapy for cancer.

1.3.3 Nucleotide excision repair

1.3.3.1 Overview of NER

Nucleotide excision repair (NER) is a DNA repair pathway that is involved in dealing with a wide range of DNA lesions. It is highly conserved, versatile and robust in eukaryotes and present in most organisms. The most common lesions processed by NER are those formed by UV radiation (such as cycolobutane-pyrimidine dimers and 6-4 photoproducts) and DNA adducts induced by compounds such as arylamine carcinogens and cisplatin (Gossage and Madhusudan 2007).

Although NER is not essential for viability, defects in NER may result in at least three diseases in human, xeroderma pigmentosum (XP), Cockayne syndrome (CS), and trichothiodystrophy (TTD) (Lehmann 1995, Lindahl and Wood 1999, Thoma 1999). Patients with XP were hypersensitive to UV radiation and had a higher risk of skin carcinomas (Friedberg 2003). Sun exposure of XP patients could cause progressive degeneration of the skin and eyes (Kraemer et al. 2007). Alteration of the NER pathway was also associated with neurological abnormalities and led to premature ageing phenotypes.

1.3.3.2 Molecular mechanism of NER

The molecular mechanism of NER is complex and involves about 30 distinct proteins which are encoded by seven XP complementation groups, XPA to XPG, *ERCC1* (excision repair cross-complementing group 1), hHR23B (human homolog of yeast RAD23), RPA (replication protein A), additional subunits of TFIIH (transcription factor with helicase activity), Cockayne syndrome proteins CSA and CSB and several other genes (de Boer and Hoeijmakers 1999).

NER is divided into two subpathways in mammals known as transcription-coupled repair (TCR-NER) pathway and global genome repair (GGR-NER) pathway. The TCR-NER pathway targets lesions specifically in the transcribed strand of expressed genes; while the GGR-NER pathway deals with lesions in non-transcribed parts of the genome, including the non-transcribed strand of transcribed genes (Friedberg 2001).

The NER pathway involves the following 4 steps (Fig. 1.7):

1) Recognition of DNA damage. In the GGR pathway, the DNA damage lesions are firstly recognized by the XPC-HR23B complex. XPC-HR23B binds to DNA distortion caused by the lesion and induces some conformational changes of the DNA helix, including local opening of DNA, which allow entry of subsequent NER factors, such as TFIIH, XPA, and RPA (Sugasawa et al. 2002, Wakasugi and Sancar 1999). XPC-HR23B was not only required for recognition of the DNA lesion but also for the recruitment of all the other NER factors in a reconstituted system, including transcription factor TFIIH (Volker et al. 2001).

The binding properties of XPC-HR23B have been the subject of extensive studies: the complex binds efficiently to ssDNA and helix distorting lesions. XPC-HR23B recognized 6-4 photoproducts but not cyclobutane pyrimidine dimers (CPDs) (Gillet and Scharer 2006). However, the CPDs were still repaired by NER. This suggests the existence of an other recognition factor responsible for recognition of these lesions. Recently, studies showed that damage-specific DNA binding protein (DDB) is involved in the recognition process of CPDs in NER (Nichols et al. 2000). The DDB complex is a heterodimer of two polypeptides, p127 and p48 (Wakasugi et al. 2001). p48, also known as DDB2, is the XPE gene product and was reported to cause conformational change to allow DNA lesion binding by the NER machinery (Kulaksiz et al. 2005).

In the TCR pathway, repair of transcription blocking lesions was thought to be initiated by an RNA polymerase, which was unable to pass the lesions (Gillet and Scharer 2006, Reardon and Sancar 2005). Cockayne syndrome proteins CSA and CSB were also involved in recognizing and binding to DNA lesions in TCR (de Waard et al. 2004). The CSA protein containing a WD-40 repair motif contributes to protein-protein interactions (Henning et al. 1995). CSA was known to regulate the ubiquitin ligase activity of the complex containing DDB1, cullin 4A, Roc1, and COP9 and this complex could be involved in the ubiquitination of RNA polymerase II. Ubiquitination of RNA polymerase II would allow access of the repair machinery to the lesion and subsequent recovery of RNA synthesis (Groisman et al. 2003). The CSB protein was able to remodel chromatin structure and directly interact with core histones. CSB is also involved in recruiting other repair proteins to the site of DNA lesions (Bradsher et al. 2002).

2) DNA helix unwinding. Once the DNA lesions are identified, the following steps in GGR and TCR are similar. XPC-HR23B or CSB and CSA recruit TFIIH to the

damage sites (Schaeffer et al. 1994). TFIIH is a ten-subunit complex, including a core complex and a CDK activating kinase subunit (Schultz et al. 2000). TFIIH was involved in initiation of RNA polymerase II transcription but could, upon DNA damage, also be recruited to perform NER functions (Hoogstraten et al. 2002). ATP-dependent helicases XPB and XPD, two subunits of TFIIH, were responsible for 3′ to 5′ direction and 5′ to 3′ direction opening of DNA around the lesion (Sancar 1996). After DNA opening by TFIIH, RPA, XPA, and XPG are recruited to the site of damage lesions to join the complex (Wakasugi and Sancar 1998). This complex was thought to be a stable state for the NER reactions where all NER factors, except ERCC1-XPF, stably bound to an open DNA bubble structure (Mu et al. 1996). RPA and XPA were considered to verify the specific NER lesions and promote the accurate assembly of the NER complex (Li et al. 1995). XPG is believed to be recruited to the complex though interaction with TFIIH (Araujo et al. 2001). The functions of XPG will be discussed later.

3) DNA dual incision. In this step, ERCC1-XPF is directly recruited to the NER complex by XPA (Li et al. 1995). Two structure-specific endonucleases XPG and ERCC1-XPF make the dual incision. XPG belongs to the FEN-1 (flap endonuclease) family of structure-specific endonucleases (Lieber 1997). It has a defined polarity that cleaves specifically at junctions between the 3′ end of ssDNA and the 5′ end of dsDNA. During the NER reaction, XPG makes the 3′ incision due to its cleavage polarity (O'Donovan et al. 1994). XPG not only performs 3′ incision in NER but is also involved in stabilizing the complex (Wakasugi et al. 1997). ERCC1-XPF is an obligate heterodimer and incises DNA with specific polarity at the 5′ side of double-strand/single-strand DNA junctions, consistent with its 5′ incision during NER (Biggerstaff et al. 1993, Sijbers et al. 1996). Unlike XPG, addition of ERCC1-XPF to the complex did not change the opened DNA structure. It has been reported that XPG could make the 3′ incision without ERCC1-XPF, while ERCC1-XPF could not make the 5′ incision in the absence of XPG (Tapias et al. 2004).

4) Repair synthesis. The excised fragment was removed and the gap was filled by two DNA polymerases δ and ε (Thoma 1999). It was observed that replication factor-C (RFC) catalyzed the ATP-dependent loading of proliferation cell nuclear antigen (PCNA) to DNA near the 3′ terminus of the primer. PCNA then facilitates DNA polymerase to add nucleotides in a 5′ to 3′ direction (Gulbis et al. 1996, Podust et al. 1992). RPA remains bound to the ssDNA following dual incision and is involved in PCNA and RFC recruitment (He et al. 1995). Finally, the gap is closed by DNA ligase I or DNA ligase III (Nocentini 1999).

Figure 1.7 Mechanism of the NER pathway

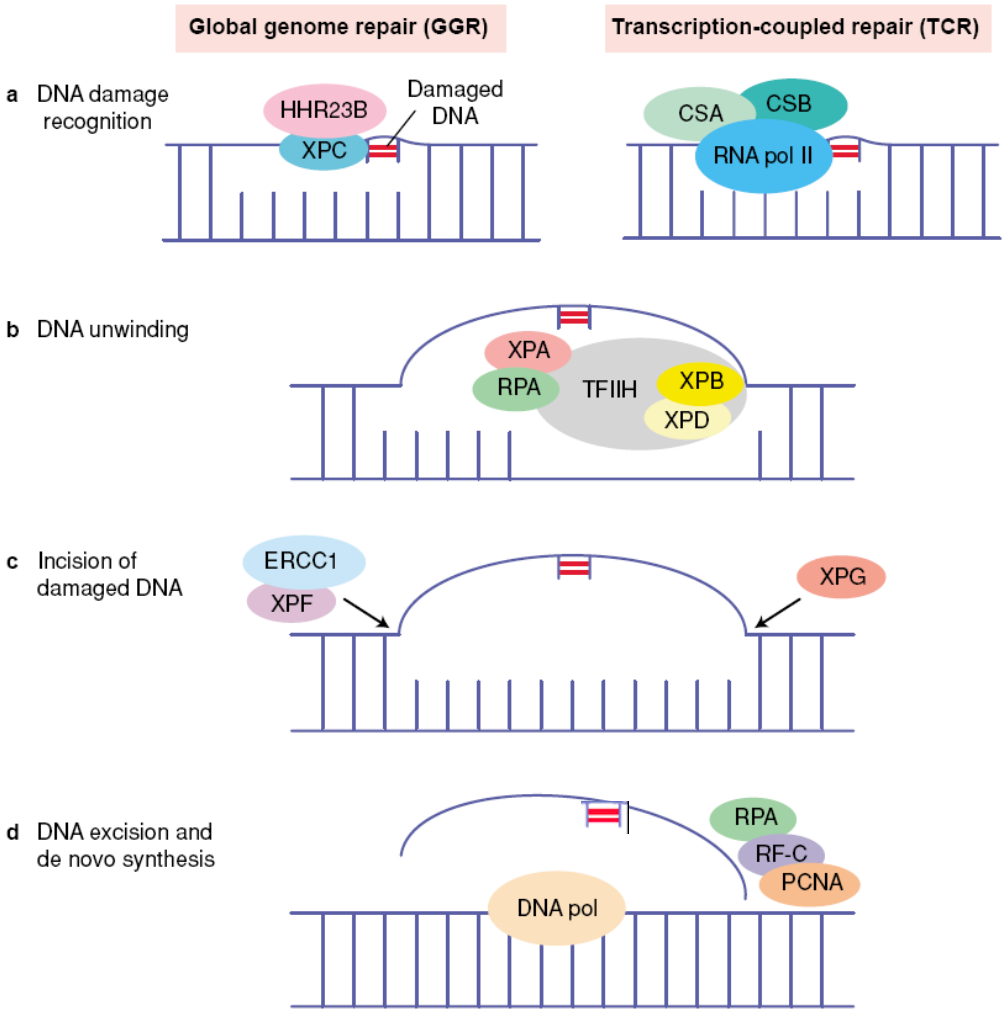

Model for mammalian nucleotide excision repair. Adapted from Matsumura and Ananthaswamy 2002. For explanation, see text.

1.3.3.3 *ERCC1* and ERCC1-XPF complex

The gene for *ERCC1* is located on chromosome 19q13.2-q13.3 and has 10 exons spread over 15kb of the genome. The molecular weight of ERCC1 is about 32.5 KD (Park et al. 1995). ERCC1 protein contains 297 amino acids and has two domains. The central domain of ERCC1 (residues 96-214) is structurally similar to the XPF nuclease domain, but is devoid of nuclease activity (Gaillard and Wood 2001). Studies showed that the ERCC1 central domain not only binds to ssDNA/dsDNA junctions with a defined cleavage polarity but also interacted with XPA (de Laat et al. 1999). The C-terminal tandem helix-hairpin-helix (HhH_2) domain of ERCC1 (residues 220-297) dimerizes with the C-terminal domain of XPF to form the functional nuclease and it also binds to DNA (de Laat et al. 1998). As the partner of *ERCC1*, *XPF* is located on chromosome 16p13.3 and has 11 exons spread over 32kb of the genome. The molecular weight of XPF is about 104.5KD. XPF protein contains 916 amino acids and has three domains (Aravind et al. 1999). An N-terminal helicase-like domain (residues 4-457) might contribute to DNA binding activities. The central nuclease domain of XPF (residues 656-813) has conserved metal-binding residues with a [V/I]ERKX_3D motif and functionally important basic residues that interact with DNA substrates (Enzlin and Scharer 2002). The C-terminal domain of XPF (residues 837-905) with HhH_2 motif dimerizes with the equivalent domain in ERCC1 and may be involved in DNA binding as well (de Laat et al. 1999).

The ERCC1-XPF complex is the last factor to join in the NER incision complex. Formation of ERCC1-XPF complex is critical for stability of both components and is required for catalytic activity of XPF (Gillet and Scharer 2006). As the previous section mentioned, the main function of ERCC1-XPF complex is to make an incision to the 5′ side of the lesion (Sijbers et al. 1996). It also has additional NER-independent functions in the repair of interstrand DNA crosslink (ICLs) and in

homologous recombination (HR) (Busch et al. 1997, Kuraoka et al. 2000, Niedernhofer et al. 2004). ICLs are an extremely toxic class of DNA damage that can be generated during normal metabolism or cancer chemotherapy. Although the mechanisms of ICL repair are still not clear, genetic data implicated the ERCC1-XPF complex as required for ICL repair (Niedernhofer et al. 2004). In the HR pathway, the ERCC1-XPF complex was involved in gene conversion and single-strand annealing (SSA) in mammalian cells (Al-Minawi et al. 2008).

1.3.3.4 *ERCC1* expression

The *ERCC1* promoter was located in a region within 170 bp upstream of the normal transcriptional start site. However this region lacked the classic promoter regulatory elements like CAAT, TATA and GC-boxes (van Duin et al. 1986). On the other hand, Wilson observed that a highly conserved region containing a CpG island and TATA box was located 5kb upstream of *ERCC1* exon1 by comparisons of the entire gene from mammalian species (Wilson et al. 2001). Hypermethylation was observed in the upstream 5kb region of the *ERCC1* promoter of cisplatin sensitive glioma cell lines (Chen et al. 2010) and it was suggested that the upstream 5kb region of *ERCC1* may be involved in regulation of *ERCC1* expression and associated with cisplatin chemosensitivity.

Expressed sequence tag (EST) assemblies for human *ERCC1* identified numerous splice variants involving exon 1, 2, 3, 7, 8, and 9 that could affect expression of *ERCC1* (Wilson et al. 2001). A 5′ variant containing a differentially spliced exon1 which spans the entire promoter region in human had been reported (van Duin et al. 1986). It suggested at least some *ERCC1* transcripts may originate from further upstream of *ERCC1*. In addition, a 42bp deletion, thought to contain the binding site for a transcriptional repressor, has been reported in exon1 of the human *ERCC1*

gene. Loss of this sequence was related to higher level of *ERCC1* mRNA in ovarian cancer specimens (Yu et al. 2001). However, previous group work indicated that alternate splicing of this 42bp sequence was not correlated with high levels of *ERCC1* expression, as suggested by Yu, and therefore its significance remains unclear (Winter et al. 2005).

A novel 1.5kb mouse skin-specific *Ercc1* transcript was identified by previous group work. According to northern blotting and RT-PCR results, the 1.5kb *Ercc1* transcript was the major transcript in mouse skin compared with the normal 1.1kb *Ercc1* transcript. This novel transcript originated from a promoter about 400bp upstream of the normal *Ercc1* promoter, not from a promoter further upstream (Song et al. 2011). However, whether similar novel transcripts exist in human skin and the functions of the novel transcript need further investigation.

1.3.3.5 Regulation of *ERCC1* expression

DNA damage induced by cisplatin, alkylating agents, and ionizing radiation resulted in the activation of c-Jun-NH2-kinase (JNK)/stress-activated protein kinase (SAPK) (Liu et al. 1996). JNK/SAPK is a subfamily of MAP kinase in the RAS pathway which enhances the phosphorylation of Jun protein. Phosphorylation of c-jun dramatically enhanced the transcriptional activity of the activated protein 1 (AP-1)-binding sites and AP-1 regulated genes (Binetruy et al. 1991, Pulverer et al. 1991, Smeal et al. 1991). The nuclear transcriptional factor AP-1 consisted of either homodimers formed between Jun and Fos or homodimers of Jun protein. AP-1 was responsible for the activation of a wide variety of genes in different cell types and tissues (Adler et al. 1992, Derijard et al. 1994, van Dam et al. 1993). The promoter of *ERCC1* was located in a region of 170 basepairs upstream of the transcriptional start site of the *ERCC1* gene (van Duin et al. 1986). The promoter region contained an

AP-1 like binding site. Cisplatin exposure had been reported to induce *ERCC1* mRNA in ovarian cancer cells. This *ERCC1* mRNA upregulation was preceded by an increase in mRNA expression of c-fos and c-jun, an increase in c-jun protein phosphorylation and an increase in nuclear extract binding activity to the AP-1 like site of *ERCC1*. It suggested that induction of *ERCC1* expression exposed to cisplatin resulted from two major factors: an increase in the expression of transactivating factors that bind the AP-1 like binding site in the promoter region of *ERCC1* and an increase in the level of c-jun phosphorylation that enhances its transactivation property. These two factors contributed to increase the activity of AP-1 binding to the *ERCC1* promoter and directly modulate *ERCC1* gene expression. (Altaha et al. 2004, Li et al. 1998a).

In addition to JNK, another MAPK, the extracellular signal regulated kinase (ERK), also responds to cisplatin treatment (Mirmohammadsadegh et al. 2007, Wang et al. 2000, Wang et al. 1998). ERK1/2 is essential in cell proliferation, survival, division, and its activity is greatly increased by exposure to cisplatin. ERCC1 induction by epidermal growth factor (EGF) depended on the MEK-ERK pathway through activation of transcriptional factor GATA-1 (Andrieux et al. 2007). Moreover, addition of MEK specific inhibitors, U0126 and PD98959, effectively inhibited ERCC1 induction by EGF in prostate carcinoma cells (Yacoub et al. 2003). Furthermore, a recent study showed that emodin induced cytotoxicity via ERCC1 downregulation through ERK1/2 inactivation in human lung cancer cells (Ko et al. 2010). Taken together, the MEK-ERK pathway may be involved in regulation of ERCC1 expression following cisplatin. Analysis of the human *ERCC1* promoter sequence with TFSEARCH identified several transcription factor motifs that could be activated by the MAPK pathway (Andrieux et al., 2007). In particular, that region contains two ETS-1 motifs, one GATA motif and two AP-1 motifs, suggesting at least one of these may be involved in the *ERCC1* increase by cisplatin through the MAPK pathway. An investigation of regulation of *ERCC1* expression by the MEK-ERK pathway following cisplatin was one of the aims of this thesis.

1.3.3.6 ERCC1 and platinum resistance

A large number of studies show that *ERCC1* mRNA and protein levels may be associated with cisplatin resistance in human cancer cells and therefore are considered as a predictive maker for chemotherapeutic outcome (Kirschner and Melton 2010). A positive association has been demonstrated between the level of *ERCC1* mRNA expression and cisplatin resistance in lung cancer. High expression of *ERCC1* mRNA has been related to poor response and survival in cisplatin-treated non-small-cell lung cancer patients (Rosell et al. 2003). Non-small-cell lung tumour patients with lower expression of *ERCC1* appear to benefit from adjuvant chemotherapy and survive longer than the control group (Olaussen et al. 2006). A 3-fold *ERCC1* mRNA increase has been reported in ovarian cancer cisplatin resistant derivatives compared with their parent cell lines (Ferry et al. 2000). In another study, cisplatin caused a time and dose dependent increase in *ERCC1* mRNA levels in A2780/CP70 human ovarian cancer cells (Li et al. 1998a). Ovarian cancer patients who were resistant to cisplatin therapy had a higher ERCC1 expression level in their tumour tissues than the patients who responded to cisplatin, suggesting that ERCC1 expression levels have a role in clinical resistance to cisplatin (Dabholkar et al. 1992). A study of a panel of 15 early-passage cervical tumour cell lines has demonstrated that *ERCC1* mRNA expression is a molecular marker for the clinically relevant cisplatin sensitivity of human cervical carcinoma cells (Britten et al. 2000). Cisplatin based chemotherapy cures over 80% of metastatic testicular germ cell tumours (TGCT). Cell lines derived from TGCT are hypersensitive to cisplatin therapy. This exceptional sensitivity is due to deficiency in interstrand-crosslink repair and low level of expression of ERCC1-XPF (Usanova et al. 2010). In another study, investigation of 35 human cell lines derived from cancers indicated that only the 6 testis tumour cell lines showed significantly lower levels of XPA, XPF and ERCC1 proteins than the other groups (Welsh et al. 2004). It suggests that lower levels of these nucleotide excision repair proteins are related to extreme chemosensitivity of testis tumours to cisplatin based chemotherapy. In patients with advanced squamous

cell carcinoma of the head and neck (SCCHN), low expression of ERCC1 was an independent predictor for prolonged survival (Jun et al. 2008). Similarly, samples from patients with gastric cancer showed that low ERCC1 correlated with a higher response to cisplatin-based chemotherapy, while high ERCC1 was a significant predictor of poor survival (Matsubara et al. 2008). ERCC1 also predicted survival in bladder cancer treated by platinum-based therapy and median survival was significantly higher in patients with low ERCC1 levels (Bellmunt et al. 2007). Taken together, the positive correlation between high expression of ERCC1 and cisplatin resistance was found in a large variety of cancer types, not just specific to one or two, and ERCC1 could be used to predict chemotherapy outcome.

Dowregulation of *ERCC1* by antisense RNA could sensitize the highly resistant OVCAR10 ovarian cancer cell line to cisplatin. In addition, immunocompromised mice transplanted with these antisense cell lines survived longer than the mice bearing control cells after cisplatin treatment (Selvakumaran et al. 2003). Knockdown of *ERCC1* expression by specific siRNA transfection also decreased DNA repair abilities in lung cancer and enhanced the cytotoxic effect induced by emodin (Ko et al. 2010). On the contrary, introduction of *ERCC1* into an *ERCC1* deficient Chinese hamster ovary cell line could restore the ability of DNA repair and make cells more resistant to cisplatin treatment (Lee et al. 1993). These data indicated that alterating expression levels of ERCC1 can affect the sensitivity of cells to cisplatin and further confirmed that ERCC1 played an important role in cisplatin resistance.

Studies showed that both Breast Cancer 1 (*BRCA1*) and *ERCC1* expression are correlated with resistance to platinum-based chemotherapy in sporadic ovarian cancer and low *BRCA1* and *ERCC1* expression predicted longer survival. Furthermore, high levels of both *BRCA1* and *ERCC1* were related to each other in patients with advanced stages of tumour and correlated with shorter survival

(Weberpals et al. 2009). It was possible that both of these two proteins take part in DSB repair pathways that complement each other. Concomitant low expression levels of ERCC1 and ribonucleotide reductase (RRM1) were reported to predict a better outcome of NSCLC patients after chemotherapy (Ceppi et al. 2006). In contrast, the best prognosis for both disease-free survival and overall survival in patients with pancreatic cancer was achieved when both these two proteins were high in the primary tumour. However, RRM1 expression seems to be involved in gemcitabine (the first line cytotoxic agent treatment of advanced pancreatic cancer) resistance. Pancreatic cancer patients with low levels of RRM1 had improved survival after gemcitabin treatment (Akita et al. 2009). This demonstrates that it is more reliable to use several protein markers to predict disease outcomes before and after chemotherapy.

A single nucleotide polymorphism (SNP) in *ERCC1* codon 118 in exon 4 leads to a C to T transition without change in the polypeptide sequence (N118N). This *ERCC1* polymorphism had been linked to decreased levels of *ERCC1* mRNA in ovarian cancer cell lines. That may explain why patients with C/C genotypes displayed reistance to chemotherapy and had a high risk for disease progression and death compared to those with C/T or T/T genotypes (Smith et al. 2007). However, the association between codon N118N transition and survival after platinum-based therapy has been corroborated in some, but not all cancers. In colorectal cancer, the T allele was linked to better response to cisplatin in some patients, but associated with cisplatin resistance and poor survival in other patients (Stoehlmacher et al. 2004, Viguier et al. 2005). For NSCLC patients, the C allele has been related to better treatment response and longer survival (Isla et al. 2004, Ryu et al. 2004, Zhou et al. 2004). However, there is no relationship between *ERCC1* genotype and treatment response in gastric cancer (Ruzzo et al. 2006). Therefore, the clinical significance of this *ERCC1* polymorphism in different cancer types needs further investigation.

The clinical observations indicated that melanoma was relatively resistant to cisplatin; however whether ERCC1 was involved in resistance to cisplatin in melanoma cells was still unclear. Our lab generated mouse *Ercc1*-deficient melanocytes using the Cre-lox system. The *Ercc1* proficient and deficient melanocytes were transplanted into nude mice where they grew as malignant melanoma. The *Ercc1* proficient xenografts grew very rapidly compared with *Ercc1* deficient xenografts. Moreover, *Ercc1* proficient melanoma xenografts developed chemotherapy resistance quickly following cisplatin treatment. ERCC1 levels were 2-fold increased in the cells re-isolated from cisplatin-resistant tumours compared with cells from untreated xenografts, while *Ercc1* deficient melanoma xenografts were cured by cisplatin. This suggested that *Ercc1* expression was related to cisplatin resistance in melanoma cells and inhibition of ERCC1 enhanced cisplatin toxicity in melanoma.

1.4 Aims

The work presented in this thesis aims to investigate several pathways related to melanoma progression and chemotherapy resistance. Chapter 3 examines the status of BRAF, ERK, MEK, and DUSP6 in the RAS/RAF/MEK/ERK (MAPK) pathway and AKT, PTEN in the PI3K/AKT (AKT) pathway in our immortal mouse melanocyte cell lines and their tumourigenic derivative cell lines to investigate the mechanisms involved in melanoma progression in our xenograft model. In chapter 4, we hope to find the specific target or critical molecules to drive our immortal mouse melanocytes to melanoma cells. Functional analyses employing ectopic overexpression reveal the roles of DUSP6 and phosphorylated ERK in melanoma progression in our xenograft model. In addition, the roles of DUSP6 in negatively regulating ERK1/2 activity and inhibiting tumourigenicity are described in a human melanoma cell line. Chapter 5 investigates the role of the MAPK pathway regulated ERCC1 and XPF expression in chemotherapy resistance. We analyze the expression levels of ERCC1 and XPF after cisplatin treatment. Moreover, using a MEK

inhibitor, we provide here correlation between activation of the MAPK pathway and ERCC1 and XPF induction in a human melanoma cell line. The roles of DUSP6 in regulation of ERCC1 and XPF and chemoresistance are also revealed in this chapter.

Chapter 2

Material and methods

2.1 Material

2.1.1 General reagents and equipment

Amersham: enhanced chemiluminescence solution (ECL) fluorescence kit.

Applied Biosystems: 7900HT Fast Real-Time PCR System, High Capacity RNA-to-cDNA Kit, TaqMan® Universal Master Mix, 384-well plates.

Bioline: DNA Hyperladder I, 5X DNA Loading Buffer Blue.

Biometra: Thermocycler.

BioRad: Gel Doc 2000 System with Quantity One 4.6 software, Mini-PROTEAN Electrophoresis System, Mini-Trans Blot Cell.

DAKO: Secondary HRP-conjugated forms of goat anti-rabbit and rabbit anti-mouse antibodies.

Fermentas: PageRuler^{TM} Plus Prestained Protein ladder.

Fisher Scientific: 3M blotting paper, absolute alcohol, chloroform, Na_2EDTA, filter paper haematoxylin, isopropanol, methanol, potassium acetate, sodium hydroxide, xylene.

GE Healthcare: Storm 865 & ImageQuant TL and Storm Image Analysis System software.

Invitrogen: agarose, subcloning efficiency DH5 a ^{TM} competent cells, ethidium bromide.

Millipore (UK) Ltd: disposable sterile filter, Immobilon P PVDF membrane.

Pierce Biotechnology: Bicinchoninic acid (BCA).

Promega: 25mM magnesium chloride, 10x PCR buffer, 5x PCR buffer, Taq DNA polymerase, Oligo dT, RNasin, pGEM-T Easy® Vector Systems.

Roche: Protease Inhibitor cocktail tablets.

Sigma-Aldrich: ammonium persulphate (APS), DMSO, DTT, Na_2EDTA, glycerol, propidium iodide, sodium chloride, sodium deoxycholate, sodium hydroxide, oligonucleotides, trypsin, Triton X-100, Tween 20.

2.1.2 DNA manipulation reagents

DNA isolation buffer: 10mM Tris HCl pH8.0, 400mM NaCl, 3mM EDTA, 1% (w/v) SDS. Stored at 4°C.

DNA agarose loading dye: 20% glycerol, 100mM EDTA, 0.1% bromophenol blue or orange G.

Proteinase K stock solution: 2mg/ml proteinase K, 100mM EDTA pH7.5, 2% (w/v) SDS. Stored at -20°C.

PCA: 25 parts redistilled phenol, 24 parts chloroform, 1 part isoamyl alcohol.

TAE electrophoresis buffer: 40mM Tris-acetate, 1mM EDTA.

TBE electrophoresis buffer: 90mM Tris-HCl, 90mM boric acid, 2mM EDTA, pH8.3.

2.1.3 RNA manipulation reagents

RNAzol^{TM}B: RNA isolation solvent.

TE buffer: 10mM Tris-HCl, 1mM EDTA, pH8.0.

2.1.4 Protein manipulation reagents

Protein sample buffer (4X): 250mM Tris-HCl, pH6.8, 2% SDS, 20% ß-mercaptoethanol, 40% glycerol, 0.5% bromophenol blue.

RIPA buffer: 25mM Tris-HCl, pH 7.2, 150mM NaCl, 1% Triton X-100, 0.1% SDS, 1% deoxycholate, 1mM EDTA, 20mM NaF, 100uM orthovanadate, 1 protease inhibitor cocktail tablet (Roche Complete)/50ml.

Running buffer: 192mM Glycine, 25 mM Tris, 0.1 % (w/v) SDS, pH8.3.

SDS PAGE separating gel: 8-15% (w/v) 29:1 acrylamide: bis-acrylamide, 0.1% (w/v) SDS, 390mM Tris-HCl, pH8.8, 0.08% (v/v) TEMED, 0.1% (w/v) APS.

SDS PAGE stacking gel: 5% (w/v) 29:1 acrylamide: bis-acrylamide, 0.1% (w/v) SDS, 129mM Tris-HCl, pH6.8, 0.1% (v/v) TEMED, 0.1% (w/v) APS.

Transfer buffer: 192mM Glycine, 25 mM Tris, pH 8.3.

TBS: 5mM Tris-HCl, 75mM NaCl, pH 7.4.

TBS-T: 5mM Tris-HCl, 75mM NaCl, 0.05-0.1% Tween-20 v/v, pH 7.4.

2.1.5 Oligonucleotides

Oligonucleotides were purchased from Sigma and resuspended in dH_2O to 100pmol/ul. Stored at -20°C.

Table 2.1 PCR primers

Name	Sequence 5'-3'	Description
BRAF exon 14 forward	TCCTGTCAGGCAGGTCAATATAG	mouse BRAF exon 14 forward primer
BRAF exon 14 reverse	ATACATACCATGTCCCACTTGTGC	mouse BRAF exon 14 reverse primer
BRAF exon 18 forward	TGTTGACTTTCAGAGGACATACG	mouse BRAF exon 18 forward primer
BRAF exon 18 reverse	CCTGTGAGTAGTGGGAACTGTGAA	mouse BRAF exon 18 reverse primer
H-exon1-A forward	CTGGCCGTGCTGGCAGTG	Normal human ERCC1 transcript forward primer
H-exon 2-3 reverse	ATTTGTGATACCCCTCGACGAG	Normal human ERCC1 transcript reverse primer
hskin2RT forward	CCACGACCTCCGCGGTCCTCCAGAACC	Larger Human ERCC1 transcript forward primer
hskin3RT forward	AAACTTAACAGTTTGGGAGCCAGATCCTC	Larger Human ERCC1 transcript forward primer
Hskin4RT forward	TGTACAGAGATCGCCCTGCTCTA	Larger Human ERCC1 transcript forward primer
Hskin5RT forward	CTGCCAGGATTCTGGGCACACA	Larger Human ERCC1 transcript forward primer
M13 Forward	GTAAAACGACGGCCAGT	Forward sequencing primer
M13 Reverse	CATGGTCATAGCTGTTTCC	Reverse sequencing primer

Table 2.2 q-PCR primers

Name	Code	Description
ERCC1 Human	Hs01012158_ml	q-PCR TaqMan ERCC1 primer pair from Applied Biosystems.

XPF Human	Hs00193342_ml	q-PCR TaqMan ERCC4 primer pair from Applied Biosystems.
ACTB Human	4310881E	q-PCR TaqMan Beta-actin primer pair from Applied Biosystems.
Larger ERCC1 Human	ERCC1-RT5-NOTSS	Custom plus TaqMan larger ERCC1 primer pair from Applied Biosystems.

Table 2.3 5′ RACE primers

Name	Sequence 5'-3'	Description
H-exon 2-3 reverse	ATTTGTGATACCCCTCGACGAG	Normal human ERCC1 transcript reverse primer
Hskin4RT reverse	TGTACAGAGATCGCCCTGCTCTATGC	Larger Human ERCC1 transcript reverse primer
REV1	CGGTCCTCCAGAACCATAGA	Larger Human ERCC1 transcript reverse primer
Oligo dT anchor	GACCACGCGTATCGATGTCGACTTTTTTTTTT TTTTTTTV (V=A, C or G)	Anchor primer
PCR anchor	GACCACGCGTATCGATGTCGA	Internal anchor primer

2.1.6 Plasmids

pcDNA3.1/V5-His-DUSP6/MKP-3 was kindly provided by Professor Toru Furukawa (Tohoku University School of Medicine, Japan). This plasmid is able to express a histidine and V5 tagged version of DUSP6 from the human cytomegalovirus (CMV) promoter and also contains a neomycin selectable marker.

The pMCL-MKK1-R4F and pMCL-MKK2-KW71A plasmids were kindly provided by Professor Natalie Ahn (University of Colorado, Boulder). pMCL-MKK1-R4F and pMCL-MKK2-KW71A are able to express the constitutively active forms of MEK1 and MEK2 from the CMV promoter. They also contain a hygromycin selectable marker.

2.1.7 Antibodies

2.1.7.1 Primary antibodies

Table 2.4 Primary antibodies in this study

Code	Target	kDa	Supplier	Dilution
9101S	Phospho-ERK (human, mouse）	42/44KD	Cell signaling	1:500
9102	ERK (human, mouse)	42/44KD	Cell signaling	1:1000
9121S	Phospho-MEK1/2 (human, mouse)	45KD	Cell signaling	1:500
9122	MEK1/2 (human, mouse)	45KD	Cell signaling	1:500
9271S	Phospho-AKT (human, mouse)	60KD	Cell signaling	1:500
9272	AKT (human, mouse)	60KD	Cell signaling	1:500
9559	PTEN (human, mouse)	54KD	Cell signaling	1:1000
SC-1207	p16 (human, mouse)	16KD	Santa Cruz	1:1000
MAB375	GAPDH (human, rat, mouse)	37KD	Chemicon	1:20000
EPR129Y	DUSP6 (human, mouse)	42KD	Abcam	1:2000
FL-297	ERCC1 (human, mouse)	35KD	Santa Cruz	1:1000
Ab-5	XPF (human, mouse)	102KD	Thermo Scientific	1:1000

2.1.7.2 Secondary antibodies

HRP-conjugated forms of goat anti-rabbit (P0448 1:3000) and rabbit anti-mouse (P0260 1:2000) antibodies were from Dako.

2.1.8 Cell culture reagents

BD Biosciences: Matrigel™ Basement Membrane Matrix.

Beckman-Coulter: Coulter counter, FACScan machine, Isoton®II diluents.

Biotium: Calcein AM.

Greiner Bio One: Cellstar® cell culture flasks, cell culture dishes, cell culture plates, pipettes, cell scrapers.

Invitrogen: GIBCO® Dulbecco's Modified Eagle's Medium without calcium (No calcium DMEM), Dulbecco's Modified Eagle's Medium (DMEM), GIBCO™ Modified Eagle's Medium (MEM) (2X)， RPMI-1640, 400mM L-glutamine, 100mM non-essential amino acids (NEAA), 100 mM sodium pyruvate (NaPy), Geneticin G-418 Sulphate, Hygromycin B.

LONZA: Foetal calf serum (FCS).

R&D Systems: Methylcellulose Stock Solution.

Sigma-Aldrich:: beta-mercaptoethanol, cholera toxin, DMSO, endothelin penicillin G, streptomycin, Corning® Transwell® polycarbonate membrane inserts (pore size 8.0µm, membrane diam. 6.5mm), keratinocyte growth factor, trichloroacetic acid (TCA).

1X HBS (HEPES buffered saline): 25mM HEPES, 140mM NaCl, 1.5mM Na_2HPO_4, pH 6.95.

PBS: 140mM NaCl, 3mM KCl, 2mM KH_2PO4, 10mM Na_2HPO4, pH 7.4.

Trypsin-EDTA**:** 10X trypsin (Cambrex) diluted in PBS to 0.25% (w/v) trypsin, 1mM EDTA. Stored at -20°C.

2.1.9 Mammalian cells and culture media

Table 2.5 Cell lines used in this study

Cell	Source	Description
A375	The European Collection of Cell Cultures (ECACC)	Human malignant melanoma
3-1-1	Melton group	Immortalized mouse melanocyte cell line
3-1-1T1	Melton group	Tumourigenic derivative of 3-1-1
3-1-1T2	Melton group	Tumourigenic derivative of 3-1-1
5-1	Melton group	Immortalized mouse melanocyte cell line
5-1T1	Melton group	Tumourigenic derivative of 5-1
5-1T2	Melton group	Tumourigenic derivative of 5-1

13-4-1	Melton group	Immortalized mouse melanocyte cell line
13-4-2	Melton group	Immortalized mouse melanocyte cell line
13-4-3	Melton group	Immortalized mouse melanocyte cell line
13-4-4	Melton group	Immortalized mouse melanocyte cell line
13-4-5	Melton group	Immortalized mouse melanocyte cell line
13-1	Melton group	Immortalized mouse melanocyte cell line
13-2	Melton group	Immortalized mouse melanocyte cell line
PEO14	Dr. Charlie Gourley, Edinburgh Cancer Research Centre	Human ovarian tumour cell line
A2780	Dr. Charlie Gourley, Edinburgh Cancer Research Centre	Human ovarian tumour cell line
HACAT	Professor N.E.Fusenig, German Cancer Research Center	Human keratinocyte cell line
MRC5V1	Prof. A. Lehmann. MRC Cell Mutation Unit, University of Sussex	Human fibroblast cell line

Human melanoma cell cultures were maintained in DMEM media with 10% FCS, 25U/ml penicillin and 25ug/ml streptomycin.

Human ovarian tumour cell cultures were maintained in DMEM media with 10% FCS, 25U/ml penicillin and 25ug/ml streptomycin.

Human fibroblast cell culture was maintained in DMEM media with 10% FCS, 25U/ml penicillin and 25ug/ml streptomycin.

Human keratinocyte cell culture was maintained in low-calcium DMEM with 8% chelexed FCS, 25U/ml penicillin and 25ug/ml streptomycin and 1ug/ml keratinocyte growth factor.

Mouse melanocyte cell cultures were maintained in RPMI-1640 media with 10% FCS, 25U/ml penicillin and 25ug/ml streptomycin.

2.1.10 Bacterial strains

Sub-cloning Efficiency™ DH5α™ Competent Cells were purchased from Invitrogen, and were grown on/in LB medium at 37°C.

2.1.11 Bacterial culture media and related reagents

Ampicillin stock solution: 50mg/ml ampicillin in dH2O. 0.2µm filter sterilised and stored at -20°C. Optimal working concentration in LB was 100µg/ml.

LB Broth media: 10g/L Tryptone, 5g/L Yeast extract, 5g/L NaCl, pH7.4.

Blue/white screen LB agar plates: 20µl of 40mg/ml X-gal was spread over LB agar plates containing the antibiotic ampicillin. The plates were dried at room temperature before being used the same day.

X-gal stock solution: 40mg/ml X-gal in dimethylformamide. Stored at -20°C and protected from light.

2.2 Methods

2.2.1 Cell culture

2.2.1.1 Mammalian cell culture

All cells were cultured using appropriate media in an incubator at 37°C with 5% CO_2. Media were changed every two days, using aseptic technique inside a Category Ⅱ Biological Safety hood. When cells were confluent, the flask was washed with PBS before being incubated with trypsin-EDTA solution. Trypsin-EDTA solution can mediate the detachment of cells from the surface of the flask. Once cells dissociated from the surface, fresh media was added and mixed with the cells. The resulting single cell suspension was centrifuged at 1,300 rpm for 5min to pellet cells. The cells were resuspended with fresh medium. The required volume of cell suspension was mixed with an appropriate volume of fresh media and transferred into a new cell culture flask.

2.2.1.2 Liquid nitrogen frozen stock

For permant storage, cells were trypsined and pelleted as described above and then resuspended in appropriate culture medium supplemented with 10% FCS and 10% DMSO. The cell stock was frozen slowly in a -70°C freezer and then transferred to a liquid nitrogen tank.

2.2.1.3 Counting of cells

Cells were diluted 1:100 in isoton and counted using the Coulter Counter Z series.

2.2.1.4 Methylcellulose assay

1.8% (w/v) agar solution was prepared in PBS and then boiled. The melted agar solution was diluted 1:1 in fresh 2X MEM medium supplemented with 10% Foetal Calf Serum (FCS), 100mM non-essential amino acids (NEAA) and 100mM penicillin-streptomycin (P/S) and then poured into 6-well tissue culture plate (1ml/well) and left until solid. 2.8% (w/v) methylcellulose solution was prepared in DMEM medium supplemented with 10% Foetl Calf Serum (FCS), 100mM non-essential amino acids (NEAA) and 100mM penicillin-streptomycin (P/S). An appropriate number of single cells were mixed with 2.8% methylcellulose solution and then 2ml was poured on the bottom agar layer. The 6-well tissue culture plate was incubated at 37°C and 5% CO_2 for up to 2 weeks. The colony number and size were counted under the microscope every three days and analyzed by Image J software.

2.2.1.5 Transwell migration assay

Matrigel was diluted 1:1 in ice cold PBS. 100ul of this dilution was added into each transwell and incubated 30min at 37°C and 5% CO_2 to allow it to set. Cell suspensions were prepared in their normal growth medium at an appropriate density. 100ul of the cell suspension was seeded onto the transwell filters. The transwells were placed carefully in the 24-well tissue culture plate and incubated for 3 hours at

37°C and 5% CO_2 to allow cells to attach to transwell filters (Fig 2.1). Then the transwells were washed with serum free DMEM medium 3 times and then set in serum free DMEM medium. Fresh DMEM medium supplemented with 10% Foetal Calf Serum (FCS), 100mM non-essential amino acids (NEAA) and 100mM penicillin-streptomycin (P/S) was gently added onto the top of the matrigel (Fig 2.1). The cells can invade into the matrigel in response to a chemotactic stimulus (in this case 10% serum) (Fig 2.1). The plate was incubated at 37°C and 5% CO_2 for 72 hours. Then cells were then labelled with calcein AM dye and visualized in the matrigel at 15um intervals by confocal sectioning. The relative cell number in each section was analyzed using Image J software and expressed relative to the cell number in the section that represented the base of the transwell filter.

Figure 2.1 Transwell migration assay

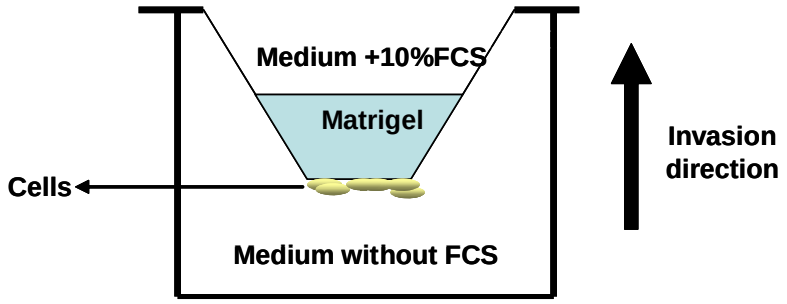

The transwell sitting in the 24-well tissue culture plate. For explanation, see text.

2.2.1.6 Drug treatments of cells

Drug (cisplatin or PD0325901) was added to the cell culture 24 hours after plating to give a designed final concentration. Treated cells were incubated at 37°C and 5% CO_2 and harvested at appropriate time points.

2.2.1.7 Sulforhodamine B (SRB) assay

Cells were plated in 96 well tissue culture plates with 150ul of medium per well at the appropriate seeding density and incubated at 37°C and 5% CO_2. To determine cell growth rate, the plates were directly assayed 72-hour (DAY3), 96-hour (DAY4) and 120-hour (DAY5) after cell plating. For drug toxicity determinations, 50ul of medium with cisplatin was added to each well of the 96-well tissue culture plate to give the designed final cisplatin concentration. The plates were assayed 120-hours (DAY 5) following the drug treatment. For the assay, 50ul of the 25% TCA solution were added to each well, and incubated at 4°C for 1h to fix the cells. Plates were washed out under running tap water for 10 times and dried at 60°C in an oven. 50ul of 0.057% (w/v) SRB Dye solution were added to each well, incubated at room temperature for 30min, washed with 1% (v/v) acetic acid for 4 times and then dried at 60°C in an oven. 150ul of 10mM Tris-base solution (pH 10.5) was added to each well and incubated at room temperature for 60min to solubilise the protein bound dye. The plates were read at 510nm by a plate reader.

2.2.1.8 Preparation of genomic DNA from mammalian cell lines

Cells were cultured till 70% confluent before being harvested. At the time of harvesting, the medium was discarded and cells were rinsed in sterile phosphate-buffered saline (PBS) twice. Trypsin-EDTA was added and the cells were incubated for 2-3min. Post incubation, fresh culture medium was added to deactivate the trypsin-EDTA. Then harvested cells were centrifuged at 1,300 rpm for 5min, the supernatant was discarded. 750ul DNA isolation buffer and 15ul proteinase K solution (20mg/ml) were added to the cells and incubated for 12h at 37℃. Then the debris was spun down and the supernatant was transferred to a fresh eppendorf containing 750ul PCA. An emulsion was formed by shaking tubes to mix the PCA

and our samples. The tubes were spun at top speed in a microfuge for 5min. Then the supernatant was transferred to another fresh tube. Isopropanol was added to the tubes to precipitate DNA. DNA was spun down at top speed for 5min and supernatant was poured off. DNA was washed in 750ul of 70% (v/v) ethanol and spun for 3min. Supernatant was poured off carefully avoiding DNA loss. DNA was allowed to air dry for 10-15min and resuspended in 150ul sterile dH_2O.

2.2.1.9 Preparation of RNA from mammalian cell lines

The total RNA extraction from mammalian cell lines was performed using RNAzol^{TM}B. Cells were cultured till 70% confluent before being harvested. First, cells were washed by cold PBS twice, and then lysed directly by the addition of RNAzol^{TM}B (0.2ml per 10^6 cells). 0.2ml chloroform per 1ml RNAzol^{TM}B was added to extract total RNA by vigorous shaking of the mixture for 30sec. The mixture was stored on ice for 5min and then centrifuged at 12,000g at 4°C for 15min. The aqueous phase where RNA remained was transferred to a fresh tube and mixed with an equal volume of isopropanol. RNA was allowed to precipitate at room temperature for 10min and then centrifuged at 7,500g for 5min. The supernatant was removed and total RNA was washed using 75% (v/v) ethanol then centrifuged at 7,500g for 5min. The pellet was allowed to air dry at room temperature and then dissolved in 50ul of RNase-free dH_2O. Total RNA was stored at -80°C before use.

2.2.1.10 Protein extraction from mammalian cell lines

Cells were cultured till 70% confluent before being harvested. First, cells were washed by cold PBS twice, and then collected in PBS by a cell scraper. After that, the harvested cells were centrifuged at 1,300 rpm for 5 minutes to remove PBS. The

cell pellet was resuspended in 50-100ul ice-cold RIPA buffer for 15 min and centrifuged at 13,000 rpm at 4°C for 15min. The supernatant containing total protein extract was collected and stored at -80°C.

2.2.2 Molecular Biology Methods

2.2.2.1 Polymerase chain reaction

Amplification of specific genes from DNA templates was performed by the Polymerase chain reaction (PCR). Routine PCRs contained 0.5pmol/ul forward and reverse primers, 0.25mM dNTPs, 2.5mM $MgCl_2$, 100ng genomic DNA template, 1U Taq DNA polymerase (Promega), Taq PCR buffer (Promega) and water in a 50ul reaction volume. A negative control containing no template DNA was also prepared. PCRs were carried out by DNA denaturation at 94°C for 5min, followed by 30-38 cycles of DNA denaturation at 94°C for 1min, primer annealing at 50-70°C for 1min and DNA polymerase extension at 72°C for 1min/kb PCR product, with a final extension of PCR products at 72°C for 5min after cycling. The primer annealing temperature was determined based on specific primer design and empirical observations. PCR products were stored at 4°C before use.

2.2.2.2 Separation of DNA fragments by electrophoresis

DNA fragments were separated by gel electrophoresis using 1-2% (w/v) agarose containing 0.5X TBE Buffer and 0.5ug/ml ethidium bromide for visualization. 5X loading dye was added to DNA samples prior to loading. Electrophoresis was performed at 30-100V in a horizontal tank with 0.5X TBE Buffer. DNA fragment bands were visualized by UV irradiation and captured using Gel Doc EQ software. DNA Hyperladder I was used as size marker.

2.2.2.3 Purification of DNA fragments from agarose gels

DNA fragments required for cloning were separated by agarose gel electrophoresis and purified using the QIAquick gel extraction kit (QIAGEN) following the manufacturer's instructions.

2.2.2.4 Quantification of DNA/RNA

The concentration of DNA/RNA was quantified by spectrophotometry at 260nm using the NanoDrop Spectrophotometer (ND-1000). 2ul of samples were loaded for quantification by measuring absorbance at 260nm after blanking. The purity of DNA and RNA samples were estimated by measuring the 260:280 absorbance ratios which are between 1.8 and 2.0 for pure preparations. Concentrations were determined based on OD260nm of 1.0 given by 50ug/ml of double-strand DNA or 40ug/ml of RNA.

2.2.2.5 DNA ligation

DNA ligation reactions were performed in a 10ul volume containing 2X Rapid Ligation Buffer (132mM Tris-HCl, 20mM $MgCl_2$, 2mM dithiohreitol, 2mM ATP, pH7.6), 3 Weiss units T4 DNA ligase and 50ng vector DNA. A 3:1 molar ratio of insert DNA to vector DNA was present in each reaction. DNA ligation reactions were incubated for either 1h at room temperature or at 4°C overnight, and then 5ul was transformed into competent bacterial cells.

2.2.2.6 Transformation of bacteria by heat shock

Aliquots of DH5α competent bacterial cells were thawed on ice. 10-100ng of plasmid DNA, or 5ul of a ligation reaction, was added to 50ul competent bacterial cells, and mixed gently. A positive control consisting of pUC19 plasmid DNA (250pg), and a negative control consisting of dH_2O alone, was also included in each group of bacterial transformations. The mixture of cells and DNA was incubated on ice for 30min, before being heat shocked in a 42°C water bath for 20s and incubated on ice for 2min. Then 950ul of LB broth was added and the transformations were incubated at 37°C for 1h with shaking (225rpm). Aliquots of the transformations were then plated out onto warm LB agar plates containing the appropriate antibiotic. The plates were inverted and incubated at 37°C overnight.

2.2.2.7 Amplification of plasmid DNA using DH5α

Single bacterial colonies that showed positive in blue/white screening for recombination (ie white colonies) were picked out and grown in 3ml LB medium containing 50ug/ml ampicillin at 37°C overnight.

2.2.2.8 Isolation of plasmid DNA from bacteria

Plasmid DNA was isolated from bacteria using Qiagen plasmid DNA Miniprep kit according to the manufacturer' instructions. Plasmid DNA was eluted in dH_2O.

2.2.2.9 DNA sequencing

All sequence analysis was carried out by the Sequencing Unit (MRC Human Genetic Unit, Edinburgh) using the BigDye Terminator V3.1 Cycle Sequencing kit (ABI). DNA sequencing reactions contained 2ul BigDye Terminator v3.1, 50-300ng DNA and 3.2pmol primer in a 10ul reaction volume. M13 forward and M13 reverse primers were used to sequence BRAF exon14 and exon18 from both sides. The PCRs were performed under the following conditions: DNA denaturation at 96°C for 1min, followed by 25 cycles of DNA denaturation 96°C for 30sec, primer annealing at 50°C for 15sec and extension at 60°C for 4 min. PCR products were cleaned up by ethanol and air dried in the dark at room temperature for 15min and then sent to the Sequencing Unit for analysis.

2.2.2.10 Transfection of mammalian cells by electroporation

50ug of plasmid DNA was suspended in 800ul 1X HBS. Cells were harvested, counted and washed with cold 1X HBS. 10^6 cells were then mixed with the plasmid DNA in 1X HBS and incubated at room temperature for 15min. The plasmid DNA/cell suspension was transferred to an electroporation cuvette and electroporated at an appropriate voltage and 500μF capacitance. After that, the mixture in the cuvette was incubated at room temperature for 10min. The cells were transferred to 90mm dishes containing fresh culture media with 10% FCS and incubated at 37°C and 5% CO_2.

2.2.2.11 Transfection of mammalian cells by calcium phosphate

Cells were plated to 90mm dishes at the required density and incubated overnight at 37°C and 5% CO_2. 10ug plasmid DNA was suspended in 1ml 1X HBS. 62ul of 2M

$CaCl_2$ was slowly added to the suspension drop by drop and incubated at room temperature for 45min. Cell culture medium was replaced with plasmid DNA/$CaCl_2$ mixture and incubated at room temperature for 20min. After that, appropriate cell growth medium was added to the dishes and they were incubated overnight at 37°C and 5% CO_2.

2.2.2.12 Selection of stable transformants

In generating stable long-term clones it was necessary to identify clones in which the DNA had integrated into the host genome. This was accomplished by the inclusion of a drug resistance marker in the transfected DNA and subsequent selection with the appropriate drug. The concentration of the drug used for selection varied according to the antibiotic and the cell line used. Cells were maintained in non-selective medium for 2-3 days post-transfection before they were replated in selective media. The selection was maintained for 1-2 weeks with frequent media changes to eliminate dead cells and continued until discrete colonies were visualized. The pooled resistant colonies were then trypsinized and transferred to a T75 flask for subsequent propagation.

2.2.2.13 5′ RACE assay

Characterisation of the 5′ end of the human larger *ERCC1* transcript was carried out using the 2nd Generation 5′/3′ RACE kit (Roche) following the manufacturer's instruction (Fig 2.2). In brief, the first strand of cDNA was synthesised from total RNA using an *ERCC1*-specific primer H exon 2-3 with deoxynucleotides and reverse transcriptase. The synthesised cDNA was then purified using High Pure PCR Product kit (Roche) and a homoploymeric A-tail was added to the 3′ end of the cDNA using terminal transferase. The tailed cDNA was PCR amplified using a second *ERCC1*-specific primer Hskin 4RT REV in combination with oligo dT-

anchor primer. To further amplify this cDNA, a further round of nested PCR was performed using internal primers PCR-anchor and REV1. The PCR products were separated by 1.5% agarose gel and cloned into the p-GEM T-EASY vector for sequencing analysis.

Figure 2.2 Flowchart of 5′ RACE assay

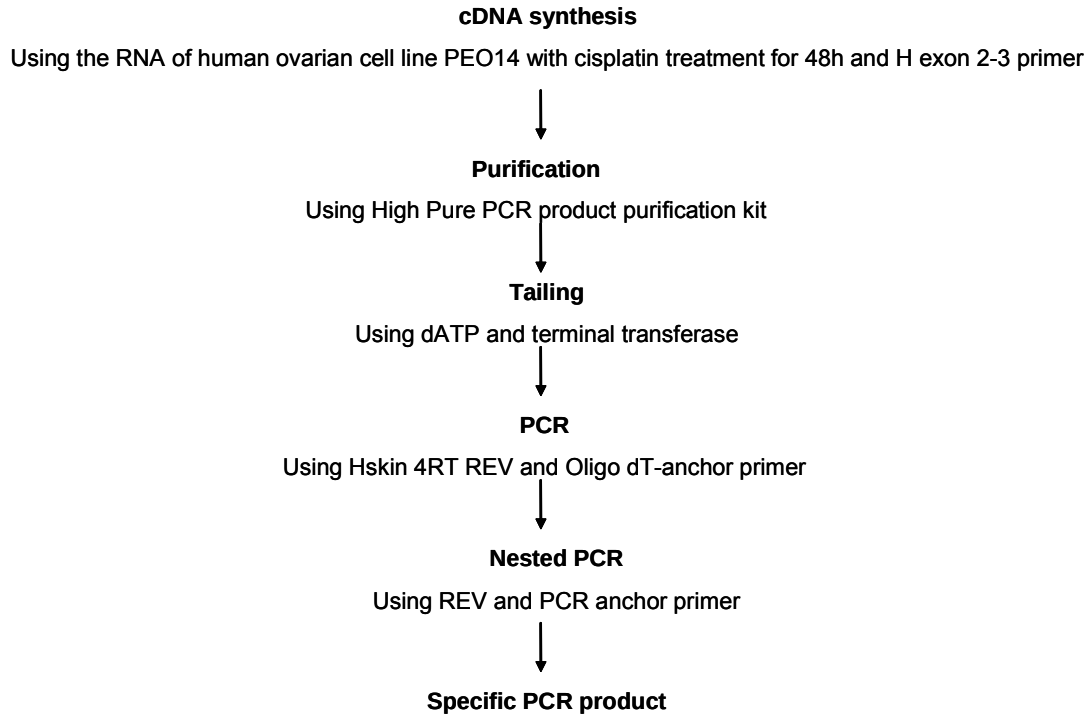

2.2.2.14 Reverse transcription of RNA

Reverse transcription of RNA was performed in a 15ul volume using High Capacity RNA-to-cDNA Master Mix containing $MgCl_2$, dNTPs, recombinant RNase inhibitor protein, reverse transcriptase, random primers and Oligo(dT) primer and stablizers. The reverse transcription of RNA reactions contained 3ul RNA (10-1000ng), 8ul deionized water and 3ul High Capacity RNA-to-cDNA Master Mix. The reverse

transcription of RNA was carried out for 25°C for 5min; 42°C for 30min, 85°C for 1min. cDNA products were stored at 4°C before use.

2.2.2.15 Real-time quantitative polymerase chain reaction

Real-time quantitative polymerase chain reactions were used to quantify the cDNAs of interest using Taqman® Gene Expression Assay and Applied Biosystems 7900HT Fast Real-Time PCR System. The Taqman probe contains a reporter dye at the 5′ end of the probe and a quencher dye at the 3′ end of the probe. During the reaction, cleavage of the probe by AmpliTaq Gold DNA Polymerase separates the reporter dye and the quencher dye, which leads to increased fluorescence of reporter. Accumulation of PCR products is detected directly by monitoring the increase of fluorescence of the reporter dye. real-time quantitative polymerase chain reactions were prepared in a 20ul volume containing 1ul specific 20X Taqman Gene Expression Assay, 10ul 20X Taqman Gene Expression Master Mix, 4ul cDNA template (10-100ng), 5ul RNase-free water. The specific Taqman Gene Expression Assays each contain specific forward and reverse primers. The Taqman Gene Expression Master Mix is optimized for TaqMan reactions and contains AmpliTaq Gold DNA Polymerase, AmpErase UNG, dNTPs with dUTP, Passive Reference dye, and optimized buffer components. Each cDNA sample was assayed in triplicate with the specific primer pair. To evaluate the primers and PCR efficiency, a dilution series of a cDNA sample was also analysed in triplicate with the specific primer pair. In addition, a no template cDNA reaction was included as the negative control. Routine real-time quantitative polymerase chain reaction conditions were as followed: AmpliTaq Gold Enzyme activation at 95°C for 10min, then 40 cycles of DNA denaturation at 95°C for 10min, primer annealing and DNA polymerase extension at 60°C for 60 sec. Data were analyzed using the Comparative C_T Method.

2.2.3 Protein detection

2.2.3.1 Protein quantification

Protein concentrations were measured using the BCA Assay Kit (Pierce) in a 96-well plate. Samples were diluted 1:10 in dH_2O to 25ul. dH_2O was used as the blank control. 200ul of the reagents of the BCA Assay Kit were mixed with protein sample and incubated at 37°C for 30min. The OD values of the protein samples were determined at 562 nm using a plate Spectrophotometer (MRX, Dynatech). The concentrations of protein samples were calculated based on the standard curve generated from the known BSA standards and were adjusted by the dilution factor.

2.2.3.2 SDS-PAGE

Proteins were separated on the basis of their molecular weight by denaturing SDS polyacrylamide gel electrophoresis (SDS PAGE). SDS-PAGE was prepared using a Mini-PROTEAN3 electrophoresis system (Bio-Rad). Two sequential gels were actually made up. The bottom gel, called the resolving gel, was to separate protein. Concentration of polyacrylamide in the resolving gel depended on the molecular weight of the protein of interest. The top gel, called the stacking gel, was to form thin, sharply defined bands. After the gels were set up, the comb in the stacking gel was removed and the gels were clamped to the electrophoretic apparatus. Then the top electrolyte compartment was filled with running buffer. Appropriate amounts of protein sample were prepared with 4X sample buffer and were heated at 95°C for 5min to improve denaturation before being added to the bottom of the gel well. 5ul of PageRuler^{TM} Plus Prestained Protein ladder (Fermentas) was loaded as size marker. Protein samples were separated by electrophoresis in running buffer at 80V for the stacking gel and 100V for the resolving gel.

2.2.3.3 Western blotting

Equivalent amounts of total protein were separated by 10% SDS-PAGE. After that, protein was transferred from SDS PAGE onto PVDF membrane according to the method of Towbin (1979) at 40 mA at 4°C overnight. The membrane was washed with TBS-T once, and then blocked with 5% non-fat milk or 5% BSA for 1 hour at room temperature and detected with primary antibody at optimal concentrations in 5% (w/v) milk or 5% (w/v) BSA for 1 hour at room temperature or overnight at 4°C. After the primary antibody incubation, membrane was washed with TBS-T for 5min, 3 times and then detected with an appropriate secondary antibody at optimal concentrations in 5% non-fat milk or 5% BSA for 45-60 min. Finally, the membrane was washed with TBS-T 3 times, 10 min each. Immunoreactive bands were visualized using enhanced chemiluminescence solution (ECL) or ECL-Plus (Amersham biosciences, Buckinghamshire, UK).

2.2.2.4 Fluorescent ECL plus western blot detection with Storm image analysis system

After protein transfer and antibody incubation, the PVDF membrane was incubated in ECL or ECL Plus detection reagent for 5min. The wet membrane was covered with a plastic hybridization bag slowly to avoid air bubbles. After that, the membrane was scanned using the Blue Fluorescence/Chemifluorescence scan mode 840 with a PMT voltage setting of between 650 and 800V. The intensities of bands on the western blot were measured and analysed using Storm Image Analysis System software.

Chapter 3

Identification of a new type of tumourigenic mouse melanocytes

3.1 Introduction

Malignant melanoma is the most aggressive tumour of the skin. If melanoma is diagnosed early it can be cured by surgical excision, with about 80% of melanoma patients being cured in this way. However, metastatic malignant melanoma is resistant to current therapeutic approaches and spreads very quickly, with a median survival of 6 to 9 months (Balch et al. 2001). Recent studies indicated that a combination of altered regulation of various effectors in different molecular pathways was involved in the progression of normal melanocytes to malignant melanoma (Smalley et al. 2006). A better understanding of molecular changes underlying melanoma progression will contribute to the diagnosis, prognosis, classification and treatment of melanoma.

Both the MAPK and the PI3K pathways were reported to be constitutively active in melanoma (Meier et al. 2005). Up to 70% of melanoma was characterized by mutations in BRAF. Mutations of BRAF have been proposed to activate the MAPK pathway. The most frequent BRAF mutation involved a glutamate for valine substitution at position 600 (V600E) (Brose et al. 2002, Gorden et al. 2003). In addition, 5-36% of primary melanomas had NRAS mutations (Carr and Mackie 1994). However, some reports also indicated that the mutations in these genes were mutually exclusive, and mutation frequencies of RAS and BRAF in primary melanoma did not seem to correlate with overall survival (Houben et al. 2004, Shinozaki et al. 2004). Moreover, only about 54% of primary human melanomas had ERK activation (Cohen et al. 2002, Uribe et al. 2006, Zhuang et al. 2005), whereas 93% of primary melanomas with BRAF V600E mutation had activated ERK (Uribe et al. 2006). Previous studies also showed that some subtypes of melanoma without BRAF or NRAS mutations did not have high level of activation of ERK (Shields et al. 2007). Furthermore, DUSP6, which can dephosphorylate activated ERK and shut down the MAPK pathway, is often lost in pancreatic, lung and ovarian cancers. Down regulation of DUSP6 may promote activation of ERK and uncontrolled cell growth (Bermudez et al. 2010).

PTEN deletion results in activation of the PI3K pathway. PTEN somatic mutations were found in 30% of melanoma cell lines and 10% of human tumour material (Lin et al. 2008). Recent studies indicated activation of AKT was associated with the activation of NF-kB which is thought to be an important transcription factor involved in the control of cell proliferation, survival and apoptosis in melanoma (Dhawan et al. 2002). Moreover, The PI3K-AKT pathway regulated proliferation of melanoma cells through the inactivation of GSK-3b, preventing cyclin D1 degradation. (Diehl et al. 1998). In addition, the activation of AKT resulted in suppression of apoptosis of melanoma cells though inactivation of many pro-apoptotic proteins including BAD and caspase-9 (Palmieri et al. 2009). Furthermore, AKT activation could lead to phosphorylation and inactivation of RAF. This inactivation of the MAPK pathway may result in loss of differentiation or senescence (Palmieri et al. 2009, Zimmermann and Moelling 1999) .

Data obtained from genetic and molecular studies over the past few years have indicated that CDKN2A mutations were more frequent in patients with a strong familial history of melanoma (Miller and Mihm 2006). CDKN2A is located on chromosome 9p21 and encodes two proteins: p16 and p14, which are known as tumour suppressors (Michaloglou et al. 2008). Studies showed that p16 was associated with melanocyte senescence. Activation of the MAPK pathway can induce cellular growth arrest by promoting cellular senescence. BRAF mutations were found to induce p16 expression and senescence in primary human melanocytes in vitro. Mutations of CDKN2A could result in inactivation of p16 and contribute to overcome senescence in melanoma (Gray-Schopfer et al. 2006, Michaloglou et al. 2005).

In our laboratory, immortal mouse melanocyte cell lines were derived from primary melanocyte cell culture of epidermis of newborn mice by infection with a retrovirus expressing SV40 T antigen (David Melton, unpublished). Studies showed that SV40

large T-antigen transformed human melanocytes cycled much more quickly and had a reduced requirement for basic fibroblast growth factor (bFGF), an essential melanocyte mitogen. However, the cells did not undergo complete transformation to the malignant phenotype remaining anchorage dependent and unable to form xenografts (Zepter et al. 1995). These features suggest that introduction of SV40 large T antigen into melanocytes produces an intermediate stage between the normal and malignant cell which may render these cells unusually susceptible to additional genetic changes necessary for full expression of the malignant phenotype. The tumourigenicity of some of these cell lines has been investigated in xenograft assays. All 12 xenografts of the human melanoma cell line, A375, grew very rapidly, taking only 21 days to reach the maximum permitted size. Compared to this, all 12 xenografts of our mouse melanocyte line, 5-1, showed a long latent period before commencing rapid growth until all reached the maximum permitted size by 59 days. Xenografts of our mouse melanocyte cell line, 3-1-1, showed an even longer latent period before commencing rapid growth and then only 2 of 12 xenografts grew, reaching the maximum permitted size by 115 days. Cells from some 5-1 and 3-1-1 xenografts were reisolated into culture for analysis. Histologicaly, all 5-1 and 3-1-1 xenografts showed the characteristics of malignant melanoma. Cells reisolated from 3-1-1 tumours were xenografted to mice again and all formed large tumours in mice in 27 days, much more quickly than the parent cell line 3-1-1.

Figure 3.1 Mouse xenograft model

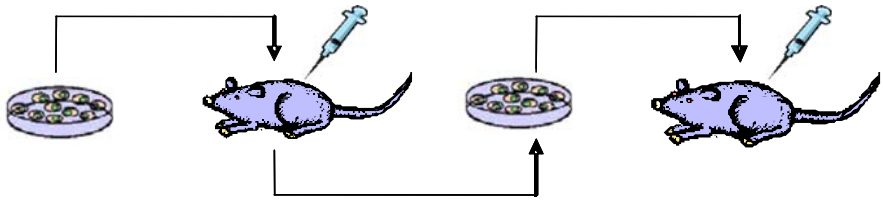

5-1	5-1T
3-1-1	5-1T
A375 (human melanoma control cell	3-1-1T
	3-1-1T

Mouse melanocyte cell lines (3-1-1, 5-1) were isolated by infection of primary mouse melanocyte cultures with retrovirus expressing SV40T antigen. These cell lines with A375 (human melanoma control) were xenografted to mice. 5-1 tumour (T) and 3-1-1 tumour cell lines were the cell lines re-isolated back into culture from independent 5-1 and 3-1-1 tumours. # 3-1-1T1 was xenografted to mice again and formed tumours more quickly than its parental cell line 3-1-1.

Figure 3.2 Growth rates of A375, 5-1, 3-1-1 and 3-1-1T1 xenograft

A **B**

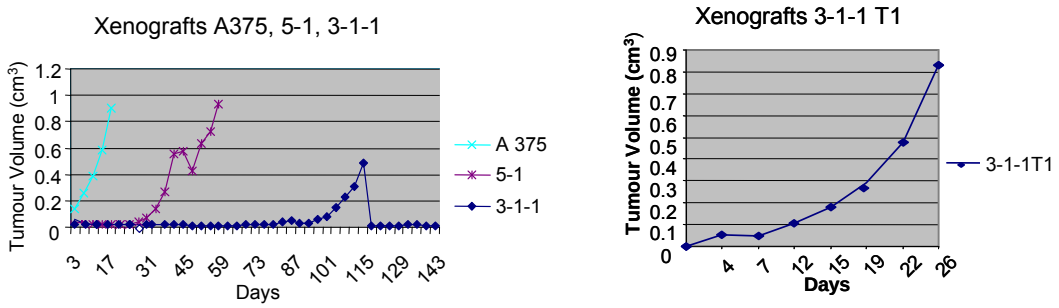

A, Growth of A375, 5-1 and 3-1-1 xenografts in nude mice. The data are provided by Professor David Melton. The light blue line represents the average volume of xenografts from 6 mice with 2 A375 xenografts per mouse. The purple line represents the average volume of xenografts from 6 mice with 2 5-1 xenografts per mouse. The dark blue line represents the average volume of xenografts from 6 mice with 2 3-1-1xenografts per mouse.

B, Growth of 3-1-1T1 xenografts in nude mice. The data are provided by David Melton. The dark blue line represents the average volume of xenografts from 6 mice with 2 3-1-1T1 xenografts per mouse.

The aim of this chapter is to investigate the genetic changes in our immortal melanocyte cell lines needed to form tumours in the xenograft experiment through comparison of 5-1 and 3-1-1 with 5-1 Tumour and 3-1-1 Tumour cell lines.

3.2 Results

3.2.1 Comparison of expression of phosphorylated ERK1/2 in our immortal mouse melanocyte cell lines and human melanoma cell line

Previous studies showed that the MAPK pathway was involved in classic melanoma progression (Smalley 2003). To investigate the genetic changes in our immortal melanocyte cell lines needed to form tumours in the xenograft experiment, we decided to compare the expression of phosphorylated ERK1/2 in the MAPK pathway between our mouse tumour cell lines and their parental cell lines.

Protein lysates obtained from our immortal mouse melanocyte cell lines (3-1-1, 3-1-1T1, 3-1-1T2, 5-1, 5-1T1, 5-1T2) and human melanoma cell line (A375) were subjected to western blot analysis using an anti-phospho-ERK antibody to detect p-ERK1 (42KD) and p-ERK2 (44KD). Total ERK and GAPDH levels of these samples were also determined by western blot to correct for different amounts of protein in the various samples. Experiments were repeated at least three times. p-ERK levels are expressed relative to total ERK levels and are normalized to human melanoma A375 cells.

Human melanoma cell line A375 showed high expression of p-ERK as expected. However, to our surprise, the expression of p-ERK was significantly lower in our tumour cell lines than their parental cell lines (Fig 3.3A). Quantification analysis showed that the expression of p-ERK in 3-1-1 tumour cell lines decreased about 10-fold compared to 3-1-1, while the expression of p-ERK in 5-1 tumour cell lines decreased 10 to 16-fold compared to 5-1 (Fig 3.3B).

Figure 3.3 p-ERK/ERK western blotting

A

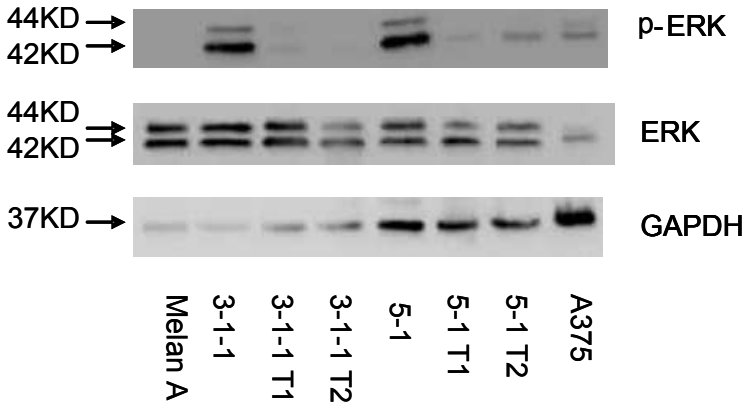

B

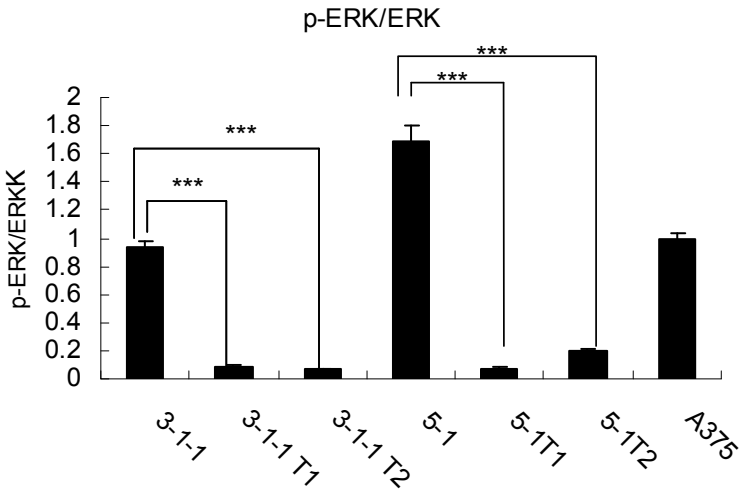

A, Western blots showing protein levels of phosphorylated ERK (p-ERK) (top panel), and total ERK (t-ERK) (middle panel) and loading control GAPDH (bottom panel) in mouse melanocytes 3-1-1, 3-1-1T1, 3-1-1T2, 5-1, 5-1T1, 5-1T2 and human melanoma A375 cells.

B, Histogram showing mean level of p-ERK (± SEM) from three independent experiments. p-ERK levels are expressed relative to total ERK levels and are normalized to human melanoma A375 cells. One way ANOVA with Bonferroni's Multiple Comparison Test was applied for statistical analysis between 3-1-1, 5-1 and their derivatives 3-1-1T1, 3-1-1T2, 5-1T1, 5-1T2. ***, $P < 0.001$.

3.2.2 Comparison of expression of phosphorylated MEK1/2 in our immortal mouse melanocyte cell lines and human melanoma cell line

To investigate whether lower expression of p-ERK comes from inactivation of its upstream effector, we next detected the expression of phosphorylated MEK1/2 in our mouse tumour cell lines and their parental cell lines. As described before, protein lysates obtained from our immortal mouse melanocyte cell lines (3-1-1, 3-1-1T1, 3-1-1T2, 5-1, 5-1T1, 5-1T2) and human melanoma cell line (A375) were subjected to western blot analysis using an anti-phospho-MEK1/2 antibody to detect p-MEK1/2. Total MEK1/2 and GAPDH levels of these samples were also determined by western blot to correct for different amounts of protein in the various samples. Experiments were repeated at least three times. p-MEK1/2 levels are expressed relative to total MEK1/2 levels and are normalized to human melanoma A375 cells.

Our results indicated that human melanoma cell line A375 showed high expression of p-MEK1/2 as expected, while our tumour cell lines had lower expression of p-MEK1/2 than their parental cell lines (Fig 3.4A). Quantification analysis showed that the expression of p-MEK1/2 in tumour cell lines was about 4-fold lower than their parental cell lines (Fig 3.4B). This suggested that lower expression of p-ERK may be due to a failure of upstream activation and that the MAPK pathway was shut down in our tumour cell lines.

Figure 3.4 p-MEK/MEK western blotting

A

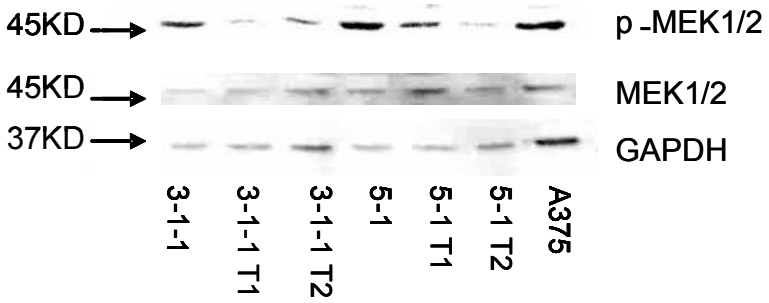

B

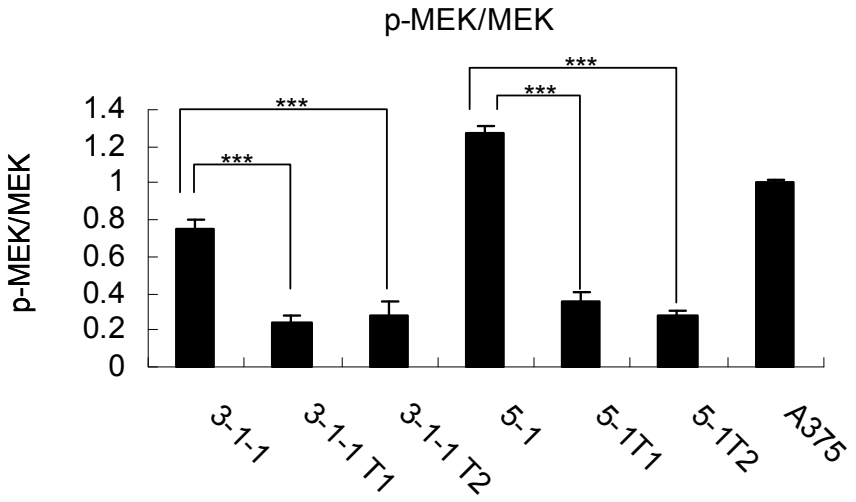

A, Western blots showing protein levels of phosphorylated MEK1/2 (p-MEK1/2) (top panel), and total MEK1/2 (MEK1/2) (middle panel) and loading control GAPDH (bottom panel) in mouse melanocytes 3-1-1, 3-1-1T1, 3-1-1T2, 5-1, 5-1T1, 5-1T2 and human melanoma A375 cells.

B, Histogram showing mean level of p-MEK1/2 (± SEM) from three independent experiments. p-MEK1/2 levels are expressed relative to total MEK levels and are normalized to human melanoma A375 cells. One way ANOVA with Bonferroni's Multiple Comparison Test was applied for statistical analysis between 3-1-1, 5-1 and their derivatives 3-1-1T1, 3-1-1T2, 5-1T1, 5-1T2. ***, $P < 0.001$.

3.2.3 Comparison of expression of DUSP6 in our immortal mouse melanocyte cell lines and human melanoma cell line

DUSP6 is the phosphatase that dephospharylates ERK1/2 and regulates the MAPK pathway through a feedback loop (Bermudez et al. 2010, Patterson et al. 2009). Higher expression of DUSP6 was found in melanoma cell lines with BRAF mutations (Bloethner et al. 2005). We suspected that overexpression of DUSP6 may also contribute to lower expression of p-ERK in our tumourigenic cell lines. Therefore, the levels of DUSP6 were detected in our immortal mouse cell lines and their tumour derivatives by western blotting. As described before, protein lysates obtained from our mouse immortal melanocyte cell lines (3-1-1, 3-1-1T1, 3-1-1T2, 5-1, 5-1T1, 5-1T2) and human melanoma cell line (A375) were subjected to western blot analysis using an anti-DUSP6 antibody to detect DUSP6. The predicted molecular weight of DUSP6 is 42KD, this anti-DUSP6 antibody can detect a band of approximately 42KD/44KD. GAPDH levels of these samples were also determined by western blot to correct for different amounts of protein in the various samples. Experiments were repeated at least three times. DUSP6 levels are expressed relative to GAPDH levels and are normalized to human melanoma A375 cells.

It was clear that the expression of DUSP6 was significantly higher in our tumour cell lines than their parental cell lines (Fig 3.5A). Quantification analysis showed that the expression of DUSP6 in 3-1-1 tumour cell lines increased about 4 to 6-fold compared to 3-1-1, while the expression of DUSP6 in 5-1 tumour cell lines increased 3 to 4-fold compared to 5-1. DUSP6 expression levels of human melanoma cell line A375 were higher than in our immortal melanocytes, but lower than in their tumour derivatives (Fig 3.5B). There was good inverse relationship between p-ERK and DUSP6 expression in our mouse cell line panel. It was possible the increased DUSP6 resulted in lower expression of p-ERK in our tumour cell lines.

Figure 3.5 DUSP6 western blotting

A

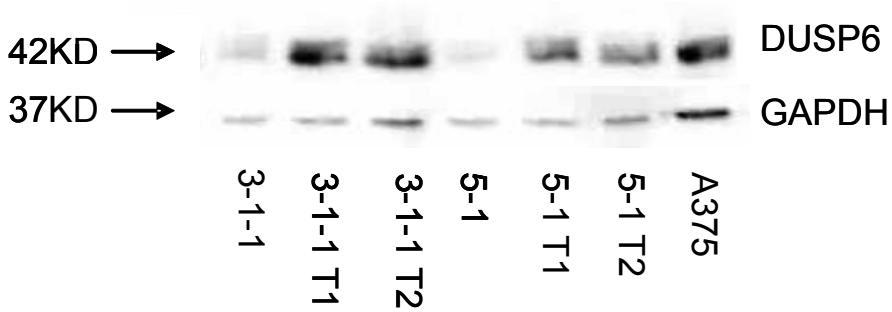

B

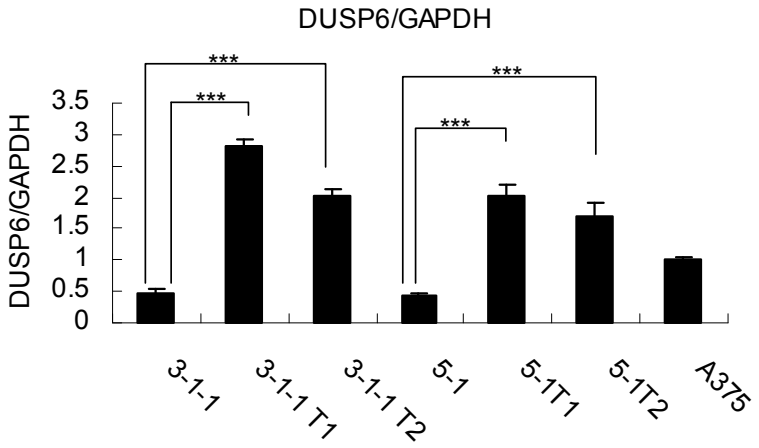

A, Western blots showing protein levels of DUSP6 (top panel) and loading control GAPDH (bottom panel) in mouse melanocytes 3-1-1, 3-1-1T1, 3-1-1T2, 5-1, 5-1T1, 5-1T2 and human melanoma A375 cells.

B, Histogram showing mean level of DUSP6 (± SEM) from three independent experiments. DUSP6 levels are expressed relative to GAPDH levels and are normalized to human melanoma A375 cells. One way ANOVA with Bonferroni's Multiple Comparison Test was applied for statistical analysis between 3-1-1, 5-1 and their derivatives 3-1-1T1, 3-1-1T2, 5-1T1, 5-1T2. ***, $P < 0.001$.

3.2.4 Comparison of expression of phosphorylation of AKT in our immortal mouse melanocyte cell lines and human melanoma cell line

Previous studies showed that the PI3K-AKT pathway was activated in human cancers (Cully et al. 2006, Hennessy et al. 2005). AKT activation can result in the phosphorylation and inactivation of RAF. This causes a decrease in downstream MEK and ERK activation and may lead to loss of differentiation or senescence (Palmieri et al. 2009, Zimmermann and Moelling 1999). Since our tumour cell lines shut down the MAPK pathway, it was possible that the PI3K-AKT pathway was activated and lower expression of p-ERK was because of hyperactivated AKT. To investigate this possibility, we examined expression of phosphorylation of AKT in our mouse cell line panel by western blotting. As described before, protein lysates obtained from our immortal mouse melanocyte cell lines (3-1-1, 3-1-1T1, 3-1-1T2, 5-1, 5-1T1, 5-1T2) and human melanoma cell line (A375) were subjected to western blot analysis using an anti-phospho-AKT antibody to detect p-AKT. Total AKT and GAPDH levels of these samples were also determined by western blot to correct for different amounts of protein in the various samples. Experiments were repeated at least three times. p-AKT levels are expressed relative to total AKT levels and are normalized to human melanoma A375 cells.

However, we found our tumour cell lines with low expression of p-ERK also had lower expression of p-AKT than their parental cell lines (Fig 3.6A). Our result also showed that molecular weight of p-AKT in the 3-1-1 tumourigenic cells was slightly higher than their parental cell line. Quantification analysis showed that the expression of p-AKT in 3-1-1 tumour cell lines was about 2-fold lower than 3-1-1, while the expression of p-AKT of 5-1 tumour cell lines was about 4 to 8-fold lower than 5-1. Human melanoma cell line A375 expressed similar low p-AKT levels as our mouse tumour cell lines (Fig 3.6B). This indicated inactivation of the MAPK pathway in our tumourigenic cell lines was not because of activation of the PI3K-AKT pathway.

Figure 3.6 p-AKT/AKT western blotting

A

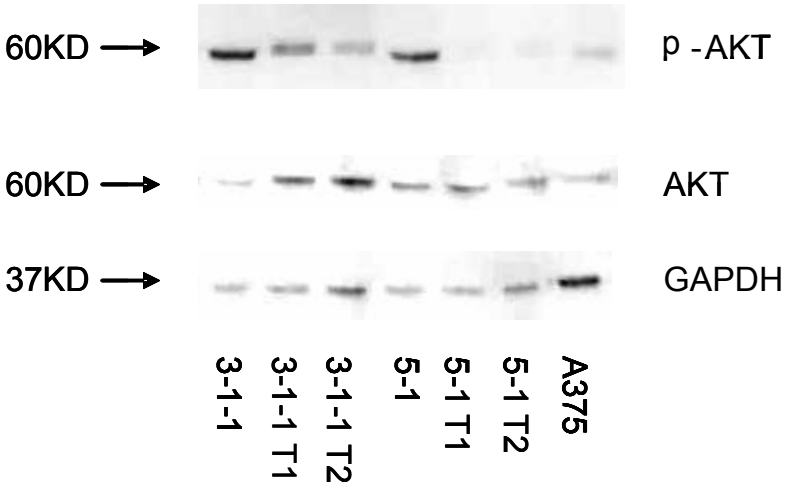

B

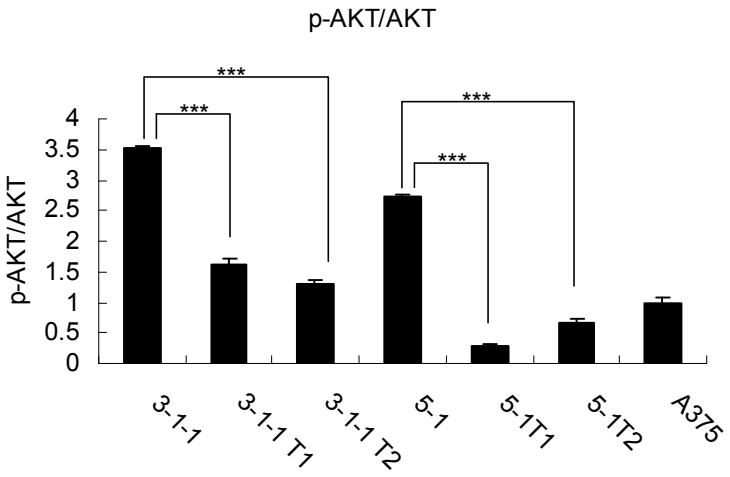

A, Western blots showing protein levels of phosphorylated AKT(p-AKT) (top panel), and total AKT (t-AKT) (middle panel) and loading control GAPDH (bottom panel) in mouse melanocytes 3-1-1, 3-1-1T1, 3-1-1T2, 5-1, 5-1T1, 5-1T2 and human melanoma A375 cells.

B, Histogram showing mean level of p-AKT (± SEM) from three independent experiments. p-AKT levels are expressed relative to total AKT levels and are normalized to human melanoma A375 cells. One way ANOVA with Bonferroni's Multiple Comparison Test was applied for statistical analysis between 3-1-1, 5-1 and their derivatives 3-1-1T1, 3-1-1T2, 5-1T1, 5-1T2. ***, $P < 0.001$.

3.2.5 Detection of PTEN in our immortal mouse melanocyte cell lines and human melanoma cell line

PTEN is a lipid phosphatase that inhibits AKT activation by PI3K. PTEN somatic mutations were found in 30% of melanoma cell lines and 10% of human tumour materials (Lin et al. 2008). To investigate whether our tumour cell lines have lost PTEN, we detected expression of PTEN in our mouse cell line panel by western blotting. As described before, protein lysates obtained from our mouse immortal melanocyte cell lines (3-1-1, 3-1-1T1, 3-1-1T2, 5-1, 5-1T1, 5-1T2) and human melanoma cell line (A375) were subjected to western blot analysis using an anti-PTEN antibody to detect PTEN. GAPDH levels of these samples were also determined by western blot to correct for different amounts of protein in the various samples. The expression of PTEN was equal in our cell line panel, there was no evidence indicating any PTEN loss (Fig 3.7).

Figure 3.7 PTEN western blotting

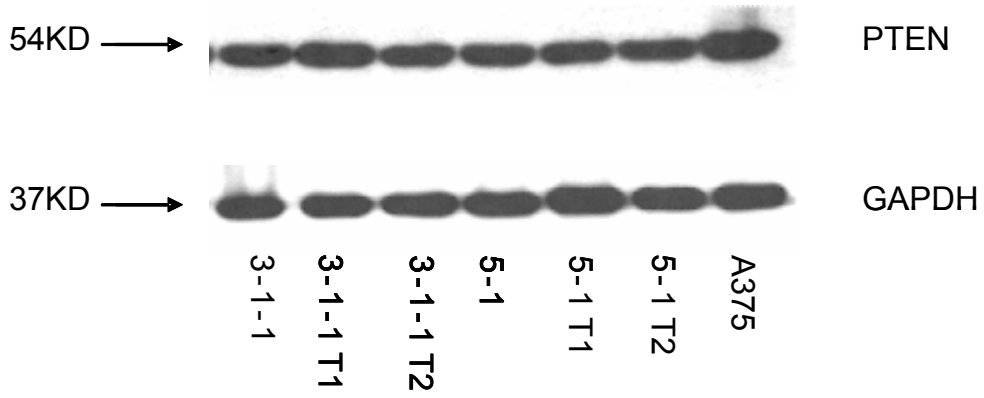

Western blots showing protein levels of PTEN (top panel) and loading control GAPDH (bottom panel) in mouse melanocytes 3-1-1, 3-1-1T1, 3-1-1T2, 5-1, 5-1T1, 5-1T2 and human melanoma A375 cells.

3.2.6 Comparison of expression of p16 in mouse melanocyte cell lines

In addition to 3-1-1 and 5-1 immortal mouse melanocyte cell lines, another immortal mouse melanocyte cell line was isolated at the same time. The #13 lines remained static for a long time and appeared senescent before a series of derivative subclones were eventually isolated, while mouse melanocyte cell lines 3-1-1, 5-1 and their tumour derivative cell lines grew quickly in cell culture. Since p16 was reported to contribute to melanocyte senescence, we decided to detect the p16 expression in these two types of mouse melanocyte cell lines.

As described before, protein lysates obtained from mouse melanocyte cell line 13 derivatives 13-4-1, 13-4-2, 13-4-3, 13-4-4, 13-4-5 and 3-1-1, 5-1 and their tumour derivative cell lines were subjected to western blot analysis using an anti-p16 antibody to detect p16. GAPDH levels of these samples were also determined by western blot to correct for different amounts of protein in the various samples. Our results indicated that all the derivatives of the senescent cell line # 13 had lost p16 expression, but 3-1-1, 5-1 and their tumour derivative cell lines 3-1-1T1 and 5-1T1 all expressed p16 (Fig 3.8).

Figure 3.8 p16 western blotting

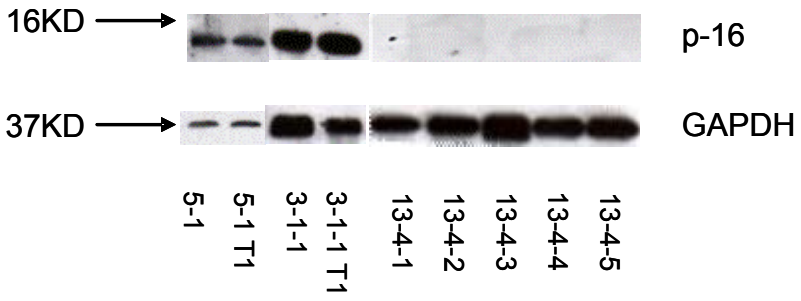

Western blots showing protein levels of p16 (top panel) and loading control GAPDH (bottom panel) in mouse melanocytes cell lines 3-1-1, 3-1-1T1, 5-1, 5-1T1 and # 13 cell lines including 13-4-1, 13-4-2, 13-4-3, 13-4-4, 13-4-5.

3.2.7 Investigation of the possibility of BRAF V600E mutations in our mouse melanocyte cell lines and their tumour derivatives

BRAF mutations are detected frequently in human melanoma. Numerous variant mutations have been identified involving codon 600 and neighbouring codons in exon 15, and less frequently in exon 11 (Spittle et al. 2007). We compared the mouse BRAF and human BRAF genes and predicted BRAF mutations may occur frequently in exon 18 and exon 14 of the mouse BRAF gene. These exons are equivalent to exon 15 and exon 11 in the human BRAF gene. To further characterize MAPK pathway activation in our panel of cell lines, we investigated whether there were mutations in these exons using the PCR sequencing method. However, the sequencing results did not provide any strong evidence for BRAF activating mutations associated with melanoma in any of our immortal mouse cell lines. For the exon 18 PCR products from genomic DNA, the sequence of 2 out of 10 5-1 sequenced sublones and 3 out of 9 5-1T1 sequenced subclones indicated sequence alteration. For the exon 14 PCR products from genomic DNA, the sequence of 2 out of 10 3-1-1 sequenced subclones, 2 out of 10 3-1-1 T1 sequenced subclones and 2 out of 10 5-1 T1 sequenced subclones indicated sequence alteration (Table 3.1).

However, for both exons, the alteration point in each subclone from the same cell line was different and these alterations were regarded as PCR or sequencing errors rather than as evidence for BRAF mutations.

Cell line / Exon	3-1-1	3-1-1 T1	5-1	5-1 T1
Exon 14	2/10	2/10	0/10	2/10
Exon 18	0/10	0/9	2/10	3/9

Table 3.1 Sequence alterations on sequenced subclones of immortal mouse melanoctye cell lines. The table shows the rate of alterations in exon 14 and exon 18 of sequenced subclones of the mouse BRAF gene from our immortal mouse melanocytes and their tumourigenic derivatives. The alteration sites of exon 14 are at positions 1613 and 1695 for 3-1-1, 1621 and 1645 for 3-1-1T1 and 1628 and 1637 for 5-1T1. The alteration sites of exon 18 are at positions 2047 and 2133 for 5-1 and 2041, 2085 and 2127 for 5-1T1.

3.2.8 Detection of anchorage independent growth ability of our mouse melanocyte cell lines and their tumour derivatives

The ability to form colonies in methylcellulose is a good in vitro surrogate for an in vivo tumourigenicity assay (Lauring et al. 2008, Runge et al. 1985). The methylcellulose system required fewer additives than necessary in the soft agar system. In addition, the quantification of the colony size and colony number in the methylcellulose system was easier than in the soft agar system. More important, colony growth of our immortal mouse melanocyte cell lines in the soft agar system was less predictable and often unsuccessful. Therefore, we decided to use the methylcellulose assay to assess the anchorage independent growth ability of our mouse melanocyte cell lines and their tumour derivatives.

10000 cells of 3-1-1, 3-1-1T1, 3-1-1T2 and 5-1, 5-1T1, 5-1T2 were seeded into methylcellulose. Colony size and number were detected under the microscope every

three days for 12 days. Image J software was used to analyze the relative colony size and colony number per photographic field at day 12. Minimum colony size cut off was set at 30um for Day 12. The data collected from three independent experiments indicated our mouse tumourigenic cell lines formed larger and more colonies than their parental cell lines (Fig 3.9A, Fig 3.9B). Quantification analysis showed that the average colony size of the 3-1-1 tumour cell lines increased 2 to 3-fold compared to 3-1-1; the colony number of the 3-1-1 tumour cell lines also increased 2.5 to 3-fold compared to 3-1-1 (Fig 3.9C, Fig 3.9D). The increase in 5-1 tumour cell lines was larger than 3-1-1 tumour cell lines: the average colony size of 5-1 tumour cell lines increased 7 to 23 fold compared to 5-1; the colony number of 5-1 tumour cell lines also increased 3 to 4-fold compared to 5-1 (Fig 3.9E, Fig 3.9F) These data suggested that our tumour cell lines had enhanced anchorage independent growth ability and that this may contribute to their ability to form tumours more easily in mice.

Figure 3.9 Detection of anchorage independent growth ability of our immortal mouse melanocytes by the methylcellulose assay

A

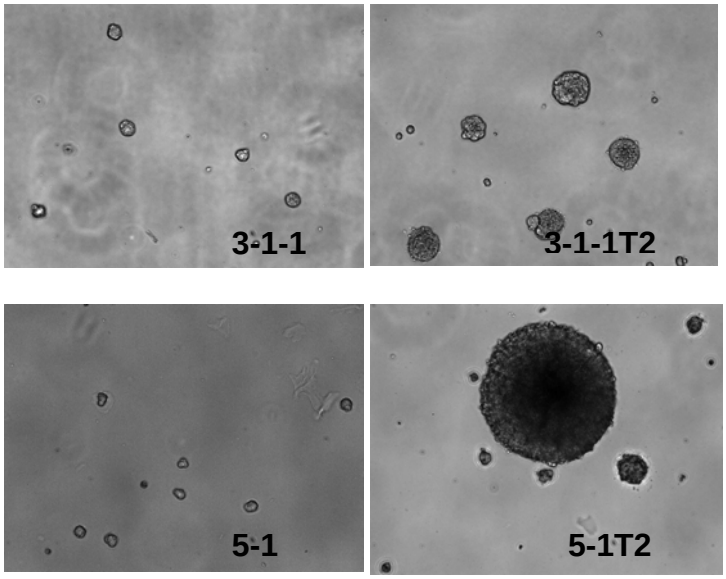

B

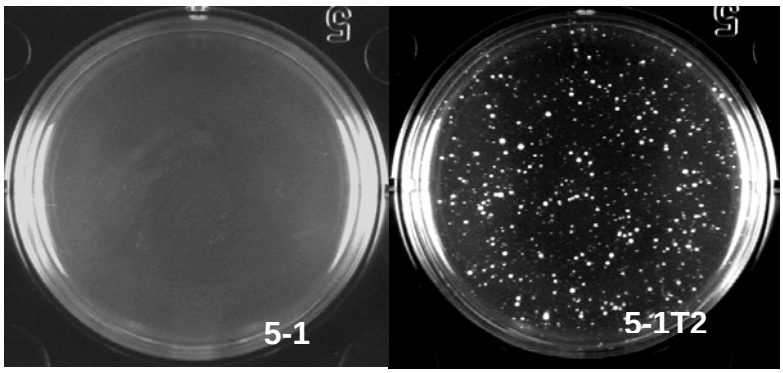

C

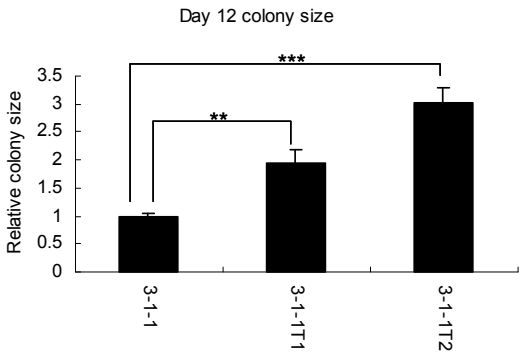

D

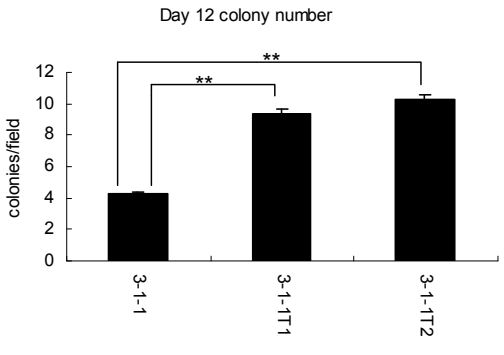

E

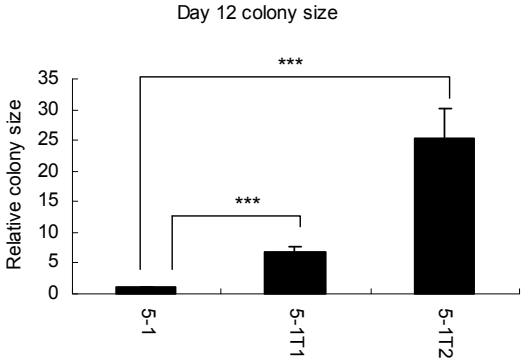

F

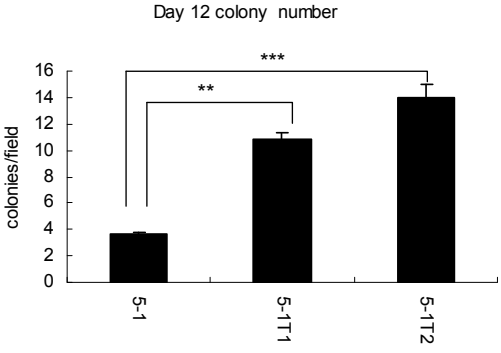

A, 3-1-1, 3-1-1T1, 3-1-1T2 and 5-1, 5-1 T1, 5-1 T2 were mixed with methylcellulose and seeded into 6-well plates to form colonies for 12 days. Images are representative of 3-1-1, 3-1-1T2, 5-1 and 5-1T2 colonies at Day 12.

B, 3-1-1, 3-1-1T1, 3-1-1T2 and 5-1, 5-1 T1, 5-1 T2 were mixed with methylcellulose and seeded into 6-well plates to form colonies for 12 days. Images are representative of 5-1 and 5-1T2 wells at Day 12.

C, Average colony size of 3-1-1, 3-1-1T1, 3-1-1T2. Colony areas were measured with Image J software. Histogram shows mean colony size (± SEM) from three independent experiments. Average colony size of 3-1-1T1 and 3-1-1T2 are standardised to 3-1-1. One way ANOVA with Bonferroni's Multiple Comparison Test was applied for statistical analysis between 3-1-1 and 3-1-1T1, 3-1-1T2 **, $P<0.01$. ***, $P < 0.001$.

D, Total number of colonies counted per photographic field. Each field is approximately 0.59 mm^2 of culture dish. At least 6 fields were counted for each dish. Histogram shows mean colony number (± SEM) from three independent experiments. One way ANOVA with Bonferroni's Multiple Comparison Test was applied for statistical analysis between 3-1-1 and 3-1-1T1, 3-1-1T2. **, $P<0.01$.

E, Average colony size of 5-1, 5-1T1, 5-1T2. Colony areas were measured with Image J software. Histogram shows mean colony size (± SEM) from three independent experiments. Average colony size of 5-1T1 and 5-1T2 are standardised to 5-1. One way ANOVA with Bonferroni's Multiple Comparison Test was applied for statistical analysis between 5-1 and 5-1T1, 5-1T2. ***, $P < 0.001$.

F, Total number of colonies counted per photographic field. Each field is approximately 0.59 mm^2 of culture dish. At least 6 fields were counted for each dish. Histogram shows mean colony number (± SEM) from three independent experiments. One way ANOVA with Bonferroni's Multiple Comparison Test was applied for statistical analysis between 5-1 and 5-1T1, 5-1T2. **, $P<0.01$. ***, $P < 0.001$.

3.2.9 Detection of invasive ability of our mouse melanocyte cell lines and their tumour derivatives

Matrigel is considered as an in vitro model for basement membrane and is generated from EHS sarcoma cells. Matrigel contains not only basement membrane components (collagens, laminin, and proteoglycans), but also matrix degrading enzymes. Migration through an extracellular matrix is a prerequisite for local

invasion and metastasis (Kleinman and Martin 2005). The transwell migration assay is a useful tool to compare invasive ability between our tumour cell lines and their parental cell lines. Our immortal mouse cell lines (3-1-1, 3-1-1T1, 3-1-1T2 and 5-1, 5-1T1, 5-1T2) and human melanoma cell line A375 as a positive control were seeded onto transwell filters to invade into matrigel in response to a chemotactic stimulus (in this case 10% serum). After 72 hours, cells were labelled with calcein AM dye and visualized in the matrigel at 15um intervals by confocal sectioning. The cell number invading to 45um was expressed relative to the cell number in the section that represented the base of the transwell filter. Our mouse tumourigenic cell lines displayed greater chemotactic invasion relative to their parental cell lines (Fig 3.10A, Fig 3.10C). Quantification analysis showed that the relative cell number at 45um increased 1.5-fold compared to 3-1-1 and increased 8-fold compared to 5-1 (Fig 3.10B, Fig 3.10D). The difference within the 5-1 series in the transwell migration assay was larger than in the 3-1-1 series. Human melanoma cell lines A375 invaded further in matrigel than any of our immortal mouse cell lines.

Figure 3.10 Detection of invasive ability of our immortal mouse melanocytes by the transwell migration assay

A

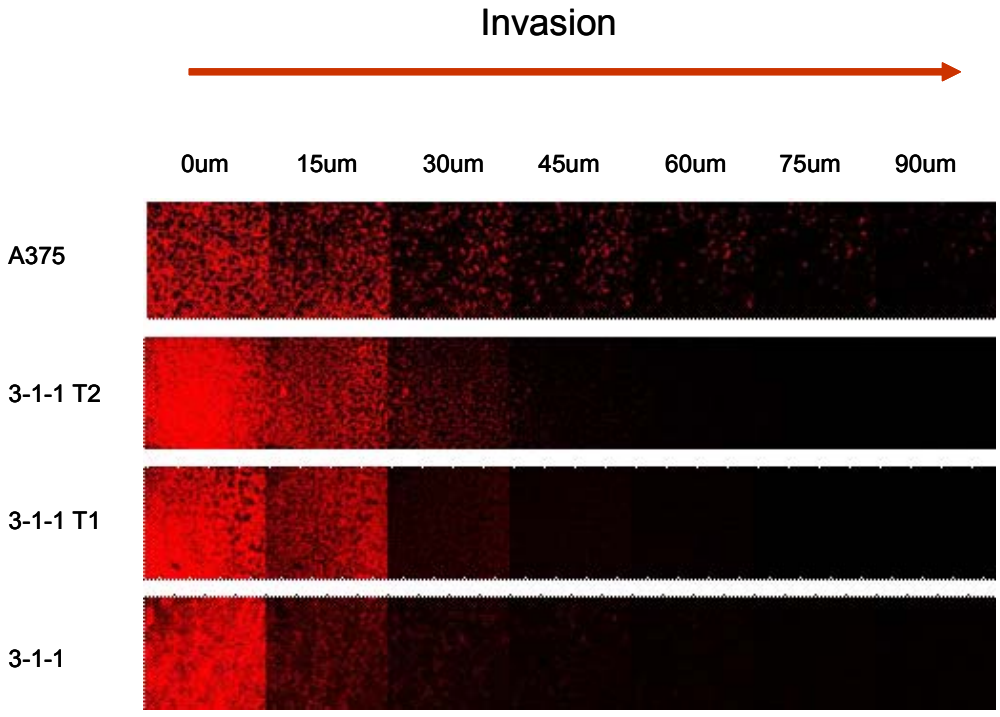

B

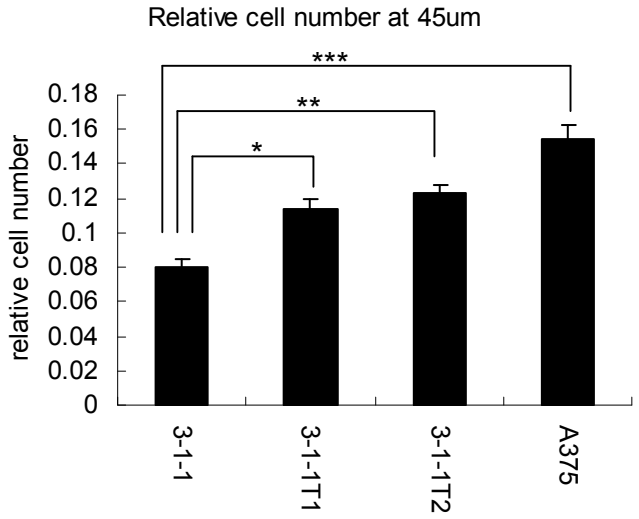
Relative cell number at 45um
relative cell number
0.18
0.16
0.14
0.12
0.1
0.08
0.06
0.04
0.02
0
***
**
*
3-1-1
3-1-1T1
3-1-1T2
A375

C

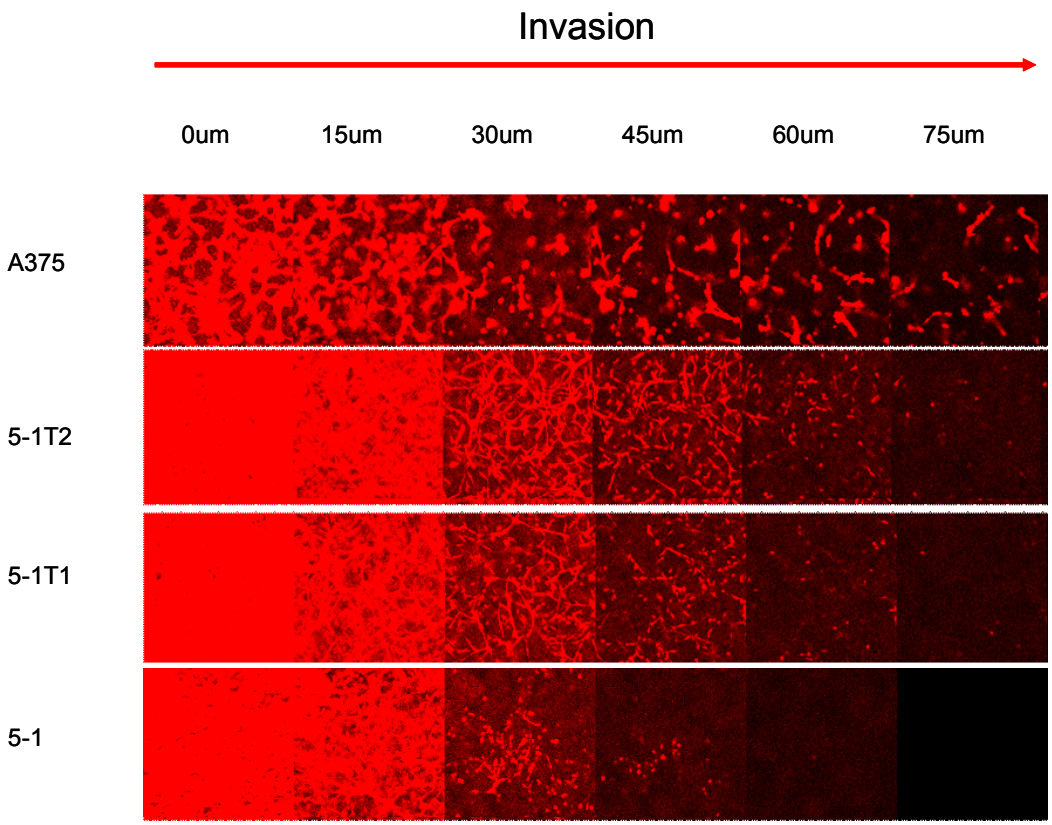
Invasion
0um
15um
30um
45um
60um
75um
A375
5-1T2
5-1T1
5-1

D

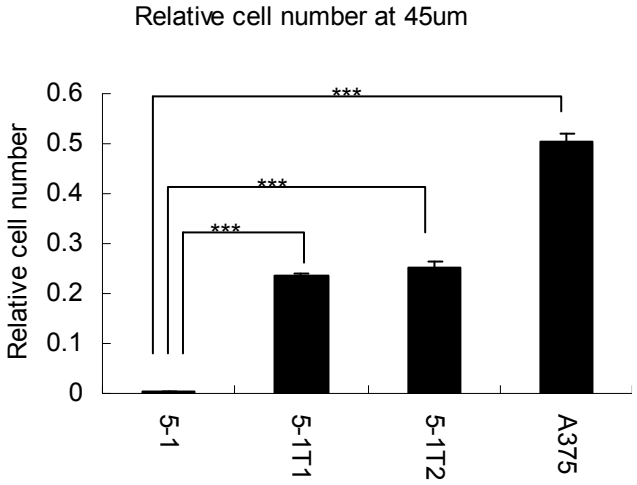

A, 3-1-1, 3-1-1T1, 3-1-1T2 and A375 were seeded on transwell filters and allowed to invade through Matrigel along a serum gradient. After 96 hours cells were labelled with calcein AM and visualized in the Matrigel at 15µm intervals by Olympus FV1000 confocal microscopy.

B, Histogram shows the quantitation of invasion at 45um for panel A. The amount of dye (positive pixels) was calculated for each z-section using Image J software, and expressed relative to the signal in the section that represented the base of the transwell filter. One way ANOVA with Bonferroni's Multiple Comparison Test was applied for statistical analysis between 3-1-1 and 3-1-1T1, 3-1-1T2, A375. *, $P < 0.05$. **, $P < 0.01$.***, $P < 0.001$.

C, 5-1, 5-1T1, 5-1T2 and A375 were seeded on transwell filters and allowed to invade through Matrigel along a serum gradient. After 96 hours cells were labelled with calcein AM and visualized in the Matrigel at 15µm intervals by Olympus FV1000 confocal microscopy.

D, Histogram shows the quantitation of invasion at 45um for panel C. The amount of dye (positive pixels) was calculated for each z-section using Image J software, and expressed relative to the signal in the section that represented the base of the transwell filter. One way ANOVA with Bonferroni's Multiple Comparison Test was applied for statistical analysis between 5-1 and 5-1T1, 5-1T2, A375. ***, $P < 0.001$.

3.3 Discussion

To begin the characterization of our mouse melanocyte cell lines, we investigated the expression of a series of cell cycle control and proliferation markers by western-blotting: p-ERK, p-MEK, DUSP6, P-AKT, PTEN and p16.

The MAPK pathway plays an important role in various cellular responses, including cell proliferation, differentiation, survival and apoptosis. Constitutive activation of the MAPK pathway seemed to link with development and progression of tumours (Ramos 2008). Therefore, the activation of the MAPK pathway in our mouse melanocyte cell lines was examined. To our surprise, the results indicated that our tumourigenic cell lines have lower expression of p-ERK than their parental cell lines 5-1 and 3-1-1. Our results agreed with a report that ERK was phosphorylated in only a minority of melanoma cells. This report showed regulated MAP kinase signalling in the majority of tumour cells rather than a continuous activation of this pathway (Houben et al. 2008). In contrast, it was reported that ERK phosphorylation appeared in the majority of cutaneous melanoma (Cohen et al. 2002). However, the authors did not report on the proportion of phospho-ERK-positive tumour cells. Recently Zhuang described that about 65% and 77% of cells were phospho-ERK-positive in melanomas (Zhuang et al. 2005). While Uribe showed that ERK phosphorylation was detected in only a low proportion of melanoma cells. Moreover, 15% of the primary tumours were completely p-ERK negative (Uribe et al. 2006). Rarely, a high proportion of phospho-ERK-positive cells were observed in metastatic melanoma (Mirmohammadsadegh et al. 2007).

As described previously, in xenograft experiments, A375 formed tumours very quickly, while 5-1 and 3-1-1 formed tumours very slowly. However when we xenografted 3-1-1 Tumour 1a into mice again, it formed tumours much more quickly than 3-1-1. Is absence of p-ERK related to melanoma progression in this xenograft assay? The importance of absence of p-ERK in cancer progression had been

previously described in prostate cancer (Paweletz et al. 2001). Recently, a melanoma subtype with epithelial characteristics, which lacked p-ERK activation, had been reported (Curtin et al. 2006, Shields et al. 2007). Moreover, melanoma lacking activation of the RAS-RAF-MEK-ERK pathway had increased expression of cyclin–dependent kinase 4 (CDK4) and cyclin D1 (CCND 1) which were downstream components of the RAS and BRAF pathway. That implied that their upregulation can occur through alternative molecular mechanisms (Curtin et al. 2006). It was possible that our 5-1 and 3-1-1 tumourigenic cell lines with a low level of p-ERK had the same characteristics as these types of melanoma. The role of lower expression of p-ERK in melanoma progression in our mouse xenograft assay needed further investigation.

We next examined expression of p-MEK to assess the overall activation of the MAPK pathway. The result indicated that p-MEK expression levels of 5-1 tumour and 3-1-1 tumour cell lines are lower than their parental cell lines. Activation of MEKs can phosphorylate Tyr and Thr residues of ERKs, causing their activation. Moreover, ERKs seemed to be the only substrates of MEKs and these kinases served as the specificity determining components of ERKs (Shaul and Seger 2007). Therefore, the low expression of p-ERK in our tumour cell lines may be due to low levels of upstream MEK and our tumour cell lines possibly shut down the RAS-RAF-MEK-ERK pathway.

The delayed phase of ERK inactivation involves specific phosphatases with a dual specificity for Ser/Thr and Tyr. They are known as the dual specificity phosphatase (DUSP) family. While DUSP1 and DUSP4 are nuclear and dephosphorylate both ERKs and the p38 and JNK, DUSP6 is cytoplasmic and specific to the ERKs (Bluthgen et al. 2009). DUSP6 can dephosphorylate ERKs and reduce the expression of p-ERK. Upregulated genes in melanoma cell lines with MAPK pathway activation were described, including DUSP6 and Sprouty 2 (Bloethner et al. 2005). There was increasing evidence that DUSP6 may be abnormally regulated and so

dephosphorylate ERKs in tumours (Bermudez et al. 2010). We suspected that a signal for ERK inhibition in our tumour cell lines may come from DUSP6. Therefore, DUSP6 expression in our panel of cell lines was detected. As expected the level of DUSP6 was higher in the 3-1-1 and 5-1 tumour cell lines than their parent cell lines. However, whether over-expression of DUSP6 was a cause of the malignant phenotype rather than simply being a consequence of cell transformation was still unclear.

The inactivation of the MAPK pathway in our mouse tumourigenic cell lines leaves room for speculation that other pathways may contribute to melanoma progression in the mouse xenograft assay. Previous studies showed that the PI3K-AKT pathway was an established regulator of cell survival in many human cancers (Cully et al. 2006, Hennessy et al. 2005). High expression of p-AKT was correlated with melanoma progression and worse patient survival in melanomas (Dai et al. 2005). Importantly, phosphorylation of RAF by AKT inhibited activation of the MAPK pathway and changed the cellular response in a human breast cancer cell line from cell cycle arrest to proliferation (Zimmermann and Moelling 1999). Therefore, we speculated that inactivation of the MAPK pathway in our tumour cell lines may arise because of hyperactivation of the P13K pathway. However, our result indicated that 5-1 and 3-1-1 had higher expression of p-AKT than 5-1 and 3-1-1 tumourigenic cell derivatives. The cell lines with a low level of p-ERK had lower expression of p-AKT as well. These data suggested that the PI3K-AKT pathway was not activated in our tumour cell lines and there was not a simple relationship between levels of p-AKT and p-ERK and tumourigenesis. The reasons for the possible high molecular weight of p-AKT in the 3-1-1 tumourigenic cells compared to the 3-1-1 parental cells are not clear and needed further investigation.

PTEN (phosphatase and tensin homolog deleted on chromosome 10) functioned as a highly effective tumour suppressor in a wide variety of tumour tissues (Suzuki et al. 2008) by regulating the PI3K/AKT pathway (Maehama and Dixon 1998). Loss of

PTEN had been implicated in the development of melanoma (Wu et al. 2003) and a high frequency of PTEN mutations had been detected in malignant melanomas (Bonneau and Longy 2000). The potential genetic interaction among NRAS, BRAF, and PTEN may play a critical role in melanoma development. PTEN expression was also detected in our cell line panel by western blot. PTEN expression was equal in all our cell lines and there was no evidence for any PTEN loss.

Mutations in BRAF were found through the genome-wide cancer sequencing programe, and were reported to occur in 50-70% of human melanoma. One specific mutation was V600E BRAF mutation, accounting for more than 90% of all BRAF mutations in melanoma (Dahl and Guldberg 2007). However whether BRAF mutations occurred in mouse melanoma was not clear. We did not find any activating mutations associated with melanoma in our immortal mouse cell lines. However, this study had some limitations. Firstly, we did not have a mouse BRAF mutation positive control. Secondly, we only sequenced exon 14 and exon 18 of the mouse BRAF gene not the whole mouse BRAF sequence. Although these exons were equivalent to exon 15 and exon 11 of human BRAF gene where mutations were most frequently found, we can not rule out that mouse BRAF mutations occurred in other exons in our cell lines.

Our results also showed that derivatives of another immortal mouse melanocyte cell line, #13, which remained static for an extensive period had all lost p16 expression, while 5-1 and 3-1-1 which grew rapidly had retained high expression of p16. This was in contrast to a previous study which showed that p16 played a very important role in cell senescence and the absence of p16 may favour melanoma progression (Sviderskaya et al. 2002). A possibility was that although derivatives of the immortal mouse melanocyte cell line, #13, had lost p16, there were other tumour suppressors associated with melanocyte senescence that retarded cell growth. The p53 tumour suppressor was mutated or otherwise inactivated in a wide range of human cancers (Dahl and Guldberg 2007). Recently, a powerful genetic model of murine melanoma was established to assess the functional roles of p53 and ARF in murine

melanomagenesis. The result demonstrated p53-independent tumour suppressive activity of ARF. ARF can function as a melanoma tumour suppressor in the absence of p53 (Widlund and Fisher 2007). We can not rule out the possibility that p53 and ARF rather than p16 were responsible for the senescence of our mouse melanocyte cell line 13 and its derivatives.

The methylcellulose assay and transwell migration assays showed the tumourigenetic and invasive ability of our mouse tumourigenic cells. Our results indicated that 5-1 and 3-1-1 tumourigenic cell lines formed larger and more colonies in the methylcellulose assay compared to their parent cell lines 3-1-1 and 5-1. Moreover, 5-1 and 3-1-1 tumour cell lines invaded further than their parental cell lines 3-1-1 and 5-1 in transwell migration assays. These agreed with our previous study that our mouse tumourigenic cell lines formed tumours more quickly than their parental cell line in the mouse xenograft assay. Furthermore, the methylcellulose assay and transwell migration assay provided good tools to detect biologic characteristics of our immortal mouse cell lines. These two assays can be used to examine tumourigenic changes following transfection in vitro.

To sum up, we identified a subtype of mouse melanoma cell lines in our mouse xenograft assay. These cell lines showed several characteristics that were uncommon in classic melanoma: (A) decreased ERK activation and MEK activation; (B) increased expression of DUSP6; (C) decreased levels of p-AKT; (D) without BRAF mutation; (F) without PTEN deletion. These data suggested that these mouse tumourigenic cell lines represented a molecularly distinct and unappreciated subtype of melanoma. Meanwhile, through analysis of our immortal mouse cell lines, we raised two main questions: firstly, is a lower level of p-ERK and higher expression of DUSP6 in our mouse tumourigenic cell lines related to melanoma progression in the mouse xenograft model? Secondly, why do the #13 cell line and its derivatives without p16 grow so poorly? Further investigations on our immortal mouse cell lines were needed.

Chapter 4

Roles of DUSP6 in melanoma progression

4.1 Introduction

During the progression of melanomagenesis, melanoma cells escape the normal cell growth and control systems and gain the ability to invade the surrounding tissues and organs. The RAS/RAF/MEK/ERK pathway plays an important role in cell growth, cell survival and invasion (Smalley 2003). Melanoma is known to harbour activating mutations in both RAS and BRAF (Dahl and Guldberg 2007), however the extent to which activation of their downstream factor ERK1/2 contributes to melanoma progression is still controversial.

The MKPs constitute a distinct subgroup of ten catalytically active enzymes within the larger family of cysteine-dependent dual-specificity protein phosphatases. The discovery of most of the DUSPs has occurred in the last 7 years, initiating a large amount of interest in their role and regulation. Recently, studies showed that DUSP6, dual-specificity phosphatase 6, was a negative feedback regulator for the Ras/Raf/MEK/ERK pathway, playing important roles in the maintenance of cellular homeostasis in response to growth factors (Amit et al. 2007, Bermudez et al. 2010). Disruption of this feedback loop could therefore cause neoplastic, and even malignant, transformation (Bermudez et al. 2010, Patterson et al. 2009). However, there have been few reports investigating the significance of DUSP6 in melanoma progression.

My previous work had identified lower p-ERK expression and higher DUSP6 expression in mouse melanocytes which formed tumours very quickly in a mouse xenograft assay compared to the non-tumourigenic parental melanocyte lines. The aims of the work in this chapter were to examine: firstly, whether the high level of DUSP6 was related to melanoma progression in the xenograft assay; secondly, whether absence of p-ERK contributed to melanoma progression in the xenograft assay.

4.2 Results

4.2.1 DUSP6 is a negative regulator of ERK1/2 in our mouse melanocytes

Previous studies showed that DUSP6 acted as a negative regulator of the MAPK pathway in pancreatic cancer, ovarian cancer and lung cancer (Keyse 2008). In our study, our mouse melanocye tumour cell lines expressed high DUSP6 but low phospho-ERK1/2 expression levels. We suspected that overexpression of DUSP6 resulted in reduction of phospho-ERK1/2 in our mouse tumour cell lines.

To investigate the regulatory mechanism of DUSP6 on ERK1/2 in our mouse melanocyte cell lines, the *pcDNA3.1*/*V5*-*His*-*DUSP6*/MKP-3 vector was introduced by electroporation into the 5-1 non-tumourigenic cell line which had low levels of DUSP6. This plasmid was able to express a histidine and V5 tagged version of DUSP6 from the human cytomegalovirus (CMV) promoter and also contained a neomycin selectable marker. Electroporation was used because, unlike some other transfection methods, it has no reagent-induced cytotoxicity towards the cells and can achieve good transfection efficiencies in our immortal mouse melanocytes. The 5-1 cell line was selected for the following studies, because 5-1 and its tumour derivatives showed larger difference in the methylcellose assay and the transwell-migration assay compared to the 3-1-1 series. Cells with stable expression of DUSP6 were selected with G418 for 7 days. About 100 pooled resistant colonies were used for western analyses. The DUSP6 expression level of pooled resistant colonies detected by western blot showed a better measure of the average DUSP6 expression of resistant colonies than measurements on individual colonies, where DUSP6 expression could be dependent on specific position effects on the integrated transgene in different colonies.

Protein lysates obtained from 5-1, 5-1 DUSP6 transfection pool, 5-1T1 and 5-1T2 were subjected to western blot analysis using DUSP6 antibody to detect DUSP6 expression and an anti-phospho-ERK antibody to detect p-ERK1 (42KD) and p-ERK2 (44KD). Total ERK and GAPDH levels of these samples were also determined by western blot to correct for different amounts of protein in the various samples. As described before, 5-1 expressed low levels of DUSP6 and high levels of phospho-ERK1/2, while 5-1 tumour cell lines expressed a high level of DUSP6 and a low level of phospho-ERK1/2 (Fig. 4.1A). Quantification analysis showed that DUSP6 expression increased 7-fold for 5-1 tumourigenic cell lines compared to 5-1, while the expression level of phospho-ERK1/2 reduced around 10-fold for tumourigenic cell lines compared to 5-1 (Fig. 4.1B, Fig 4.1C). Moreover, the DUSP6 expression level dramatically increased in the 5-1 DUSP6 transfection pool compared to non-transfected 5-1 cells as expected. Ectopic expression of DUSP6 in 5-1 cells reduced the expression level of phospho-ERK1/2 to that seen in 5-1 T1 and T2 (Fig. 4.1A). Quantification analysis showed that DUSP6 expression increased 6-fold for 5-1 DUSP6 transfection pool compared to 5-1, while the expression level of phospho-ERK1/2 reduced around 10-fold for 5-1 DUSP6 transfection pool compared to 5-1 (Fig. 4.1B, Fig 4.1C). These data suggested that DUSP6 negatively regulated ERK1/2 in our mouse melanocyte cell lines.

Figure 4.1 DUSP6 is a negative regulator of ERK1/2 activity in mouse melanocyte cell lines

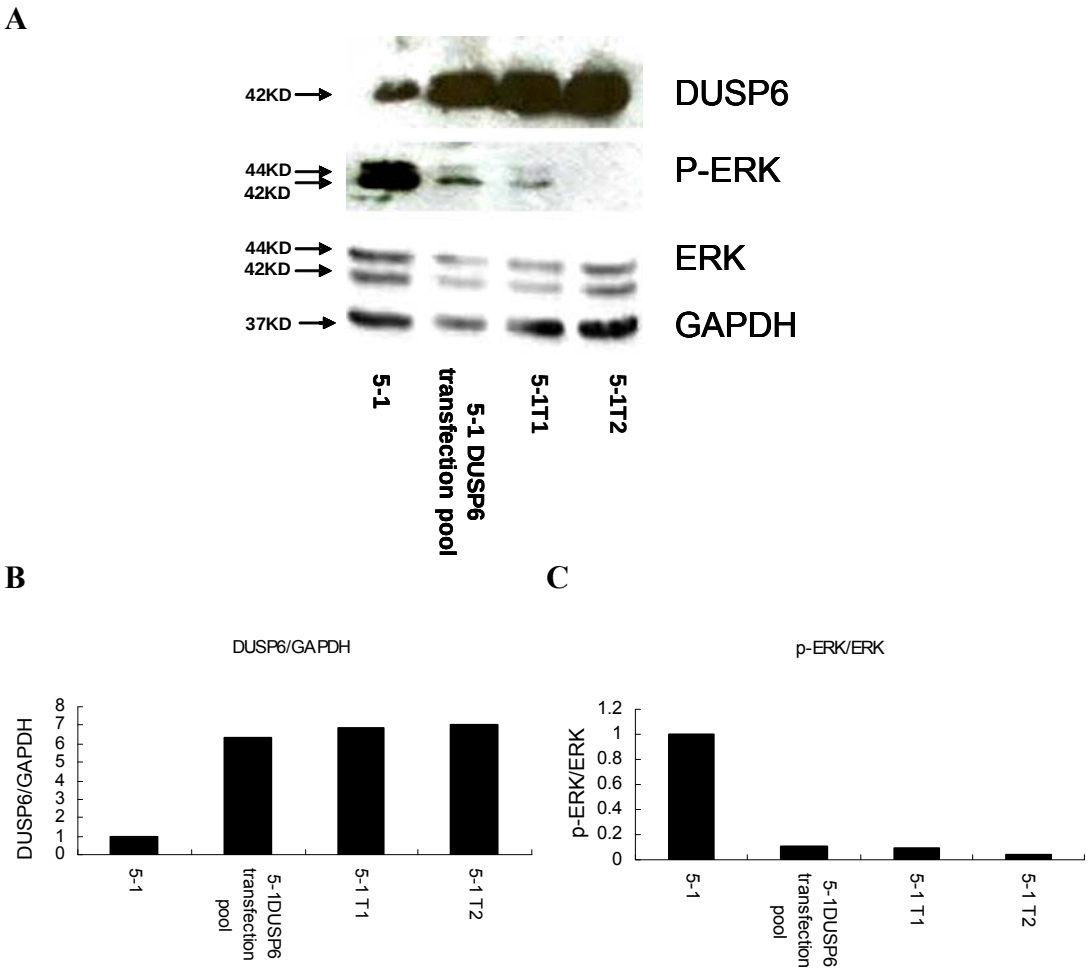

A, *pcDNA3.1/V5-His-DUSP6*/MKP-3 vector was transfected into 5-1 cells by electroporation. Western blots show protein levels of DUSP6 (top panel), phosphorylated ERK (p-ERK) (second panel), total ERK (third panel) and loading control GAPDH (bottom panel) in 5-1, 5-1 DUSP6 transfection pool, 5-1T1 and 5-1T2 cells. Stable overexpression of DUSP6 reduced phosphorylated ERK (P-ERK) level in the 5-1 DUSP6 transfection pool.

B, Histogram shows level of DUSP6. DUSP6 levels are expressed relative to loading control GAPDH and are normalized to 5-1.

C, Histogram shows level of phosphorylation ERK (p-ERK). p-ERK levels are expressed relative to total ERK levels and are normalized to 5-1.

4.2.2 Effect of DUSP6 on anchorage independent growth activity of our immortal mouse melanocytes

As described in Chapter 3, absence of DUSP6 may be associated with tumourigenicity in our mouse xenograft model. To determine the involvement of DUSP6 in melanoma progression of our immortal mouse cell lines, we assessed anchorage independent growth ability of the DUSP6 transfection pool by methylcellulose assay. 10000 cells of 5-1, 5-1 DUSP6 transfection pool, 5-1T1 and 5-1T2 were seeded into methylcellulose. Colony size and number were determined under the microscope every three days for 12 days in total. Image J software was used to analyze the relative colony size and colony number per photographic field at day 12. Minimum colony size cut off was set at 30um for Day 12.

The results showed that overexpression of DUSP6 stimulated colony formation in the methylcellulose assay. As described before in Chapter 3, the data collected from three independent experiments indicated that 5-1 tumour cell lines formed more and larger colonies than their parental cell line 5-1. Moreover, the DUSP6 transfection pool formed more and larger colonies than non-transfected 5-1 cells (Fig. 4.2A, Fig. 4.2D). Quantification analysis of microscope images by Image J indicated that the average colony size of DUSP6 transfection pool increased 5-fold compared to non-transfected 5-1 cells and the colony number of the DUSP6 transfection pool also increased nearly 3-fold compared to non-transfected 5-1 cells (Fig. 4.2B, Fig. 4.2C). This result suggests that high DUSP6 expression contributes to tumourigenicity of our mouse melanoma cells.

Figure 4.2 DUSP6 overexpression contributes to colony formation of our mouse melanocytes in the methylcellulose assay

A

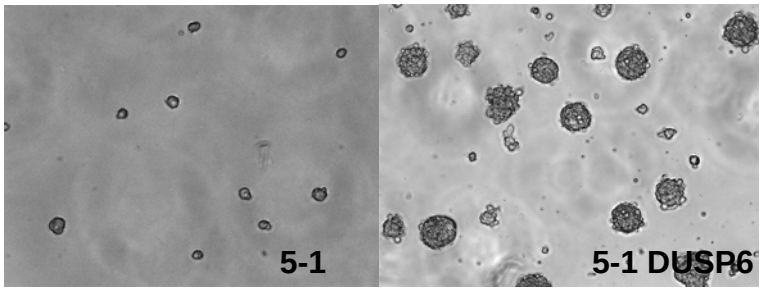

B

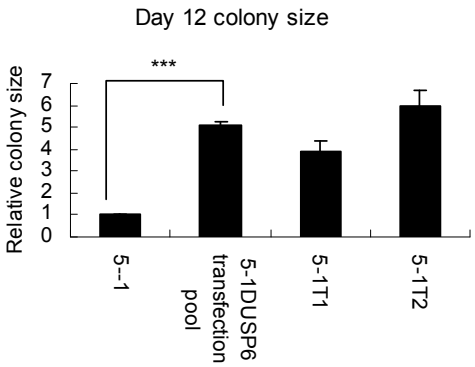

C

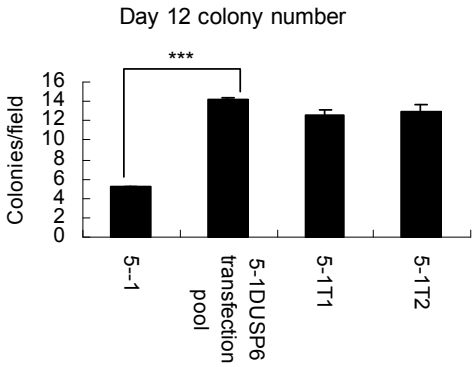

D

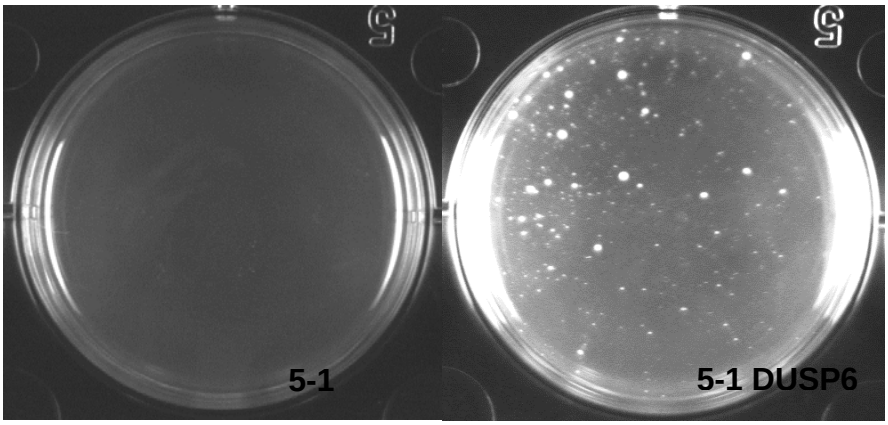

A, 5-1, 5-1 DUSP6 transfection pool, 5-1 T1 and 5-1 T2 were mixed with methylcellulose and seeded into 6-well plates to form colonies for 12 days. Images are representative of 5-1 and 5-1 DUSP6 transfection pool colonies at Day 12.

B, Average colony size of 5-1, 5-1 DUSP6 transfection pool, 5-1 T1 and 5-1 T2. Colony areas were measured with ImageJ software. Histogram shows mean colony size (± SEM) from three independent experiments. Average colony size of 5-1 DUSP6 transfection pool, 5-1 T1 and 5-1 T2 are standardized to 5-1. One way ANOVA with Bonferroni's Multiple Comparison Test was applied for statistical analysis between 5-1 and 5-1 DUSP6 transfection pool. ***, $P < 0.001$.

C, Total number of colonies counted per photographic field. Each field is approximately 0.59 mm^2 of culture dish. At least 6 fields were counted for each dish. Histogram shows mean colony number (± SEM) from three independent experiments. One way ANOVA with Bonferroni's Multiple Comparison Test was applied for statistical analysis between 5-1 and 5-1 DUSP6 transfection pool. ***, $P < 0.001$.

D, 5-1, 5-1 DUSP6 transfection pool, 5-1 T1 and 5-1 T2 were mixed with methylcellulose and seeded into 6-well plates to form colonies for 12 days. Photos are representative of entire wells from 5-1 and 5-1 DUSP6 transfection pool at Day 12 .

4.2.3 Effect of DUSP6 on invasive ability of immortal mouse melanocytes

As we had demonstrated in Chapter 3 that our mouse tumour cell lines with high levels of DUSP6 invaded further in the transwell-migration assay than their parental non-tumourigenic cell lines, we hypothesized that the DUSP6 transfection pool had enhanced capacity for invasion compared to non-transfected 5-1 cells. We therefore utilized the quantitative in vitro invasion assay to assess the ability of the DUSP6 transfection pool to invade into matrigel in response to a chemotactic stimulus (in this case 10% serum). 5-1, 5-1 DUSP6 transfection pool, 5-1T1 and 5-1T2 were seeded onto transwell filters. After 72 hours, cells were labelled with calcein AM dye, and visualized in the matrigel at 15um intervals by confocal sectioning. The relative cell number invading at 45um into 3D-gels was expressed relative to the cell number in the section that represented the base of the transwell filter. As described before, 5-1 tumour cell lines invaded further than 5-1 in matrigel. The relative cell number at 45um was around 0.37 for the tumour lines, compared to only 0.002 for 5-1. Moreover, the 5-1 DUSP6 transfection pool also displayed much more chemotactic

invasion relative to non-transfected 5-1 (Fig. 4.3A). Quantification analysis indicated that relative cell number of 5-1 DUSP6 transfection pool at 45um into 3D-gels was 0.15, 55-fold more than non-transfected 5-1 (Fig. 4.3B). These data showed that 5-1 DUSP6 transfection pool had similar increased invasive ablility as the 5-1 tumour cell lines and the increased DUSP6 expression was needed for invasion of our mouse melanoma cells.

Figure 4.3 DUSP6 is needed for mouse melanocyte invasion

A

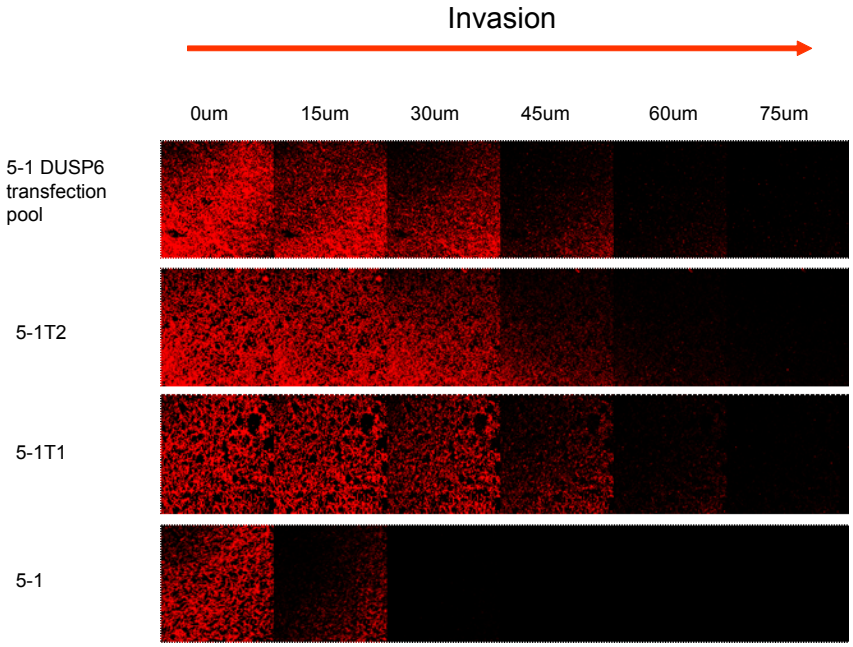

B

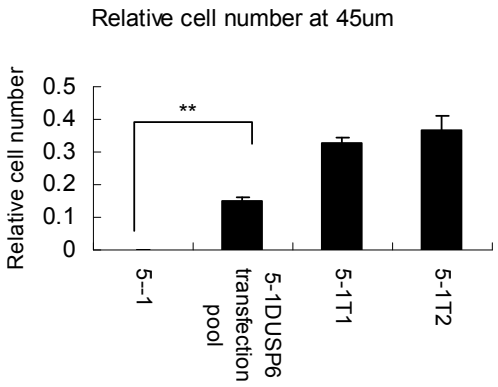

A, 5-1, 5-1 T1, 5-1 T2 and 5-1 DUSP6 transfection cells were seeded on transwell filters and allowed to invade through Matrigel along a serum gradient. After 96 hours cells were labelled

with calcein AM and visualized in the Matrigel at 15μm intervals by Olympus FV1000 confocal microscopy.

B, Histogram shows the quantitation of invasion at 45um. The amount of dye (positive pixels) was calculated for each z-section using Image J software, and expressed relative to the signal in the section that represented the base of the transwell filter. One way ANOVA with Bonferroni's Multiple Comparison Test was applied for statistical analysis between 5-1 and 5-1 DUSP6 transfection pool. **, $P < 0.01$.

4.2.4 Constitutive activation of MEK1/2 increases phosphorylation of ERK1/2 in our mouse tumour cells

As described in Chapter 3, our mouse tumour cell lines had lower phosphorylation levels of ERK1/2 than their parental cell lines, but formed tumours more quickly in the xenograft assay and displayed enhanced anchorage independent-growth and invasive abilities. Therefore, we suspected that lower phosphorylation levels of ERK1/2 may contribute to melanoma progression in our mouse xenograft model.

To investigate the functional significance of ERK1/2 activation in our mouse tumour cell lines, we ectopically expressed constitutively active versions of MEK1 and MEK2 in the 5-1 T2 cell line which had low expression of p-ERK. The pMCL-MKK1-R4F and pMCL-MKK2-KW71A plasmids were able to express the constitutively actived form of MEK1 and MEK2 from the CMV promoter. They also contained a hygromycin selectable marker. MEK1 and MEK2 are the upstream activators of ERK1 and ERK2 (Cobb 1999). Introduction of constitutively active MEK1 and MEK2 can result in increased phosphorylation of ERK1/2 (Seger et al. 1992). The 5-1 T2 cell line was selected for subsequent experiments because 5-1 T2 and its parental cell line 5-1 showed larger differences in the methylcellose assay and transwell migration assay compared to the 3-1-1 series. Polyclonal populations of transfected clones were selected in Hygromycin and used for subsequent studies. Expression of ectopic MEK1 and MEK2 in the 5-1T2 transfected population was

confirmed by western blotting. A recent study indicated that the activation of the MAPK pathway can increase the expression of DUSP6 through regulation of transcriptional factor ETS2 (Furukawa et al. 2008). To investigate whether activation of the MAPK pathway by expression of ectopic MEK1 and MEK2 can regulate DUSP6 expression in the 5-1T2 cell line, DUSP6 levels were also detected by western blotting.

Protein lysates obtained from 5-1, 5-1T1, 5-1T2 and 5-1T2 MEK1 and MEK2 transfection pool were subjected to western blot analysis using an anti-phospho-MEK antibody to detect p-MEK1/2 (45KD) expression, an anti-phospho-ERK antibody to detect p-ERK1 (42KD) and p-ERK2 (44KD) expression and a DUSP6 antibody to detect DUSP6 expression. Total MEK1/2, ERK and GAPDH levels of these samples were also determined by western blot to correct for different amounts of protein in the various samples. As described before, 5-1 had high levels of phosphorylated MEK1/2 and ERK1/2 but low levels of DUSP6, while 5-1 tumour cell lines expressed low levels of phospho-MEK1/2 and phospho-ERK1/2 but high levels of DUSP6 (Fig. 4.4A). Quantification analysis showed that the ratio of phospho-MEK1/2 over total MEK1/2 was 1.7 for 5-1, compared to 0 for 5-1 tumourigenic cell lines, while the expression level of phospho-ERK1/2 reduced around 12-fold for tumourigenic cell lines compared to 5-1 (Fig 4.4B, Fig 4.4C). The ratio of DUSP6 over GAPDH was around 6-fold increased for tumourigenic cell lines compared to 5-1 (Fig 4.4D). Moreover, ectopic expression of constitutively active MEK1/2 dramatically increased the phosphorylation level of MEK1/2 which resulted in activation of ERK1/2 as expected (Fig. 4.4A). In addition, the activation of the MAPK pathway in 5-1T2 MEK1 and MEK2 transfection pool upregulated DUSP6 expression as expected (Fig. 4.4A). Quantification analysis showed that the ratio of phospho-MEK1/2 over total MEK1/2 was 3.2 for the 5-1 T2 MEK1 and MEK2 transfection pool, compared to 0 for non-transfected 5-1 T2, while expression level of phospho-ERK1/2 increased around 13-fold for the 5-1 T2 MEK1 and MEK2 transfection pool compared to non-transfected 5-1 T2 (Fig 4.4B, Fig 4.4C). In

addition, the ratio of DUSP6 over GAPDH increased almost 2-fold for the 5-1 T2 MEK1 and MEK2 transfection pool compared to non-transfected 5-1 T2.

Figure 4.4 MEK1/2 is a positive regulator of ERK1/2 activity in transformed mouse melanocytes

A

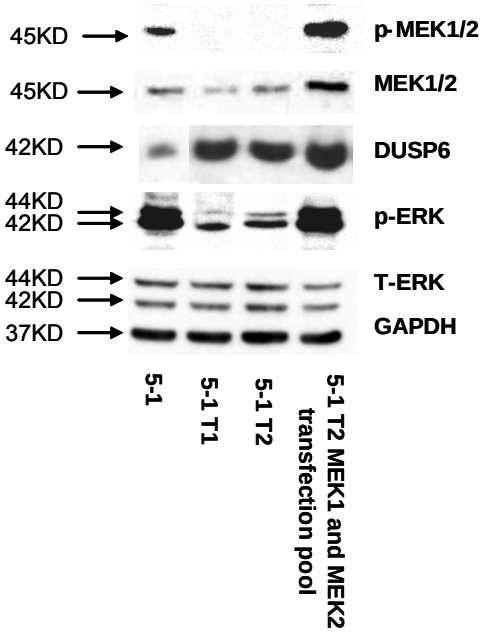

B

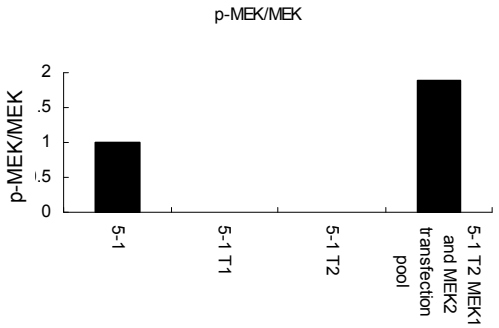

C

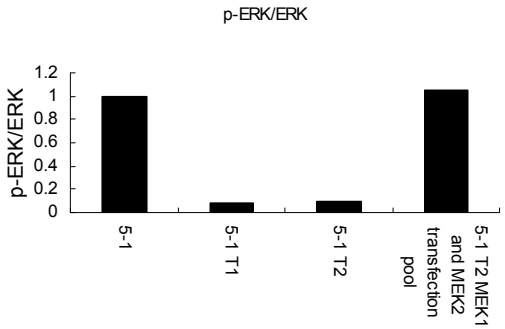

D

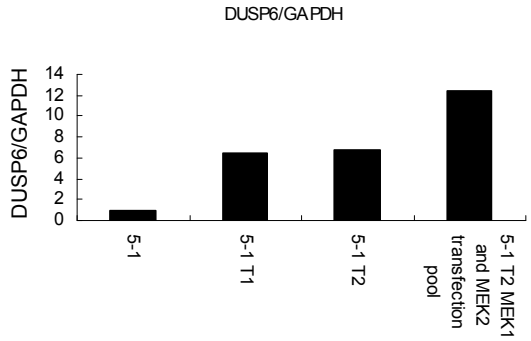

A, MEK1 and MEK2 vectors were transfected together into 5-1T2 cells by electroporation. Western blots show protein levels of phosphorylated MEK1/2 (p-MEK1/2) (top panel), total MEK (second panel), phosphorylated ERK (p-ERK) (third panel), total ERK (fourth panel) and loading control GAPDH (bottom panel) in 5-1, 5-1T1 and 5-1T2 and 5-1T2 MEK1 and MEK2 transfection pool. Increased levels of p-MEK led to increased phosphorylated ERK (P-ERK) and DUSP6 levels in the 5-1T2 MEK1 and MEK2 transfection pool.

B, Histogram shows level of phosphorylation of MEK1/2 (p-MEK1/2). p-MEK1/2 levels are expressed relative to total MEK1/2 levels and are normalized to 5-1.

C, Histogram shows level of phosphorylation of ERK (p-ERK). p-ERK levels are expressed relative to total ERK levels and are normalized to 5-1.

D, Histogram shows level of DUSP6. DUSP6 levels are expressed relative to GAPDH levels and are normalized to 5-1.

4.2.5 Effect of constitutive activation of MEK1/2 on anchorage independent growth activity of transformed mouse melanocytes

To determine the involvement of ERK1/2 in melanoma progression of our immortal mouse melanocytes, we assessed the anchorage independent growth ability of the constitutively activated MEK1/2 transfection pool by methylcellulose assay. 10000 cells of 5-1, 5-1T1, 5-1T2 and 5-1T2 MEK1/2 transfection pool were seeded into methylcellulose. Colony size and number were detected under the microscope every

three days for 12 days in total. Image J software was used to analyze the relative colony size and colony number per photographic field at day 12. Minimum colony size cut off was set at 30um for Day 12.

The results showed that enforced expression of constitutively active MEK1/2 slightly decreased colony size and total colony number, but this reduction was not significant in the methylcellulose assay. As described before, the data collected from three independent experiments indicated that 5-1 tumour cell lines formed more and larger colonies than their parental cell line 5-1. Moreover, the 5-1T2 MEK1/2 transfection pool formed less and smaller colonies than non-transfected 5-1T2 cells (Fig. 4.5A, Fig 4.5D). Quantification analysis indicated that the average colony size and total colony number of 5-1T2 MEK1/2 transfection pool slightly decreased compared to non-tansfected 5-1T2 cells (Fig. 4.5B, Fig. 4.5C). However, one way ANOVA with Bonferroni's Multiple Comparison Test statistical analysis showed that there was no significant difference between 5-1T2 and 5-1T2 MEK1/2 transfection pool in the methylcellulose assay.

Figure 4.5 Increased p-MEK levels do not inhibit colony formation of our transformed mouse melanocytes

A

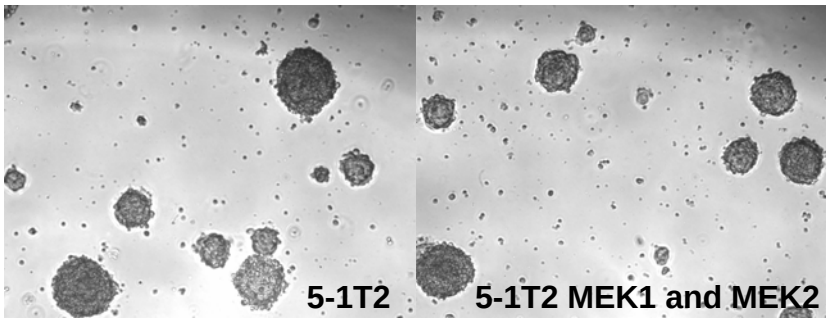

B

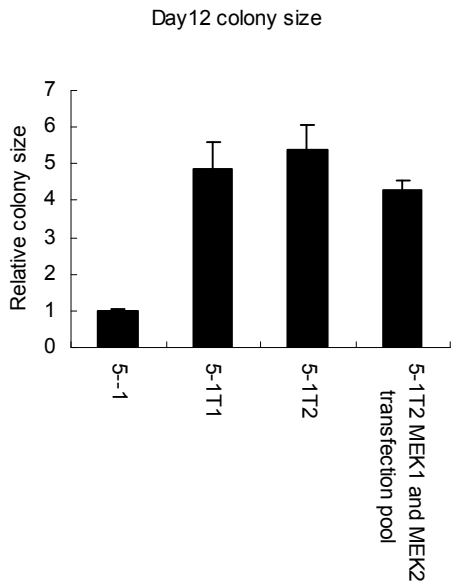

C

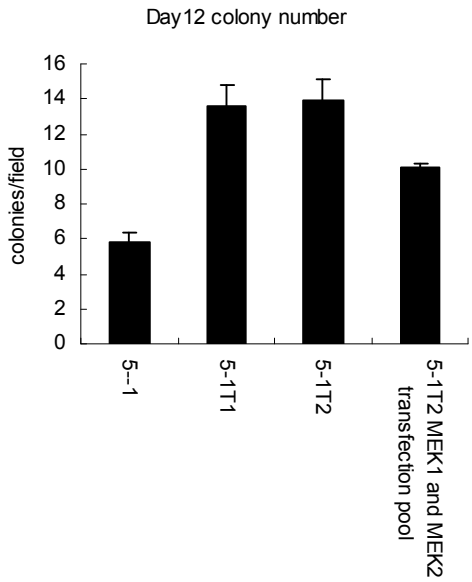

D

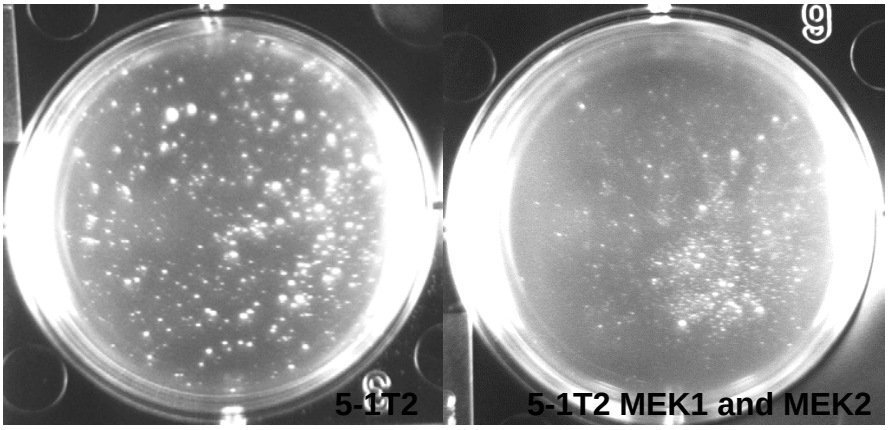

A, 5-1, 5-1T1, 5-1T2 and 5-1T2 MEK1/2 transfection pool were mixed with methylcellulose and seeded into 6 well-plates to form colonies for 12 days. Photos are representative of 5-1T2 and 5-1T2 MEK1/2 transfection colonies pool at Day 12.

B, Average colony size of 5-1, 5-1T1, 5-1T2 and 5-1T2 MEK1 and MEK2 transfection pool. Colony areas were measured with ImageJ software. Histogram shows mean colony size (± SEM) from three independent experiments. Average colony size of 5-1T1, 5-1 T2 and 5-1T2 MEK1/2 transfection pool are standardised to 5-1. One way ANOVA with Bonferroni's Multiple Comparison Test was applied for statistical analysis. There was no significant difference between 5-1T2 and 5-1T2 MEK1/2 transfection pool.

C, Total number of colonies counted per photographic field. Each field is approximately 0.59 mm^2 of culture dish. At least 6 fields were counted for each dish. Histogram shows mean colony number (± SEM) from three independent experiments. One way ANOVA with Bonferroni's Multiple Comparison Test was applied for statistical analysis. There was no significant difference between 5-1T2 and 5-1T2 MEK1/2 transfection pool.

D, 5-1, 5-1T1, 5-1T2 and 5-1T2 MEK1/2 transfection pool were mixed with methylcellulose and seeded into 6-well plates to form colonies for 12 days. Photos are representative of an entire well from 5-1T2 and 5-1T2 MEK1/2 transfection pool at Day 12.

4.2.6 Effect of constitutive active MEK1/2 on invasive ability of transformed mouse melanncytes

As demonstrated in Chapter 3, our mouse tumour cell lines with lower phosphorylation levels of ERK1/2 can invade further in matrigel than their parental cell lines, we hypothesized that lower expression of ERK1/2 may be involved in invasion of our mouse tumour cell line. Therefore, we introduced constitutively active MEK1/2 into the 5-1 tumour cell line to activate ERK1/2. A quantitative in vitro invasion assay was used to assess the ability of the MEK1/2 transfection pool to invade into matrigel in response to a chemotactic stimulus (in this case 10% serum). 5-1, 5-1T1, 5-1T2 and 5-1T2 MEK1 and MEK2 transfection pool were seeded onto transwell filters. After 72 hours, cells were labelled with calcein AM dye and visualized in the matrigel at 15um intervals by confocal sectioning. The cell number invading at 45um into 3D-gels was expressed relative to the cell number in the section that represented the base of the transwell filter. As described before, 5-1T1 and 5-1T2 invaded further than 5-1 in matrigel. The relative cell number at 45um was around 0.20 for the tumour lines, compared to 0.026 for 5-1. Moreover, ectopic expression of constitutively active MEK1/2 significantly suppressed the invasive capacity of 5-1T2 cells (Fig. 4.5A). Quantification analysis indicated that the relative cell number of 5-1T2 MEK1/2 transfection pool at 45um into 3D-gels was 0.07, 3-fold less than non-transfected 5-1T2 cells (Fig. 4.5B). These data showed that 5-1T2

MEK1/2 transfection pool had similar reduced invasive ablility as 5-1 and that lower levels of p-ERK may contribute to invasive ablility of our mouse melanocytes.

Figure 4.6 Increased levels of p-MEK1/2 are needed for inhibition of mouse melanocyte invasion

A

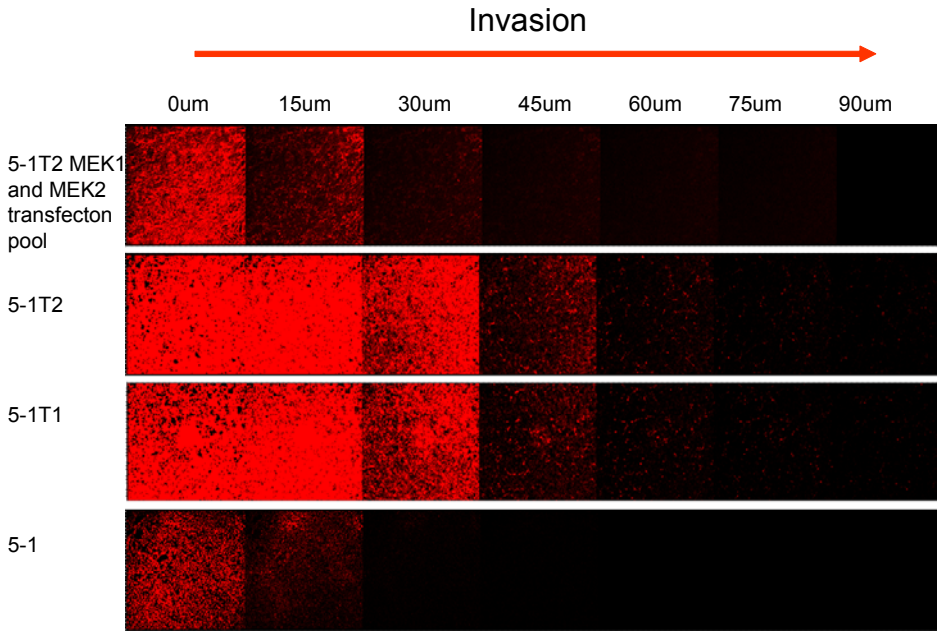

B

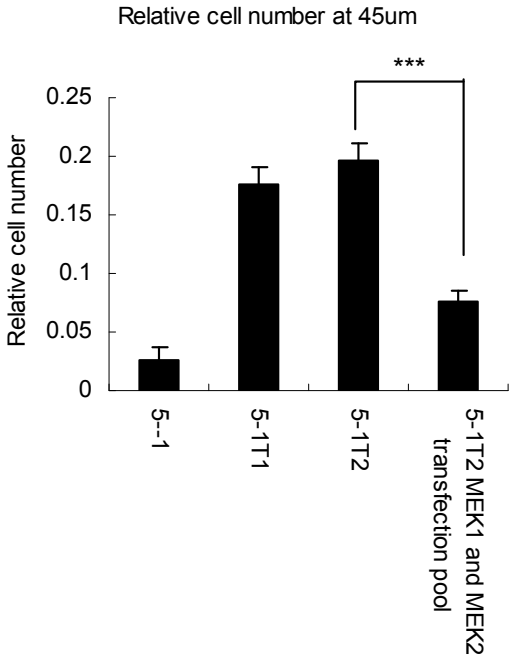

A, 5-1, 5-1 T1, 5-1 T2 and 5-1T2 MEK1 and MEK2 transfection pool cells were seeded on transwell filters and allowed to invade through Matrigel along a serum gradient. After 96 hours cells were labelled with calcein AM and visualized in the Matrigel at 15μm intervals by Olympus FV1000 confocal microscopy.

B, Histogram shows the quantitation of invasion at 45um. The amount of dye (positive pixels) was calculated for each z-section using Image J software, and expressed relative to the signal in the section that represented the base of the transwell filter. One way ANOVA with Bonferroni's Multiple Comparison Test was applied for statistical analysis between 5-1T2 and 5-1T2 MEK1/2 transfection pool. ***, $P < 0.001$.

4.2.7 DUSP6 is a negative regulator of ERK1/2 in human melanoma cells

Our study already showed that DUSP6 overexpression increased the tumourigenic potential of our transformed mouse melanocytes. To investigate the effect of DUSP6 in classic human melanoma cells, the *pcDNA3.1/V5-His-DUSP6*/MKP-3 vector was introduced into the A375 human melanoma cell line by CaPO4 transfection. This plasmid was able to express a histidine and V5 tagged version of DUSP6 from the CMV promoter and also contained a neomycin selectable marker. A375 was selected for this study as it was a classic human melanoma cell line harbouring the BRAF V600E mutation which occurs in around 70% of human melanoma patients. The calcium phosphate transfection method is generally used to generate stably transfected cell lines, allowing for long term gene expression studies. However one of the disadvantages of this transfection method is its toxicity especially to some cell types. A375 cells were better able to withstand the reagent-induced toxicity while our immortal mouse melanocytes could not survive in the culture medium with CaPO4. A375 cells stably expressing DUSP6 were selected with G418 for 7 days. As before, the pooled resistant colonies were used for western analyses.

Protein lysates obtained from two independent A375 dishes: A375 1 and A375 2, and A375 DUSP6 transfected pool 3 and A375 DUSP6 transfected pool 4 were subjected to western blot analysis using a DUSP6 antibody to detect DUSP6 expression and an anti-phospho-ERK antibody to detect p-ERK1 (42KD) and p-ERK2 (44KD). Total ERK and GAPDH levels of these samples were also determined by western blot to correct for different amounts of protein in the various samples. Our data indicated that the DUSP6 expression levels dramatically increased in A375 DUSP6 transfection pools compared to non-transfected A375 cells as expected (Fig. 4.7A). Quantification analysis showed that DUSP6 expression increased 2 to 3.2-fold for DUSP6 transfection pool compared to non-transfected A375 (Fig. 4.7B). Ectopic expression of DUSP6 in A375 cells reduced the expression levels of phospho-ERK1/2 (Fig. 4.7A) Quantification analysis showed that the level of p-ERK reduced 2 to 3-fold for DUSP6 transfection pools compared to non-transfected A375 (Fig. 4.7C). These data suggested that DUSP6 negatively regulated ERK1/2 in human melanoma cells as well.

Figure 4.7 DUSP6 is a negative regulator of ERK1/2 activity in human melanoma cells

A

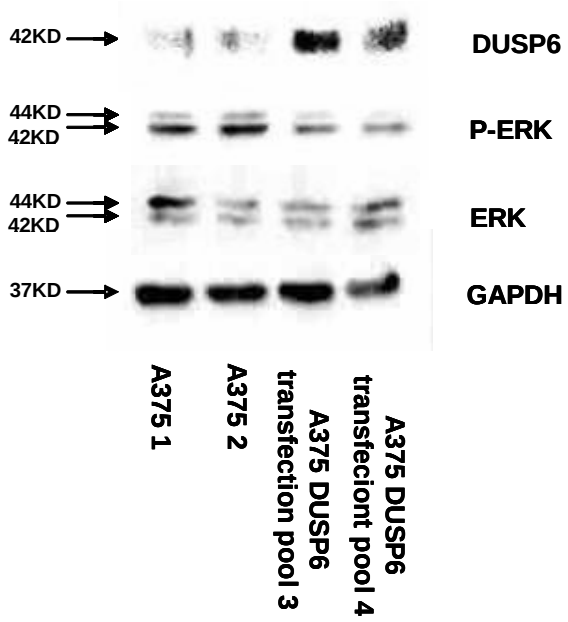

B **C**

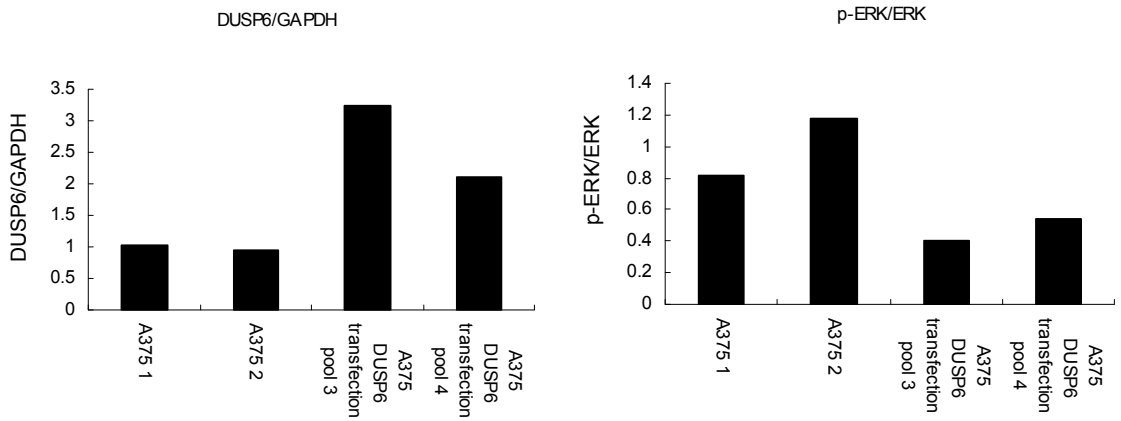

A, The *pcDNA3.1/V5-His-DUSP6*/MKP-3 vector was transfected into A375 cells by CaPO4. Western blots show protein levels of DUSP6 (top panel), phosphorylated ERK (p-ERK) (second panel), total ERK (third panel) and loading control GAPDH (bottom panel) in A375 1, A375 2, A375 DUSP6 transfection pool 3 and A375 DUSP6 transfection pool 4. Stable overexpression of DUSP6 reduced phosphorylated ERK (P-ERK) level in the A375 DUSP6 transfection pools.

B, Histogram shows level of DUSP6. DUSP6 levels are expressed relative to loading control GAPDH and are normalized to mean level of A375 1 and A375 2.

C, Histogram shows level of phosphorylation of ERK (p-ERK). p-ERK levels are expressed relative to total ERK levels and are normalized to mean level of A375 1 and A375 2.

4.2.8 Effect of DUSP6 on anchorage independent growth activity of human melanoma cells

In our distinct subtype of mouse melanoma, DUSP6 played an important role in colony formation in methylcellulose. To investigate whether DUSP6 was also involved in colony formation in classic human melanoma cells, we assessed anchorage independent-growth ability of the A375 DUSP6 transfection pool by methylcellulose assay. 5000 cells of A375, A375 DUSP6 transfection pool 3 and A375 DUSP6 transfection pool 4 were seeded into methylcellulose. Colony size and number were detected under the microscope every three days for 12 days. Image J

software was used to analyze the relative colony size and colony number per photographic field at day 7. Minimum colony size cut off was set at 50um for Day 7.

In contrast to the methylcellulose assay results of our distinct subtype of mouse melanoma, enforced expression of DUSP6 suppressed colony formation in human melanoma cells. The data collected from three independent experiments indicated A375 DUSP6 transfection pools formed less and smaller colonies than non-transfected A375 cells (Fig. 4.8A, Fig. 4.8D). Quantification analysis per photographic field by Image J showed that the average colony size of A375 DUSP6 transfection pools was reduced 2-fold compared to non-transfected A375 cells; the colony number of the DUSP6 transfection pools was also decreased 2-fold compared to non-transfected A375 cells (Fig. 4.8B, Fig. 4.8C). These data suggested that overexpression of DUSP6 can reduce anchorage independent growth ability of A375 human melanoma cells.

Figure 4.8 DUSP6 overexpression inhibits colony formation in human melanoma cells

A

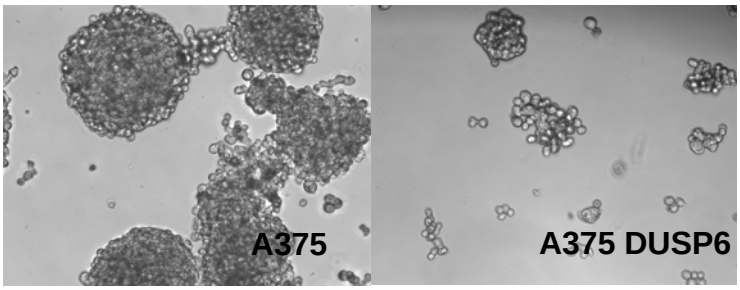

B

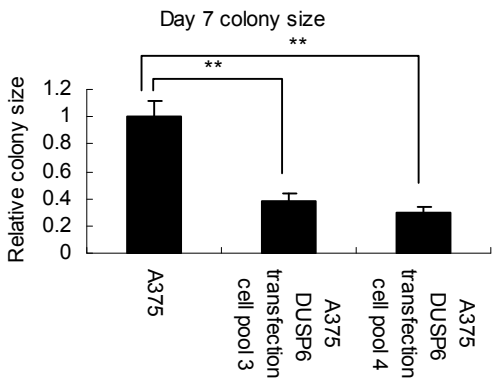

C

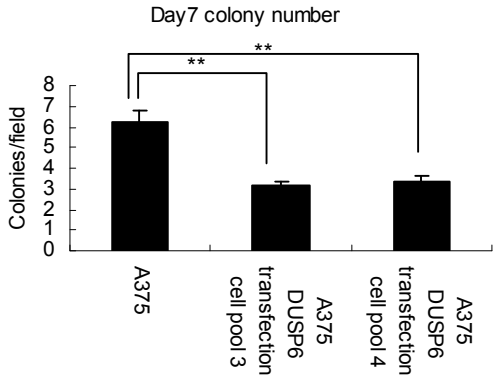

D

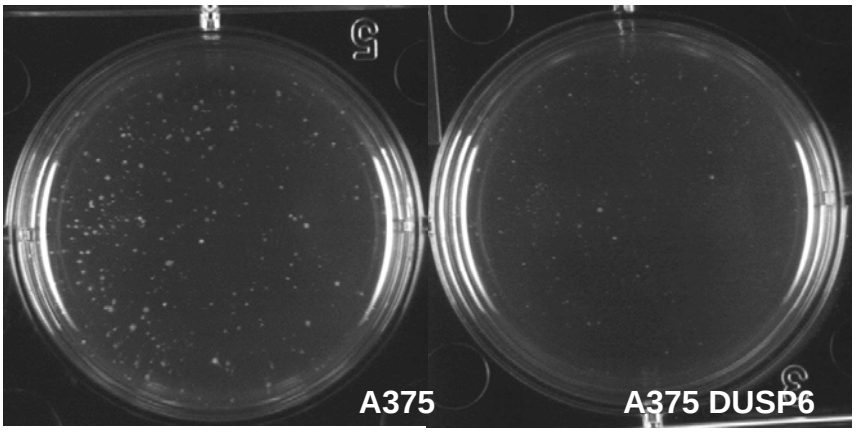

A, A375, A375 DUSP6 transfection pool 3 and A375 DUSP6 transfection pool 4 were mixed with methylcellulose and seeded into 6-well plates to form colonies for 12 days. Photos are representative of A375 and A375 DUSP6 transfection pool 3 colonies at Day 12.

B, Average colony size of A375, A375 DUSP6 transfection pool 3 and A375 DUSP6 transfection pool 4. Colony areas were measured with Image J software. Histogram shows mean colony size (± SEM) from three independent experiments. Average colony size of A375 DUSP6 transfection pool 3 and A375 DUSP6 transfection pool 4 are standardised to A375. One way ANOVA with Bonferroni's Multiple Comparison Test was applied for statistical analysis between A375 and A375 DUSP6 transfection pools. **, $P < 0.01$.

C, Total number of colonies counted per photographic field. Each field is approximately 0.59 mm^2 of culture dish. At least 6 fields were counted for each dish. Histogram shows mean colony number (± SEM) from three independent experiments. One way ANOVA with Bonferroni's Multiple Comparison Test was applied for statistical analysis between A375 and A375 DUSP6 transfection pool. **, $P < 0.01$.

D, A375, A375 DUSP6 transfection pool 3 and A375 DUSP6 transfection pool 4 were mixed with methylcellulose and seeded into 6-well plates to form colonies for 12 days. Photos are representative of entire well from A375 and A375 DUSP6 transfection pool 3 at Day 12.

4.2.9 Effect of DUSP6 on invasive ability of human melanoma cells

In our distinct subtype of mouse melanoma cells, enforced expression of DUSP6 increased invasive ability. To investigate the effect of DUSP6 on invasive ability of human melanoma cells, the transwell migration assay was used to assess the ability of the DUSP6 transfection pools to invade into matrigel in response to a chemotactic stimulus (in this case 10% serum). A375, A375 DUSP6 transfection pool 3, A375 DUSP6 transfection pool 4 were seeded onto transwell filters. After 72 hours, cells were labelled with calcein AM dye and visualized in the matrigel at 15um intervals by confocal sectioning. The cell number invading at 45um into 3D-gels was expressed relative to the cell number in the section that represented the base of the transwell filter. Invasion was significantly reduced in the A375 DUSP6 transfected pools (relative cell number around 0.05), compared to 0.24 in non-transfected A375 (Fig. 4.9A). Quantification analysis indicated that the relative cell number of A375 DUSP6 transfection pools 45um into the 3D-gels decreased 3-5 fold compared to non-transfected A375 (Fig. 4.9B). In contrast to the transwell migration assay results of our distinct subtype of mouse melanoma, the result with classic human melanoma cells suggested that the enforced expression of DUSP6 can reduce invasive ability of A375 cells in matrigel.

Figure 4.9 DUSP6 overexpression inhibits invasion of human melanoma cells

A

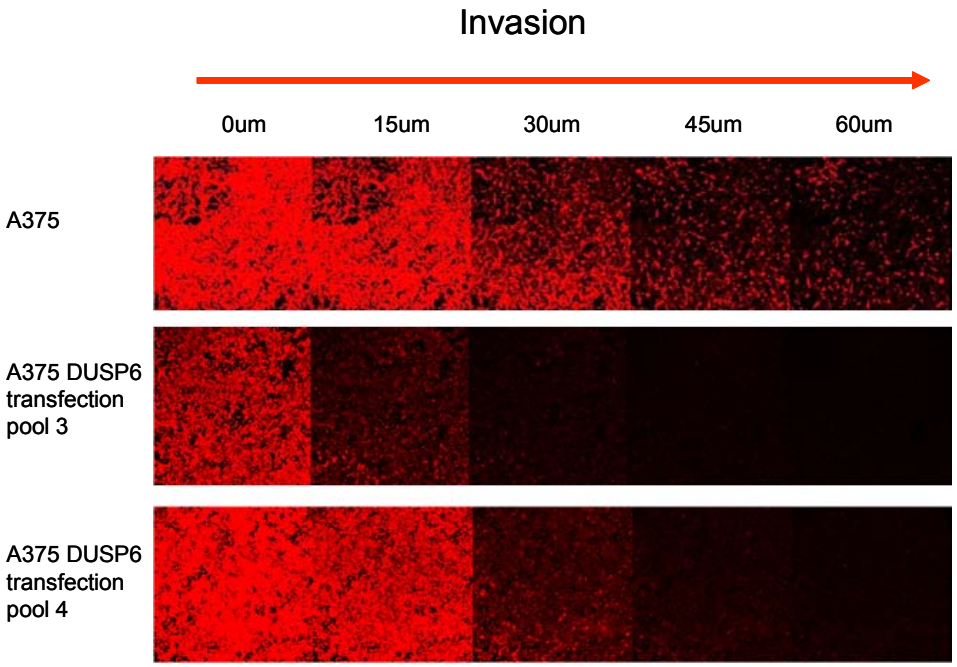

B

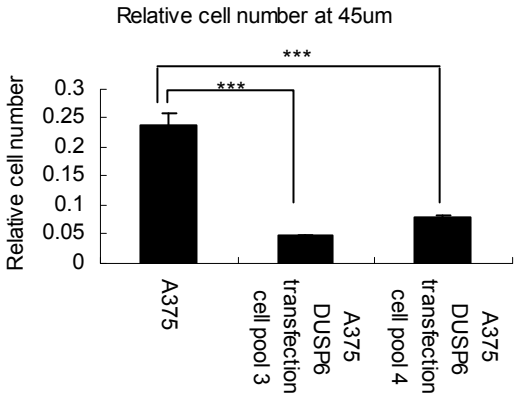

A, A375, A375 DUSP6 transfection pool 3 and A375 DUSP6 transfection pool 4 were seeded on transwell filters and allowed to invade Matrigel towards a serum gradient. After 96 hours cells were labelled with calcein AM and visualized in the Matrigel at 15µm intervals by Olympus FV1000 confocal microscopy.

B, Histogram shows the quantitation of invasion at 45um. The amount of dye (positive pixels) was calculated for each z-section using Image J software, and expressed relative to the signal in

the section that represented the base of the transwell filter. One way ANOVA with Bonferroni's Multiple Comparison Test was applied for statistical analysis between A375 and A375 DUSP6 transfection pools. ***, $P < 0.001$.

4.3 Discussion

DUSP6 was overexpressed in our mouse melanocyte tumour cell lines compared to their parental non-tumourigenic cell lines. Overexpression of DUSP6 was associated with low levels of phospho-ERK1/2 in our mouse tumour cells. Moreover, ectopic expression of DUSP6 increased anchorage independent growth ability and invasive ability of our mouse non-tumourigenic melanocytes. This may contribute to the ability to form tumours in the xenograft assay. DUSP6 also negatively regulated phosphorylation of ERK1/2 in human melanoma cell line, but ectopic expression of DUSP6 led to decreased anchorage independent growth ability and invasive ability. Considering that these opposing results were obtained with different species and subtypes of melanoma, we will discuss the results for mouse and human separately.

Some studies showed that activation of the MAPK pathway may be involved in the oncogenic behaviour of classic melanoma (Smalley 2003). The activation of RAS and BRAF was frequently found in metastatic melanoma. The mutated RAS and BRAF can result in activation of ERK1/2. Activated ERK1/2 transfers into the nucleus to induce expression of various genes (Dahl and Guldberg 2007). However, previous studies have also identified subgroups of melanoma lacking mutations in NRAS and BRAF genes (Goel et al. 2006). Some distinct melanoma subtypes with overexpression of c-kit and CDK4 did not require ERK activation (Smalley et al. 2008). The MAPK activity was subject to regulation even in BRAF/NRAS mutant melanoma cells and high activity of the MAPK pathway may be important only in distinct subsets of melanoma cells (Houben et al. 2008). Furthermore, some studies indicated that the absence of cytoplasmic ERK activation became an independent adverse prognostic factor in primary cutaneous melanoma and it was speculated that

melanomas may be associated with activation of some other pathway leading to tumour progression and adverse outcome (Jovanovic et al. 2008). Our results also indicated that our tumourigenic mouse melanocyte cell lines have a lower phosphorylation level of ERK1/2. Meanwhile, these cell lines showed high expression levels of DUSP6. DUSP6 is one of the MKPs members which binds to and inactivates ERK1/2 in mammalian cells. DUSP6 plays an important role in regulating the duration, magnitude and subcellular compartmentalization of ERK1/2 expression through a negative feedback mechanism. Disruption of this feedback loop was directly relevant to the initiation and development of pancreatic cancer, lung cancer and ovarian cancer (Bermudez et al. 2010). The roles of DUSP6 in melanoma are still unclear. We suspected that overexpression of DUSP6 was associated with the lower levels of p-ERK in our mouse tumour cells. If higher expression of DUSP6 promotes growth of our transformed melanocytes in the xenograft assay, then enforced expression of DUSP6 in the non-transformed parental cells should inactivate ERK and contribute to melanoma progression. Therefore, a vector harbouring DUSP6 was introduced into the 5-1 cell line to test the effect of DUSP6 overexpression. Indeed, the result showed that exogenous expression of DUSP6 dramatically decreased the phosphorylation of ERK1/2. Moreover, overexpression of DUSP6 increased anchorage independent growth ability and invasive ability of our immortal mouse melanocytes. This suggests that DUSP6 is involved in melanoma progression and contributes to the transformation of our immortal mouse melanocytes in the xenograft assay.

One question remaining is at which stage the DUSP6 expression increase occurs in 5-1 and 3-1-1 cell lines. One possibility is that high levels of DUSP6 preexist in some cells in the 5-1 and 3-1-1 populations prior to xenograft. These cells then grow fast in the mouse xenografts and form tumours. We can not rule out another possiblility that genetic changes occur in some xenografted cells which are then selected by their ability to form a tumour. Either possibility would explain how DUSP6 expression was increased in the tumourigenic derivatives.

To investigate whether absence of ERK1/2 was required for melanoma progression in our xenograft assay, we next introduced vectors harbouring constitutively active MEK1 and MEK2 into the 5-1 T2 cell line which had high expression of DUSP6 and low expression of p-ERK. Constitutively active MEKs act as dual specificity kinases and phosphorylate the regulatory Tyr and Thr residues of ERKs in the cascade (Shaul and Seger 2007). If inactivation of MEKs is responsible for the lower level of phosphorylation of ERK1/2 and tumour formation in the xenograft assay, exogenous expression of constitutively active MEK1 and MEK2 should activate ERK and suppress melanoma progression. Our data indicated that exogenous expression of constitutively active MEK1/2 increased levels of phosphorylation of ERK1/2 as expected. In addition, this efficiently suppressed invasion of 5-1T2 cells in the transwell migration assay. It suggested that inactivation of the MAPK pathway contributed to invasion of our mouse tumour cells. Furthermore, exogenous expression of constitutively active MEK1 and MEK2 inhibited the colony formation in the methylcellulose assay, but the differences of colony size and colony number between the 5-1T2 MEK1 and MEK2 transfection pools and non-transfected 5-1T2 cells were not significant. The ability of anchorage independent growth of our mouse tumour cells may be more dependent on increased expression of DUSP6 and ERK inactivation, rather than reduced activation of ERKs by MEKs. Exogenous expression of constitutively active MEK1 and MEK2 not only increased the level of phospho-ERK but also increased DUSP6 expression in our mouse tumourigenic cells. It agrees with a report which showed that the activation of the MAPK pathway can increase the expression of DUSP6 through regulation of transcriptional factor ETS2 (Furukawa et al. 2008). An increase of DUSP6 would contribute to anchorage independent-growth of our mouse tumour cells and so impair the suppression of colony formation induced by introduction of constitutively active MEK1 and MEK2. We also can not rule out the possibility that DUSP6 controlled the anchorage independent growth of our mouse tumour cells through other uncharacterized targets and pathways rather than the MAPK pathway. In either case this would explain why we did not observe the significant changes in the methylcellulose assays following introduction of constitutively active MEK1 and MEK2.

In this study, the DUSP6 plasmid was introduced into the classic human melanoma cell line A375 as well. The human melanoma cell line A375 which expresses the oncogenic BRAF V600E mutation has constitutively elevated ERK activity and activation of the MAPK pathway is required for its proliferation. A MEK inhibitor that blocked this constitutive activation of ERK1/2, inhibited DNA synthesis and induced cell death in A375 cells (Cheng et al. 2007). If the MAPK pathway contributes to proliferation of A375 human melanoma cells, enforced expression of DUSP6 may decrease phosphorylation of ERK1/2 and stop or retard the A375 cell growth. To investigate this hypothesis, DUSP6 was introduced to A375 cells. We demonstrated that exogenous expression of DUSP6 dephosphorylated ERK1/2 in DUSP6 transfected A375 pools. Although the DUSP6 transfected A375 pools had the same growth rate as non-transfected A375 cells in cell culture (see Chapter 5), DUSP6 A375 transfected pools formed smaller and fewer colonies than non-transfected A375 cells in the methylcellulose assay. These data suggested that DUSP6 can not only regulate the activation of the MAPK pathway in our mouse immortal cells but also can control the MAPK pathway in human melanoma cells. Furthermore, the enforced expression of DUSP6 decreased anchorage-independent growth ability of the A375 human melanoma cell line. Our data provided the first direct evidence for the role of DUSP6 on human melanoma development. This finding was comparable with previous observations in human pancreatic cancers. The upregulation of DUSP6 was reported in the majority of dysplastic cells in pancreatic tumours, but downregulation was seen in invasive carcinoma cells. Adenovirus-mediated transfer of DUSP6 into cultured pancreatic cancer cells led to suppression of growth and induction of apoptosis (Furukawa et al. 2003). In addition, knockdown of endogenous DUSP6 increased ERK1/2 activity which contributed to cell proliferation and anchorage-independent growth ability of the A2780 ovarian cell line. On the contrary, enforced expression of a DUSP6 in DUSP6 deficient ovarian cell line suppressed cell growth, anchorage-independent growth ability and tumour growth in nude mice (Chan et al. 2008). Recent study also indicated that overexpression of DUSP6 markedly inhibited the growth of lung cancer cell lines

and that the expression decreased with the progression of grade and stage of lung cancers (Okudela et al. 2009).

Our results also indicated that A375 DUSP6 transfected cells are less invasive than non-transfected A375 cells in matrigel. It was possible that enforced expression of DUSP6 inhibited melanoma cell invasion through inactivation of the MAPK pathway. As described in the general introduction (Chapter 1), the MAPK pathway played important roles in classic melanoma invasion. Firstly, constitutive activation of the MAPK pathway appears to be associated with downregulated E-cadherin expression. Inactivation of the MAPK pathway can block the decrease of E-cadherin and inhibit melanoma invasion (Meier et al. 2005). In addition, the constitutive activation of the MAPK pathway can upregulate integrin expression which contributes to melanoma survival and invasive growth in ECM (Schwartz et al. 1995). The expression of $\alpha_V\beta_3$ integrin was involved in melanoma invasion (Albelda et al. 1990). Furthermore, the constitutive activation of the MAPK pathway increased expression and activity of proteolytic enzymes that helped melanoma cells degrade the ECM. MMP-2 and MMP-9, which degrade basement membrane collagen, were reported to be particularly important proteolytic enzymes involved in melanoma invasion (MacDougall et al. 1999, Vaisanen et al. 1999). Treatment of A375 melanoma cells with MEK inhibitors U1026 and PD98059 reduced matrigel invasion. This suppression of invasion was associated with inhibition of MMP-9 and uPA expression (Ge et al. 2002). Enforced expression of DUSP6 dephosphorylated ERK1/2 and blocked the MAPK pathway in A375 human melanoma cell line. This inactivation may result in upregulated expression of E-cadherin and downregulated expression of integrin and MMPs which reduce the matrigel invasion of classic human melanoma cells.

As demonstrated, overexpression of DUSP6 in our immortal mouse melanocyte cells led to increased tumourigenicity and invasive ability, while enforced expression of DUSP6 in classic human melanoma cell caused inhibition of anchorage-independent

colony formation and invasion in matrigel. One reason for the difference may result from the species difference. It is possible that mice and humans have different mechanisms involved in melanoma formation. We can not rule out that DUSP6 may interact with different targets and control different pathways in human and mouse cells. We also considered that our mouse tumour cell lines may resemble a distinct molecular subtype of human melanoma with decreased levels of p-ERK and p-AKT which were uncommon in classic melanoma (Curtin et al. 2006, Shields et al. 2007). In addition, our mouse tumour cells did not have a BRAF V600E equivalent mutation, while A375 human melanoma cells harboured the BRAF V600E mutation. Some studies showed that there were different mechanisms underlying melanoma progression in melanoma cell lines with BRAF mutations and those without BRAF mutations (Bloethner et al. 2005, Pratilas et al. 2009, Ryu et al. 2007). Therefore, DUSP6 may play different roles in our distinct subtype of mouse melanoma compared to classic human melanoma A375.

There is limited information about the roles of DUSP6 on melanoma progression. Our studies provide the first direct evidence that DUSP6 may be involved in development of melanoma. Our results also demonstrated that introduction of constitutively active MEK1/2 to our mouse tumourigenic melanocytes inhibited invasion in matrigel. The previous studies of roles of the MAPK pathway activation on development of mouse melanoma are controversial. One study showed that introduction of constitutively active MAP kinase kinase (MAPKK) into immortalized melanocytes L10BIOBR led to tumourigenesis in nude mice (Govindarajan et al. 2003). However, another study also indicated that metastasis in an orthotopic murine model of melanoma is not dependent of elevated phosphorylated ERK (Rozenberg et al. 2010). In addition, growth of oncogenic BRAF overexpressing tumours with hyperactivation of ERK was inhibited in nude mice (Maddodi et al. 2010).

To sum up, we investigated the functions of DUSP6 in melanoma cells in this chapter. We concluded that DUSP6 regulated phosphorylation of ERK1/2 in both our

tumourigenic mouse melanocytes and human melanoma cell lines. In our distinct subtype of mouse melanoma, overexpression of DUSP6 may contribute to melanoma formation in the xenograft assay. Introduction of constitutively active MEK1 and MEK2 into our mouse tumourigenic cells can suppress the invasion in matrigel, but did not result in significant changes of anchorage independent growth in the methylcellulose assay. In classic human melanoma, inhibition of anchorage independent growth and invasion were observed after exogenous expression of DUSP6. DUSP6 may act as a tumour suppressor in classic melanoma cells. We hope our efforts will contribute to better understanding the mechanisms underlying of melanoma progression and assist the development of new therapeutic interventions for this disease.

Chapter 5

Cisplatin resistance and ERCC1

5.1 Introduction

Cisplatin (CDDP) is one of the most widely used chemotherapeutic agents for treatment of tumours. It is particularly active against germ-cell tumours, prolongs survival in ovarian cancer and in non-small cell lung cancer, and plays an important role in the treatment of oesophageal, cervical, gastric and prostate cancer (Lebwohl and Canetta 1998). However, the efficacy of cisplatin is hampered by resistance of cancer cells to its cytotoxicity. The cellular toxicity of cisplatin occurs primarily through its ability to bind to DNA to generate DNA adducts leading to intrastrand or interstrand cross links which disrupt the structure of the DNA molecule, leading to steric changes in the helix. Cells can become resistant to cisplatin through enhanced ability to remove DNA adducts and so repair cisplatin-induced lesions in DNA (Martin et al. 2008).

Nucleotide excision repair (NER) levels are involved in determining resistance or sensitivity to cisplatin (Rabik and Dolan 2007). The nucleotide excision repair system can recognize cisplatin induced DNA lesions, which alter the helical structure of the DNA molecule, followed by complex formation to unwind the DNA around the lesions and excise them. The excised portion is resynthesized and ligated to repair the cisplatin induced DNA damage and rescue DNA replication and transcription over the damage region (Rabik and Dolan 2007). *ERCC1* is one of the critical repair genes in NER. ERCC1 forms a complex with xeroderma pigmentosum complementation group F protein to excise cisplatin induced DNA lesions (Evans et al. 1997). Overexpression of ERCC1 was found in various types of cancers, including non-small cell lung cancer (NSCLC), ovarian, colorectal and gastric cancers and this overexpression was related to the formation of cellular and clinical drug resistance. By contrast, with lack of ERCC1 expression, repair of cisplatin induced DNA adducts disappeared and cancer cells were more sensitive to cisplatin (Gossage and Madhusudan 2007). However, whether cisplatin treatment can increase

ERCC1 expression in melanoma cell lines and, if so, what kinds of mechanisms are involved in ERCC1 overexpression by cisplatin is still unclear.

The MAPK signaling pathway is constitutively activated via multiple mechanisms in malignant melanoma (Oliveria et al. 2006). The MAPK signal transduction pathway regulates cell survival, proliferation and invasion, key functions in the progression of melanoma (Hoshino et al. 1999). Treatment of melanoma cell lines with cisplatin did not cause the anticipated decrease of ERK1/2 phosphorylation, to the contrary, it resulted in increased ERK1/2 phosphorylation (Mirmohammadsadegh et al. 2007). Moreover, a recent study shows that the MAPK pathway plays an important role in the regulation of ERCC1 expression by EGF in human hepatoma cells (Andrieux et al. 2007). Therefore, we wished to investigate the possibility that cisplatin activates ERK1/2 which regulates ERCC1 overexpression to protect tumour cells from DNA damage.

DUSP6 is a member of the subfamily of protein tyrosine phosphatases known as dual-specificity phosphatases. DUSP6 can dephosphorylate ERK1/2 by protein-protein interaction via a mitogen-activatated protein kinase interaction motif within the N-terminal ERK1/2-binding domain (Bermudez et al. 2010). A recent study has shown that cisplatin might cause degradation of DUSP6, which in turn leads to aberrant ERK1/2 activation and contributes to chemoresistance of human ovarian cancer cells (Chan et al. 2008). In addition, cisplatin-mediated transcriptional inhibition of DUSP6 contributes to the delayed and long lasting accumulation of ERK 1/2 phosphorylation that is driven by cisplatin in neurons (Gozdz et al. 2008). However, there is a lack of similar reports in other human cancers so far. We postulated that decreased DUSP6 levels contribute to activation of ERK1/2 during cisplatin treatment in melanoma cells.

In our study, we analyzed ERCC1 expression as well as XPF expression in the

human melanoma cell line A375 treated by cisplatin. The results provide evidence that p-ERK levels show a time dependent increase after cisplatin treatment, while ERCC1 and XPF expression are both augmented by cisplatin. Use of a MEK inhibitor showed ERCC1 induction was dependent on the MAPK pathway. The DUSP6 level decreased after cisplatin treatment, while overexpression of DUSP6 inhibited ERCC1 induction by cisplatin and reduced resistance to cisplatin.

5. 2 Results

5.2.1 Detection of ERK phosphorylation and ERCC1 and XPF induction after cisplatin treatment in a melanoma cell line

To evaluate the molecular mechanisms of cisplatin induced drug resistance in melanoma, human melanoma A375 cells were treated with cisplatin (6uM) for 12h, 24h, 36h, 48h and 72h. Protein lysates obtained at various times from untreated and CDDP-treated cells were subjected to western blot analysis using an anti-phospho-ERK antibody to detect p-ERK1 (42KD) and p-ERK2 (44KD) and an anti-ERCC1 antibody to detect ERCC1 (39KD) induction. Total ERK and GAPDH levels of these samples were also determined by western blot to correct for different amounts of protein in the various samples (Fig. 5.1A).

Cisplatin treatment caused a time dependent increase in levels of phosphorylated ERK1/2 while total ERK 1/2 expression was unaffected. Activation of ERK1/2 increased 24 h after incubation with cisplatin and eventually attained a peak 3.5-fold increase at 48 h after cisplatin administration. The activation of ERK1/2 was decreased by 72 h (Fig. 5.1B). Cisplatin induced a similar time dependent ERCC1 increase. Expression of ERCC1 protein was increased at 24h and peaked at 48h with an approximate 5-fold increase after cisplatin exposure. The induction of ERCC1 by cisplatin was also reduced at 72h (Fig. 5.1C).

Given that ERCC1 was induced in the melanoma cell line A375 by cisplatin treatment, it was important to detect the XPF protein level too since it forms a complex with ERCC1 to excise cisplatin induced DNA lesions. Human melanoma cell line A375 was treated with cisplatin (6uM) for 12h, 24h, 36h and 72h. XPF and loading control GAPDH levels from samples at various times were detected by western blot. As shown in the upper panel, cisplatin induced a time dependent XPF increase up to 72 hours (Fig. 5.2A). The protein quantification analysis showed a 2 to 5-fold XPF induction after cisplatin treatment (Fig. 5.2B). Next, the role of ERK1/2 in the regulation of ERCC1 and XPF was investigated in more detail.

Figure 5.1 Cisplatin activates ERK1/2 and induces ERCC1 overexpression

A

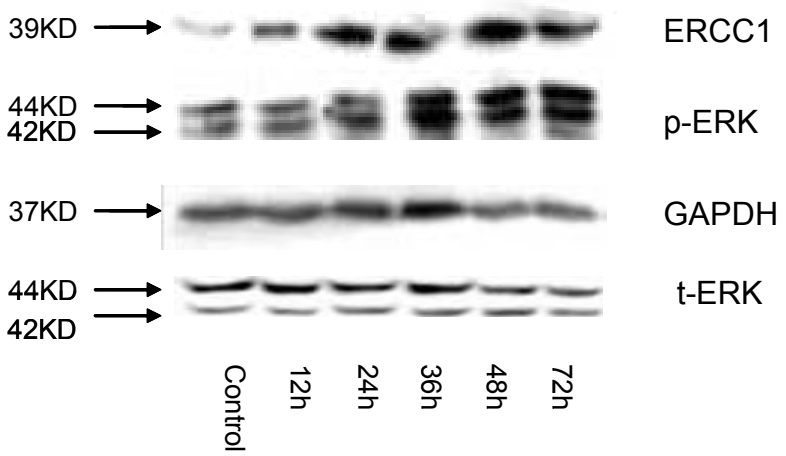

B

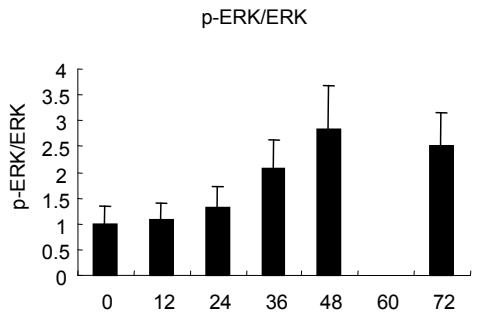

C

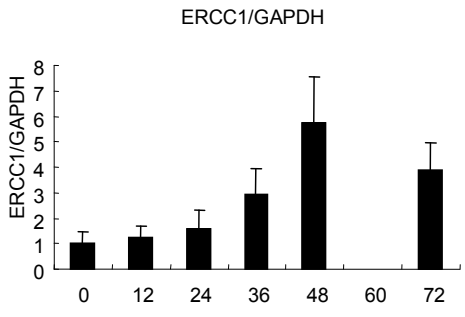

A, Western blots showing protein levels of ERCC1 (top panel), phosphorylated ERK (p-ERK)

and loading control GAPDH (middle panel) and total ERK (t-ERK) (bottom panel) in human melanoma A375 cells treated with cisplatin (6uM) for 12, 24, 36, 48 and 72h.

B, Histogram showing mean level of p-ERK (± SEM) from three independent experiments. p-ERK levels are expressed relative to total ERK levels and are normalized to the non-cisplatin treated control.

C, Histogram showing mean level of ERCC1 (± SEM) from three independent experiments. ERCC1 levels are expressed relative to loading control GAPDH levels and are normalized to the non-cisplatin treated control.

Figure 5.2 Cisplatin induces XPF overexpression

A

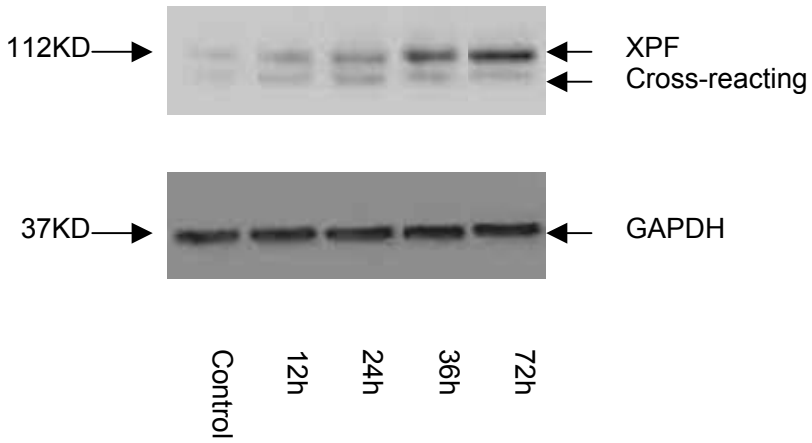

B

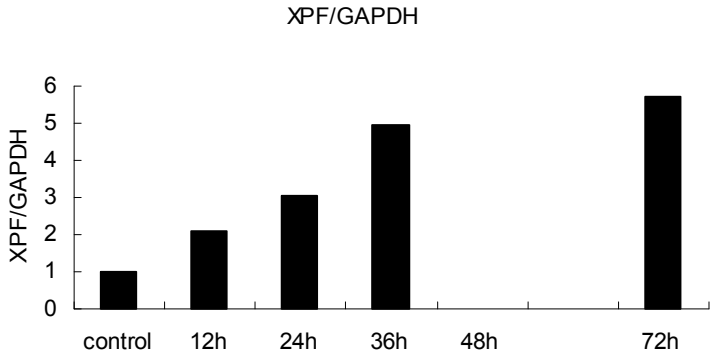

A, Western blots showing protein levels of XPF (top panel) and loading control GAPDH (bottom panel) in human melanoma A375 cells treated with cisplatin (6uM) for 12, 24, 36 and 72h. Cross-reacting bands, XPF and GAPDH bands are indicated by arrows on the right.

B, Histogram showing level of XPF. XPF levels are expressed relative to loading control GAPDH and are normalized to the non-cisplatin treated control. There is no error bar for this experiment as it was only done once.

5.2.2 MAPK pathway regulates ERCC1 protein level following cisplatin treatment

A specific inhibitor of MEK1/2, PD0325901, has been developed, which is highly selective in preventing ERK activation (Ciuffreda et al. 2009). It was used to evaluate whether ERK activation regulated ERCC1 induction following cisplatin treatment. Human melanoma cell line A375 was treated with cisplatin (6uM), PD0325901 (1uM), or both cisplatin and PD0325901 for 24h, 48h and 72h. PD0325901 was added 30 min before cisplatin treatment. Protein lysates obtained at various times from untreated and treated cells were subjected to western blot analysis using an anti-phospho-ERK antibody and an anti-ERCC1 antibody to detect phosphorylated ERK and ERCC1 induction. Total ERK and GAPDH levels of these samples were also determined by western blot to correct for different amounts of protein in the various samples.

As shown in Figure 3A, PD0325901 successfully inhibited ERK1/2 activation following cisplatin treatment (Fig. 5.3A). ERK1/2 phosphorylation levels in cisplatin treated cells significantly increased about 3-fold at 48h, while there were no bands showing ERK1/2 activation in the cells treated with PD0325901 or in cells treated with both cisplatin and PD0325901 (Fig. 5.3B). Neither cisplatin nor PD0325901 affected total ERK1/2 expression (Fig. 5.3A).

As in the previous experiment cisplatin treatment resulted in increased ERCC1 protein levels, the peak was at 4.5-fold the control level at 48 hours (Fig 5.3C). The

MEK inhibitor efficiently prevented this cisplatin-induced increase in ERCC1 protein. PD0325901 on its own did not affect the basal level of ERCC1 protein at 48 and 72 hours (Fig 5.3C). I conclude that ERK activation plays an important role in the regulation of ERCC1 levels after cisplatin treatment in melanoma cells.

Figure 5.3 ERCC1 protein levels are regulated by the MAPK pathway

A

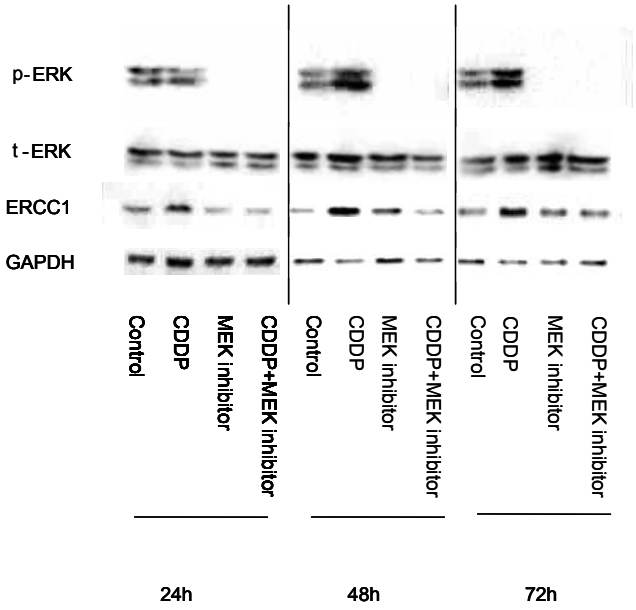

B

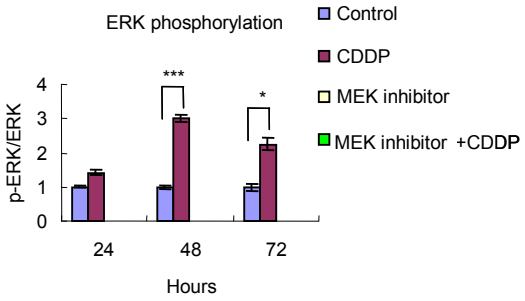

C

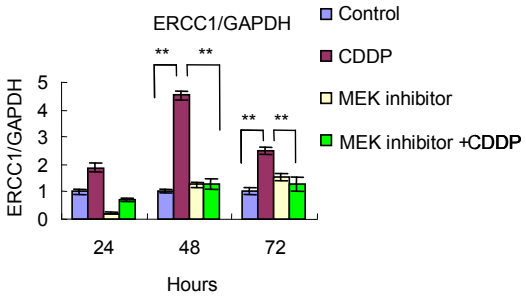

A, Western blots showing protein levels of phosphorylated ERK (p-ERK) (top panel), total ERK (t-ERK) (second panel), ERCC1 (third panel) and loading control GAPDH (bottom panel) in human melanoma A375 cells treated with cisplatin (6uM), MEK inhibitor, PD0325901 (1uM), or both cisplatin and MEK inhibitor for 24h, 48h and 72h. PD0325901 was added 30 min before cisplatin treatment.

B, Histogram showing mean level of p-ERK (± SEM) from three independent experiments. p-ERK levels are expressed relative to total ERK levels. At each time point, p-ERK levels are standardized to the non-cisplatin treated control. Control, CDDP, MEK inhibitor and both MEK inhibitor and CDDP groups are plotted in blue, purple, yellow and green columns, respectively. One way ANOVA with Bonferroni's Multiple Comparison Test was applied for statistical analysis among control, cisplatin, PD0325901 and both cisplatin and PD0325901 groups. *, $P < 0.05$ and ***, $P < 0.001$.

C, Histogram shows mean level of ERCC1 (± SEM) from three independent experiments. ERCC1 levels are expressed relative to loading control GAPDH levels. At each time point, ERCC1 levels are standardized to the non-cisplatin treated control. Control, CDDP, MEK inhibitor and both MEK inhibitor and CDDP groups are plotted in blue, purple, yellow and green columns, respectively. One way ANOVA with Bonferroni's Multiple Comparison Test was applied for statistical analysis among control, cisplatin, PD0325901 and both cisplatin and PD0325901 groups. **, $P < 0.01$.

5.2.3 *ERCC1* and *XPF* transcription level changes following cisplatin treatment

To determine whether *ERCC1* and *XPF* transcription levels were also increased following cisplatin treatment and whether the MAPK pathway regulated *ERCC1* and *XPF* mRNA induction, human melanoma cell line A375 was treated with cisplatin (6uM), PD0325901 (1uM), or both cisplatin and PD0325901 for 24h, 48h and 72h. As before, PD0325901 was added 30 min before cisplatin treatment. Total mRNA was extracted at various times from treated cells and control cells. Reverse transcription was performed and *ERCC1* and *XPF* mRNA levels were determined by performing real time RT-PCR. Beta-actin was used as the internal control in order to normalize the expression of *ERCC1* and *XPF*. A standard curve was first run for each gene specific PCR reaction in order to demonstrate whether PCR efficiencies of target and internal control gene were approximately equal. If the absolute value of the slope of the plot of log dilution factor vs. $\Delta C_T < 0.1$, then the comparative C_T method can be used to analyze real time RT-PCR data (Livak and Schmittgen 2001).

The relative efficiency plot for *ERCC1* vs. Beta-actin showed that the absolute value of the slope was 0.0467 (Fig. 5.4A) and the relative efficiency plot for *XPF* vs. Beta-actin showed that the absolute value of the slope was 0.0551(Fig 5.4B), so both passed this test. Therefore, the comparative C_T method was used to measure relative concentrations of *ERCC1* and *XPF* mRNA.

As in the previous protein experiment cisplatin treatment also resulted in increased *ERCC1* mRNA levels, the peak was at 3.5-fold the control level at 48 hours (Fig 5.5). The MEK inhibitor efficiently prevented this cisplatin-induced increase in *ERCC1* mRNA. PD032501 on its own did not affect the basal level of *ERCC1* mRNA at 48 and 72 hours (Fig 5.5). It suggested that ERK activation played an important role in the regulation of *ERCC1* transcriptional levels after cisplatin treatment in melanoma cells. Cisplatin treatment also resulted in increased *XPF* mRNA levels; the peak was at 2.5 fold the control level at 24 hours. Although *XPF* mRNA induction by cisplatin was slightly reduced by the MEK inhibitor, unlike the changes with *ERCC1* mRNA, statistical analysis indicated that this reduction was not significant. PD032501 on its own did not affect the basal level of *XPF* mRNA at 48 and 72 hours (Fig. 5.6).

Figure 5.4 Validation of qPCR expression data for *ERCC1* and *XPF*

A

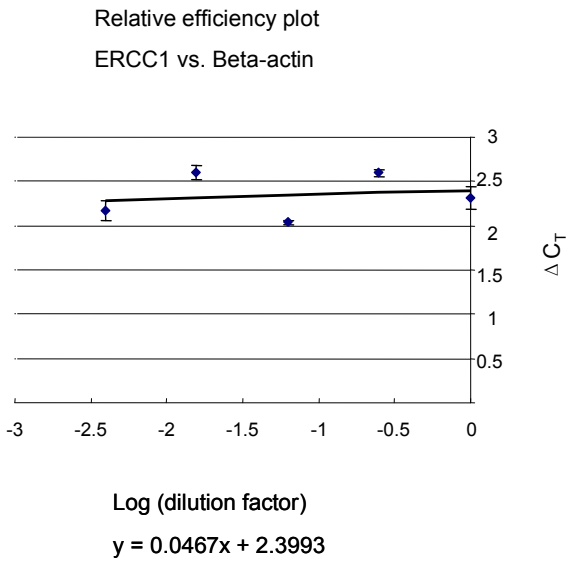

B

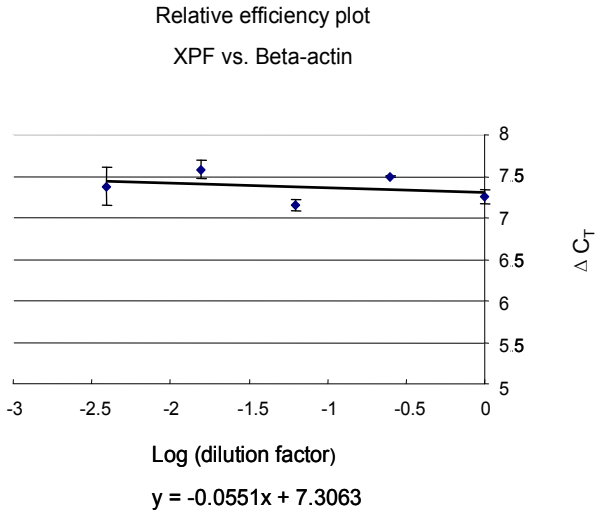

A, Relative qPCR efficiency plot for *ERCC1* and Beta-actin. Delta CT values are the means of three independent experiments. The absolute value of the slope of log dilution factor vs. delta CT is 0.0467.

B, Relative qPCR efficiency plot for XPF and Beta-actin. Delta CT values are the means of three independent experiments. The absolute value of the slope of log dilution factor vs. delta CT is 0.0551.

Figure 5.5 *ERCC1* transcriptional levels are regulated by the MAPK pathway

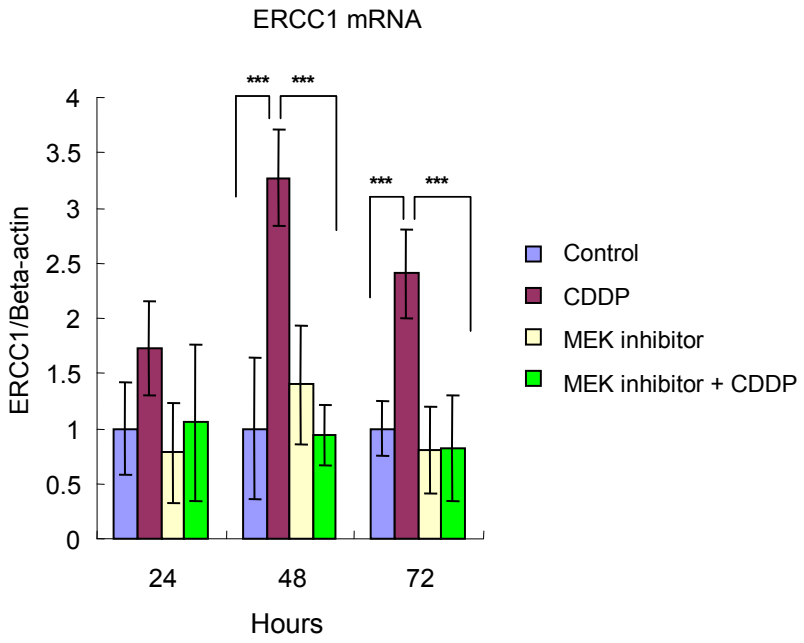

The histogram shows the mean level (± SEM) of *ERCC1* mRNA relative to beta-actin mRNA in human melanoma cells determined from three independent experiments by qPCR. Cells are untreated (blue), or treated with cisplatin (6uM) (purple), or treated with the MEK inhibitor, PD0325901 (1uM) (yellow), or treated with both cisplatin and MEK inhibitor (green). The MEK inhibitor was added 30 minutes before cisplatin treatment. Samples were collected at 24, 48 and 72h. One way ANOVA with Bonferroni's Multiple Comparison Test was applied for statistical analysis among control, cisplatin, PD0325901 and both cisplatin and PD0325901 groups. ***, $P < 0.001$.

Figure 5.6 *XPF* transcriptional levels are regulated by cisplatin but are not regulated by the MAPK pathway

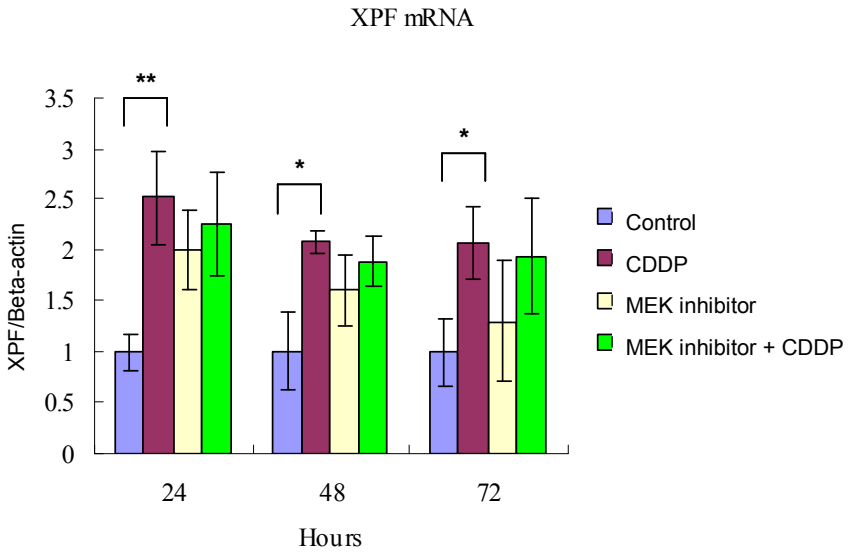

The histogram shows the mean level (± SEM) of *XPF* mRNA relative to beta-actin mRNA in human melanoma cells determined from three independent experiments by qPCR. Cells were untreated (blue), or treated with cisplatin (6uM) (purple), or treated with the MEK inhibitor, PD0325901 (1uM) (yellow), or treated with both cisplatin and MEK inhibitor (green). The MEK inhibitor was added 30 minutes before cisplatin treatment. Samples were collected at 24, 48 and 72h. One way ANOVA with Bonferroni's Multiple Comparison Test was applied for statistical analysis among control, cisplatin, PD0325901 and both cisplatin and PD0325901 groups. *, $P < 0.05$ and **, $P < 0.01$.

5.2.4 DUSP6 changes following cisplatin treatment

It has been demonstrated that the level of ERK1/2 phosphorylation increased after cisplatin treatment in a melanoma cell line in a previous study (Mirmohammadsadegh et al. 2007). However mechanisms of activation of ERK1/2 during cisplatin treatment were still unclear. As ERK1/2 could be inactivated by dephosphorylation, it was possible that inhibition of DUSP6 could lead to accumulation of active ERK1/2 (Bermudez et al. 2010). To test whether inhibition of DUSP6 may be involved in cisplatin effects on human melanoma, A375 cells were treated with cisplatin (6uM) for 24h, 48h and 72h. Protein lysates obtained at various times from untreated and treated cells were subjected to western blot analysis using an anti-phospho-ERK antibody and an anti-DUSP6 antibody to detect phosphorylated ERK and DUSP6. Total ERK and GAPDH levels of these samples were also determined by western blot to correct for different amounts of protein in the various samples.

As in the previous experiment, western blot results showed that ERK1/2 phosphorylation levels significantly increased during cisplatin treatment, while DUSP6 levels decreased under the same conditions (Fig. 5.7A). Protein quantification analysis revealed around a 3-fold ERK1/2 activation increase at 48 hours after cisplatin treatment (Fig. 5.7B). On the contrary, cisplatin reduced expression of DUSP6 3-fold at 48 hours (Fig. 5.7C). Cisplatin did not affect basal levels of total ERK and GAPDH. There was a good reverse correlation between ERK1/2 phosphorylation and DUSP6 expression. The data suggested that DUSP6 may be involved in MAPK pathway activation and *ERCC1* induction during cisplatin treatment to protect tumour cells from DNA damage.

Figure 5.7 DUSP6 may be involved in the MAPK pathway activation after cisplatin treatment

A

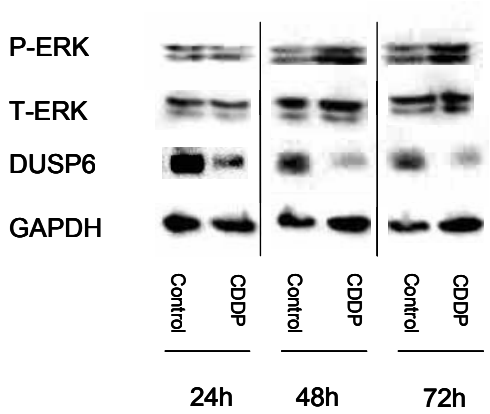

B

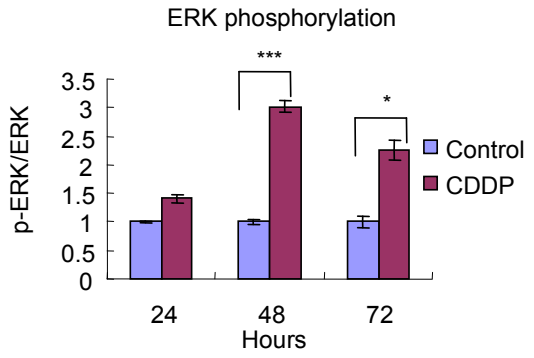

C

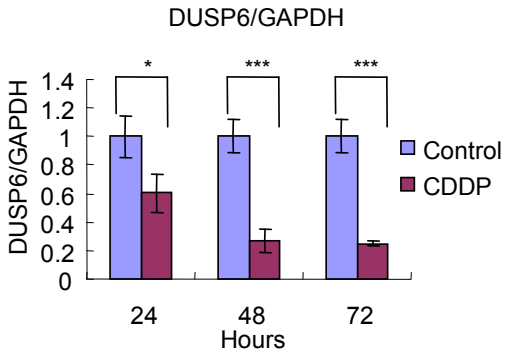

A, Western blots showing protein levels of phosphorylated ERK (p-ERK) (top panel), total ERK (T-ERK) (second panel), DUSP6 (third panel) and loading control GAPDH (bottom panel) in human melanoma A375 cells treated with cisplatin (6uM) for 24h, 48h, 72h. PD0325901 was added 30 min before cisplatin treatment.

B, Histogram showing mean level of p-ERK (± SEM) from three independent experiments. p-ERK levels are expressed relative to total ERK levels. At each time point, p-ERK levels are standardized to the non-cisplatin treated control. One way ANOVA with Bonferroni's Multiple Comparison Test was applied for statistical analysis between control and cisplatin groups. *, $P < 0.05$ and ***, $P < 0.001$.

C, Histogram showing mean level of DUSP6 (± SEM) from three independent experiments. DUSP6 levels are expressed relative to loading control GAPDH levels. At each time point, DUSP6 levels are standardized to the non-cisplatin treated control. One way ANOVA with Bonferroni's Multiple Comparison Test was applied for statistical analysis between control and cisplatin groups. *, $P < 0.05$ and ***, $P < 0.001$.

5.2.5 DUSP6 overexpression inhibited induction of *ERCC1* and *XPF* mRNA following cisplatin treatment

To investigate whether DUSP6 reduction was involved in *ERCC1* and *XPF* induction following cisplatin treatment, human melanoma cell line A375 was transfected with plasmids carrying the DUSP6 gene and the hygromycin resistance selection marker. Cells stably expressing DUSP6 were selected with Hygromycin. Two independent pools of resistant colonies were used for the following experiments. Successful transfection was confirmed by western blots for DUSP6 as described in Chapter 4. Because 48h treatment with cisplatin seemed to be optimal for the *ERCC1* and *XPF* increase as well as for ERK activation in our culture conditions, this time point was selected to study the cisplatin effect on DUSP6 transfected A375 cell pools and non-transfected A375 cells. Relative concentrations of *ERCC1* and *XPF* mRNA were detected by real time RT-PCR as described before. DUSP6 overexpression in A375 significantly reduced *ERCC1* basal mRNA levels around 5-fold, but did not affect *XPF* basal mRNA levels (Fig. 5.8A, Fig. 5.8B). Furthermore, as in the previous experiment *ERCC1* and *XPF* mRNA levels were augmented in non-transfected A375 cells stimulated by cisplatin. On the contrary, under the same condition of cisplatin treatment, overexpression of DUSP6 in A375 cells resulted in no induction of *ERCC1* and *XPF* mRNA compared with non-transfected cells (Fig. 5.8C, Fig. 5.8D). These studies were performed in triplicate. The data suggested that DUSP6 negatively regulated *ERCC1* and *XPF* induction by cisplatin treatment in melanoma cancer cells.

Figure 5.8 DUSP6 overexpression inhibits induction of *ERCC1* and *XPF* mRNA after cisplatin treatment

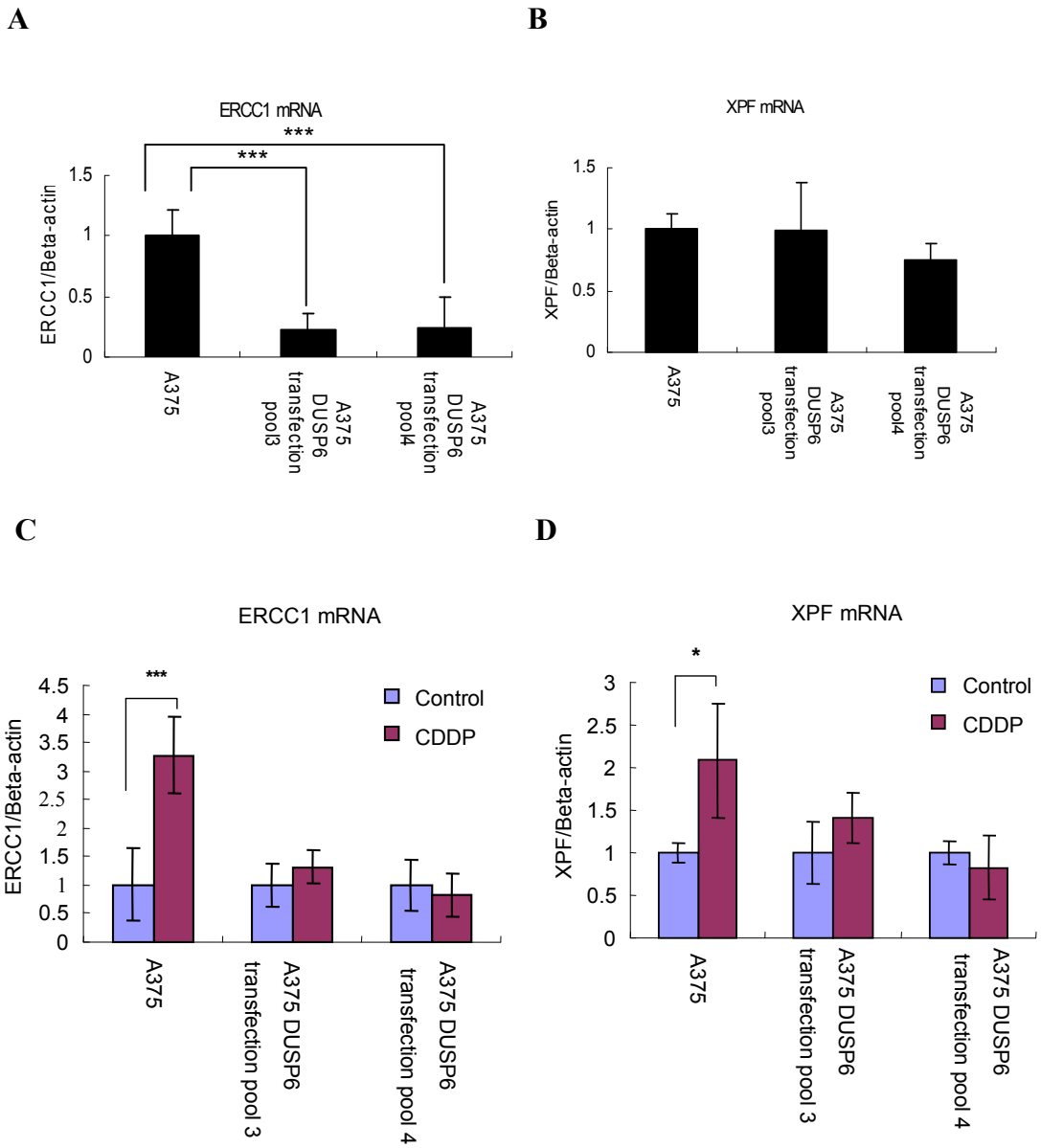

A, Histogram showing the mean level (± SEM) of *ERCC1* mRNA relative to beta-actin mRNA in human melanoma A375, A375 DUSP6 transfection pool 3 and A375 DUSP6 transfection pool 4 determined from three independent experiments by qPCR. Samples were collected at 48h. *ERCC1* mRNA levels of A375 DUSP6 transfection pools were standardized to non-transfected A375. One way ANOVA with Bonferroni's Multiple Comparison Test was applied for statistical analysis between A375 and A375 DUSP6 transfection pools. ***, $P < 0.001$.

B, Histogram showing the mean level (± SEM) of *XPF* mRNA relative to beta-actin mRNA in human melanoma A375, A375 DUSP6 transfection pool 3 and A375 DUSP6 transfection pool 4 determined from three independent experiments by qPCR. Samples were collected at 48h. *XPF* mRNA levels of A375 DUSP6 transfection pools were standardized to non-transfected A375. One way ANOVA with Bonferroni's Multiple Comparison Test was applied for statistical analysis between A375 and A375 DUSP6 transfection pools. There was no significant difference between A375 DUSP6 transfection pools and non-transfected A375.

C, Histogram showing the mean level (± SEM) of *ERCC1* mRNA relative to beta-actin mRNA in human melanoma A375, A375 DUSP6 transfection pool 3 and A375 DUSP6 transfection pool 4 determined from three independent experiments by qPCR. Cells were untreated (blue), or treated with cisplatin (6uM) (purple). Samples were collected at 48h. For each cell line *ERCC1* mRNA levels after cisplatin treatment were standardized to the non-treated control. One way ANOVA with Bonferroni's Multiple Comparison Test was applied for statistical analysis between control and cisplatin groups. ***, $P < 0.001$.

D, Histogram showing the mean level (± SEM) of *XPF* mRNA relative to beta-actin mRNA in human melanoma A375, A375 DUSP6 transfection pool 3 and A375 DUSP6 transfection pool 4 determined from three independent experiments by qPCR. Cells were untreated (blue), or treated with cisplatin (6uM) (purple). Samples were collected at 48h. For each cell line *XPF* mRNA levels after cisplatin treatment were standardized to the non-treated control. One way ANOVA with Bonferroni's Multiple Comparison Test was applied for statistical analysis between control and cisplatin groups. *, $P < 0.05$.

5.2.6 DUSP6 overexpression reduced cisplatin resistance of melanoma cells

In order to further understand the effect of reduction of *ERCC1* and *XPF* induction by overexpression of DUSP6 on cisplatin resistance, cytotoxicity of the cells to cisplatin was determined by the Sulforhodamine B assay. A growth rate experiment was firstly carried out in control medium with the different cell populations. The growth rates of non-transfected A375 cells, DUSP6 transfected A375 cell pool 3 and DUSP6 transfected A375 cell pool 4 were determined by Sulforhodamine B assay.

Cells were plated into 96-well plates with starting cell density 300 cells/ well and 150ul culture media. The plates were harvested at day 3, day4 and day5. The relative growth of the different cell populations was analyzed and plotted using a histogram. The data showed that there was no significant difference in growth rate between non-transfected A375 cells and DUSP6 transfected A375 cell pools (Fig. 5.9). Thus any difference in the response to cisplatin between the cell lines could not be explained simply on the basis of different growth rates of the untreated cell lines.

The sensitivities of non-transfected A375 cells, DUSP6 transfected A375 cell pool 3 and DUSP6 transfected A375 cell pool 4 to cisplatin were examined by Sulforhodamine B assay. Cells were plated into 96-well plates as described before. The desired amount of cisplatin mixed with 50ul culture media was added to each well to make a total volume of 200ul media with a final concentration of cisplatin ranging from 0.1uM to 3uM. For corresponding controls, 50ul culture media without cisplatin was added to each well. The plates were incubated for 5 days. Then the plates were harvested and assayed.

The growth of non-transfected A375 cells, DUSP6 transfected A375 cell pool 3 and DUSP6 transfected A375 cell pool 4 with different concentration of cisplatin relative to untreated controls was analyzed and plotted using a growth curve. Figure 5.10 shows the relative growth on day 5. The half maximal inhibitory concentration (IC_{50}) was used to compare sensitivities of different cell populations to cisplatin. IC_{50} is a measure of the effectiveness of a compound in inhibiting biological or biochemical function. This quantitative measure indicates how much of a particular drug is needed to inhibit a given biological process by half. It is commonly used as a measure of antagonist drug potency in pharmacological research (Soothill et al. 1992). Our data showed the cells with DUSP6 overexpression were more sensitive to cisplatin compared with non-transfected cells. The IC_{50} for A375 was 0.59 ± 0.05uM while the IC_{50} for A375 transfection pool 3 was 0.30 ± 0.02uM. In a separate experiment, the IC_{50} for A375 was 0.51 ± 0.03uM while the IC_{50} for A375 transfection pool 4 was 0.31 ± 0.02uM (Figure 5.10). One way ANOVA with

Bonferroni's Multiple Comparison was applied for statistical analysis of IC_{50} between A375 and A375 transfection pools and showed that the IC_{50} values in the DUSP6 overexpression pools were significantly reduced compared to A375.

Figure 5.9 A375 and A375 DUSP6 transfectant cell lines have similar growth rate

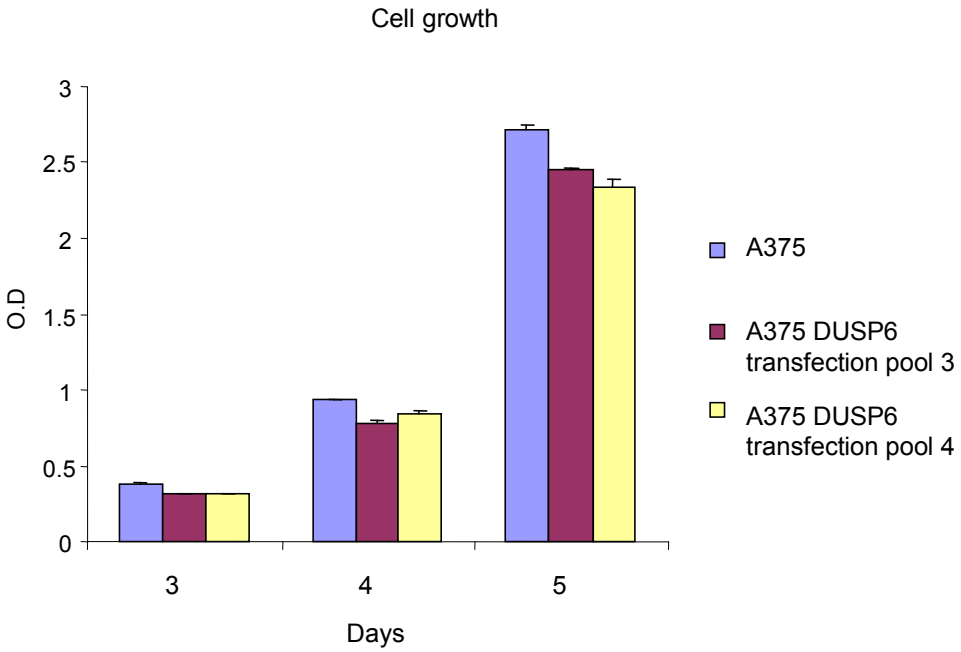

Gowth rate of human melanoma A375 cells and A375 DUSP6 transfection pools 3 and 4 were determined by SRB growth assay. Histogram shows the O.D value at 510nm for the SRB assay. Mean O.D level (± SEM) from 8 independent wells of A375, A375 DUSP6 transfection cell pool 3 and A375 DUSP6 transfection cell pool 4 are plotted as blue, purple and yellow columns. Y-axis shows the O.D values while X-axis shows different days following cell plating. Statistical analysis was performed by one way ANOVA with Bonferroni's Multiple Comparison Test. There were no statistically significant differences between A375 and DUSP6 transfection cell lines, $P>0.05$.

Figure 5.10 DUSP6 overexpression sensitizes human melanoma A375 cells to cisplatin

A **B**

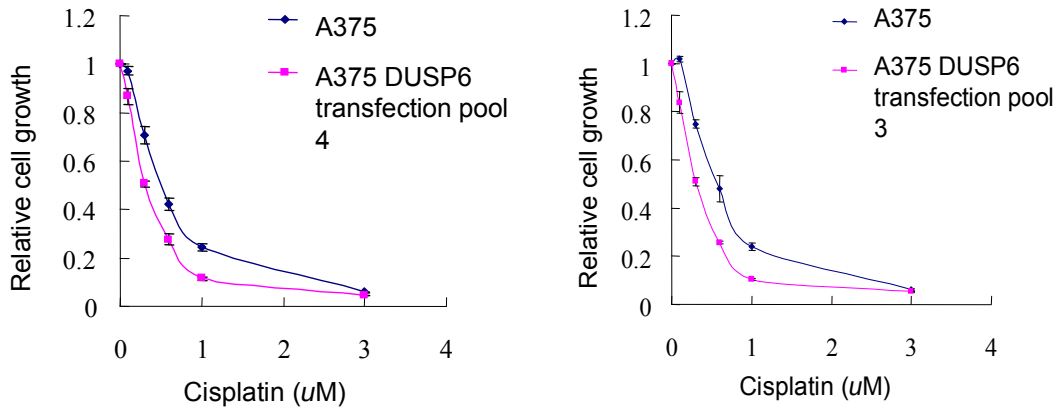

A, Resistance to cisplatin of human melanoma A375 cells and A375 DUSP6 transfection pool 4 were determined by SRB growth assay. Cells in 96-well plates were treated with various concentration of cisplatin for 5 days before being stained and extracted to determine the amount of growth. Growth of cisplatin treated cells is expressed relative to untreated control cells. Data shown are mean levels (± SEM) from three independent experiments. The IC_{50} for A375 was 0.51±0.03uM, the IC_{50} for A375 transfection pool 4 was 0.31±0.02uM. One way ANOVA with Bonferroni's Multiple Comparison was applied for statistical analysis of IC_{50} between A375 and A375 transfection pool 4. ***, $P < 0.001$.

B, Resistance to cisplatin of human melanoma A375 cells and A375 DUSP6 transfection pool 3 were determined by SRB growth assay. Cells in 96-well plates were treated with various concentration of cisplatin for 5 days before being stained and extracted to determine the amount of growth. Growth of cisplatin treated cells was expressed relative to untreated control cells. Data shown are mean levels (± SEM) from three independent experiments. The IC_{50} for A375 was 0.59± 0.05uM, the IC_{50} for A375 transfection pool 3 was 0.30±0.02uM. One way ANOVA with Bonferroni's Multiple Comparison was applied for statistical analysis of IC_{50} between A375 and A375 transfection pool 3. ***, $P < 0.001$.

5.2.7 Longer *ERCC1* transcripts following cisplatin treatment

A previous study in our group showed that a larger *Ercc1* transcript encoded ERCC1 protein in mouse skin and cultured mouse keratinocytes and this novel transcript originated from an upstream promoter, but no such transcript has previously been clearly demonstrated in human cells (Song et al. 2011). As cisplatin induced an *ERCC1* mRNA increase following cisplatin treatment in human melanoma A375 cells, we postulated that larger *ERCC1* transcripts in human cells could also be induced by cisplatin.

An RT-PCR assay was used to detect novel *ERCC1* transcripts originating upstream of the normal transcription initiation site. Several novel forward primers were designed located upstream of the normal human *ERCC1* initiation site as shown in Figure 5.11A. If novel *ERCC1* transcripts originating upstream existed, these primers in combination with reverse primer H-exon 2-3, which is located in *ERCC1* exon 2, should generate PCR products from 291bp to 419bp (Fig. 5.11A). H-exon1-A forward primer in combination with H-exon 2-3 reverse primer was used to detect the exon1 to exon2 region of all *ERCC1* transcripts (Fig. 5.11A) (Winter et al. 2005). The 164bp PCR product seen with the exon1 to exon2 region was generated by alternative splicing of a 42bp region in *ERCC1* exon1 from the expected 206bp band. Loss of this sequence during splicing has been reported before (Winter et al. 2005).

The search for larger *ERCC1* transcripts was carried out first in human melanoma cell line A375. The total mRNA was extracted from untreated human melanoma A375 cells. Reverse transcription was performed to generate a pool of A375 cDNA. PCR using H-exon1-A and H-exon 2-3 was then performed on the A375 cDNA pool to amplify the sequence between *ERCC1* exon 1 and exon 2. PCRs using different combinations of novel primers with H-exon 2-3 were also performed on the A375 cDNA pool to amplify any transcripts initiating upstream and extending through exon 2. The PCR products were electrophoresed on a 1.5% agarose gel and

visualized by ethidium bromide staining. As shown in the Figure 5.11B, for the products common to all *ERCC1* transcripts, two clear bands at the predicted sizes of 206bp and 164bp were observed. For the larger products from upstream transcripts, two bands 42bp apart were detected with all primer pairs (Fig. 5.11B). The sizes of the gel bands with the different primer pairs agreed with our prediction (Fig. 5.11B). This result indicated that novel larger *ERCC1* transcripts originating upstream of *ERCC1* existed in human melanoma cells. Although the RT-PCR assay was only semi-quantitative, it was noted that the ratio of alternatively spliced to the normal product appeared different between the total and upstream transcripts. Quantification of *ERCC1* RT-PCR bands was achieved by densitometry and expressed as the ratio of signal from the alternative spliced band relative to signal from the normal band. The ratio of the alternative spliced band relative to normal band in the *ERCC1* all transcripts assay was 0.5, while in the upstream *ERCC1* transcripts assay the ratio was around 1.6. It suggested that more of the transcripts originating upstream contained the alternative splice than those originating from the normal start site (Fig. 5.11B).

To investigate whether the larger *ERCC1* transcripts were present in other human cell lines and whether they could be induced by cisplatin, semi-quantitative RT-PCR analysis of *ERCC1* transcripts was carried out on human melanoma cell line A375, ovarian cancer cell lines A2870 and PEO14, human keratinocyte cell line HACAT and human fibroblast cell line MRC5V1 following 48h cisplatin (6uM) treatment, or combined cisplatin and MEK inhibitor (PD0325901, 1uM) treatment. The primer pair Hexon1A and Hexon2-3 was used to detect all *ERCC1* transcripts, while the primers Hskin3RT specific to *ERCC1* transcripts initiating upstream, and Hexon2-3 were used to detect the larger *ERCC1* products from upstream transcripts. The RT-PCR assays were performed as described before.

For the products common to all *ERCC1* transcripts, two bands at the predicted 164bp and 206bp size were observed in all samples (Fig. 5.12). For the larger products from

upstream transcripts, two bands at the predicted 333bp and 375bp size were detected as well (Fig. 5.12). The data indicated that all the human cell lines assayed had larger *ERCC1* larger transcripts; although the amounts seemed to vary. Moreover, in all cases, the level of the upstream transcript was increased following cisplatin treatment, Although the levels of the increase varied between cell lines, this induction was abrogated by the MEK inhibitor (Fig. 5.12). Furthermore, although the resolution of these gels was not as good as in Figure 5.11B, the ratio of the alternatively spliced band relative to the normal band again appeared to be higher for upstream transcripts than normal transcripts (Fig. 5.12).

Figure 5.11 An upstream *ERCC1* transcript in human cell lines

A

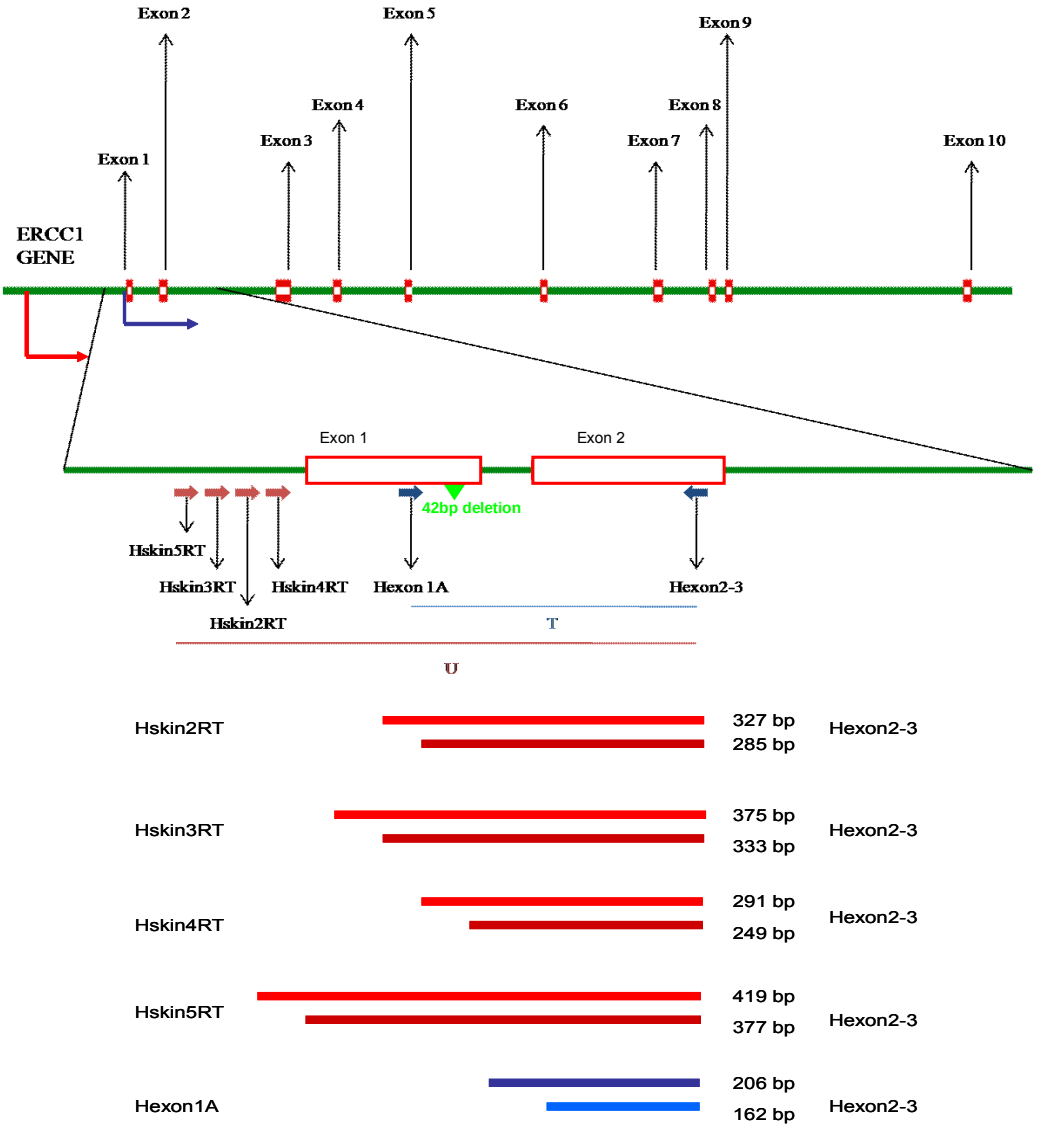

B

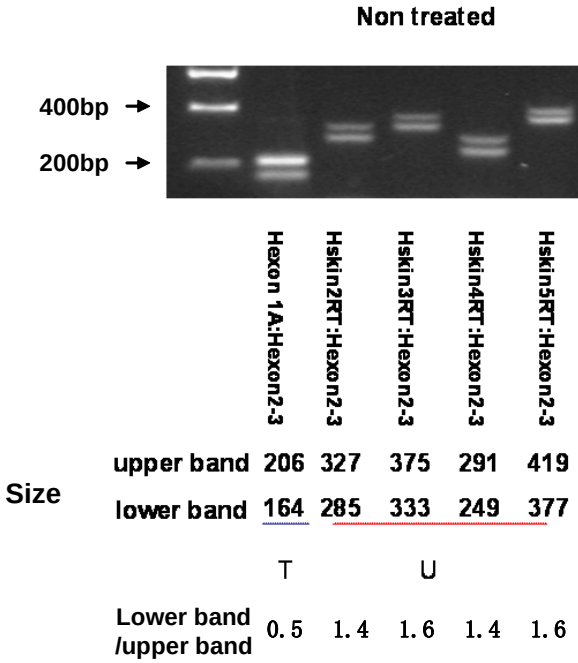

A, schematic of human *ERCC1* gene showing the exons, location of the normal transcription initiation site (blue arrow) and presumed location of the upstream initiation site (red arrow). The positions of primers used to detect all *ERCC1* transcripts (T) and predicted sizes of PCR products are indicated. The positions of the various primers used to detect the upstream *ERCC1* transcripts (U) and predicted size of PCR products are also indicated. Normal and alternatively spliced products (generates a 42bp smaller product in all cases) are demonstrated.

B, RT-PCR on mRNA extracted from human melanoma A375 cells. T, detection of all *ERCC1* transcripts with primer pair of Hexon1A and H-exon 2-3. U, detection of *ERCC1* transcripts initiating upstream with primer pairs of hskin2RT and H-exon2-3, hskin3RTand H-exon2-3, hskin4RTand H-exon2-3, hskin5RTand H-exon2-3. The sizes all the PCR products are indicated. Quantification of *ERCC1* RT-PCR bands was achieved by densitometry and expressed as the ratio of signal from the alternative spliced band relative to signal from the normal band.

Figure 5.12 Cisplatin induces an upstream *ERCC1* transcript

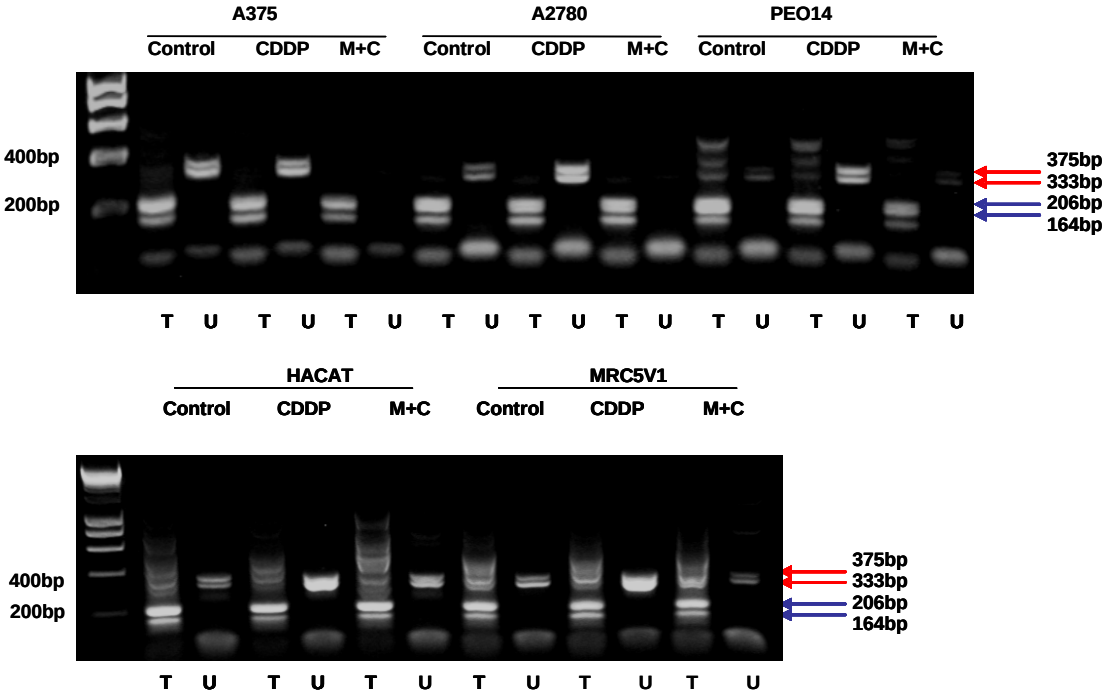

ERCC1 transcripts were analyzed in human melanoma (A375), ovarian cancer (A2780,PEO14), keratinocyte (HACAT) and fibroblast (MRC5V1) cell lines. Cells were untreated or treated for 48h with cisplatin (6uM) or both cisplatin (6uM) and MEK inhibitor, PD0325901 (1uM) before RNA was extracted and RT-PCR was carried out. T, detection of all *ERCC1* transcripts with primer pair Hexon1A and H-exon 2-3. U, detection of *ERCC1* transcripts initiating upstream with primer pair hskin3RT and H-exon 2-3. Blue arrows, product common to all transcripts; red arrows, product from upstream transcripts. PCR was performed with the following thermocycling profiles: 35 cycles (30 for melanoma cell line A375) of 94°C for 1min, 60°C for 1min and 72°C for 1min.

5.2.8 Regulation of *ERCC1* upstream transcript levels

To investigate the relationship between total *ERCC1* transcripts, upstream *ERCC1* transcripts and cisplatin induction quantitatively, Taqman qPCR analysis of total *ERCC1* transcripts and *ERCC1* upstream transcripts was performed on human melanoma cell line A375 and ovarian cancer cell lines A2780 and PEO14 following 48h cisplatin (6uM) treatment, or combined cisplatin and MEK inhibitor

(PD0325901, 1uM) treatment. Beta-actin was used as the internal control in order to normalize the expression of total *ERCC1* and larger *ERCC1* transcripts. Relative concentrations of total *ERCC1* were detected by qPCR as described before. For the upstream transcript detection, a custom Taqman q-RT PCR assay was ordered based on the 139bp of *ERCC1* 5′ upstream sequence between Hskin5RT and the normal *ERCC1* initiation site. A standard curve of qPCR for larger *ERCC1* and Beta-actin was run first. If the absolute value of the slope of the plot of log dilution factor vs. $\Delta C_T < 0.1$, then the comparative C_T method can be used to analyze real time RT-PCR data (Livak and Schmittgen 2001). The relative efficiency plot for larger *ERCC1* vs. Beta-actin showed that the absolute value of the slope was 0.0888 which passed the test (Fig. 5.13). Therefore, the comparative C_T method could be used to measure relative concentrations of larger *ERCC1* mRNA.

Cisplatin treatment caused a 4.1-fold, 2.6-fold and 6.5-fold increase in larger *ERCC1* mRNA in human melanoma cell line A375, ovarian cancer cell lines A2780 and PEO14, respectively. In each case, the MEK inhibitor efficiently prevented this cisplatin-induced increase in larger *ERCC1* mRNA (Fig. 5.14A, C, E). This confirmed our RT-PCR results that expression of upstream *ERCC1* transcripts were increased following cisplatin treatment and this increase was regulated by the MAPK pathway. Cisplatin treatment also resulted in a 3.3-fold, 2.3-fold and 1.6-fold increase in total *ERCC1* mRNA in human melanoma cell line A375, and ovarian cancer cell lines A2780 and PEO14, respectively. In addition, the MEK inhibitor completely abrogated the cisplatin-induce total *ERCC1* mRNA increase in human melanoma cell line A375, but did not significantly reduce this induction in ovarian cancer cell lines A2780 and PEO14 (Fig. 5.14B, D, F).

We also compared the larger *ERCC1* and total *ERCC1* mRNA basal levels between human melanoma cell line and ovarian cancer cell lines. Larger *ERCC1* mRNA basal levels were 2 to 7-fold higher in melanoma cell line A375 than ovarian cell lines A2780 and PEO14 (Fig 5.15A). Moreover, total *ERCC1* mRNA basal levels were

10 to 20-fold higher in melanoma cell line A375 than ovarian cell lines A2780 and PEO14 (Fig 5.15B).

To further investigate the contribution that cisplatin induction of the larger *ERCC1* mRNA made to the increase in total ERCC1 mRNA after cisplatin, the ratios of larger *ERCC1* relative to total *ERCC1* mRNA were analyzed using the relative standard method in human melanoma cell line A375 and ovarian cancer cell lines A2780 and PEO14 following 48h cisplatin (6uM) treatment, or combined cisplatin and MEK inhibitor (PD0325901, 1uM) treatment. After cisplatin treatment, the ratios of larger *ERCC1* relative to total *ERCC1* mRNA in human melanoma cell line A375 increased from 15% to 28%, while for ovarian cancer cell lines A2780 and PEO14, the increases were from 54% to 72% and 41% to 98%, respectively (Fig 5.16A, B, C). Moreover, the cisplatin induced increase in the larger *ERCC1*/total *ERCC1* mRNA ratio increase was inhibited by the MEK inhibitor in all three cell lines (Fig 5.16A, B, C).

Figure 5.13 Validation of qPCR expression data for the larger *ERCC1* transcript

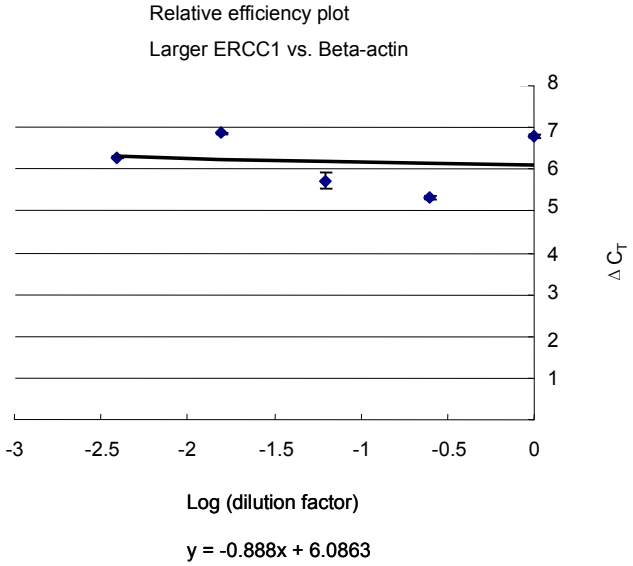

Relative qPCR efficiency plot for larger *ERCC1* and beta-actin transcripts. delta CT values are the means from three independent experiments. The absolute value of the slope of log dilution factor vs. delta CT is 0.0888.

Figure 5.14 Cisplatin induced expression of the larger *ERCC1* transcript

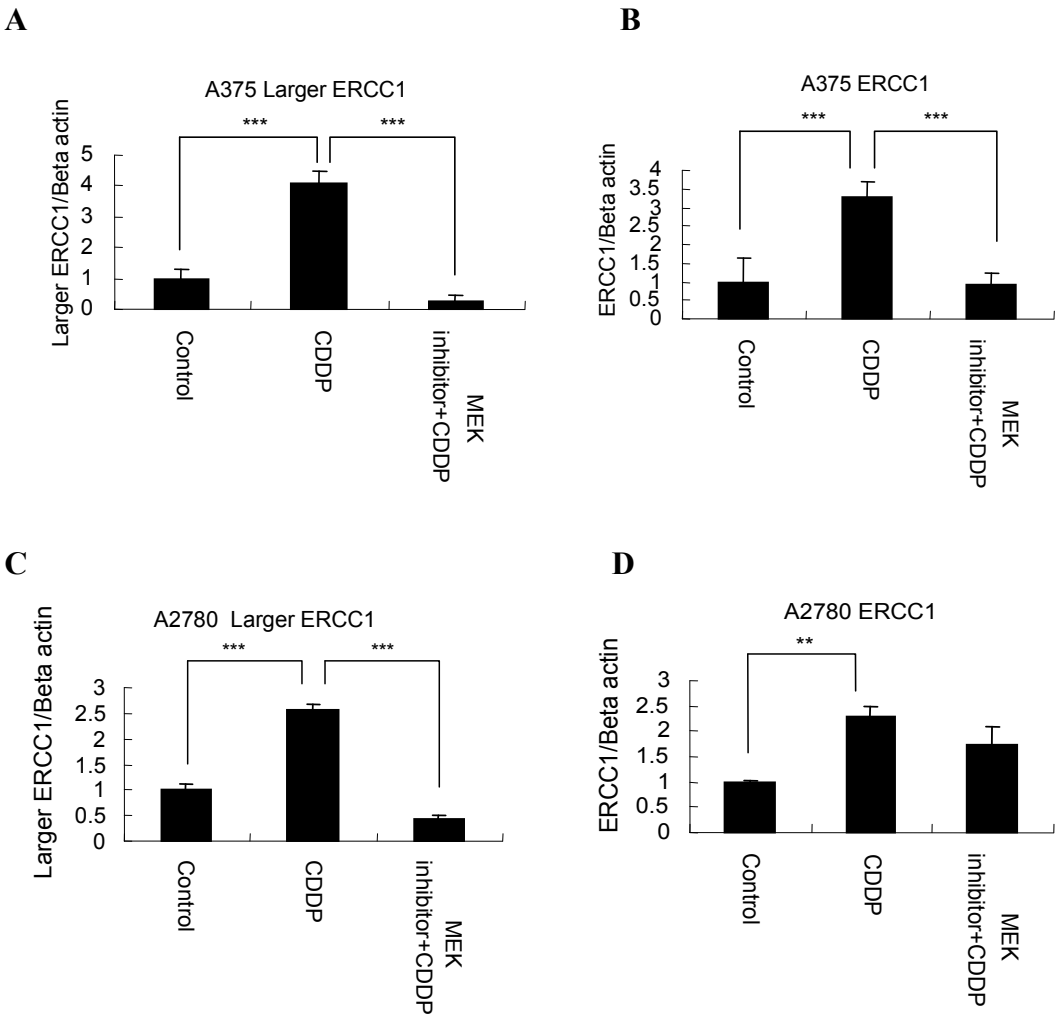

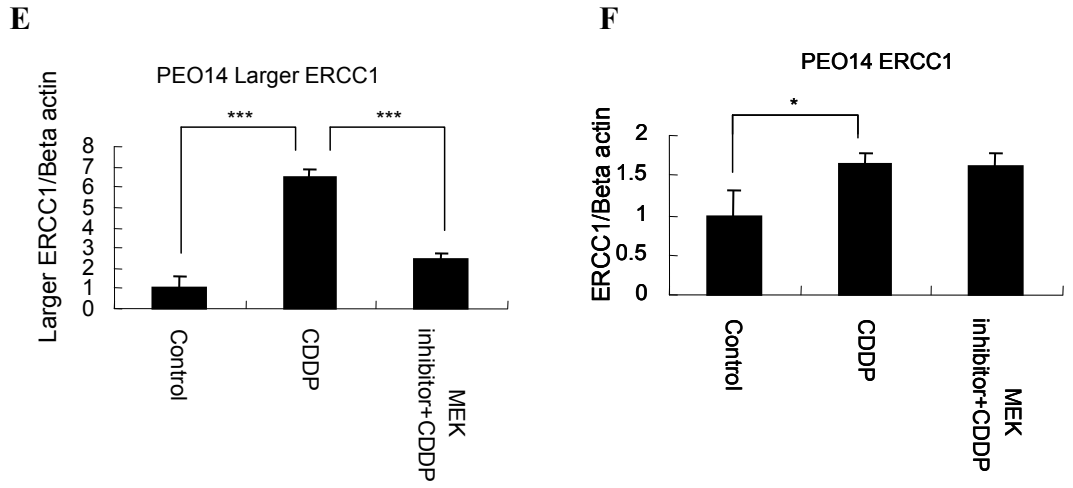

A, Histogram shows the mean level (± SEM) of larger *ERCC1* mRNA relative to beta-actin mRNA in human melanoma cell line A375 determined from three independent experiments by qPCR. In this panel and in panels B-F, Cells were untreated, or treated with cisplatin (6uM), or treated with both cisplatin and MEK inhibitor for 48h. The MEK inhibitor was added 30 minutes before cisplatin treatment. One way ANOVA with Bonferroni's Multiple Comparison Test was applied for statistical analysis among control, cisplatin, and both cisplatin and PD0325901 groups. *, $P < 0.05$. **, $P < 0.01$. ***, $P < 0.001$.

B, Histogram shows the mean level (± SEM) of total *ERCC1* mRNA relative to beta-actin mRNA in human melanoma cell line A375 determined from three independent experiments by qPCR.

C, Histogram shows the mean level (± SEM) of larger *ERCC1* mRNA relative to beta-actin mRNA in human ovarian cell line A2780 determined from three independent experiments by qPCR.

D, Histogram shows the mean level (± SEM) of total *ERCC1* mRNA relative to beta-actin mRNA in human ovarian cell line A2780 determined from three independent experiments by qPCR.

E, Histogram shows the mean level (± SEM) of larger *ERCC1* mRNA relative to beta-actin mRNA in human ovarian cell line PEO14 determined from three independent experiments by qPCR.

F, Histogram shows the mean level (± SEM) of total *ERCC1* mRNA relative to beta-actin mRNA in human ovarian cell line PEO14 determined from three independent experiments by qPCR.

Figure 5.15 Basal levels of larger *ERCC1* and total *ERCC1* transcripts

A **B**

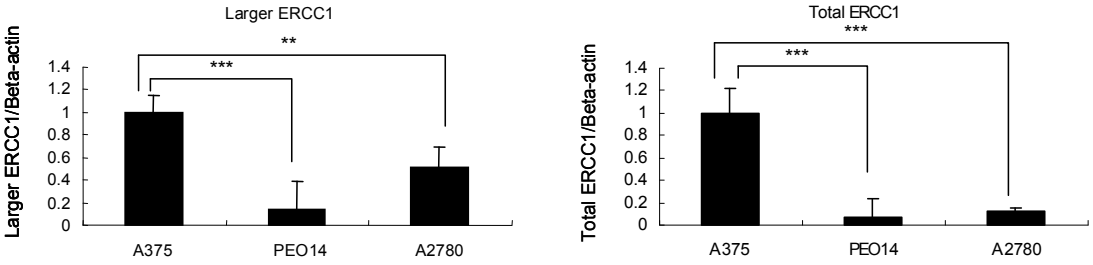

A, Histogram shows the mean level (± SEM) of larger *ERCC1* mRNA relative to beta-actin mRNA in human melanoma cell line A375, ovarian cell lines PEO14 and A2780 determined from three independent experiments by qPCR. Data were normalized to the mean level of larger *ERCC1* mRNA relative to beta-actin mRNA in human melanoma cell line A375. One way ANOVA with Bonferroni's Multiple Comparison Test was applied for statistical analysis between human melanoma cell line A375, ovarian cell lines PEO14 and A2780. **, $P < 0.01$. ***, $P < 0.001$.

B, Histogram shows the mean level (± SEM) of total *ERCC1* mRNA relative to beta-actin mRNA in human melanoma cell line A375, ovarian cell lines PEO14 and A2780 determined from three independent experiments by qPCR. Data were normalized to the mean level of total *ERCC1* mRNA relative to beta-actin mRNA in human melanoma cell line A375. One way ANOVA with Bonferroni's Multiple Comparison Test was applied for statistical analysis between human melanoma cell line A375, ovarian cell lines PEO14 and A2780. ***, $P < 0.001$.

Figure 5.16 Ratio of larger *ERCC1*/total *ERCC1*

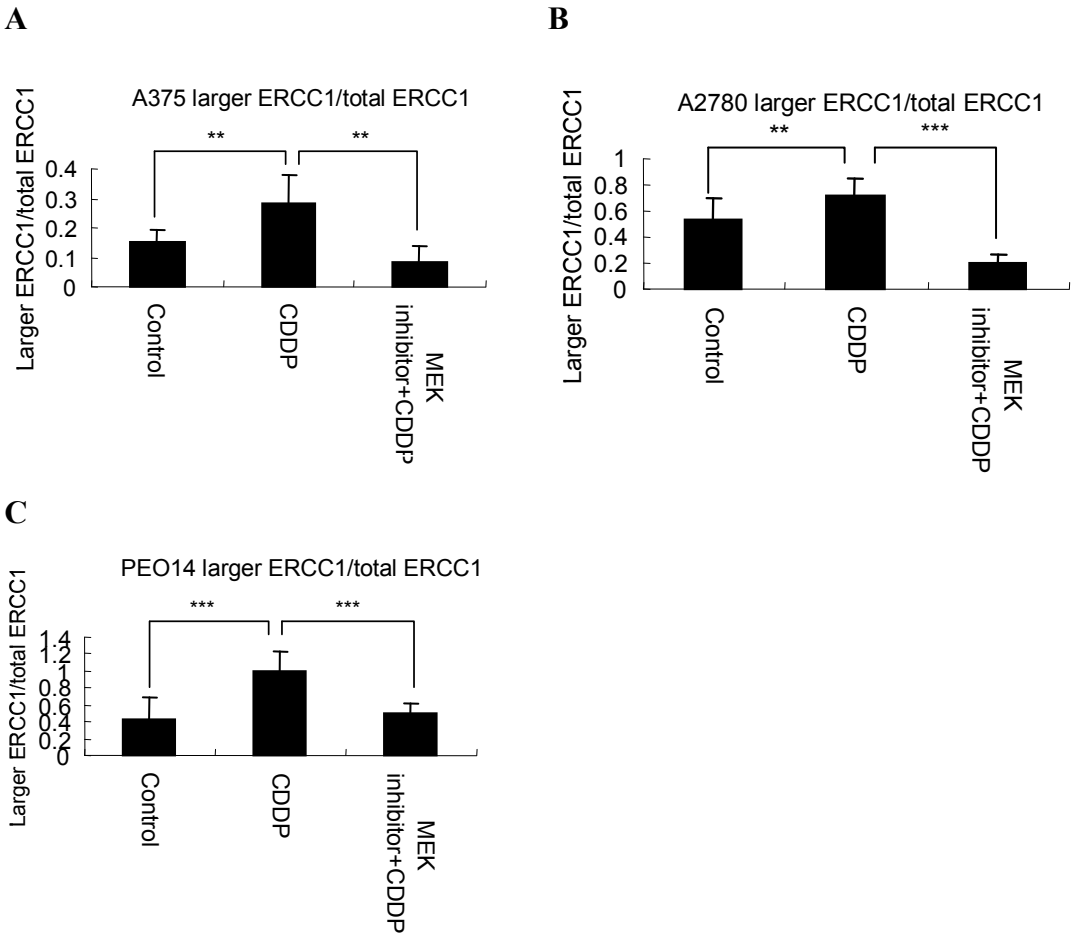

A, Histogram shows the mean ratio (± SEM) of larger *ERCC1* mRNA over total *ERCC1* mRNA in human melanoma cell line A375 determined from three independent experiments by qPCR. Larger *ERCC1* mRNA and total *ERCC1* mRNA levels were each calculated relative to beta-actin. In this panel and in panels B and C, Cells were untreated, or treated with cisplatin (6uM), or treated with both cisplatin and MEK inhibitor for 48h. The MEK inhibitor was added 30 minutes before cisplatin treatment. One way ANOVA with Bonferroni's Multiple Comparison Test was applied for statistical analysis among control, cisplatin, and both cisplatin and PD0325901 groups. **, $P < 0.01$.

B, Histogram shows the mean ratio (± SEM) of larger *ERCC1* mRNA over total *ERCC1* mRNA in ovarian cancer cell line A2780 determined from three independent experiments by qPCR. Larger *ERCC1* mRNA and total *ERCC1* mRNA levels were each calculated relative to beta-actin. **, $P < 0.01$. ***, $P < 0.001$.

C, Histogram shows the mean ratio (± SEM) of larger *ERCC1* mRNA over total *ERCC1* mRNA in ovarian cancer cell line PEO14 determined from three independent experiments by qPCR. Larger *ERCC1* mRNA and total *ERCC1* mRNA levels were each calculated relative to beta-actin. ***, $P < 0.001$.

5.2.9 5′ RACE to investigate the origin of the larger *ERCC1* transcript

To characterise the 5′ end of the larger *ERCC1* transcript, 5′ RACE analysis was performed on human ovarian cell line PEO14 with cisplatin treatment using 5′ RACE kit. The PEO14 cell line was selected for the 5′ RACE study, because the expression of the larger *ERCC1* transcript in PEO14 cell line showed larger difference between cisplatin treatment group and control group compared to other cell lines in the RT-PCR and qPCR assay.

Total RNA was freshly isolated from human ovarian cell line PEO14 with cisplatin treatment (6uM) for 48h. The first strand cDNA synthesis was performed using the *ERCC1* specific reverse primer H exon 2-3 (Fig 5.17A). Then synthesised *ERCC1* cDNA was purified using the high pure PCR product purification kit. A homopolymeric A-tail was added to the 3′ end of *ERCC1* cDNA and then it was amplified using Oligo-DT anchor primer in combination with *ERCC1* specific reverse primer Hskin 4RT REV (Fig 5.17A). The PCR products were electrophored on a 1.5% agarorse gel and visualised by ethidium bromide staining. A single weak band was detected at around 400bp (Fig 5.17B). To further amplify PCR products, a further round of nested PCR was carried out using internal primers PCR-anchor and REV1 (Fig 5.17A). A single clear band was detected at around 400bp (Fig 5.17B). This product was slightly shorter than the product in the first round of PCR as expected. The 400bp band was then purified and cloned into p-GEM T EASY vector by the LacZ blue white screen. 25 positive clones were sequenced and analyzed to map the 5′ end of novel larger *ERCC1* transcript.

Figure 5.17 Investigation of the origin of the larger *ERCC1* transcript by 5′ RACE

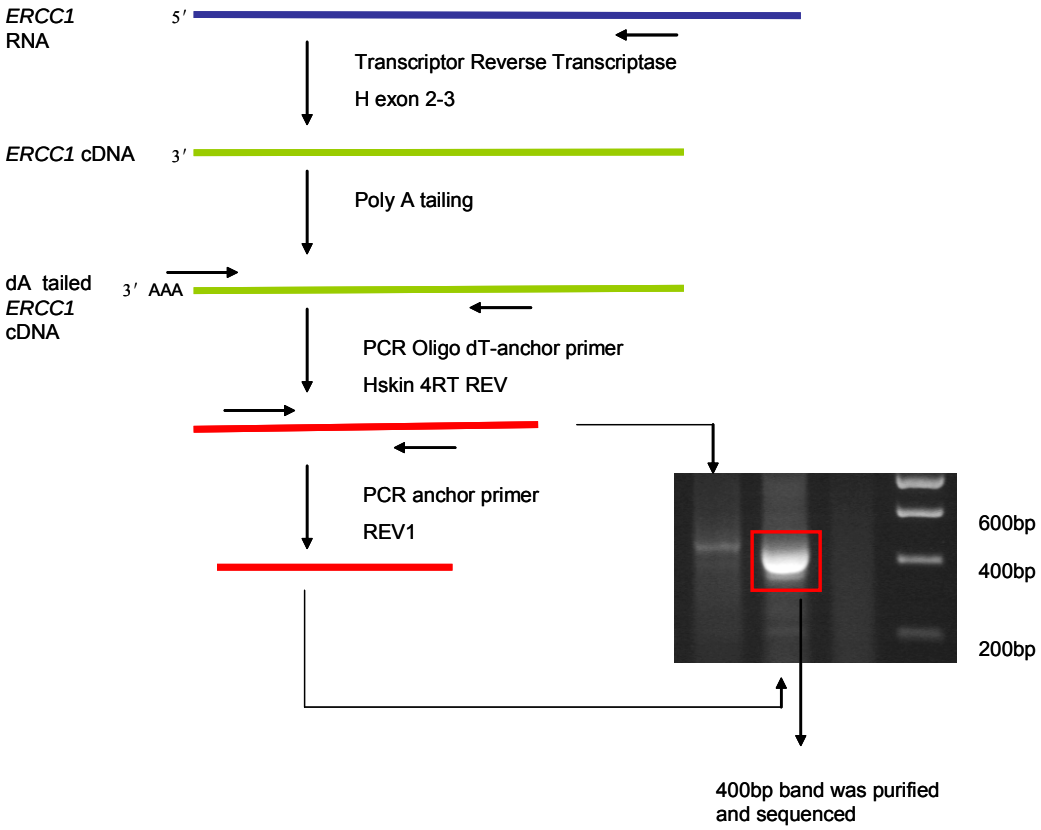

A schematic representation of the investigation of the origin of the larger ERCC1 transcripts using 5′ RACE. The tailed *ERCC1* cDNA was amplified using PCR Oligo dT-anchor forward primer and Hskin 4RT REV reverse primer. The PCR product was visualized at the position around 400bp in the first lane line from the left on the gel shown. The further round of nested PCR was performed using internal PCR anchor forward primer and REV1 reverse primer. The PCR product was visualized at the position around 400bp in the second lane line from the left on the gel.

The suquencing results showed that *ERCC1* 5′ RACE endpoints determined on the RNA of human ovarian cell line PEO14 with cisplatin treatment were much further upstream than the normal transcriptional start site. The endpoints of 23 independent 5′ RACE clones are shown in the Figure 5.18 aligned alongside the human genomic

DNA sequence. The endpoint of the longest clone mapped to -669, around 500bp upstream of the normal transcriptional start site (Fig 5.18).

Figure 5.18 Sequence analysis of 5′ RACE results aligned with human genomic DNA

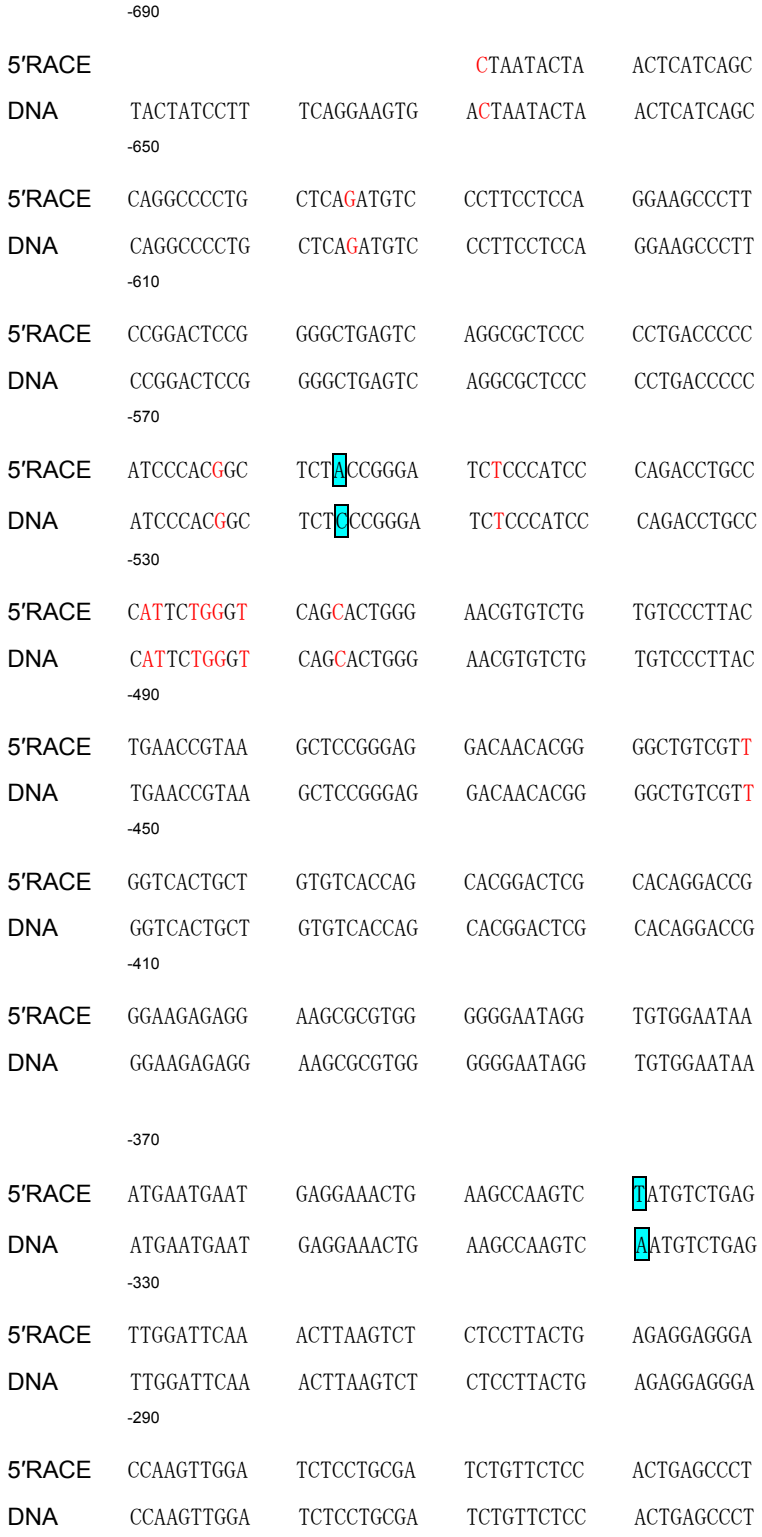

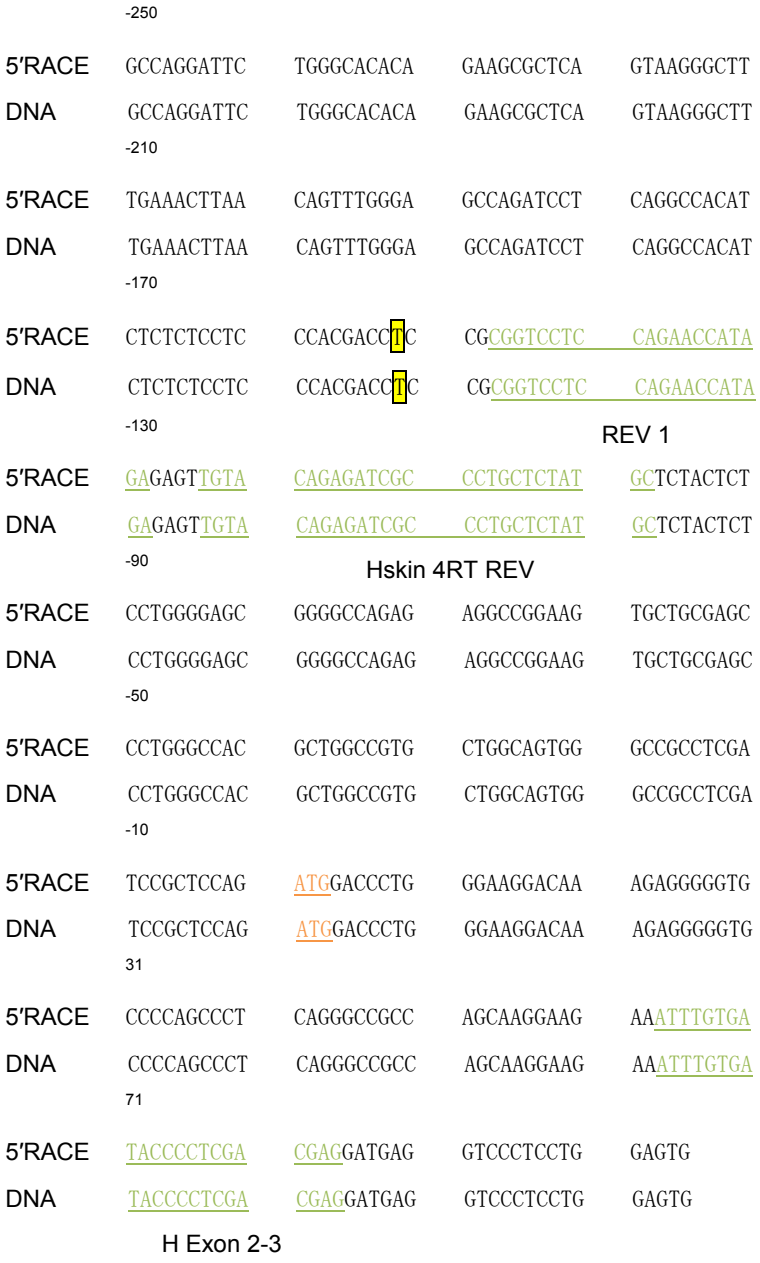

Start points of human *ERCC1* larger transcript by 5′ RACE. The sequence of the longest 5′ RACE clone determined using human ovarian cell line PEO14 is shown, aligned against the human genome DNA sequence. The sequence is numbered from the translational initiation codon in orange in exon 2, with intron 1 omitted. The start points of 5′ RACE clones are indicated in red. Mismatched sequence is indicated in light blue. The H exon2-3, Hskin 4RT REV and REV1 primers used in the 5′ RACE assay are indicated in green. TSS, normal transcription start site is shown in yellow at -152bp.

5.3 Discusssion

The MAPK pathway plays a major role in regulation of cell growth and differentiation, often induced by growth factors, cytokines and phorbol esters (Johnson and Vaillancourt 1994, Niedernhofer et al. 2006). It is also activated by some conditions of stress, particularly oxidant injury, and is believed to confer a survival advantage to cells (Guyton et al. 1996). Many studies have demonstrated an activation of the MAPK in response to CDDP treatment (Brown et al. 1993, Mirmohammadsadegh et al. 2007). However, the role of the MAPK pathway in response to cisplatin is complex (Brozovic and Osmak 2007). Although some studies showed a role for the MAPK pathway in the induction of apoptosis (Wang et al. 2000), most reports suggest that activation of the MAPK pathway enhances the resistance to cisplatin and plays an important role in enhancing survival of CDDP-treated cells (Persons et al. 1999, Wang et al. 1998). In melanoma, overexpression of activated N-RAS has been reported to protect melanoma cells and induce cisplatin resistance (Jansen et al. 1997). In this chapter, we focused on the molecular mechanisms underlying activation of the MAPK pathway by CDDP and enhanced chemotherapy resistance.

The use of cisplatin in cancer chemotherapy is limited by acquired or intrinsic resistance of cells to the drug. Acquired resistance developed in patients undergoing cisplatin treatment, increasing concentration of cisplatin treatment could reduce sensitivity to cisplatin. Resistance was described as intrinsic when patients' tumours were naturally unaffected by cisplatin (Kartalou and Essigmann 2001). Melanoma shows intrinsic resistance to cisplatin. The mechanisms involved in cisplatin resistance had been proposed in previous studies. Firstly, increased reflux, or increased inactivation by sulfhydryl molecules, such as glutathione, could result in resistance to cisplatin. Secondly, changes of expression level of regulatory proteins involved in signal transduction pathways that control the apoptotic pathway could also cause cisplatin resistance. Moreover, an increased level of DNA repair in

tumour cells was also suggested to be a cause of cisplatin resistance (Kartalou and Essigmann 2001). An improved understanding of the mechanisms of resistance contributed to increase the utility of cisplatin for the treatment of cancer.

ERCC1 is essential in the NER pathway where it forms a tight heterodimer with XPF protein. Its role is to incise DNA on the 5′ side of a lesion such as platinum-DNA adducts (Andrieux et al. 2007). In this chapter we assayed mRNA and protein levels of two NER proteins, ERCC1 and XPF, in human melanoma cell line A375 following cisplatin treatment. In our study we noticed that cisplatin induced a time dependent increase in both ERCC1 and XPF and that induction by cisplatin occurred at both protein and transcriptional levels. Previous studies have shown that higher levels of ERCC1 were observed in other cisplatin resistant tumours as well. Overexpression of ERCC1 in non small lung tumours are significantly related with resistance to cisplatin and cisplatin resistance decreases after antisense RNA inhibition of ERCC1 in non small lung tumour cell lines (Rosell et al. 2003). In addition, overexpression of ERCC1 in human ovarian cancer cells has been associated with repair of cisplatin-induced DNA damage and clinical resistance to cisplatin (Li et al. 1998a). Ovarian cell lines that developed resistance in vitro after exposure to cisplatin are found to have increased ERCC1 levels (Ferry et al. 2000). Furthermore, testicular cancer treatment was one of the most successful cisplatin-based treatments. About 95 percent of testicular cancer patients were sensitive to cisplatin and achieved a cure (Bosl and Motzer 1997). Several reports indicated that most testicular cancer cell lines are NER deficient (Koberle et al. 1997, Koberle et al. 1999). In particular, ERCC1 and XPF DNA repair protein levels decreased in these cell lines (Welsh et al. 2004). Our data agreed with these observations and suggested that ERCC1 and XPF induction during cisplatin treatment might contribute to development of resistance to chemotherapy in melanoma.

After the identification of *ERCC1* and *XPF* as cisplatin induced genes, the major object of this study was to identify the mechanism of induction of ERCC1 and XPF

by cisplatin. Protein kinases regulate signaling pathways for a broad spectrum of cellular response including proliferation, differentiation, apoptosis and DNA damage (Cantley et al. 1991). It was reasonable to speculate that one or more protein kinases were involved in induction of ERCC1 and XPF expression in response to DNA damage.

ERK1/2 is one of the important kinases in the MAPK pathway that regulates cell growth and death. Several studies showed that ERK1/2 was activated in response to DNA damage agents, including UV radiation, ionizing radiation, alkylating agents and cisplatin (Stecca and Gerber 1998). Our findings indicated that ERK1/2 was activated by cisplatin in the human melanoma cell line A375. This data confirmed previous results that treatment with cisplatin increased the activation of ERK1/2 in melanoma cell lines and induced drug resistance (Mirmohammadsadegh et al. 2007). This permitted us to investigate whether ERK1/2 activation was responsible for ERCC1 and XPF induction following cisplatin treatment. Indeed, we noticed that inactivation of MEK1/2-ERK1/2 by the specific MEK inhibitor PD0325901 prevented the cisplatin induced increase of ERCC1 protein and mRNA. Previous studies have shown that ERCC1 induction by EGF was dependent on the MAPK pathway, which was regulated by the activation of the GATA transcription factor (Andrieux et al. 2007). Activated H-Ras could up-regulate ERCC1 induction through increased transcriptional activity of AP-1 in NIH3T3 and MCF-7 cells (Agar and Young 2005). In addition, the ionizing radiation-induced ERCC1 increase also depended on ERK1/2 activation in prostate cancer cells (Yacoub et al. 2003). Moreover, blocking ERK1/2 activation by the MEK inhibitor U0126 decreased cisplatin-induced ERCC1 protein levels in lung cancer cell lines (Ko et al. 2010). In a similar way, our data indicated that the MAPK pathway took part in regulation of ERCC1 mRNA and protein levels following cisplatin treatment in melanoma cells.

We next sought to determine whether cisplatin directly activated the ERK1/2 signaling cascade or acted indirectly through cellular damage. In contrast to the usual

rapid and transient activation of this pathway in response to various other stimuli such as growth factors, UV damage, or cytokines (Xia et al. 1995), the time course for activation of ERK1/2 following cisplatin treatment showed that activation of ERK1/2 was only observed after 24 hour following initiation of cisplatin treatment and was then sustained to 72 hours. It suggested that phosphorylation of ERK1/2 might occur indirectly through cisplatin induced cellular damage. ERK1/2 activation may result from activation of upstream members of the MAPK pathway. An important role for RAS activation in accumulation of *ERCC1* mRNA by insulin had been described (Lee-Kwon et al. 1998). However, another cause seemed to be inhibition of ERK1/2 phosphatases. ERK1/2 activation was opposed by ERK1/2 phosphatases like DUSP6 (Kondoh and Nishida 2007). Both mathematical models and experimental data showed that DUSP6 was the principal time regulator of the ERK1/2 signaling (Ekerot et al. 2008). It was tempting to speculate that cisplatin mediated delayed and long lasting activation of ERK1/2 was, at least in part, due to inhibition of the ERK1/2-specific phosphatase DUSP6.

In this study we found that the DUSP6 protein levels showed a time dependent decrease following cisplatin treatment. In addition, overexpression of DUSP6 in human melanoma cells could reduce the basal mRNA levels of *ERCC1*, but did not affect the basal mRNA levels of *XPF*, suggesting that expression of DUSP6 is involved in *ERCC1* basal expression, but does not regulate *XPF* basal expression. Furthermore, the induction of *ERCC1* and *XPF* mRNA by cisplatin was inhibited by introduction of DUSP6 to melanoma cells. It suggests that cisplatin mediated DUSP6 inhibition could upregulate phosphorylation of ERK1/2 which may induce *ERCC1* and *XPF* expression. In the SRB assay for detecting cisplatin cytotoxity and resistance, the DUSP6 overexpression transfection pools were more sensitive to cisplatin compared with non-tranfected cells. Either the ERCC1 basal expression decrease or the cisplatin-induced *ERCC1* and *XPF* expression decrease by overexpression of DUSP6 could increase the sensitivity to cisplatin. DUSP6 appears to play a crucial role in resistance of melanoma to cisplatin. Overexpression of DUSP6 has previously been found to reduce ERK activity and sensitize ovarian

cancer cells to cisplatin induced cell death (Chan et al. 2008). On the contrary, knockdown of DUSP6 by siRNA increased ovarian cancer cells resistance to cisplatin (Chan et al. 2008).

An increase in ERCC1 expression can only boost repair if there is a corresponding increase in expression of its partner XPF. We found XPF protein and mRNA levels were also increased by cisplatin treatment. However, unlike ERCC1, this XPF increase was not inhibited by the MEK specific inhibitor PD0325901, but was by DUSP6 overexpression. Our observations agreed with another report which showed that DUSP6 overexpression enhanced sensitivity of ovarian cancer cells to cisplatin more strongly than the MEK inhibitor treatment. Overexpression of DUSP6 had a stronger influence on the suppression of ERK1/2 activity and cisplatin resistance (Chan et al. 2008). It was possible that DUSP6 overexpression in melanoma cells could not only block the MAPK pathway but also inhibit other pathways which may regulate XPF induction, so that XPF mRNA and protein induction following cisplatin was reduced by DUSP6 overexpression but not by the MEK inhibitor.

Previous study in our lab showed a novel *Ercc1* mRNA in mouse skin that originated from an alternative upstream promoter (Song et al. 2011). Levels of this skin-specific transcript were low in embryonic skin and increased rapidly after birth, but there was no induction by UV radiation (Song et al. 2011). In this study, RT-PCR results showed that larger *ERCC1* transcript also existed in a series of human cells (human melanoma cell line, ovarian cancer cell lines, keratinocyte cell line and human fibroblast cell line). Moreover, larger *ERCC1* transcripts could be induced by cisplatin and inhibited by inactivation of ERK1/2. It suggested that larger *ERCC1* transcripts are regulated by the MAPK pathway. These results were confirmed by the qPCR assay. Furthermore, the qPCR assay results revealed that the ratios of larger *ERCC1* relative to total *ERCC1* mRNA increased following cisplatin treatment and this increase could be abrogated by the MEK inhibitor. It implied cisplatin may preferentially induce larger *ERCC1* transcripts rather than normal *ERCC1* transcripts

through the MAPK pathway or that induction of normal transcripts is less affected by the MEK inhibitor. The function of novel *ERCC1* transcripts is possibly related to cisplatin resistance and contributes to protect cells. Finally, the origin of the larger *ERCC1* transcript was investigated by 5′ RACE assay. The *ERCC1* 5′ RACE endpoints determined on the RNA of human ovarian cell line PEO14 with cisplatin treatment were mapped to around 500bp upstream of the normal transcriptional start site. This novel transcript in human cell lines is similar to the novel transcript of *Ercc1* in mouse skin which mapped to 400bp upstream of the normal transcriptional start point (Song et al. 2011). We concluded that there is another *ERCC1* promoter upstream of the mormal promoter and additional upstream elements to regulate the expression of larger ERCC1 transcripts following cisplatin treatment.

Although cisplatin increased total *ERCC1* mRNA and larger *ERCC1* mRNA levels in all assayed cell lines, there were still some differences in expression of *ERCC1* between melanoma cell line and ovarian cancer cell lines. Firstly, the cisplatin induced total *ERCC1* mRNA increase was completely inhibited by the MEK inhibitor in the human melanoma cell line, but was not significantly reduced by the MEK inhibitor in ovarian cancer cell lines. We can not rule out the possibility that beside the MAPK pathway, other pathways may also regulate expression of *ERCC1* in ovarian cancer cell lines. Some studies have demonstrated that the activation of c-Jun-NH2-kinase(JNK)/stress-activated protein kinase (SAPK) pathway was related to regulation of *ERCC1* expression in ovarian cancer cells (Altaha et al. 2004, Li et al. 1998a). Secondly, the melanoma cell line had both higher total *ERCC1* mRNA and larger *ERCC1* mRNA basal levels than ovarian cell lines. Finally, the cisplatin induced larger *ERCC1*/total *ERCC1* mRNA ratio increase was more obvious in ovarian cancer cell lines than in the melanoma cell line. These findings may explain why melanoma patients are naturally unaffected by cisplatin while ovarian cancer patients are sensitive to cisplatin treatment firstly, but soon develop cisplatin resistance.

We also noticed that there was another smaller band showing in both normal *ERCC1* transcript detection and larger *ERCC1* transcript detection. Previous studies showed that the *ERCC1* exon 1 region contains a 42bp sequence which is often lost during splicing (Yu et al. 2001). Loss of this sequence produced a shorter transcript that was reported to be correlated with higher levels of *ERCC1* mRNA in ovarian cancer speciments (Yu et al. 2001). In this study, the ratio of the alternatively spliced product relative to normal product in upstream *ERCC1* transcripts was higher than in all *ERCC1* transcripts. The previous study in our group indicated that the lack of the 42bp sequence in exon 1 transcripts was not correlated with high levels of *ERCC1* expression and had limited significance in ovarian cancer and melanoma cells (Winter et al. 2005). We have no evidence to support the suggestion that this alternatively spliced transcript contributes to expression of *ERCC1*.

Clinical failure of chemotherapy is mainly due to drug resistance in cancer cells. Thus, it is very important to understand the molecular mechanisms underlying resistance to chemotherapy. This was the first time that cisplatin induced expression of two NER proteins, ERCC1 and XPF, to repair DNA damage had been demonstrated in melanoma cells. These inductions contribute to increase drug resistance which is one of the major obstacles to melanoma treatment. This showed us a hint that ERCC1 or XPF inhibitors could be used to enhance the effectiveness of cisplatin treatment. Furthermore, our observations revealed a new molecular mechanism that ERCC1 induction by cisplatin was regulated by activation of ERK1/2 in melanoma cells. We also provided the first direct evidence for DUSP6 reduction following cisplatin treatment and showed that its disruption was involved in ERCC1 induction by cisplatin. The understanding of this molecular mechanism may assist the development of new therapeutic interventions for melanoma. Simultaneous treatment with cisplatin and MEK inhibitor may result in synergistic therapeutic effects at tolerable doses of cisplatin. In addition, a novel larger *ERCC1* transcript was found in human cell lines and was upregulated by cisplatin. The functions of this larger *ERCC1* transcript on cisplatin resistance deserve further study.

Chapter 6

General conclusion

.

Malignant melanoma is notorious for therapeutic resistance. There are no FDA-approved agents so far that can alter the natural history of metastatic melanoma in large randomized clinical trails. Therefore, one of the major goals of the work in this thesis was to increase our understanding of melanoma biology and discover new targets for therapeutic intervention. The work in Chapter 3 identified and characterised a molecularly distinct subtype of melanoma, Chapter 4 explored the role of DUSP6 and p-ERK in melanoma progression and Chapter 5 studied the mechanisms underlying cisplatin resistance in melanoma cell lines.

Due to the limitation of using human subjects for disease pathogenesis studies, we used a mouse xenograft model to investigate molecular pathology of melanoma. Our immortal mouse melanocyte cell lines were derived from primary melanocyte cell culture of epidermis of newborn mice by infection with a retrovirus expressing SV40 T antigen. SV40 T antigen promotes cell growth and renders these cells immortal and susceptible to the additional genetic changes necessary for full expression of the malignant phenotype. Some of these cell lines were xenografted to mice. Cells from some 5-1 and 3-1-1 xenografts were reisolated into cell culture. When these cells were xenografted into mice again, they formed large tumours much more quickly than their parental cells. That provides a good platform to investigate genetic changes in melanoma progression through comparison of 5-1 and 3-1-1 Tumour cell lines with their parental cell lines.

The MAPK and the PI3K-AKT signalling pathways modulate the function of numerous substrates involved in the regulation of cell survival, proliferation and invasion. In melanoma, both the MAPK and PI3K-AKT pathways play important roles in melanoma development and progression. It is worth noting that DUSP6 acts as a phosphatase which can inactivate ERK1/2 through a feedback loop. Overexpression of DUSP6 has been reported in melanoma cell lines. We hypothesised that some molecular changes in the MAPK pathway and PI3K-AKT pathway may contribute to melanoma formation in our mouse xenograft model. Therefore, we decided to examine p-ERK, p-MEK, DUSP6 and BRAF in the MAPK

pathway and p-AKT, PTEN in the PI3K-AKT pathway in our mouse melanocyte cell line panel.

Interestingly, we found that our mouse tumour cell lines have lower expression of ERK and MEK but higher expression of DUSP6 than their parental cell lines. Meanwhile, we did not find any BRAF activating mutations associated with melanoma in our immortal mouse cell lines. All these data suggest that our tumour cell lines have shut down the MAPK pathway. As previous study showed that phosphorylation of RAF by AKT can inhibit activation of the MAPK pathway, we suspected that the inactivation of the MAPK may come from hyperactivation of the PI3K-AKT pathway. However, our mouse tumour cell lines also have decreased levels of p-AKT compare to their parental cell lines. In addition, there was no evidence for any PTEN loss in our tumour cell lines. Therefore, the PI3K-AKT pathway was not activated in our tumour cell lines and the inactivation of the MAPK pathway was not because of activation of the PI3K-AKT pathway. The MAPK pathway inactivation and the PI3K-AKT pathway inactivation observed in our mouse tumourigenic cell lines are uncommon in classic melanoma. These tumour cell lines represent a molecularly distinct and unappreciated subtype of melanoma.

Through analysis of our immortal mouse cell lines, we raised the questions: is higher expression of DUSP6 and lower level of p-ERK in our mouse tumour cell lines related to melanoma progression in the xenograft mouse model? Our results showed that overexpression of DUSP6 inactivated ERK1/2 in our immortal mouse melanocytes. Moreover, enforced expression of DUSP6 indeed increased anchorage independent-growth ability and invasive ability of our immortal mouse melanocytes. It suggests that DUSP6 may indeed be involved in melanoma progression in the xenograft assay and contributes to transform our immortal mouse melanocytes to melanoma cells. Our data also indicated that increasing phosphorylation of ERK1/2 suppressed invasion of our mouse tumour cell lines in the transwell migration assay. However, introduction of constitutively active MEK1 and MEK2 into mouse tumour

cells only slightly reduced anchorage independent growth ability. The differences between the MEK1 and MEK2 transfected and non-transfected cells were not significant in the methylcellulose assay. As DUSP6 is regulated by the MAPK pathway, exogenous expression of constitutively active MEK1 and MEK2 can induce DUSP6 expression which in turn impairs colony formation caused by the MAPK pathway activation. We can not rule out the possibility that DUSP6 can interact with other uncharacterized targets and pathways to control colony formation in the methylcellulose assay.

In contrast, although overexpression of DUSP6 also results in dephosphorylation of ERK1/2 in human melanoma cell line A375, enforced expression of DUSP6 decreased anchorage independent-growth ability and invasive ability. It is possible that mice and human have slightly different mechanisms involved in melanoma development and progression. We also consider that our mouse tumour cell lines are identified as a molecularly distinct subtype of melanoma. DUSP6 may play different roles in our distinct subtype of melanoma compared to classic melanoma exemplified by A375. In addition, there is BRAF V600E mutation in A375 human melanoma cells but not in our mouse tumour cells. The mechanisms underlying melanoma progression are possibly different in A375 human melanoma cell line with BRAF mutations and our mouse tumour cell lines without BRAF mutations.

Recent study showed that treatment of melanoma cell lines with cisplatin increased the phosphorylation of ERK1/2. The MAPK pathway activation was reported to play an important role in the regulation of *ERCC1* gene expression by insulin and EGF. Overexpression of ERCC1 has been associated with repair of cisplatin-induced DNA damage and clinical resistance to cisplatin in NSCLC, ovarian, colorectal and gastric cancers. Therefore, cisplatin is able to activate ERK1/2 and induce ERCC1 and XPF overexpression which can protect tumour cells from DNA damage and enhance resistance to cisplatin. In Chapter 5, we explored the phosphorylation level of ERK1/2 and the mRNA and protein level of *ERCC1* and its partner *XPF* following

cisplatin treatment. The results provide evidence that cisplatin induced a time dependent increase in expression of p-ERK, ERCC1 and XPF. Moreover, use of a MEK inhibitor showed ERCC1 induction by cisplatin was dependent on the MAPK pathway, while cisplatin induced XPF expression through not only the MAPK pathway but also other pathways. We also found that the DUSP6 level decreased after cisplatin treatment and overexpression of DUSP6 inhibited ERCC1 and XPF induction by cisplatin and reduced resistance to cisplatin. DUSP6 appears to play a crucial role in resistance of melanoma to cisplatin.

Previous study in our lab showed a novel *Ercc1* mRNA in mouse skin that originated from an alternative upstream promoter (Song et al. 2011). In this study, our findings showed that the larger *ERCC1* transcripts also existed in a series of human cells and originated from around 500bp upstream of the normal ERCC1 transcriptional start site. In addition, both larger *ERCC1* and total *ERCC1* basal mRNA expression levels are higher in melanoma cells than in ovarian cancer cells. That may contribute to the greater cisplatin resistance of melanoma compared to ovarian cancer. Moreover, larger *ERCC1* transcripts could be induced by cisplatin and regulated by the MAPK pathway. Furthermore, the ratios of larger *ERCC1* relative to total *ERCC1* mRNA increase following cisplatin treatment through activation of the MAPK pathway. It implied cisplatin may preferentially induce larger *ERCC1* transcripts rather than normal *ERCC1* transcripts through the MAPK pathway. The function of novel *ERCC1* transcripts is possibly related to cisplatin resistance and contributes to protect cells. To investigate this, functional analysis of the role of the larger *ERCC1* transcript should be carried out.

In conclusion, the present study described in this thesis revealed the roles of the MAPK pathway and DUSP6 in melanoma progression and cisplatin resistance. It is hoped that our work can contribute to improve understanding of molecular mechanisms underlying melanoma development and chemotherapy resistance. There is great hope that the understanding of these molecular mechanisms may assist the

development of new therapeutic interventions for melanoma in the future.

References

Adler, V., C. C. Franklin, and A. S. Kraft. 1992. Phorbol esters stimulate the phosphorylation of c-Jun but not v-Jun: regulation by the N-terminal delta domain. *Proc Natl Acad Sci U S A* 89: 5341-5.

Agar, N., and A. R. Young. 2005. Melanogenesis: a photoprotective response to DNA damage? *Mutat Res* 571: 121-32.

Akita, H., Z. Zheng, Y. Takeda, C. Kim, N. Kittaka, S. Kobayashi, S. Marubashi, I. Takemasa, H. Nagano, K. Dono, S. Nakamori, M. Monden, M. Mori, Y. Doki, and G. Bepler. 2009. Significance of RRM1 and ERCC1 expression in resectable pancreatic adenocarcinoma. *Oncogene* 28: 2903-9.

Al-Minawi, A. Z., Y. F. Lee, D. Hakansson, F. Johansson, C. Lundin, N. Saleh-Gohari, N. Schultz, D. Jenssen, H. E. Bryant, M. Meuth, J. M. Hinz, and T. Helleday. 2009. The ERCC1/XPF endonuclease is required for completion of homologous recombination at DNA replication forks stalled by inter-strand cross-links. *Nucleic Acids Res* 37: 6400-13.

Al-Minawi, A. Z., N. Saleh-Gohari, and T. Helleday. 2008. The ERCC1/XPF endonuclease is required for efficient single-strand annealing and gene conversion in mammalian cells. *Nucleic Acids Res* 36: 1-9.

Al-Sarraf, M., W. Fletcher, N. Oishi, R. Pugh, J. S. Hewlett, L. Balducci, J. McCracken, and F. Padilla. 1982. Cisplatin hydration with and without mannitol diuresis in refractory disseminated malignant melanoma: a southwest oncology group study. *Cancer Treat Rep* 66: 31-5.

Albelda, S. M., S. A. Mette, D. E. Elder, R. Stewart, L. Damjanovich, M. Herlyn, and C. A. Buck. 1990. Integrin distribution in malignant melanoma: association of the beta 3 subunit with tumor progression. *Cancer Res* 50: 6757-64.

Altaha, R., X. Liang, J. J. Yu, and E. Reed. 2004. Excision repair cross complementing-group 1: gene expression and platinum resistance. *Int J Mol Med* 14: 959-70.

Amaravadi, R. K., L. M. Schuchter, D. F. McDermott, A. Kramer, L. Giles, K. Gramlich, M. Carberry, A. B. Troxel, R. Letrero, K. L. Nathanson, M. B. Atkins, P. J. O'Dwyer, and K. T. Flaherty. 2009. Phase II Trial of Temozolomide and Sorafenib in Advanced Melanoma Patients with or without Brain Metastases. *Clin Cancer Res* 15: 7711-7718.

Amit, I., A. Citri, T. Shay, Y. Lu, M. Katz, F. Zhang, G. Tarcic, D. Siwak, J. Lahad, J. Jacob-Hirsch, N. Amariglio, N. Vaisman, E. Segal, G. Rechavi, U. Alon, G. B. Mills, E. Domany, and Y. Yarden. 2007. A module of negative feedback regulators defines growth factor signaling. *Nat Genet* 39: 503-12.

Andrieux, L. O., A. Fautrel, A. Bessard, A. Guillouzo, G. Baffet, and S. Langouet. 2007. GATA-1 is essential in EGF-mediated induction of nucleotide excision repair activity and ERCC1 expression through ERK2 in human hepatoma cells. *Cancer Res* 67: 2114-23.

Araujo, S. J., E. A. Nigg, and R. D. Wood. 2001. Strong functional interactions of TFIIH with XPC and XPG in human DNA nucleotide excision repair, without a preassembled repairosome. *Mol Cell Biol* 21: 2281-91.

Aravind, L., D. R. Walker, and E. V. Koonin. 1999. Conserved domains in DNA repair proteins and evolution of repair systems. *Nucleic Acids Res* 27: 1223-42.

Atkins, M. B., L. Kunkel, M. Sznol, and S. A. Rosenberg. 2000. High-dose recombinant interleukin-2 therapy in patients with metastatic melanoma: long-term survival update. *Cancer J Sci Am* 6 Suppl 1: S11-4.

Balch, C. M., A. C. Buzaid, S. J. Soong, M. B. Atkins, N. Cascinelli, D. G. Coit, I. D. Fleming, J. E. Gershenwald, A. Houghton, Jr., J. M. Kirkwood, K. M. McMasters, M. F. Mihm, D. L. Morton, D. S. Reintgen, M. I. Ross, A. Sober, J. A. Thompson, and J. F. Thompson. 2001. Final version of the American Joint Committee on Cancer staging system for cutaneous melanoma. *J Clin Oncol* 19: 3635-48.

Balch, C. M., S. Soong, M. I. Ross, M. M. Urist, C. P. Karakousis, W. J. Temple, M. C. Mihm, R. L. Barnhill, W. R. Jewell, H. J. Wanebo, and R. Harrison. 2000. Long-term results of a multi-institutional randomized trial comparing prognostic factors and surgical results for intermediate thickness melanomas (1.0 to 4.0 mm). Intergroup Melanoma Surgical Trial. *Ann Surg Oncol* 7: 87-97.

Beck, D. J., and R. R. Brubaker. 1973. Effect of cis-platinum(II)diamminodichloride on wild type and deoxyribonucleic acid repair deficient mutants of Escherichia coli. *J Bacteriol* 116: 1247-52.

Bellmunt, J., L. Paz-Ares, M. Cuello, F. L. Cecere, S. Albiol, V. Guillem, E. Gallardo, J. Carles, P. Mendez, J. J. de la Cruz, M. Taron, R. Rosell, and J. Baselga. 2007. Gene expression of ERCC1 as a novel prognostic marker in advanced bladder cancer patients receiving cisplatin-based chemotherapy. *Ann Oncol* 18: 522-8.

Berk, L. B. 2008. Radiation therapy as primary and adjuvant treatment for local and regional melanoma. *Cancer Control* 15: 233-8.

Bermudez, O., G. Pages, and C. Gimond. 2010. The dual-specificity MAP kinase phosphatases: critical roles in development and cancer. *Am J Physiol Cell Physiol* 299: C189-202.

Bevona, C., W. Goggins, T. Quinn, J. Fullerton, and H. Tsao. 2003. Cutaneous melanomas associated with nevi. *Arch Dermatol* 139: 1620-4; discussion 1624.

Biggerstaff, M., D. E. Szymkowski, and R. D. Wood. 1993. Co-correction of the ERCC1, ERCC4 and xeroderma pigmentosum group F DNA repair defects in vitro. *Embo J* 12: 3685-92.

Binetruy, B., T. Smeal, and M. Karin. 1991. Ha-Ras augments c-Jun activity and stimulates phosphorylation of its activation domain. *Nature* 351: 122-7.

Bloethner, S., B. Chen, K. Hemminki, J. Muller-Berghaus, S. Ugurel, D. Schadendorf, and R. Kumar. 2005. Effect of common B-RAF and N-RAS mutations on global gene expression in melanoma cell lines. *Carcinogenesis* 26: 1224-32.

Bluthgen, N., S. Legewie, S. M. Kielbasa, A. Schramme, O. Tchernitsa, J. Keil, A. Solf, M. Vingron, R. Schafer, H. Herzel, and C. Sers. 2009. A systems biological approach suggests that transcriptional feedback regulation by dual-specificity phosphatase 6 shapes extracellular signal-related kinase activity in RAS-transformed fibroblasts. *Febs J* 276: 1024-35.

Bonneau, D., and M. Longy. 2000. Mutations of the human PTEN gene. *Hum Mutat* 16: 109-22.

Bosl, G. J., and R. J. Motzer. 1997. Testicular germ-cell cancer. *N Engl J Med* 337: 242-53.

Bradsher, J., J. Auriol, L. Proietti de Santis, S. Iben, J. L. Vonesch, I. Grummt, and J. M. Egly. 2002. CSB is a component of RNA pol I transcription. *Mol Cell* 10: 819-29.

Britten, R. A., D. Liu, A. Tessier, M. J. Hutchison, and D. Murray. 2000. ERCC1 expression as a molecular marker of cisplatin resistance in human cervical tumor cells. *Int J Cancer* 89: 453-7.

Brose, M. S., P. Volpe, M. Feldman, M. Kumar, I. Rishi, R. Gerrero, E. Einhorn, M. Herlyn, J. Minna, A. Nicholson, J. A. Roth, S. M. Albelda, H. Davies, C. Cox, G. Brignell, P. Stephens, P. A. Futreal, R. Wooster, M. R. Stratton, and B. L. Weber. 2002. BRAF and RAS mutations in human lung cancer and melanoma. *Cancer Res* 62: 6997-7000.

Brown, R., C. Clugston, P. Burns, A. Edlin, P. Vasey, B. Vojtesek, and S. B. Kaye. 1993. Increased accumulation of p53 protein in cisplatin-resistant ovarian cell lines. *Int J Cancer* 55: 678-84.

Brozovic, A., and M. Osmak. 2007. Activation of mitogen-activated protein kinases by cisplatin and their role in cisplatin-resistance. *Cancer Lett* 251: 1-16.

Busch, D. B., H. van Vuuren, J. de Wit, A. Collins, M. Z. Zdzienicka, D. L. Mitchell, K. W. Brookman, M. Stefanini, R. Riboni, L. H. Thompson, R. B. Albert, A. J. van Gool, and J. Hoeijmakers. 1997. Phenotypic heterogeneity in nucleotide excision repair mutants of rodent complementation groups 1 and 4. *Mutat Res* 383: 91-106.

Cantley, L. C., K. R. Auger, C. Carpenter, B. Duckworth, A. Graziani, R. Kapeller, and S. Soltoff. 1991. Oncogenes and signal transduction. *Cell* 64: 281-302.

Carr, J., and R. M. Mackie. 1994. Point mutations in the N-ras oncogene in malignant melanoma and congenital naevi. *Br J Dermatol* 131: 72-7.

Cascinelli, N., S. Zurrida, V. Galimberti, C. Bartoli, R. Bufalino, I. Del Prato, L. Mascheroni, A. Testori, and C. Clemente. 1994. Acral lentiginous melanoma. A histological type without prognostic significance. *J Dermatol Surg Oncol* 20: 817-22.

Casula, M., M. Colombino, M. P. Satta, A. Cossu, A. Lissia, M. Budroni, E. Simeone, R. Calemma, C. Loddo, C. Caraco, N. Mozzillo, A. Daponte, G. Comella, S. Canzanella, M. Guida, G. Castello, P. A. Ascierto, and G. Palmieri. 2007. Factors predicting the occurrence of germline mutations in candidate genes among patients with cutaneous malignant melanoma from South Italy. *Eur J Cancer* 43: 137-43.

Ceppi, P., M. Volante, S. Novello, I. Rapa, K. D. Danenberg, P. V. Danenberg, A. Cambieri, G. Selvaggi, S. Saviozzi, R. Calogero, M. Papotti, and G. V. Scagliotti. 2006. ERCC1 and RRM1 gene expressions but not EGFR are predictive of shorter survival in advanced non-small-cell lung cancer treated with cisplatin and gemcitabine. *Ann Oncol* 17: 1818-25.

Chan, D. W., V. W. Liu, G. S. Tsao, K. M. Yao, T. Furukawa, K. K. Chan, and H. Y. Ngan. 2008. Loss of MKP3 mediated by oxidative stress enhances tumorigenicity and chemoresistance of ovarian cancer cells. *Carcinogenesis* 29: 1742-50.

Chapman, P. B., L. H. Einhorn, M. L. Meyers, S. Saxman, A. N. Destro, K. S. Panageas, C. B. Begg, S. S. Agarwala, L. M. Schuchter, M. S. Ernstoff, A. N. Houghton, and J. M. Kirkwood. 1999. Phase III multicenter randomized trial of the Dartmouth regimen versus dacarbazine in patients with metastatic melanoma. *J Clin Oncol* 17: 2745-51.

Chen, H. Y., C. J. Shao, F. R. Chen, A. L. Kwan, and Z. P. Chen. 2010. Role of ERCC1 promoter hypermethylation in drug resistance to cisplatin in human gliomas. *Int J Cancer* 126: 1944-54.

Cheng, S. L., R. Huang-Liu, J. N. Sheu, S. T. Chen, S. Sinchaikul, and G. J. Tsay. 2007. Toxicogenomics of A375 human malignant melanoma cells. *Pharmacogenomics* 8: 1017-36.

Chi, H., S. P. Barry, R. J. Roth, J. J. Wu, E. A. Jones, A. M. Bennett, and R. A. Flavell. 2006. Dynamic regulation of pro- and anti-inflammatory cytokines by MAPK phosphatase 1 (MKP-1) in innate immune responses. *Proc Natl Acad Sci U S A* 103: 2274-9.

Chin, L. 2003. The genetics of malignant melanoma: lessons from mouse and man. *Nat Rev Cancer* 3: 559-70.

Chipchase, M. D., and D. W. Melton. 2002. The formation of UV-induced chromosome aberrations involves ERCC1 and XPF but not other nucleotide excision repair genes. *DNA Repair (Amst)* 1: 335-40.

Chu, G. 1994. Cellular responses to cisplatin. The roles of DNA-binding proteins and DNA repair. *J Biol Chem* 269: 787-90.

Ciuffreda, L., D. Del Bufalo, M. Desideri, C. Di Sanza, A. Stoppacciaro, M. R. Ricciardi, S. Chiaretti, S. Tavolaro, B. Benassi, A. Bellacosa, R. Foa, A. Tafuri, F. Cognetti, A. Anichini, G. Zupi, and M. Milella. 2009. Growth-inhibitory and antiangiogenic activity of the MEK inhibitor PD0325901 in malignant melanoma with or without BRAF mutations. *Neoplasia* 11: 720-31.

Clark, W. H., Jr., and M. C. Mihm, Jr. 1969. Lentigo maligna and lentigo-maligna melanoma. *Am J Pathol* 55: 39-67.

Cobb, M. H. 1999. MAP kinase pathways. *Prog Biophys Mol Biol* 71: 479-500.

Cohen, C., A. Zavala-Pompa, J. H. Sequeira, M. Shoji, D. G. Sexton, G. Cotsonis, F. Cerimele, B. Govindarajan, N. Macaron, and J. L. Arbiser. 2002. Mitogen-actived protein kinase activation is an early event in melanoma progression. *Clin Cancer Res* 8: 3728-33.

Crews, C. M., A. Alessandrini, and R. L. Erikson. 1992. The primary structure of MEK, a protein kinase that phosphorylates the ERK gene product. *Science* 258: 478-80.

Cully, M., H. You, A. J. Levine, and T. W. Mak. 2006. Beyond PTEN mutations: the PI3K pathway as an integrator of multiple inputs during tumorigenesis. *Nat Rev Cancer* 6: 184-92.

Curtin, J. A., K. Busam, D. Pinkel, and B. C. Bastian. 2006. Somatic activation of KIT in distinct subtypes of melanoma. *J Clin Oncol* 24: 4340-6.

Dabholkar, M., F. Bostick-Bruton, C. Weber, V. A. Bohr, C. Egwuagu, and E. Reed. 1992. ERCC1 and ERCC2 expression in malignant tissues from ovarian cancer patients. *J Natl Cancer Inst* 84: 1512-7.

Dahl, C., and P. Guldberg. 2007. The genome and epigenome of malignant melanoma. *Apmis* 115: 1161-76.

Dai, D. L., M. Martinka, and G. Li. 2005. Prognostic significance of activated Akt expression in melanoma: a clinicopathologic study of 292 cases. *J Clin Oncol* 23: 1473-82.

de Boer, J., and J. H. Hoeijmakers. 1999. Cancer from the outside, aging from the inside: mouse models to study the consequences of defective nucleotide excision repair. *Biochimie* 81: 127-37.

de Laat, W. L., N. G. Jaspers, and J. H. Hoeijmakers. 1999. Molecular mechanism of nucleotide excision repair. *Genes Dev* 13: 768-85.

de Laat, W. L., A. M. Sijbers, H. Odijk, N. G. Jaspers, and J. H. Hoeijmakers. 1998. Mapping of interaction domains between human repair proteins ERCC1 and XPF. *Nucleic Acids Res* 26: 4146-52.

de Waard, H., J. de Wit, J. O. Andressoo, C. T. van Oostrom, B. Riis, A. Weimann, H. E. Poulsen, H. van Steeg, J. H. Hoeijmakers, and G. T. van der Horst. 2004. Different effects of CSA and CSB deficiency on sensitivity to oxidative DNA damage. *Mol Cell Biol* 24: 7941-8.

Denkert, C., W. D. Schmitt, S. Berger, A. Reles, S. Pest, A. Siegert, W. Lichtenegger, M. Dietel, and S. Hauptmann. 2002a. Expression of mitogen-activated protein kinase phosphatase-1 (MKP-1) in primary human ovarian carcinoma. *Int J Cancer* 102: 507-13.

Denkert, C., A. Siegert, A. Leclere, A. Turzynski, and S. Hauptmann. 2002b. An inhibitor of stress-activated MAP-kinases reduces invasion and MMP-2 expression of malignant melanoma cells. *Clin Exp Metastasis* 19: 79-85.

Derijard, B., M. Hibi, I. H. Wu, T. Barrett, B. Su, T. Deng, M. Karin, and R. J. Davis. 1994. JNK1: a protein kinase stimulated by UV light and Ha-Ras that binds and phosphorylates the c-Jun activation domain. *Cell* 76: 1025-37.

Dhawan, P., A. B. Singh, D. L. Ellis, and A. Richmond. 2002. Constitutive activation of Akt/protein kinase B in melanoma leads to up-regulation of nuclear factor-kappaB and tumor progression. *Cancer Res* 62: 7335-42.

Diehl, J. A., M. Cheng, M. F. Roussel, and C. J. Sherr. 1998. Glycogen synthase kinase-3beta regulates cyclin D1 proteolysis and subcellular localization. *Genes Dev* 12: 3499-511.

Dong, J., R. G. Phelps, R. Qiao, S. Yao, O. Benard, Z. Ronai, and S. A. Aaronson. 2003. BRAF oncogenic mutations correlate with progression rather than initiation of human melanoma. *Cancer Res* 63: 3883-5.

Ekerot, M., M. P. Stavridis, L. Delavaine, M. P. Mitchell, C. Staples, D. M. Owens, I. D. Keenan, R. J. Dickinson, K. G. Storey, and S. M. Keyse. 2008. Negative-feedback regulation of FGF signalling by DUSP6/MKP-3 is driven by ERK1/2 and mediated by Ets factor binding to a conserved site within the DUSP6/MKP-3 gene promoter. *Biochem J* 412: 287-98.

Elwood, J. M. 1992. Melanoma and sun exposure: contrasts between intermittent and chronic exposure. *World J Surg* 16: 157-65.

Emuss, V., M. Garnett, C. Mason, and R. Marais. 2005. Mutations of C-RAF are rare in human cancer because C-RAF has a low basal kinase activity compared with B-RAF. *Cancer Res* 65: 9719-26.

Enzlin, J. H., and O. D. Scharer. 2002. The active site of the DNA repair endonuclease XPF-ERCC1 forms a highly conserved nuclease motif. *Embo J* 21: 2045-53.

Eskandarpour, M., S. Kiaii, C. Zhu, J. Castro, A. J. Sakko, and J. Hansson. 2005. Suppression of oncogenic NRAS by RNA interference induces apoptosis of human melanoma cells. *Int J Cancer* 115: 65-73.

Evans, E., J. G. Moggs, J. R. Hwang, J. M. Egly, and R. D. Wood. 1997. Mechanism of open complex and dual incision formation by human nucleotide excision repair factors. *EMBO J* 16: 6559-73.

Fecher, L. A., S. D. Cummings, M. J. Keefe, and R. M. Alani. 2007. Toward a molecular classification of melanoma. *J Clin Oncol* 25: 1606-20.

Fecher, L. A., and K. T. Flaherty. 2009. Where are we with adjuvant therapy of stage III and IV melanoma in 2009? *J Natl Compr Canc Netw* 7: 295-304.

Feramisco, J. R., M. Gross, T. Kamata, M. Rosenberg, and R. W. Sweet. 1984. Microinjection of the oncogene form of the human H-ras (T-24) protein results in rapid proliferation of quiescent cells. *Cell* 38: 109-17.

Ferry, K. V., T. C. Hamilton, and S. W. Johnson. 2000. Increased nucleotide excision repair in cisplatin-resistant ovarian cancer cells: role of ERCC1-XPF. *Biochem Pharmacol* 60: 1305-13.

Fisher, L. A., M. Bessho, and T. Bessho. 2008. Processing of a psoralen DNA interstrand cross-link by XPF-ERCC1 complex in vitro. *J Biol Chem* 283: 1275-81.

Flaherty, K. T. 2006. Chemotherapy and targeted therapy combinations in advanced melanoma. *Clin Cancer Res* 12: 2366s-2370s.

Flotte, T. J., and M. C. Mihm, Jr. 1999. Lentigo maligna and malignant melanoma in situ, lentigo maligna type. *Hum Pathol* 30: 533-6.

Frankenberg-Schwager, M., D. Kirchermeier, G. Greif, K. Baer, M. Becker, and D. Frankenberg. 2005. Cisplatin-mediated DNA double-strand breaks in replicating but not in quiescent cells of the yeast Saccharomyces cerevisiae. *Toxicology* 212: 175-84.

Fraval, H. N., C. J. Rawlings, and J. J. Roberts. 1978. Increased sensitivity of UV-repair-deficient human cells to DNA bound platinum products which unlike thymine dimers are not recognized by an endonuclease extracted from Micrococcus luteus. *Mutat Res* 51: 121-32.

Friedberg, E. C. 2001. How nucleotide excision repair protects against cancer. *Nat Rev Cancer* 1: 22-33.

—. 2003. DNA damage and repair. *Nature* 421: 436-40.

Furukawa, T., M. Sunamura, F. Motoi, S. Matsuno, and A. Horii. 2003. Potential tumor suppressive pathway involving DUSP6/MKP-3 in pancreatic cancer. *Am J Pathol* 162: 1807-15.

Furukawa, T., E. Tanji, S. Xu, and A. Horii. 2008. Feedback regulation of DUSP6 transcription responding to MAPK1 via ETS2 in human cells. *Biochem Biophys Res Commun* 377: 317-20.

Gaillard, P. H., and R. D. Wood. 2001. Activity of individual ERCC1 and XPF subunits in DNA nucleotide excision repair. *Nucleic Acids Res* 29: 872-9.

Gandini, S., F. Sera, M. S. Cattaruzza, P. Pasquini, R. Zanetti, C. Masini, P. Boyle, and C. F. Melchi. 2005. Meta-analysis of risk factors for cutaneous melanoma: III. Family history, actinic damage and phenotypic factors. *Eur J Cancer* 41: 2040-59.

Garbe, C., P. Buttner, J. Weiss, H. P. Soyer, U. Stocker, S. Kruger, M. Roser, J. Weckbecker, R. Panizzon, F. Bahmer, and et al. 1994. Associated factors in

the prevalence of more than 50 common melanocytic nevi, atypical melanocytic nevi, and actinic lentigines: multicenter case-control study of the Central Malignant Melanoma Registry of the German Dermatological Society. *J Invest Dermatol* 102: 700-5.

Ge, X., Y. M. Fu, and G. G. Meadows. 2002. U0126, a mitogen-activated protein kinase kinase inhibitor, inhibits the invasion of human A375 melanoma cells. *Cancer Lett* 179: 133-40.

Geller, A. C., K. Emmons, D. R. Brooks, Z. Zhang, C. Powers, H. K. Koh, A. J. Sober, D. R. Miller, F. Li, F. Haluska, and B. A. Gilchrest. 2003a. Skin cancer prevention and detection practices among siblings of patients with melanoma. *J Am Acad Dermatol* 49: 631-8.

Geller, A. C., A. J. Sober, Z. Zhang, D. R. Brooks, D. R. Miller, A. Halpern, and B. A. Gilchrest. 2002. Strategies for improving melanoma education and screening for men age >or= 50 years: findings from the American Academy of Dermatological National Skin Cancer Sreening Program. *Cancer* 95: 1554-61.

Geller, A. C., Z. Zhang, A. J. Sober, A. C. Halpern, M. A. Weinstock, S. Daniels, D. R. Miller, M. F. Demierre, D. R. Brooks, and B. A. Gilchrest. 2003b. The first 15 years of the American Academy of Dermatology skin cancer screening programs: 1985-1999. *J Am Acad Dermatol* 48: 34-41.

Giles, R. H., J. H. van Es, and H. Clevers. 2003. Caught up in a Wnt storm: Wnt signaling in cancer. *Biochim Biophys Acta* 1653: 1-24.

Gillet, L. C., and O. D. Scharer. 2006. Molecular mechanisms of mammalian global genome nucleotide excision repair. *Chem Rev* 106: 253-76.

Glover, D., J. H. Glick, C. Weiler, K. Fox, and D. Guerry. 1987. WR-2721 and high-dose cisplatin: an active combination in the treatment of metastatic melanoma. *J Clin Oncol* 5: 574-8.

Goel, V. K., A. J. Lazar, C. L. Warneke, M. S. Redston, and F. G. Haluska. 2006. Examination of mutations in BRAF, NRAS, and PTEN in primary cutaneous melanoma. *J Invest Dermatol* 126: 154-60.

Goldstein, A. M., and M. A. Tucker. 1993. Etiology, epidemiology, risk factors, and public health issues of melanoma. *Curr Opin Oncol* 5: 358-63.

Goldstein, B. G., and A. O. Goldstein. 2001. Diagnosis and management of malignant melanoma. *Am Fam Physician* 63: 1359-68, 1374.

Gorden, A., I. Osman, W. Gai, D. He, W. Huang, A. Davidson, A. N. Houghton, K. Busam, and D. Polsky. 2003. Analysis of BRAF and N-RAS mutations in metastatic melanoma tissues. *Cancer Res* 63: 3955-7.

Gossage, L., and S. Madhusudan. 2007. Current status of excision repair cross complementing-group 1 (ERCC1) in cancer. *Cancer Treat Rev* 33: 565-77.

Govindarajan, B., X. Bai, C. Cohen, H. Zhong, S. Kilroy, G. Louis, M. Moses, and J. L. Arbiser. 2003. Malignant transformation of melanocytes to melanoma by constitutive activation of mitogen-activated protein kinase kinase (MAPKK) signaling. *J Biol Chem* 278: 9790-5.

Gozdz, A., A. Vashishta, K. Kalita, E. Szatmari, J. J. Zheng, S. Tamiya, N. A. Delamere, and M. Hetman. 2008. Cisplatin-mediated activation of extracellular signal-regulated kinases 1/2 (ERK1/2) by inhibition of ERK1/2 phosphatases. *J Neurochem* 106: 2056-67.

Gray-Schopfer, V. C., S. C. Cheong, H. Chong, J. Chow, T. Moss, Z. A. Abdel-Malek, R. Marais, D. Wynford-Thomas, and D. C. Bennett. 2006. Cellular senescence in naevi and immortalisation in melanoma: a role for p16? *Br J Cancer* 95: 496-505.

Groisman, R., J. Polanowska, I. Kuraoka, J. Sawada, M. Saijo, R. Drapkin, A. F. Kisselev, K. Tanaka, and Y. Nakatani. 2003. The ubiquitin ligase activity in the DDB2 and CSA complexes is differentially regulated by the COP9 signalosome in response to DNA damage. *Cell* 113: 357-67.

Guadagnolo, B. A., and G. K. Zagars. 2009. Adjuvant radiation therapy for high-risk nodal metastases from cutaneous melanoma. *Lancet Oncol* 10: 409-16.

Gulbis, J. M., Z. Kelman, J. Hurwitz, M. O'Donnell, and J. Kuriyan. 1996. Structure of the C-terminal region of p21(WAF1/CIP1) complexed with human PCNA. *Cell* 87: 297-306.

Gulmann, C., K. M. Sheehan, R. M. Conroy, J. D. Wulfkuhle, V. Espina, M. J. Mullarkey, E. W. Kay, L. A. Liotta, and E. F. Petricoin, 3rd. 2009. Quantitative cell signalling analysis reveals down-regulation of MAPK pathway activation in colorectal cancer. *J Pathol* 218: 514-9.

Guyton, K. Z., Y. Liu, M. Gorospe, Q. Xu, and N. J. Holbrook. 1996. Activation of mitogen-activated protein kinase by H2O2. Role in cell survival following oxidant injury. *J Biol Chem* 271: 4138-42.

Hammer, M., J. Mages, H. Dietrich, A. Servatius, N. Howells, A. C. Cato, and R. Lang. 2006. Dual specificity phosphatase 1 (DUSP1) regulates a subset of LPS-induced genes and protects mice from lethal endotoxin shock. *J Exp Med* 203: 15-20.

He, Z., L. A. Henricksen, M. S. Wold, and C. J. Ingles. 1995. RPA involvement in the damage-recognition and incision steps of nucleotide excision repair. *Nature* 374: 566-9.

Hennessy, B. T., D. L. Smith, P. T. Ram, Y. Lu, and G. B. Mills. 2005. Exploiting the PI3K/AKT pathway for cancer drug discovery. *Nat Rev Drug Discov* 4: 988-1004.

Henning, K. A., L. Li, N. Iyer, L. D. McDaniel, M. S. Reagan, R. Legerski, R. A. Schultz, M. Stefanini, A. R. Lehmann, L. V. Mayne, and E. C. Friedberg. 1995. The Cockayne syndrome group A gene encodes a WD repeat protein that interacts with CSB protein and a subunit of RNA polymerase II TFIIH. *Cell* 82: 555-64.

Hirobe, T. 1995. Structure and function of melanocytes: microscopic morphology and cell biology of mouse melanocytes in the epidermis and hair follicle. *Histol Histopathol* 10: 223-37.

Hoogstraten, D., A. L. Nigg, H. Heath, L. H. Mullenders, R. van Driel, J. H. Hoeijmakers, W. Vermeulen, and A. B. Houtsmuller. 2002. Rapid switching of TFIIH between RNA polymerase I and II transcription and DNA repair in vivo. *Mol Cell* 10: 1163-74.

Hoshino, R., Y. Chatani, T. Yamori, T. Tsuruo, H. Oka, O. Yoshida, Y. Shimada, S. Ari-i, H. Wada, J. Fujimoto, and M. Kohno. 1999. Constitutive activation of the 41-/43-kDa mitogen-activated protein kinase signaling pathway in human tumors. *Oncogene* 18: 813-22.

Houben, R., J. C. Becker, A. Kappel, P. Terheyden, E. B. Brocker, R. Goetz, and U. R. Rapp. 2004. Constitutive activation of the Ras-Raf signaling pathway in metastatic melanoma is associated with poor prognosis. *J Carcinog* 3: 6.

Houben, R., C. S. Vetter-Kauczok, S. Ortmann, U. R. Rapp, E. B. Broecker, and J. C. Becker. 2008. Phospho-ERK staining is a poor indicator of the mutational status of BRAF and NRAS in human melanoma. *J Invest Dermatol* 128: 2003-12.

Isla, D., C. Sarries, R. Rosell, G. Alonso, M. Domine, M. Taron, G. Lopez-Vivanco, C. Camps, M. Botia, L. Nunez, M. Sanchez-Ronco, J. J. Sanchez, M. Lopez-Brea, I. Barneto, A. Paredes, B. Medina, A. Artal, and P. Lianes. 2004. Single nucleotide polymorphisms and outcome in docetaxel-cisplatin-treated advanced non-small-cell lung cancer. *Ann Oncol* 15: 1194-203.

Jamieson, E. R., and S. J. Lippard. 1999. Structure, Recognition, and Processing of Cisplatin-DNA Adducts. *Chem Rev* 99: 2467-98.

Jansen, B., H. Schlagbauer-Wadl, H. G. Eichler, K. Wolff, A. van Elsas, P. I. Schrier, and H. Pehamberger. 1997. Activated N-ras contributes to the chemoresistance of human melanoma in severe combined immunodeficiency (SCID) mice by blocking apoptosis. *Cancer Res* 57: 362-5.

Jeffrey, K. L., T. Brummer, M. S. Rolph, S. M. Liu, N. A. Callejas, R. J. Grumont, C. Gillieron, F. Mackay, S. Grey, M. Camps, C. Rommel, S. D. Gerondakis, and C. R. Mackay. 2006. Positive regulation of immune cell function and inflammatory responses by phosphatase PAC-1. *Nat Immunol* 7: 274-83.

Jimbow, K., O. Oikawa, S. Sugiyama, and T. Takeuchi. 1979. Comparison of eumelanogenesis and pheomelanogenesis in retinal and follicular melanocytes; role of vesiculo-globular bodies in melanosome differentiation. *J Invest Dermatol* 73: 278-84.

Johnson, G. L., and R. R. Vaillancourt. 1994. Sequential protein kinase reactions controlling cell growth and differentiation. *Curr Opin Cell Biol* 6: 230-8.

Jovanovic, B., D. Krockel, D. Linden, B. Nilsson, S. Egyhazi, and J. Hansson. 2008. Lack of cytoplasmic ERK activation is an independent adverse prognostic factor in primary cutaneous melanoma. *J Invest Dermatol* 128: 2696-704.

Jun, H. J., M. J. Ahn, H. S. Kim, S. Y. Yi, J. Han, S. K. Lee, Y. C. Ahn, H. S. Jeong, Y. I. Son, J. H. Baek, and K. Park. 2008. ERCC1 expression as a predictive marker of squamous cell carcinoma of the head and neck treated with cisplatin-based concurrent chemoradiation. *Br J Cancer* 99: 167-72.

Kartalou, M., and J. M. Essigmann. 2001. Mechanisms of resistance to cisplatin. *Mutat Res* 478: 23-43.

Kaskel, P., S. Sander, M. Kron, P. Kind, R. U. Peter, and G. Krahn. 2001. Outdoor activities in childhood: a protective factor for cutaneous melanoma? Results of a case-control study in 271 matched pairs. *Br J Dermatol* 145: 602-9.

Kawakami, Y., J. Rodriguez-Leon, C. M. Koth, D. Buscher, T. Itoh, A. Raya, J. K. Ng, C. R. Esteban, S. Takahashi, D. Henrique, M. F. Schwarz, H. Asahara, and J. C. Izpisua Belmonte. 2003. MKP3 mediates the cellular response to FGF8 signalling in the vertebrate limb. *Nat Cell Biol* 5: 513-9.

Keys, H. M., B. N. Bundy, F. B. Stehman, L. I. Muderspach, W. E. Chafe, C. L. Suggs, 3rd, J. L. Walker, and D. Gersell. 1999. Cisplatin, radiation, and adjuvant hysterectomy compared with radiation and adjuvant hysterectomy for bulky stage IB cervical carcinoma. *N Engl J Med* 340: 1154-61.

Keyse, S. M. 2000. Protein phosphatases and the regulation of mitogen-activated protein kinase signalling. *Curr Opin Cell Biol* 12: 186-92.

—. 2008. Dual-specificity MAP kinase phosphatases (MKPs) and cancer. *Cancer Metastasis Rev* 27: 253-61.

Kim, M., G. H. Cha, S. Kim, J. H. Lee, J. Park, H. Koh, K. Y. Choi, and J. Chung. 2004. MKP-3 has essential roles as a negative regulator of the Ras/mitogen-activated protein kinase pathway during Drosophila development. *Mol Cell Biol* 24: 573-83.

Kirschner, K., and D. W. Melton. 2010. Multiple roles of the ERCC1-XPF endonuclease in DNA repair and resistance to anticancer drugs. *Anticancer Res* 30: 3223-32.

Kleinman, H. K., and G. R. Martin. 2005. Matrigel: basement membrane matrix with biological activity. *Semin Cancer Biol* 15: 378-86.

Ko, J. C., Y. J. Su, S. T. Lin, J. Y. Jhan, S. C. Ciou, C. M. Cheng, and Y. W. Lin. 2010. Suppression of ERCC1 and Rad51 expression through ERK1/2 inactivation is essential in emodin-mediated cytotoxicity in human non-small cell lung cancer cells. *Biochem Pharmacol* 79: 655-64.

Ko, J. M., and D. E. Fisher. 2010. A new era: melanoma genetics and therapeutics. *J Pathol* 223: 241-50.

Koberle, B., K. A. Grimaldi, A. Sunters, J. A. Hartley, L. R. Kelland, and J. R. Masters. 1997. DNA repair capacity and cisplatin sensitivity of human testis tumour cells. *Int J Cancer* 70: 551-5.

Koberle, B., J. R. Masters, J. A. Hartley, and R. D. Wood. 1999. Defective repair of cisplatin-induced DNA damage caused by reduced XPA protein in testicular germ cell tumours. *Curr Biol* 9: 273-6.

Kolch, W. 2000. Meaningful relationships: the regulation of the Ras/Raf/MEK/ERK pathway by protein interactions. *Biochem J* 351 Pt 2: 289-305.

Kondoh, K., and E. Nishida. 2007. Regulation of MAP kinases by MAP kinase phosphatases. *Biochim Biophys Acta* 1773: 1227-37.

Kortylewski, M., P. C. Heinrich, M. E. Kauffmann, M. Bohm, A. MacKiewicz, and I. Behrmann. 2001. Mitogen-activated protein kinases control p27/Kip1 expression and growth of human melanoma cells. *Biochem J* 357: 297-303.

Kraemer, K. H., N. J. Patronas, R. Schiffmann, B. P. Brooks, D. Tamura, and J. J. DiGiovanna. 2007. Xeroderma pigmentosum, trichothiodystrophy and Cockayne syndrome: a complex genotype-phenotype relationship. *Neuroscience* 145: 1388-96.

Kulaksiz, G., J. T. Reardon, and A. Sancar. 2005. Xeroderma pigmentosum complementation group E protein (XPE/DDB2): purification of various complexes of XPE and analyses of their damaged DNA binding and putative DNA repair properties. *Mol Cell Biol* 25: 9784-92.

Kuphal, S., and A. K. Bosserhoff. 2006. Influence of the cytoplasmic domain of E-cadherin on endogenous N-cadherin expression in malignant melanoma. *Oncogene* 25: 248-59.

Kuraoka, I., W. R. Kobertz, R. R. Ariza, M. Biggerstaff, J. M. Essigmann, and R. D. Wood. 2000. Repair of an interstrand DNA cross-link initiated by ERCC1-XPF repair/recombination nuclease. *J Biol Chem* 275: 26632-6.

Lauring, J., A. M. Abukhdeir, H. Konishi, J. P. Garay, J. P. Gustin, Q. Wang, R. J. Arceci, W. Matsui, and B. H. Park. 2008. The multiple myeloma associated

MMSET gene contributes to cellular adhesion, clonogenic growth, and tumorigenicity. *Blood* 111: 856-64.

Lebwohl, D., and R. Canetta. 1998. Clinical development of platinum complexes in cancer therapy: an historical perspective and an update. *Eur J Cancer* 34: 1522-34.

Lee-Kwon, W., D. Park, and M. Bernier. 1998. Involvement of the Ras/extracellular signal-regulated kinase signalling pathway in the regulation of ERCC-1 mRNA levels by insulin. *Biochem J* 331 (Pt 2): 591-7.

Lee, J. W., Y. H. Soung, S. Y. Kim, W. S. Park, S. W. Nam, W. S. Min, S. H. Kim, J. Y. Lee, N. J. Yoo, and S. H. Lee. 2005. Mutational analysis of the ARAF gene in human cancers. *Apmis* 113: 54-7.

Lee, K. B., R. J. Parker, V. Bohr, T. Cornelison, and E. Reed. 1993. Cisplatin sensitivity/resistance in UV repair-deficient Chinese hamster ovary cells of complementation groups 1 and 3. *Carcinogenesis* 14: 2177-80.

Lehmann, A. R. 1995. Nucleotide excision repair and the link with transcription. *Trends Biochem Sci* 20: 402-5.

Lenormand, P., C. Sardet, G. Pages, G. L'Allemain, A. Brunet, and J. Pouyssegur. 1993. Growth factors induce nuclear translocation of MAP kinases (p42mapk and p44mapk) but not of their activator MAP kinase kinase (p45mapkk) in fibroblasts. *J Cell Biol* 122: 1079-88.

Li, L., X. Lu, C. A. Peterson, and R. J. Legerski. 1995. An interaction between the DNA repair factor XPA and replication protein A appears essential for nucleotide excision repair. *Mol Cell Biol* 15: 5396-402.

Li, Q., K. Gardner, L. Zhang, B. Tsang, F. Bostick-Bruton, and E. Reed. 1998a. Cisplatin induction of ERCC-1 mRNA expression in A2780/CP70 human ovarian cancer cells. *J Biol Chem* 273: 23419-25.

Li, X., B. Chen, S. D. Blystone, K. P. McHugh, F. P. Ross, and D. M. Ramos. 1998b. Differential expression of alphav integrins in K1735 melanoma cells. *Invasion Metastasis* 18: 1-14.

Lieber, M. R. 1997. The FEN-1 family of structure-specific nucleases in eukaryotic DNA replication, recombination and repair. *Bioessays* 19: 233-40.

Lin, A. W., M. Barradas, J. C. Stone, L. van Aelst, M. Serrano, and S. W. Lowe. 1998. Premature senescence involving p53 and p16 is activated in response to constitutive MEK/MAPK mitogenic signaling. *Genes Dev* 12: 3008-19.

Lin, J. Y., and D. E. Fisher. 2007. Melanocyte biology and skin pigmentation. *Nature* 445: 843-50.

Lin, W. M., A. C. Baker, R. Beroukhim, W. Winckler, W. Feng, J. M. Marmion, E. Laine, H. Greulich, H. Tseng, C. Gates, F. S. Hodi, G. Dranoff, W. R. Sellers, R. K. Thomas, M. Meyerson, T. R. Golub, R. Dummer, M. Herlyn, G. Getz, and L. A. Garraway. 2008. Modeling genomic diversity and tumor dependency in malignant melanoma. *Cancer Res* 68: 664-73.

Lindahl, T., and R. D. Wood. 1999. Quality control by DNA repair. *Science* 286: 1897-905.

Lippard, S. J. 1982. New chemistry of an old molecule: cis-[Pt(NH3)2Cl2]. *Science* 218: 1075-82.

Liu, D., Z. Liu, S. Condouris, and M. Xing. 2007. BRAF V600E maintains proliferation, transformation, and tumorigenicity of BRAF-mutant papillary thyroid cancer cells. *J Clin Endocrinol Metab* 92: 2264-71.

Liu, Z. G., R. Baskaran, E. T. Lea-Chou, L. D. Wood, Y. Chen, M. Karin, and J. Y. Wang. 1996. Three distinct signalling responses by murine fibroblasts to genotoxic stress. *Nature* 384: 273-6.

Livak, K. J., and T. D. Schmittgen. 2001. Analysis of relative gene expression data using real-time quantitative PCR and the 2(-Delta Delta C(T)) Method. *Methods* 25: 402-8.

Loda, M., P. Capodieci, R. Mishra, H. Yao, C. Corless, W. Grigioni, Y. Wang, C. Magi-Galluzzi, and P. J. Stork. 1996. Expression of mitogen-activated protein kinase phosphatase-1 in the early phases of human epithelial carcinogenesis. *Am J Pathol* 149: 1553-64.

Loehrer, P. J., and L. H. Einhorn. 1984. Drugs five years later. Cisplatin. *Ann Intern Med* 100: 704-13.

MacDougall, J. R., M. R. Bani, Y. Lin, R. J. Muschel, and R. S. Kerbel. 1999. 'Proteolytic switching': opposite patterns of regulation of gelatinase B and its inhibitor TIMP-1 during human melanoma progression and consequences of gelatinase B overexpression. *Br J Cancer* 80: 504-12.

MacKie, R. M. 1985. Malignant melanocytic tumours. *J Cutan Pathol* 12: 251-65.

Maddodi, N., W. Huang, T. Havighurst, K. Kim, B. J. Longley, and V. Setaluri. 2010. Induction of autophagy and inhibition of melanoma growth in vitro and in vivo by hyperactivation of oncogenic BRAF. *J Invest Dermatol* 130: 1657-67.

Maehama, T., and J. E. Dixon. 1998. The tumor suppressor, PTEN/MMAC1, dephosphorylates the lipid second messenger, phosphatidylinositol 3,4,5-trisphosphate. *J Biol Chem* 273: 13375-8.

Magi-Galluzzi, C., R. Montironi, M. G. Cangi, K. Wishnow, and M. Loda. 1998. Mitogen-activated protein kinases and apoptosis in PIN. *Virchows Arch* 432: 407-13.

Markovic, S. N., L. A. Erickson, R. D. Rao, R. H. Weenig, B. A. Pockaj, A. Bardia, C. M. Vachon, S. E. Schild, R. R. McWilliams, J. L. Hand, S. D. Laman, L. A. Kottschade, W. J. Maples, M. R. Pittelkow, J. S. Pulido, J. D. Cameron, and E. T. Creagan. 2007. Malignant melanoma in the 21st century, part 1: epidemiology, risk factors, screening, prevention, and diagnosis. *Mayo Clin Proc* 82: 364-80.

Martin, L. P., T. C. Hamilton, and R. J. Schilder. 2008. Platinum resistance: the role of DNA repair pathways. *Clin Cancer Res* 14: 1291-5.

Matsubara, J., T. Nishina, Y. Yamada, T. Moriwaki, T. Shimoda, T. Kajiwara, T. E. Nakajima, K. Kato, T. Hamaguchi, Y. Shimada, Y. Okayama, T. Oka, and K. Shirao. 2008. Impacts of excision repair cross-complementing gene 1 (ERCC1), dihydropyrimidine dehydrogenase, and epidermal growth factor receptor on the outcomes of patients with advanced gastric cancer. *Br J Cancer* 98: 832-9.

McCubrey, J. A., L. S. Steelman, W. H. Chappell, S. L. Abrams, E. W. Wong, F. Chang, B. Lehmann, D. M. Terrian, M. Milella, A. Tafuri, F. Stivala, M. Libra, J. Basecke, C. Evangelisti, A. M. Martelli, and R. A. Franklin. 2007. Roles of the Raf/MEK/ERK pathway in cell growth, malignant transformation and drug resistance. *Biochim Biophys Acta* 1773: 1263-84.

McMasters, K. M., and S. M. Swetter. 2003. Current management of melanoma: benefits of surgical staging and adjuvant therapy. *J Surg Oncol* 82: 209-16.

Meier, F., B. Schittek, S. Busch, C. Garbe, K. Smalley, K. Satyamoorthy, G. Li, and M. Herlyn. 2005. The RAS/RAF/MEK/ERK and PI3K/AKT signaling pathways present molecular targets for the effective treatment of advanced melanoma. *Front Biosci* 10: 2986-3001.

Melton, D. W., A. M. Ketchen, F. Nunez, S. Bonatti-Abbondandolo, A. Abbondandolo, S. Squires, and R. T. Johnson. 1998. Cells from ERCC1-deficient mice show increased genome instability and a reduced frequency of S-phase-dependent illegitimate chromosome exchange but a normal frequency of homologous recombination. *J Cell Sci* 111 (Pt 3): 395-404.

Meyer, L. J., and J. H. Zone. 1994. Genetics of cutaneous melanoma. *J Invest Dermatol* 103: 112S-116S.

Michaloglou, C., L. C. Vredeveld, W. J. Mooi, and D. S. Peeper. 2008. BRAF(E600) in benign and malignant human tumours. *Oncogene* 27: 877-95.

Michaloglou, C., L. C. Vredeveld, M. S. Soengas, C. Denoyelle, T. Kuilman, C. M. van der Horst, D. M. Majoor, J. W. Shay, W. J. Mooi, and D. S. Peeper. 2005. BRAFE600-associated senescence-like cell cycle arrest of human naevi. *Nature* 436: 720-4.

Middleton, M. R., J. J. Grob, N. Aaronson, G. Fierlbeck, W. Tilgen, S. Seiter, M. Gore, S. Aamdal, J. Cebon, A. Coates, B. Dreno, M. Henz, D. Schadendorf, A. Kapp, J. Weiss, U. Fraass, P. Statkevich, M. Muller, and N. Thatcher. 2000. Randomized phase III study of temozolomide versus dacarbazine in the treatment of patients with advanced metastatic malignant melanoma. *J Clin Oncol* 18: 158-66.

Miller, A. J., and M. C. Mihm, Jr. 2006. Melanoma. *N Engl J Med* 355: 51-65.

Mirmohammadsadegh, A., R. Mota, A. Gustrau, M. Hassan, S. Nambiar, A. Marini, H. Bojar, A. Tannapfel, and U. R. Hengge. 2007. ERK1/2 is highly phosphorylated in melanoma metastases and protects melanoma cells from cisplatin-mediated apoptosis. *J Invest Dermatol* 127: 2207-15.

Morris, M., P. J. Eifel, J. Lu, P. W. Grigsby, C. Levenback, R. E. Stevens, M. Rotman, D. M. Gershenson, and D. G. Mutch. 1999. Pelvic radiation with concurrent chemotherapy compared with pelvic and para-aortic radiation for high-risk cervical cancer. *N Engl J Med* 340: 1137-43.

Mu, D., D. S. Hsu, and A. Sancar. 1996. Reaction mechanism of human DNA repair excision nuclease. *J Biol Chem* 271: 8285-94.

Nazarian, R., H. Shi, Q. Wang, X. Kong, R. C. Koya, H. Lee, Z. Chen, M. K. Lee, N. Attar, H. Sazegar, T. Chodon, S. F. Nelson, G. McArthur, J. A. Sosman, A. Ribas, and R. S. Lo. 2010. Melanomas acquire resistance to B-RAF(V600E) inhibition by RTK or N-RAS upregulation. *Nature* 468: 973-7.

Nelemans, P. J., F. H. Rampen, D. J. Ruiter, and A. L. Verbeek. 1995. An addition to the controversy on sunlight exposure and melanoma risk: a meta-analytical approach. *J Clin Epidemiol* 48: 1331-42.

Newell, G. R., J. G. Sider, L. Bergfelt, and M. L. Kripke. 1988. Incidence of cutaneous melanoma in the United States by histology with special reference to the face. *Cancer Res* 48: 5036-41.

Nichols, A. F., T. Itoh, J. A. Graham, W. Liu, M. Yamaizumi, and S. Linn. 2000. Human damage-specific DNA-binding protein p48. Characterization of XPE mutations and regulation following UV irradiation. *J Biol Chem* 275: 21422-8.

Niedernhofer, L. J., G. A. Garinis, A. Raams, A. S. Lalai, A. R. Robinson, E. Appeldoorn, H. Odijk, R. Oostendorp, A. Ahmad, W. van Leeuwen, A. F. Theil, W. Vermeulen, G. T. van der Horst, P. Meinecke, W. J. Kleijer, J. Vijg, N. G. Jaspers, and J. H. Hoeijmakers. 2006. A new progeroid syndrome reveals that genotoxic stress suppresses the somatotroph axis. *Nature* 444: 1038-43.

Niedernhofer, L. J., H. Odijk, M. Budzowska, E. van Drunen, A. Maas, A. F. Theil, J. de Wit, N. G. Jaspers, H. B. Beverloo, J. H. Hoeijmakers, and R. Kanaar. 2004. The structure-specific endonuclease Ercc1-Xpf is required to resolve DNA interstrand cross-link-induced double-strand breaks. *Mol Cell Biol* 24: 5776-87.

Nocentini, S. 1999. Rejoining kinetics of DNA single- and double-strand breaks in normal and DNA ligase-deficient cells after exposure to ultraviolet C and gamma radiation: an evaluation of ligating activities involved in different DNA repair processes. *Radiat Res* 151: 423-32.

O'Donovan, A., A. A. Davies, J. G. Moggs, S. C. West, and R. D. Wood. 1994. XPG endonuclease makes the 3' incision in human DNA nucleotide excision repair. *Nature* 371: 432-5.

Okudela, K., T. Yazawa, T. Woo, M. Sakaeda, J. Ishii, H. Mitsui, H. Shimoyamada, H. Sato, M. Tajiri, N. Ogawa, M. Masuda, T. Takahashi, H. Sugimura, and H. Kitamura. 2009. Down-regulation of DUSP6 expression in lung cancer: its mechanism and potential role in carcinogenesis. *Am J Pathol* 175: 867-81.

Olaussen, K. A., A. Dunant, P. Fouret, E. Brambilla, F. Andre, V. Haddad, E. Taranchon, M. Filipits, R. Pirker, H. H. Popper, R. Stahel, L. Sabatier, J. P. Pignon, T. Tursz, T. Le Chevalier, and J. C. Soria. 2006. DNA repair by ERCC1 in non-small-cell lung cancer and cisplatin-based adjuvant chemotherapy. *N Engl J Med* 355: 983-91.

Oliveria, S. A., M. Saraiya, A. C. Geller, M. K. Heneghan, and C. Jorgensen. 2006. Sun exposure and risk of melanoma. *Arch Dis Child* 91: 131-8.

Omholt, K., A. Platz, U. Ringborg, and J. Hansson. 2001. Cytoplasmic and nuclear accumulation of beta-catenin is rarely caused by CTNNB1 exon 3 mutations in cutaneous malignant melanoma. *Int J Cancer* 92: 839-42.

Owens, D. M., and S. M. Keyse. 2007. Differential regulation of MAP kinase signalling by dual-specificity protein phosphatases. *Oncogene* 26: 3203-13.

Pages, G., P. Lenormand, G. L'Allemain, J. C. Chambard, S. Meloche, and J. Pouyssegur. 1993. Mitogen-activated protein kinases p42mapk and p44mapk are required for fibroblast proliferation. *Proc Natl Acad Sci U S A* 90: 8319-23.

Palmieri, G., M. Capone, M. L. Ascierto, G. Gentilcore, D. F. Stroncek, M. Casula, M. C. Sini, M. Palla, N. Mozzillo, and P. A. Ascierto. 2009. Main roads to melanoma. *J Transl Med* 7: 86.

Park, C. H., T. Bessho, T. Matsunaga, and A. Sancar. 1995. Purification and characterization of the XPF-ERCC1 complex of human DNA repair excision nuclease. *J Biol Chem* 270: 22657-60.

Patil, M. A., S. A. Lee, E. Macias, E. T. Lam, C. Xu, K. D. Jones, C. Ho, M. Rodriguez-Puebla, and X. Chen. 2009. Role of cyclin D1 as a mediator of c-Met- and beta-catenin-induced hepatocarcinogenesis. *Cancer Res* 69: 253-61.

Patterson, K. I., T. Brummer, P. M. O'Brien, and R. J. Daly. 2009. Dual-specificity phosphatases: critical regulators with diverse cellular targets. *Biochem J* 418: 475-89.

Paweletz, C. P., L. Charboneau, V. E. Bichsel, N. L. Simone, T. Chen, J. W. Gillespie, M. R. Emmert-Buck, M. J. Roth, I. E. Petricoin, and L. A. Liotta. 2001. Reverse phase protein microarrays which capture disease progression show activation of pro-survival pathways at the cancer invasion front. *Oncogene* 20: 1981-9.

Persons, D. L., E. M. Yazlovitskaya, W. Cui, and J. C. Pelling. 1999. Cisplatin-induced activation of mitogen-activated protein kinases in ovarian carcinoma cells: inhibition of extracellular signal-regulated kinase activity increases sensitivity to cisplatin. *Clin Cancer Res* 5: 1007-14.

Podust, V. N., A. Georgaki, B. Strack, and U. Hubscher. 1992. Calf thymus RF-C as an essential component for DNA polymerase delta and epsilon holoenzymes function. *Nucleic Acids Res* 20: 4159-65.

Polyak, K., M. H. Lee, H. Erdjument-Bromage, A. Koff, J. M. Roberts, P. Tempst, and J. Massague. 1994. Cloning of p27Kip1, a cyclin-dependent kinase inhibitor and a potential mediator of extracellular antimitogenic signals. *Cell* 78: 59-66.

Popoff, S. C., D. J. Beck, and W. D. Rupp. 1987. Repair of plasmid DNA damaged in vitro with cis- or trans-diamminedichloroplatinum(II) in Escherichia coli. *Mutat Res* 183: 129-37.

Pratilas, C. A., B. S. Taylor, Q. Ye, A. Viale, C. Sander, D. B. Solit, and N. Rosen. 2009. (V600E)BRAF is associated with disabled feedback inhibition of RAF-MEK signaling and elevated transcriptional output of the pathway. *Proc Natl Acad Sci U S A* 106: 4519-24.

Prota, G., H. Rorsman, A. M. Rosengren, and E. Rosengren. 1976. Occurrence of trichochromes in the urine of a melanoma patient. *Experientia* 32: 1122-4.

Pulverer, B. J., J. M. Kyriakis, J. Avruch, E. Nikolakaki, and J. R. Woodgett. 1991. Phosphorylation of c-jun mediated by MAP kinases. *Nature* 353: 670-4.

Rabik, C. A., and M. E. Dolan. 2007. Molecular mechanisms of resistance and toxicity associated with platinating agents. *Cancer Treat Rev* 33: 9-23.

Ramos, J. W. 2008. The regulation of extracellular signal-regulated kinase (ERK) in mammalian cells. *Int J Biochem Cell Biol* 40: 2707-19.

Reardon, J. T., and A. Sancar. 2005. Nucleotide excision repair. *Prog Nucleic Acid Res Mol Biol* 79: 183-235.

Rees, J. L. 2004. The genetics of sun sensitivity in humans. *Am J Hum Genet* 75: 739-51.

Rose, P. G., B. N. Bundy, E. B. Watkins, J. T. Thigpen, G. Deppe, M. A. Maiman, D. L. Clarke-Pearson, and S. Insalaco. 1999. Concurrent cisplatin-based radiotherapy and chemotherapy for locally advanced cervical cancer. *N Engl J Med* 340: 1144-53.

Rosell, R., M. Taron, A. Barnadas, G. Scagliotti, C. Sarries, and B. Roig. 2003. Nucleotide excision repair pathways involved in Cisplatin resistance in non-small-cell lung cancer. *Cancer Control* 10: 297-305.

Rosenberg, B. 1985. Fundamental studies with cisplatin. *Cancer* 55: 2303-l6.

Rosenberg, B., L. VanCamp, J. E. Trosko, and V. H. Mansour. 1969. Platinum compounds: a new class of potent antitumour agents. *Nature* 222: 385-6.

Rozenberg, G. I., K. B. Monahan, C. Torrice, J. E. Bear, and N. E. Sharpless. 2010. Metastasis in an orthotopic murine model of melanoma is independent of RAS/RAF mutation. *Melanoma Res* 20: 361-71.

Ruiz, P., D. Dunon, A. Sonnenberg, and B. A. Imhof. 1993. Suppression of mouse melanoma metastasis by EA-1, a monoclonal antibody specific for alpha 6 integrins. *Cell Adhes Commun* 1: 67-81.

Runge, H. M., H. A. Neumann, W. Bucke, and A. Pfleiderer. 1985. Cloning ovarian carcinoma cells in an agar double layer versus a methylcellulose monolayer system. A comparison of two methods. *J Cancer Res Clin Oncol* 110: 51-5.

Ruzzo, A., F. Graziano, K. Kawakami, G. Watanabe, D. Santini, V. Catalano, R. Bisonni, E. Canestrari, R. Ficarelli, E. T. Menichetti, D. Mari, E. Testa, R. Silva, B. Vincenzi, P. Giordani, S. Cascinu, L. Giustini, G. Tonini, and M. Magnani. 2006. Pharmacogenetic profiling and clinical outcome of patients with advanced gastric cancer treated with palliative chemotherapy. *J Clin Oncol* 24: 1883-91.

Ryu, B., D. S. Kim, A. M. Deluca, and R. M. Alani. 2007. Comprehensive expression profiling of tumor cell lines identifies molecular signatures of melanoma progression. *PLoS One* 2: e594.

Ryu, J. S., Y. C. Hong, H. S. Han, J. E. Lee, S. Kim, Y. M. Park, Y. C. Kim, and T. S. Hwang. 2004. Association between polymorphisms of ERCC1 and XPD and survival in non-small-cell lung cancer patients treated with cisplatin combination chemotherapy. *Lung Cancer* 44: 311-6.

Sancar, A. 1995. Excision repair in mammalian cells. *J Biol Chem* 270: 15915-8.

—. 1996. DNA excision repair. *Annu Rev Biochem* 65: 43-81.

Saxena, M., and T. Mustelin. 2000. Extracellular signals and scores of phosphatases: all roads lead to MAP kinase. *Semin Immunol* 12: 387-96.

Schaeffer, L., V. Moncollin, R. Roy, A. Staub, M. Mezzina, A. Sarasin, G. Weeda, J. H. Hoeijmakers, and J. M. Egly. 1994. The ERCC2/DNA repair protein is associated with the class II BTF2/TFIIH transcription factor. *Embo J* 13: 2388-92.

Schilcher, R. B., M. Wessels, N. Niederle, S. Seeber, and C. G. Schmidt. 1984. Phase II evaluation of fractionated low and single high dose cisplatin in various tumors. *J Cancer Res Clin Oncol* 107: 57-60.

Schultz, P., S. Fribourg, A. Poterszman, V. Mallouh, D. Moras, and J. M. Egly. 2000. Molecular structure of human TFIIH. *Cell* 102: 599-607.

Schwartz, M. A., M. D. Schaller, and M. H. Ginsberg. 1995. Integrins: emerging paradigms of signal transduction. *Annu Rev Cell Dev Biol* 11: 549-99.

Seger, R., N. G. Ahn, J. Posada, E. S. Munar, A. M. Jensen, J. A. Cooper, M. H. Cobb, and E. G. Krebs. 1992. Purification and characterization of mitogen-activated protein kinase activator(s) from epidermal growth factor-stimulated A431 cells. *J Biol Chem* 267: 14373-81.

Sekulic, A., P. Haluska, Jr., A. J. Miller, J. Genebriera De Lamo, S. Ejadi, J. S. Pulido, D. R. Salomao, E. C. Thorland, R. G. Vile, D. L. Swanson, B. A. Pockaj, S. D. Laman, M. R. Pittelkow, and S. N. Markovic. 2008. Malignant melanoma in the 21st century: the emerging molecular landscape. *Mayo Clin Proc* 83: 825-46.

Selvakumaran, M., D. A. Pisarcik, R. Bao, A. T. Yeung, and T. C. Hamilton. 2003. Enhanced cisplatin cytotoxicity by disturbing the nucleotide excision repair pathway in ovarian cancer cell lines. *Cancer Res* 63: 1311-6.

Shaul, Y. D., and R. Seger. 2007. The MEK/ERK cascade: from signaling specificity to diverse functions. *Biochim Biophys Acta* 1773: 1213-26.

Shelton, J. G., L. S. Steelman, S. L. Abrams, F. E. Bertrand, R. A. Franklin, M. McMahon, and J. A. McCubrey. 2005. The epidermal growth factor receptor gene family as a target for therapeutic intervention in numerous cancers: what's genetics got to do with it? *Expert Opin Ther Targets* 9: 1009-30.

Sherr, C. J. 1994. G1 phase progression: cycling on cue. *Cell* 79: 551-5.

Sherr, C. J., and J. M. Roberts. 1995. Inhibitors of mammalian G1 cyclin-dependent kinases. *Genes Dev* 9: 1149-63.

Shields, J. M., N. E. Thomas, M. Cregger, A. J. Berger, M. Leslie, C. Torrice, H. Hao, S. Penland, J. Arbiser, G. Scott, T. Zhou, M. Bar-Eli, J. E. Bear, C. J. Der, W. K. Kaufmann, D. L. Rimm, and N. E. Sharpless. 2007. Lack of extracellular signal-regulated kinase mitogen-activated protein kinase signaling shows a new type of melanoma. *Cancer Res* 67: 1502-12.

Shinozaki, M., A. Fujimoto, D. L. Morton, and D. S. Hoon. 2004. Incidence of BRAF oncogene mutation and clinical relevance for primary cutaneous melanomas. *Clin Cancer Res* 10: 1753-7.

Sijbers, A. M., W. L. de Laat, R. R. Ariza, M. Biggerstaff, Y. F. Wei, J. G. Moggs, K. C. Carter, B. K. Shell, E. Evans, M. C. de Jong, S. Rademakers, J. de Rooij, N. G. Jaspers, J. H. Hoeijmakers, and R. D. Wood. 1996. Xeroderma pigmentosum group F caused by a defect in a structure-specific DNA repair endonuclease. *Cell* 86: 811-22.

Small, G. W., Y. Y. Shi, L. S. Higgins, and R. Z. Orlowski. 2007. Mitogen-activated protein kinase phosphatase-1 is a mediator of breast cancer chemoresistance. *Cancer Res* 67: 4459-66.

Smalley, K., and T. Eisen. 2000. The involvement of p38 mitogen-activated protein kinase in the alpha-melanocyte stimulating hormone (alpha-MSH)-induced melanogenic and anti-proliferative effects in B16 murine melanoma cells. *FEBS Lett* 476: 198-202.

Smalley, K. S. 2003. A pivotal role for ERK in the oncogenic behaviour of malignant melanoma? *Int J Cancer* 104: 527-32.

Smalley, K. S., R. Contractor, T. K. Nguyen, M. Xiao, R. Edwards, V. Muthusamy, A. J. King, K. T. Flaherty, M. Bosenberg, M. Herlyn, and K. L. Nathanson. 2008. Identification of a novel subgroup of melanomas with KIT/cyclin-dependent kinase-4 overexpression. *Cancer Res* 68: 5743-52.

Smalley, K. S., N. K. Haass, P. A. Brafford, M. Lioni, K. T. Flaherty, and M. Herlyn. 2006. Multiple signaling pathways must be targeted to overcome drug resistance in cell lines derived from melanoma metastases. *Mol Cancer Ther* 5: 1136-44.

Smeal, T., B. Binetruy, D. A. Mercola, M. Birrer, and M. Karin. 1991. Oncogenic and transcriptional cooperation with Ha-Ras requires phosphorylation of c-Jun on serines 63 and 73. *Nature* 354: 494-6.

Smith, S., D. Su, I. A. Rigault de la Longrais, P. Schwartz, M. Puopolo, T. J. Rutherford, G. Mor, H. Yu, and D. Katsaros. 2007. ERCC1 genotype and phenotype in epithelial ovarian cancer identify patients likely to benefit from

paclitaxel treatment in addition to platinum-based therapy. *J Clin Oncol* 25: 5172-9.

Song, L., A. G. Winter, J. Selfridge, and D. W. Melton. 2011. A novel transcript for DNA repair gene Ercc1 in mouse skin. *Transgenic Res*. 20:109-22.

Soothill, J. S., R. Ward, and A. J. Girling. 1992. The IC50: an exactly defined measure of antibiotic sensitivity. *J Antimicrob Chemother* 29: 137-9.

Spittle, C., M. R. Ward, K. L. Nathanson, P. A. Gimotty, E. Rappaport, M. S. Brose, A. Medina, R. Letrero, M. Herlyn, and R. H. Edwards. 2007. Application of a BRAF pyrosequencing assay for mutation detection and copy number analysis in malignant melanoma. *J Mol Diagn* 9: 464-71.

Stecca, C., and G. B. Gerber. 1998. Adaptive response to DNA-damaging agents: a review of potential mechanisms. *Biochem Pharmacol* 55: 941-51.

Stoehlmacher, J., D. J. Park, W. Zhang, D. Yang, S. Groshen, S. Zahedy, and H. J. Lenz. 2004. A multivariate analysis of genomic polymorphisms: prediction of clinical outcome to 5-FU/oxaliplatin combination chemotherapy in refractory colorectal cancer. *Br J Cancer* 91: 344-54.

Stokoe, D., S. G. Macdonald, K. Cadwallader, M. Symons, and J. F. Hancock. 1994. Activation of Raf as a result of recruitment to the plasma membrane. *Science* 264: 1463-7.

Sugasawa, K., Y. Shimizu, S. Iwai, and F. Hanaoka. 2002. A molecular mechanism for DNA damage recognition by the xeroderma pigmentosum group C protein complex. *DNA Repair (Amst)* 1: 95-107.

Sulaimon, S. S., and B. E. Kitchell. 2003. The biology of melanocytes. *Vet Dermatol* 14: 57-65.

Suzuki, A., T. Nakano, T. W. Mak, and T. Sasaki. 2008. Portrait of PTEN: messages from mutant mice. *Cancer Sci* 99: 209-13.

Sviderskaya, E. V., S. P. Hill, T. J. Evans-Whipp, L. Chin, S. J. Orlow, D. J. Easty, S. C. Cheong, D. Beach, R. A. DePinho, and D. C. Bennett. 2002. p16(Ink4a) in melanocyte senescence and differentiation. *J Natl Cancer Inst* 94: 446-54.

Takata, M., and T. Saida. 2006. Genetic alterations in melanocytic tumors. *J Dermatol Sci* 43: 1-10.

Tapias, A., J. Auriol, D. Forget, J. H. Enzlin, O. D. Scharer, F. Coin, B. Coulombe, and J. M. Egly. 2004. Ordered conformational changes in damaged DNA induced by nucleotide excision repair factors. *J Biol Chem* 279: 19074-83.

Theodosiou, A., and A. Ashworth. 2002. MAP kinase phosphatases. *Genome Biol* 3: REVIEWS3009.

Thoma, F. 1999. Light and dark in chromatin repair: repair of UV-induced DNA lesions by photolyase and nucleotide excision repair. *Embo J* 18: 6585-98.

Thomas, N. E., M. Berwick, and M. Cordeiro-Stone. 2006. Could BRAF mutations in melanocytic lesions arise from DNA damage induced by ultraviolet radiation? *J Invest Dermatol* 126: 1693-6.

Titus-Ernstoff, L., A. E. Perry, S. K. Spencer, J. J. Gibson, B. F. Cole, and M. S. Ernstoff. 2005. Pigmentary characteristics and moles in relation to melanoma risk. *Int J Cancer* 116: 144-9.

Treisman, R. 1994. Ternary complex factors: growth factor regulated transcriptional activators. *Curr Opin Genet Dev* 4: 96-101.

Tsang, M., S. Maegawa, A. Kiang, R. Habas, E. Weinberg, and I. B. Dawid. 2004. A role for MKP3 in axial patterning of the zebrafish embryo. *Development* 131: 2769-79.

Tsao, H., and K. Niendorf. 2004. Genetic testing in hereditary melanoma. *J Am Acad Dermatol* 51: 803-8.

Tsao, H., and A. J. Sober. 2005. Melanoma treatment update. *Dermatol Clin* 23: 323-33.

Tsao, H., X. Zhang, E. Benoit, and F. G. Haluska. 1998. Identification of PTEN/MMAC1 alterations in uncultured melanomas and melanoma cell lines. *Oncogene* 16: 3397-402.

Tucker, M. A., W. A. Crutcher, P. Hartge, and R. W. Sagebiel. 1993. Familial and cutaneous features of dysplastic nevi: a case-control study. *J Am Acad Dermatol* 28: 558-64.

Uribe, P., L. Andrade, and S. Gonzalez. 2006. Lack of association between BRAF mutation and MAPK ERK activation in melanocytic nevi. *J Invest Dermatol* 126: 161-6.

Usanova, S., A. Piee-Staffa, U. Sied, J. Thomale, A. Schneider, B. Kaina, and B. Koberle. 2010. Cisplatin sensitivity of testis tumour cells is due to deficiency in interstrand-crosslink repair and low ERCC1-XPF expression. *Mol Cancer* 9: 248.

Vaisanen, A., M. Kallioinen, K. von Dickhoff, L. Laatikainen, M. Hoyhtya, and T. Turpeenniemi-Hujanen. 1999. Matrix metalloproteinase-2 (MMP-2) immunoreactive protein--a new prognostic marker in uveal melanoma? *J Pathol* 188: 56-62.

van Dam, H., M. Duyndam, R. Rottier, A. Bosch, L. de Vries-Smits, P. Herrlich, A. Zantema, P. Angel, and A. J. van der Eb. 1993. Heterodimer formation of cJun and ATF-2 is responsible for induction of c-jun by the 243 amino acid adenovirus E1A protein. *Embo J* 12: 479-87.

van Duin, M., J. de Wit, H. Odijk, A. Westerveld, A. Yasui, M. H. Koken, J. H. Hoeijmakers, and D. Bootsma. 1986. Molecular characterization of the human excision repair gene ERCC-1: cDNA cloning and amino acid homology with the yeast DNA repair gene RAD10. *Cell* 44: 913-23.

Veierod, M. B., E. Weiderpass, M. Thorn, J. Hansson, E. Lund, B. Armstrong, and H. O. Adami. 2003. A prospective study of pigmentation, sun exposure, and risk of cutaneous malignant melanoma in women. *J Natl Cancer Inst* 95: 1530-8.

Viguier, J., V. Boige, C. Miquel, M. Pocard, B. Giraudeau, J. C. Sabourin, M. Ducreux, A. Sarasin, and F. Praz. 2005. ERCC1 codon 118 polymorphism is a predictive factor for the tumor response to oxaliplatin/5-fluorouracil combination chemotherapy in patients with advanced colorectal cancer. *Clin Cancer Res* 11: 6212-7.

Volker, M., M. J. Mone, P. Karmakar, A. van Hoffen, W. Schul, W. Vermeulen, J. H. Hoeijmakers, R. van Driel, A. A. van Zeeland, and L. H. Mullenders. 2001. Sequential assembly of the nucleotide excision repair factors in vivo. *Mol Cell* 8: 213-24.

Wajapeyee, N., R. W. Serra, X. Zhu, M. Mahalingam, and M. R. Green. 2008. Oncogenic BRAF induces senescence and apoptosis through pathways mediated by the secreted protein IGFBP7. *Cell* 132: 363-74.

Wakasugi, M., J. T. Reardon, and A. Sancar. 1997. The non-catalytic function of XPG protein during dual incision in human nucleotide excision repair. *J Biol Chem* 272: 16030-4.

Wakasugi, M., and A. Sancar. 1998. Assembly, subunit composition, and footprint of human DNA repair excision nuclease. *Proc Natl Acad Sci U S A* 95: 6669-74.

—. 1999. Order of assembly of human DNA repair excision nuclease. *J Biol Chem* 274: 18759-68.

Wakasugi, M., M. Shimizu, H. Morioka, S. Linn, O. Nikaido, and T. Matsunaga. 2001. Damaged DNA-binding protein DDB stimulates the excision of cyclobutane pyrimidine dimers in vitro in concert with XPA and replication protein A. *J Biol Chem* 276: 15434-40.

Wan, P. T., M. J. Garnett, S. M. Roe, S. Lee, D. Niculescu-Duvaz, V. M. Good, C. M. Jones, C. J. Marshall, C. J. Springer, D. Barford, and R. Marais. 2004. Mechanism of activation of the RAF-ERK signaling pathway by oncogenic mutations of B-RAF. *Cell* 116: 855-67.

Wang, X., J. L. Martindale, and N. J. Holbrook. 2000. Requirement for ERK activation in cisplatin-induced apoptosis. *J Biol Chem* 275: 39435-43.

Wang, X., J. L. Martindale, Y. Liu, and N. J. Holbrook. 1998. The cellular response to oxidative stress: influences of mitogen-activated protein kinase signalling pathways on cell survival. *Biochem J* 333 (Pt 2): 291-300.

Warmka, J. K., L. J. Mauro, and E. V. Wattenberg. 2004. Mitogen-activated protein kinase phosphatase-3 is a tumor promoter target in initiated cells that express oncogenic Ras. *J Biol Chem* 279: 33085-92.

Weberpals, J., K. Garbuio, A. O'Brien, K. Clark-Knowles, S. Doucette, O. Antoniouk, G. Goss, and J. Dimitroulakos. 2009. The DNA repair proteins BRCA1 and ERCC1 as predictive markers in sporadic ovarian cancer. *Int J Cancer* 124: 806-15.

Weinstock, M. A., M. J. Stampfer, R. A. Lew, W. C. Willett, and A. J. Sober. 1992. Case-control study of melanoma and dietary vitamin D: implications for advocacy of sun protection and sunscreen use. *J Invest Dermatol* 98: 809-11.

Wellbrock, C., S. Rana, H. Paterson, H. Pickersgill, T. Brummelkamp, and R. Marais. 2008. Oncogenic BRAF regulates melanoma proliferation through the lineage specific factor MITF. *PLoS One* 3: e2734.

Welsh, C., R. Day, C. McGurk, J. R. Masters, R. D. Wood, and B. Koberle. 2004. Reduced levels of XPA, ERCC1 and XPF DNA repair proteins in testis tumor cell lines. *Int J Cancer* 110: 352-61.

Whitwam, T., M. W. Vanbrocklin, M. E. Russo, P. T. Haak, D. Bilgili, J. H. Resau, H. M. Koo, and S. L. Holmen. 2007. Differential oncogenic potential of activated RAS isoforms in melanocytes. *Oncogene* 26: 4563-70.

Widlund, H. R., and D. E. Fisher. 2007. Potent p53-independent tumor suppressor activity of ARF in melanoma-genesis. *Pigment Cell Res* 20: 339-40.

Widlund, H. R., M. A. Horstmann, E. R. Price, J. Cui, S. L. Lessnick, M. Wu, X. He, and D. E. Fisher. 2002. Beta-catenin-induced melanoma growth requires the downstream target Microphthalmia-associated transcription factor. *J Cell Biol* 158: 1079-87.

Wilhelm, S. M., C. Carter, L. Tang, D. Wilkie, A. McNabola, H. Rong, C. Chen, X. Zhang, P. Vincent, M. McHugh, Y. Cao, J. Shujath, S. Gawlak, D. Eveleigh, B. Rowley, L. Liu, L. Adnane, M. Lynch, D. Auclair, I. Taylor, R. Gedrich,

A. Voznesensky, B. Riedl, L. E. Post, G. Bollag, and P. A. Trail. 2004. BAY 43-9006 exhibits broad spectrum oral antitumor activity and targets the RAF/MEK/ERK pathway and receptor tyrosine kinases involved in tumor progression and angiogenesis. *Cancer Res* 64: 7099-109.

Wilson, M. D., C. C. Ruttan, B. F. Koop, and B. W. Glickman. 2001. ERCC1: a comparative genomic perspective. *Environ Mol Mutagen* 38: 209-15.

Winter, A. G., C. Dorgan, and D. W. Melton. 2005. Expression of a splicing variant in the 5'-UTR of the human ERCC1 gene is not cancer related. *Oncogene* 24: 2110-3.

Wood, R. D. 1997. Nucleotide excision repair in mammalian cells. *J Biol Chem* 272: 23465-8.

Woods, D., H. Cherwinski, E. Venetsanakos, A. Bhat, S. Gysin, M. Humbert, P. F. Bray, V. L. Saylor, and M. McMahon. 2001. Induction of beta3-integrin gene expression by sustained activation of the Ras-regulated Raf-MEK-extracellular signal-regulated kinase signaling pathway. *Mol Cell Biol* 21: 3192-205.

Wu, H., V. Goel, and F. G. Haluska. 2003. PTEN signaling pathways in melanoma. *Oncogene* 22: 3113-22.

Wu, J. J., R. J. Roth, E. J. Anderson, E. G. Hong, M. K. Lee, C. S. Choi, P. D. Neufer, G. I. Shulman, J. K. Kim, and A. M. Bennett. 2006. Mice lacking MAP kinase phosphatase-1 have enhanced MAP kinase activity and resistance to diet-induced obesity. *Cell Metab* 4: 61-73.

Xia, Z., M. Dickens, J. Raingeaud, R. J. Davis, and M. E. Greenberg. 1995. Opposing effects of ERK and JNK-p38 MAP kinases on apoptosis. *Science* 270: 1326-31.

Yacoub, A., R. McKinstry, D. Hinman, T. Chung, P. Dent, and M. P. Hagan. 2003. Epidermal growth factor and ionizing radiation up-regulate the DNA repair genes XRCC1 and ERCC1 in DU145 and LNCaP prostate carcinoma through MAPK signaling. *Radiat Res* 159: 439-52.

Yu, J. J., K. Thornton, Y. Guo, H. Kotz, and E. Reed. 2001. An ERCC1 splicing variant involving the 5'-UTR of the mRNA may have a transcriptional modulatory function. *Oncogene* 20: 7694-8.

Zamble, D. B., and S. J. Lippard. 1995. Cisplatin and DNA repair in cancer chemotherapy. *Trends Biochem Sci* 20: 435-9.

Zepter, K., A. C. Haffner, U. Trefzer, and C. A. Elmets. 1995. Reduced growth factor requirements and accelerated cell-cycle kinetics in adult human melanocytes transformed with SV40 large T antigen. *J Invest Dermatol* 104: 755-62.

Zhang, Y., J. N. Blattman, N. J. Kennedy, J. Duong, T. Nguyen, Y. Wang, R. J. Davis, P. D. Greenberg, R. A. Flavell, and C. Dong. 2004. Regulation of innate and adaptive immune responses by MAP kinase phosphatase 5. *Nature* 430: 793-7.

Zhou, W., S. Gurubhagavatula, G. Liu, S. Park, D. S. Neuberg, J. C. Wain, T. J. Lynch, L. Su, and D. C. Christiani. 2004. Excision repair cross-complementation group 1 polymorphism predicts overall survival in advanced non-small cell lung cancer patients treated with platinum-based chemotherapy. *Clin Cancer Res* 10: 4939-43.

Zhuang, L., C. S. Lee, R. A. Scolyer, S. W. McCarthy, A. A. Palmer, X. D. Zhang, J. F. Thompson, L. P. Bron, and P. Hersey. 2005. Activation of the extracellular signal regulated kinase (ERK) pathway in human melanoma. *J Clin Pathol* 58: 1163-9.

Zimmermann, S., and K. Moelling. 1999. Phosphorylation and regulation of Raf by Akt (protein kinase B). *Science* 286: 1741-4.